R-08-93

Bedrock hydrogeochemistry Laxemar

Site descriptive modelling SDM-Site Laxemar

Marcus Laaksoharju, Geopoint
John Smellie, Conterra
Eva-Lena Tullborg, Terralogica
Bill Wallin, Geokema
Henrik Drake, Isochron Geokonsulting HB
Mel Gascoyne, Gascoyne Geoprojects Inc
Maria Gimeno, University of Zaragoza
Ioana Gurban, 3D Terra
Lotta Hallbeck, Microbial Analytics
Jorge Molinero, Amphos
Ann-Chatrin Nilsson, Geosigma
Nick Waber, University of Bern

June 2009

Svensk Kärnbränslehantering AB
Swedish Nuclear Fuel
and Waste Management Co

Box 250, SE-101 24 Stockholm
Phone +46 8 459 84 00

SKB

ISSN 1402-3091
SKB Rapport R-08-93

Bedrock hydrogeochemistry Laxemar

Site descriptive modelling SDM-Site Laxemar

Marcus Laaksoharju, Geopoint
John Smellie, Conterra
Eva-Lena Tullborg, Terralogica
Bill Wallin, Geokema
Henrik Drake, Isochron Geokonsulting HB
Mel Gascoyne, Gascoyne Geoprojects Inc
Maria Gimeno, University of Zaragoza
Ioana Gurban, 3D Terra
Lotta Hallbeck, Microbial Analytics
Jorge Molinero, Amphos
Ann-Chatrin Nilsson, Geosigma
Nick Waber, University of Bern

June 2009

Preface

This Background Report document forms the final component of the hydrogeochemical site descriptive modelling associated with the complete site investigation stage of Laxemar and the larger Laxemar-Simpevarp area leading to a hydrogeochemical site descriptive model version SDM-Site Laxemar, as based on available primary data from the 'Extended data freeze Laxemar 2.3' at Laxemar (November 30, 2007). SKB's ChemNet group, consisting of consultants and university personnel, carried out the data interpretation and modelling during the period November 2007 to November 2008. The Insite and Sierg review comments on the earlier model versions of Laxemar-Simpevarp area were considered in this work. Several groups within ChemNet were involved and the evaluation was conducted using different approaches ranging from expert knowledge to geochemical and transport modelling. During regular ChemNet meetings the results were presented and discussed and directions for subsequent analysis were issued. The underlying original work by the ChemNet participants is presented in six level III reports /Drake and Tullborg 2009a, Hallbeck and Pedersen 2008b, Gimeno et al. 2009, Smellie and Tullborg 2009, Waber et al. 2009, Kalinowski (ed) 2009/ which contain complementary information for the bedrock hydro-geochemistry Laxemar Site Descriptive Model (SDM-Site Laxemar) level II report (this report), as given by the figure below. The former Level III reports include descriptions of fracture mineralogy, explorative analyses of microbes, colloids asnd gases, water-rock interaction modelling and uncertainties of mixing modelling, background complementary studies and porewater in the rock matrix.

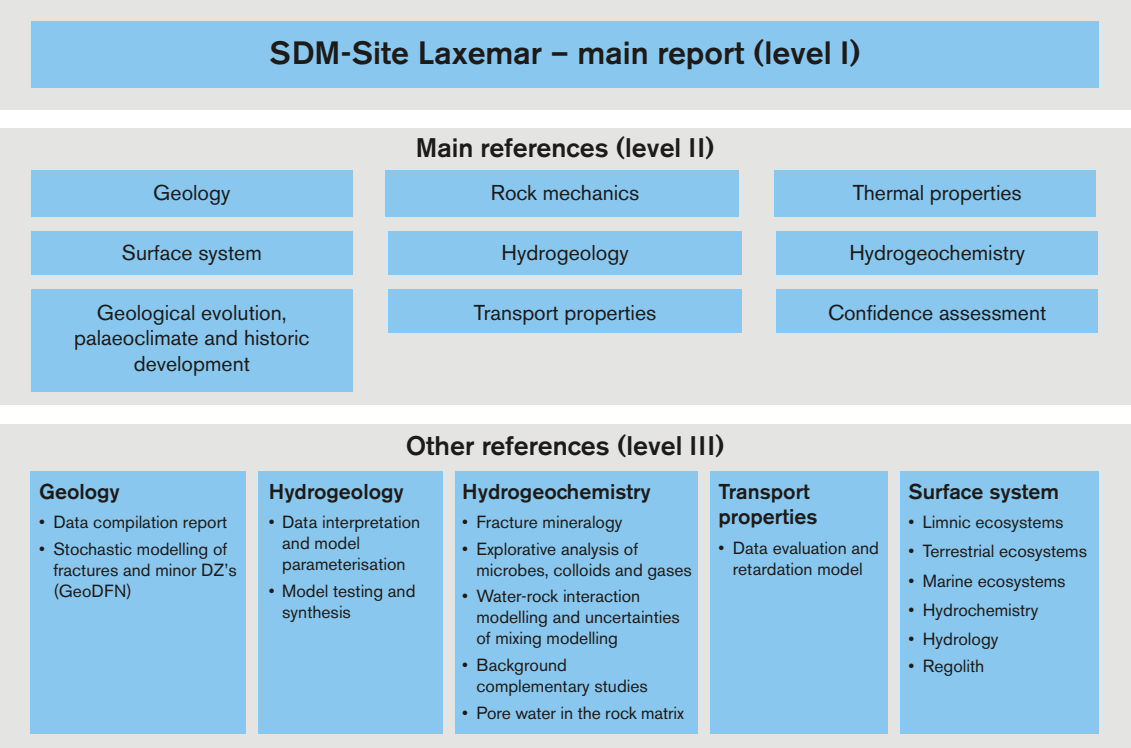

The views presented in the level III reports reflect those of the individual authors and do not neccessarily coincide with the views expressed in this integrated Background Report which represents the collective views of the ChemNet Core Group (CCG). The ChemNet members contributing to this report are (in alphabetic order):

Patricia Acero, University of Zaragoza, Spain.
David Arcos, Amphos, Barcelona, Spain.
Luis Auqué, University of Zaragoza, Spain.
Henrik Drake, University of Gothenburg, Sweden.
Lara Duro, Amphos, Barcelona, Spain.
Mel Gascoyne, GGP Inc. Pinawa, Canada.
María Gimeno, University of Zaragoza, Spain.
Thomas Gimmi, University of Bern, Switzerland.
Javier Gómez, University of Zaragoza, Spain.
Ioana Gurban, 3D-Terra, Montreal, Canada.
Lotta Hallbeck, Micro Analytics, Gothenburg, Sweden.
Jorge Molinero, Amphos, Barcelona, Spain.
Ann-Chatrin Nilsson, Geosigma AB, Uppsala, Sweden.
Karsten Pedersen, Microbial Analytics, Gothenburg, Sweden.
John Smellie, Conterra AB, Stockholm, Sweden (CCG).
Eva-Lena Tullborg, Terralogica AB, Gråbo, Sweden (CCG).
Nick Waber, University of Bern, Switzerland.
Bill Wallin, Geokema AB, Sweden (CCG).

Marcus Laaksoharju, ChemNet project leader.

Summary

The overall objectives of the hydrogeochemical description for the Laxemar-Simpevarp area, south-eastern Sweden, are to first establish a detailed understanding of the hydrogeochemical conditions at the site, and to use this understanding to develop models that address the needs identified by the safety assessment group during the site investigation phase /Ström et al. 2008/. Issues of concern to safety assessement are radionuclide transport and technical barrier behaviour, both of which are dependent on the current chemistry of groundwater and matrix porewater and their evolution with time in the future. The specific aims of the hydrogeochemical work were:

- To document the hydrogeochemistry in the Laxemar subarea and the larger Laxemar-Simpevarp area, with focus on the development of conceptual understanding to describe and visualise the sites.
- To provide relevant parameter values to be used for safety assessment calculations.
- To provide the hydrogeochemical basis for the modelling work by other teams, in particular hydrogeology.
- To take account of the feedback from the SR-Can safety assessment work /SKB 2006a/ that bears relevance to the hydrogeochemical modelling work.

The groundwaters have been interpreted in relation to their *composition, origin and evolution*, which require close integration with geological, climatological and hydrogeological information. Past climate changes are among the major driving forces for long term hydrogeochemical changes (hundreds to thousands of years) and are, therefore, of fundamental importance for understanding the palaeohydrogeological, palaeohydrogeochemical and present evolution of groundwater in the Fennoscandian crystalline bedrock.

The SDM-Site Laxemar hydrochemistry modelling has resulted in improved robustness of model versions Laxemar 1.2 and Laxemar 2.1 concerning site understanding. The many consistent temporal and spatial data support the description concerning the groundwater origin, most of the major end members and major hydrochemical processes. Integration with hydrogeology supports the palaeohydrogeological description of the site. Chemical reaction modelling, the use of different isotope ratios (of the elements Sr, S, C, B, Cl, O, H and the U-decay series) and measurements of Eh, pH and microbe population data, support the process understanding. Matrix porewater compositions have now been fairly well established and their compositional variation with depth is determined. Important input from the fracture mineralogical study also supports the palaeohydrogeological and process understanding of the site. Confidence concerning the three-dimensional variability of processes and properties was improved by the addition of new data in previously drilled boreholes and from new boreholes in important key areas.

Hydrogeologically the Laxemar subarea is an area of groundwater recharge and shows classic systematic changes in groundwater chemistry with depth which accompany increasingly lower hydraulic conductivity values and lower groundwater flow rates in the bedrock. Although such changes lead to greater water-rock interactions, the major groundwater feature is that the groundwater composition is mainly a result of transport (mixing), of groundwaters from different origins (deep groundwater, glacial water, Littorina Sea water and meteoric water). The groundwater compositions are, or have been, modified by reactions ranging from fast (e.g. redox reactions catalysed by microorganisms, ion exchange, calcite equilibrium) to long term water-rock reactions such as aluminosilicate equilibrium at depth. Despite these changes, the alkalinity and redox buffer capacity provided by the bedrock and the microbial metabolisms is driven by comparatively fast reactions (hundreds of years). Hence, the pH and Eh variability of the contacting groundwaters are restricted to a narrow and stable range provided that appropriate alkalinity and redox buffer capacities are present.

Post glacial meteoric water dominates in the depth interval between 100 to 150 metres of the bedrock and may be present as decreasing components also at intermediate depth. Only part of the Laxemar subarea was covered by the Littorina Sea water and even this has had limited impact, resulting in a relatively minor influence, especially in the central part and towards the west and north-west. Weak

Littorina signatures are found in groundwaters in boreholes KLX01, KLX10A and KLX15A located to the north-east, east-central and south-central areas respectively at various depths between 200 and 680 m. Clear evidence of glacial water components is commonly present at the approximately 300 to 600 m depth interval, especially in the west and central parts of the area. These waters are usually low in chloride (1,000–2,500 mg/L Cl). Decreasing transmissivity of the deformation zones with depth is reflected in different mixing/reaction environments, and increasing residence times of the groundwater. At depths greater than 1,200 m low flow to effectively stagnant conditions prevail.

Dissolved oxygen is consumed in the shallow, upper part (50 m) of the bedrock, generally resulting in reducing groundwater conditions already at these depths. Redox sensitive species such as iron and manganese are generally present in low concentrations in the deeper groundwaters at Laxemar (less than 1 mg/L Fe^{2+} and 0.5 mg/L Mn^{2+}) compared with the near surface waters (up to 10 mg/L Fe^{2+} and below 2.0 mg/L Mn^{2+}). However, iron- and manganese-reducing bacteria are identified at all depths analysed for microbes. Easily accessible Fe-oxyhydroxides and Mn-oxides on the fracture walls decrease with depth, and the relatively low Eh (–275 mV) measured at shallow depths (~170 m) indicate that the importance of iron- and manganese-reducers in the control of the redox system is most prominent in the very upper part of the bedrock (potentially down to around 100 m). At greater depths, between 170 to 500 m, measured Eh values are well below –200 mV and seem to correlate with the number of sulphate-reducing bacteria. Furthermore, high $\delta^{34}S_{(SO4)}$ values and correspondingly low sulphate contents occur together, which describes the importance of sulphate reduction at depths between 100 m to at least 500 m. At greater depths, less information is available on the redox system with only one measured Eh-value (KLX01:–680 m elevation) and only one section analysed for microbe identification (KLX03:–922 m elevation). Taking into consideration that the system below 600 m is much less dynamic, and thus nutrition may be limited for microbial activity, lower sulphide production is assumed at these depths. Nevertheless, dissolved sulphide has been measured in several borehole sections sampled below 550 m, implying that the redox is less well characterised at these depths.

The measured colloid content decreases with depth which is expected due to the increasing ionic strength which destabilises the colloids, for example, the colloid content is less than 20 µg/L at depths greater than 350 m. The measured gas contents in the groundwaters are 50–110 ml/L and dominated by N_2. The helium and argon contents increase with depth indicating a possible input from deep-seated gas sources.

The major groundwater features are:

- The 0–20 m depth interval is hydrogeologically active (residence times in the order of years to decades) and dominated by modern recharge meteoric water or Fresh groundwater (< 200 mg/L Cl) of Na-Ca-HCO_3 (SO_4) type showing large variations in pH and redox conditions.
- The 20–250 m depth interval is dominated by Fresh–Mixed Brackish–Brackish Glacial groundwaters of Na-Ca-HCO_3 (SO_4) to Na-Ca-Cl-HCO_3 type, showing a transition to stable reducing conditions with increasing depth. The residence times of the groundwaters are in the order of decades to several thousands of years.
- The 250–600 m depth interval is dominated by Brackish Glacial–Brackish Non-marine–Transition groundwaters of Na-Ca-Cl-(HCO_3) type. Redox conditions are reducing and low Eh values (–245 to –303 mV) are typically controlled by the interplay between the iron and especially the sulphur systems. The significant portions of glacial waters in this depth interval, and the equally significant increase of non-marine groundwaters with depth, indicates that groundwaters older than the last deglaciation at around 14,000 years ago are becoming increasingly important.
- The 600–1,200 m depth interval is dominated by Brackish Non-marine–Saline (±Brackish Glacial and Transition) groundwater of Na-Ca Cl-(SO_4) to Ca-Na Cl-(SO_4) type. These groundwaters show very low magnesium values and are clearly reducing (–220 to –265 mV). Interpretation of chlorine-36 measurements suggests long residence times of hundreds of thousands of years, supported hydrogeologically by low flow to near stagnant conditions.
- The pH values are between 7.2 and 8.6 in the groundwaters and do not show any clear variation trend with depth. pH is mainly controlled by calcite dissolution-precipitation reactions and, probably, by microbial activities. Of secondary importance is the influence of other common chemical processes, such as aluminosilicate dissolution-precipitation or cation exchange.

Contents

1 Introduction

1.1 Scope and objectives

The Swedish Nuclear Fuel and Waste Management Company (SKB) has undertaken site characterisation at two different locations, the Laxemar-Simpevarp and Forsmark areas, with the objective of siting a geological repository for spent nuclear fuel. The investigations were conducted in campaigns with periodic 'data freezes', i.e. allocation of specific dates when no further data were incorporated in the database for interpretation and modelling of that specific dataset. After each data freeze, the site data were analysed and site descriptive modelling was carried out with the purpose of developing a Site Descriptive Model (SDM) of the site. An SDM is a synthesis of hydrogeochemistry, geology, rock mechanics, thermal properties, hydrogeology, bedrock transport properties and surface system description.

The overall objectives of the SDM-Site Laxemar hydrogeochemical modelling project were to first establish a detailed understanding of the hydrogeochemical conditions at the site, and to use this understanding to develop models that address the needs identified by the safety assessment groups during the site investigation phase. Issues of concern to safety assessement are radionuclide transport and technical barrier behaviour, both of which are dependent on the chemistry of groundwater and porewater and their likely future evolution with time. The specific aims of the SDM Site Laxemar hydrogeochemical work were:

- To document the hydrogeochemistry in Laxemar and the larger Laxemar-Simpevarp area with focus on the development of conceptual models to describe and visualise the hydrogeochemical situation at the site.
- To provide relevant parameter values to be used in safety assessment calculations.
- To provide the hydrogeochemical basis for the modelling work by other teams, in particular hydrogeology.
- To take account of the feedback from the SR-Can safety assessment work /SKB 2006a/ that bears relevance to the hydrogeochemical modelling work.

The work has involved the development of descriptive and mathematical models for groundwaters in relation to rock domains, fracture domains and deformation zones, and importantly also hydraulic rock and fracture domains. In this report, the groundwaters have been interpreted in relation to their *composition, origin and evolution*, requiring close integration with geological, climatological and hydrogeological information. Past climate changes are one of the major driving forces for long term hydrogeochemical changes (hundreds to thousands of years) and are, therefore, of fundamental importance for understanding the palaeohydrogeological, palaeohydrogeochemical and present evolution of groundwater in the Fennoscandian crystalline bedrock. Despite these changes, the alkalinity and redox buffer capacities of the bedrock are controlled by relatively fast and reversible processes which occur over time scales of hundreds of years. Hence, the pH and Eh variability of the contacting groundwaters are restricted to a narrow and stable range provided that the appropriate alkalinity and redox buffer capacities are present.

This Background Report provides an integrated link between the condensed account of the hydrogeochemical modelling provided in the SDM Level 1 report /SKB 2009/, and the Level 3 reports /Drake and Tullborg 2009a, Hallbeck and Pedersen 2008b, Gimeno et al. 2009, Smellie and Tullborg 2009, Waber et al. 2009, Kalinowski (ed) 2009/ which present full background information and documentation and, in some cases, interpretation of the hydrogeochemical data.

1.2 Methodology

The main task of the hydrochemistry evaluation work is to describe the hydrochemical conditions in and around the rock volume surrounding the repository. The investigations were focused to fulfil various requirements, where one is related to information on features (parameters) used to calculate the long term stability and safety of the disposal. The second requirement includes the understanding

of the chemical conditions, including active processes, and changes and development in the hydrogeochemical situation to the present time (palaeohydrogeochemistry). For example, the first step in the modelling work is to reconstruct the palaeohydrogeochemical model at the site (e.g. Section 2.5).

Understanding the current undisturbed hydrochemical conditions and past hydrogeochemical evolution at the proposed repository site is important when predicting future changes in groundwater chemistry. Such future changes may jeopardise the long term integrity of the currently planned SKB repository system, in particular copper corrosion and/or bentonite degradation. Therefore, the following variables are of particular interest for the hydrogeochemical site descriptive modelling: pH, Eh, sulphur system, iron, manganese, carbonate, phosphate, acetate, nitrogen species, total dissolved solids (TDS), isotopes, colloids, fulvic and humic acids, and microorganisms. In addition, dissolved gases (e.g. carbon dioxide, methane and hydrogen) are of interest because of their likely participation in microbial reactions.

In order to establish hydrogeochemical site understanding the sequence of investigations, evaluations and modelling exercises outlined in Figure 1-1 were initially established as guidelines to the hydrogeochemical programme. Some of the methods are based on expert knowledge, whereas others are based on mathematical modelling. The applied methodology is described in detail by (e.g. /Smellie et al. 2002, Laaksoharju et al. 2008/) and the specific hydrogeochemical methodology used within the SKB site investigation programme is published in a special issue of Applied Geochemistry /Gascoyne and Laaksoharju 2008/.

In brief, the raw chemical data are initially screened to remove any obvious analytical or sampling artefacts based on specified laboratory and field procedures. These screened data are then entered into the SKB Sicada database and subsequently made available in this form for hydrochemical evaluation. The quality of the data is then rigorously assessed with respect to their representativity based on an integrated approach involving hydrochemical, geological and hydrogeological considerations. Specific data judged to be prerequisite for the understanding, interpretation and modelling of the groundwater conditions are then selected, and from these the most suitable samples are identified for different modelling purposes. Examples include field redox potential measurements and analysed Fe(tot) and Fe(II) values for redox modelling of the groundwater system, and major ion and environmental isotope data input to hydrogeological model calibrations.

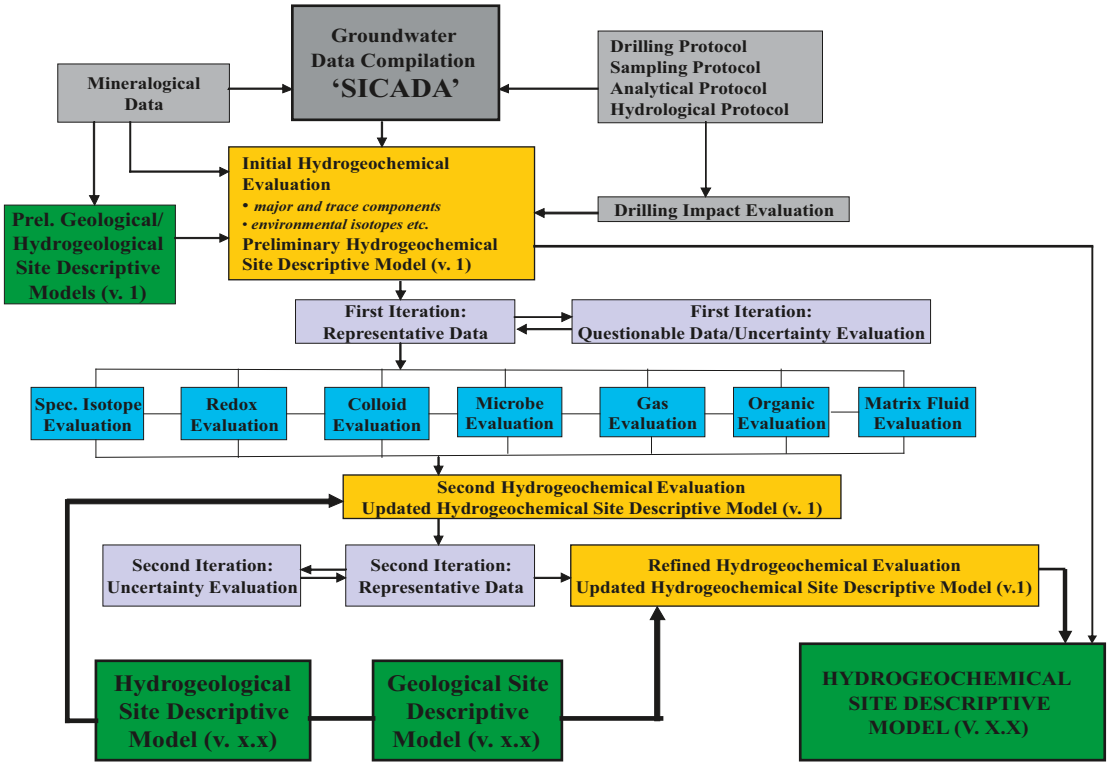

Figure 1-1. *Schematic work flow and modelling steps for the implementation of the hydrochemical modelling /Smellie et al. 2002/.*

The next step is a general examination of the data using traditional geochemical approaches to describe the data and provide an initial insight and understanding of the site, i.e. the construction of a preliminary conceptual model for the area. Based on this hydrochemical framework, selected data are further evaluated using different modelling approaches, for example, geochemical equilibrium modelling, mixing modelling and finally using coupled modelling codes. The results from these modelling exercises are presented as 2D/3D visualisations of the model volume based on the measured constituents from the modelled area. These descriptions are compared and integrated with independent modelled results for the area, for example, the geological and hydrogeological models.

The evaluation stages were repeated after each data freeze when new and modified data became available. Each data freeze represents data collected up to a predetermined date set by SKB, after which no new data are accepted in the site descriptive modelling; this allows all participant groups to share the same dataset. For internal consistency, at each new hydrogeochemical data freeze and modelling stage, the updated datasets are checked against the previous versions to identify anomalous or erroneous data which may require additional sampling and/or analysis to reduce uncertainties and increase reliability. The data freeze is also an important QA control to ensure that all end-users work with the same dataset. Thus, the final hydrogeochemistry site descriptive model of Laxemar as presented and described in this report is the result of an iterative, step by step development during the period of the site investigations, i.e. through modelling stages 1.1 and 1.2 for the Simpevarp subarea /Laaksoharju 2004, SKB 2004/ and the subsequent hydrogeochemical model versions 1.2 and 2.1 /SKB 2006bc/ (no full SDM was produced for model step Laxemar 2.1) for the Laxemar subarea.

The work within the SDM-Site Laxemar hydrogeochemistry modelling further developed the conceptual models and the understanding of the site as presented in earlier model stages. Integration with the hydrogeology, surface system and transport modelling groups was more effective than was previously the case due to the large amount of new interpreted data which brought the hydrogeochemical programme into consistency with the progress of the other groups.

The importance of mineralogy has been underlined in site understanding, for example, as input to the geochemical equilibrium modelling. From a palaeohydrogeological viewpoint, geochemical and mineralogical information from fracture minerals, altered rock and the reference rock matrix has been compiled in /Drake and Tullborg 2009a, Sandström et al. 2008/ where analysis of these data are restricted to the pH and redox buffering capacity of the host rock.

Further to the groundwater hydrochemical studies, detailed investigations of matrix porewaters have been carried out for the first time in a crystalline rock environment. The major findings from the porewater investigations and fracture mineral studies have been integrated into the site description.

Important feedback from SR-Can /SKB 2006a/ and Insite (the international review group established by the authorities) and Sierg (SKB's independent international review group) was integrated into the modelling. The list of critical issues established by the authorities represented important input to the investigations, aiming to improve various aspects of the site descriptive model and site understanding. Of the issues proposed, some were addressed already in /SKB 2006a/, but additional data during model version SDM-Site Laxemar faciliated further modification. The issues addressed at different levels of detail were:

- Eh and pH buffering capacity.
- Interaction between deep and shallow groundwater systems.
- Alternative models, uncertainties and data bias.
- Confirming site scale models in relation to groundwater flow system.
- Geochemical and isotopic data for palaeohydrogeology and groundwater evolution.
- Mineralogical and petrographical characterisation of fracture and matrix minerals.
- Groundwater compositions at repository depth.
- Spatial variability of hydrochemical data.
- Characterisation of colloidal, organic, microbial and gaseous species in groundwaters.
- Data from pre-existing boreholes in and near the sites.
- Geochemical analogues of safety-related radionuclides.

Details of the hydrogeochemistry work have been addressed and reported in /Drake and Tullborg 2009b, Hallbeck and Pedersen 2008b, Gimeno et al. 2009, Smellie and Tullborg 2009, Waber et al. 2009, Kalinowski 2009/. The sampling at Laxemar was often complex which led to some problems with sample quality; this is documented in detail in /Bergelin et al. 2009/.

1.3 Nomenclature and processes

The nomenclature and processes described in this section are important to understanding the various concepts used in this report.

The sample coding used in this report:

- A specific sample from a single borehole is prefixed by the borehole number followed by the elevation in metres, i.e. 'KLX02:–455 m elevation'. This coordinate refers to the mid point of the corresponding packed-off section in the borehole.
- A specific vertical depth interval is labelled as '–404 to –420 m elevation'.
- An approximate vertical depth or depth interval is labelled 'about or approximately 500 m depth' or 'about or approximately 500 to 700 m depth'.
- Any location related to borehole length is signified specially as '432 m borehole length' in the text (i.e. KLX02:432 m borehole length), or generally as 'about or approximately 500 to 700 m borehole length'.
- Repository depth refers to '–400 to –700 m elevation'.

The nomenclature of the groundwater types used depends on the purpose of the modelling and a distinction can be made between the following.

1) *Current groundwater types*, i.e. these are the types that are now used to distinguish different waters as sampled and analysed *in situ* today. The nomenclature of these present water types is related to the perceived main origin of these waters (i.e. meteoric, Littorina, glacial meltwaters etc.) but their compositions have subsequently been altered by mixing and reactions.

2) *Origins of current groundwater types*. This relates to the chemical composition of the real groundwater end members, i.e. the 'actual' precipitation, the 'real' glacial meltwater, the 'best estimate' Littorina Sea water, etc. 'End member' therefore refers to a modern or older water type which constitutes an important component to the presently measured groundwaters in the Laxemar-Simpevarp area. The end-member compositions identified and used for the site modelling are listed in Table 1-1 and their influence on the groundwater composition is based on the palaeohydrochemical conceptual model. The compositions of the end members are based on measured and modelled values and are described in detail by /Gurban 2009, Gimeno et al. 2009/.

The description of the current groundwater types in the Laxemar (and Simpevarp) subarea is based on the salinity content of the water (e.g. Fresh, Brackish, Saline and Highly Saline). Brackish waters may be subdivided into Brackish Glacial, Brackish Marine and Brackish Non-marine, mainly based on $\delta^{18}O$ and marine indicators such as magnesium and chloride-bromide ratios. As a consequence, the same water type can be described in some samples as, for example, Brackish Glacial or a mixture of Glacial and Brackish Non-marine with subordinate Littorina water.

The names of the water types used in the different evaluations and modelling activities based on /Smellie et al. 2008/ and documented in /Gimeno et al. 2009, Gurban 2009, Molinero 2009, Hallbeck and Pedersen 2009/ are as follows:

1) **Palaeohydrogeochemical description:** Highly Saline, Old Meteoric ± Old Glacial, Last Deglaciation, Littorina and Present Meteoric.

(Note: '± Old Glacial' means that the Old Meteoric water may or may not contain an Old Glacial component; Last deglaciation means 'final stage of the last phase of ice sheet coverage').

2) **Mixing end members (M3) modelling:** Deep Saline, Glacial, Littorina and Altered Meteoric. (Note: 'Old Meteoric + Glacial' was tested as a modelling alternative at an early stage by /Gurban 2009/).

3) **Site descriptive model:** Highly saline, Saline, Brackish Marine, Brackish Non-marine, Transition (mixture between marine and non-marine water), Brackish Glacial, Mixed Brackish and Fresh.

To understand, interpret and conceptualise the groundwater evolution, the following issues need to be considered.

1) **The 'original' composition of the water present in the bedrock:** This is essentially unknown, but evidence from fracture groundwaters and rock matrix porewaters indicates that resident groundwaters prior to the last deglaciation were a mixture of old meteoric ± old glacial and saline in type as a function of depth. Note that the uncertainty in recognising groundwater components older than the last deglaciation increases considerably with age, (cf /Laaksoharju et al. 2008a, Smellie et al. 2008/).

2) **Effects of the last deglaciation:** Includes incursion of glacial meltwater.

3) **Introduction of more recent groundwater types (post glacial):** Because the studied site is situated close to the Baltic Sea coast, it is evident that both fresh meteoric water and brackish marine sea waters of different salinities may have played important roles. Fresh meteoric waters from very different climates (e.g. ranging from temperate to cold) may also have been recharged repeatedly.

4) **Factors influencing groundwater flow that largely determine the resulting groundwater chemistry:** These include topography, bedrock hydraulic conductivity, interconnection of different fractures and fracture networks, density differences and potential glacial loading and unloading.

5) **The reactions taking place in the soil cover and bedrock which modify the original signature of the recharge water:** Examples are redox reactions mostly mediated by microbial activity involving oxygen consumption, and reactions with manganese, iron, sulphide and carbon. In addition, water-rock reactions such as ion exchange, calcite dissolution/precipitation, and silicate weathering will have occurred, together with mixing and also diffusion (e.g. exchange with matrix porewater).

Table 1-1. End-member compositions used for the SDM-Site Laxemar site descriptive hydrogeochemistry modelling.

Parameter	Deep Saline	Littorina	Glacial	Old Meteoric + Glacial**	Altered Meteoric Laxemar #10231
pH (units)	8	7.6	–	–	8.17
Alkalinity(mg/L)	14.1	92.5	0.12	0.12	265.0
Cl (mg/L)	47,200	6,500	0.5	0.5	23.0
SO_4^{2-}(mg/L)	906.0	890	0.5	0.5	35.8
Br (mg/L)	323.66	22.2	–	–	–
Ca (mg/L)	19,300	151	0.18	0.18	11.2
Mg (mg/L)	2.12	448	0.1	0.1	3.6
Na (mg/L)	8,500	3,674	0.17	0.17	110.0
K (mg/L)	45.5	134	0.4	0.4	3.0
Si (mg/L)	2.9	3.94	–	–	7.0
δ^2H (‰ VSMOW*)	–44.9	–37.8	–158.0	–118	–76.5
δ^{18}O (‰ VSMOW*)	–8.9	–4.7	–21.0	–16.0	–10.9

*Vienna Standard Mean Ocean Water

** Tested as a modelling alternative at an early stage /Gurban 2009/

– No data available

1.4 Abbreviations

Symbols, subscripts, and abbreviations used in this report are listed and explained in Table 1-2 below. These are provided to simplify reference in the text to special names, chemical and physical parameters, elements, compounds, isotopes and biochemical compounds.

Stable isotope ratios ($^{2}H/^{1}H$, $^{11}B/^{10}B$, $^{13}C/^{12}C$, $^{18}O/^{16}O$, $^{37}Cl/^{35}Cl$ and $^{34}S/^{32}S$) are referenced to a standard (e.g. VSMOW, PDB or CDT) and expressed in per mil (‰) deviations (δ values) from the appropriate standard where δ is defined as:

$$\delta = [\ (R_{sample}/R_{standard}) - 1\ ] \times 1{,}000$$

and R is e.g. $^{18}O/^{16}O$.

Table 1-2. Explanation of symbols, subscripts and abbreviations used in this report.

Symbol/abbreviation	Description
^{40}Ar	Radiogen isotope formed from ^{40}K.
^{39}Ar	Isotope formed as a result of induced neutron activation of ^{39}K
ATP	Adenosine-Tri-Phosphate
AA	Autotrophic Acetogenic bacteria
HA	Heterotrophic Acetogenic bacteria
AM	Autotrophic Methanogen bacteria
HM	Heterotrophic Methanogen bacteria
AOM	Anaerobic Oxidation of Methane
$^{11}B/^{10}B$	Ratio for boron isotopes
pCO_2	Partial pressure of carbon dioxide
CCC	Complete Chemical Characterisation
CDT	Cañon Diablo Troilite (Standard used for $\delta^{34}S$)
CHAB	Cultivable Heterotrophic Aerobic Bacteria
Cond.	Electric conductivity (field)
^{12}C	Light stable carbon isotope
^{13}C	Heavy stable carbon isotope
^{14}C	Radioactive carbon isotope (half-life 5,730 ± 40 years)
$^{14}C_{(TIC)}$	Carbon-14 concentration in total inorganic carbon
pmC	Percent modern carbon
^{35}Cl	Light stable isotope of chlorine
^{37}Cl	Stable isotope of chlorine
^{36}Cl	Radioactive isotope of chlorine (half-life = 301,000 years)
Deuterium	(^{2}H) The heavy stable isotope for hydrogen
DIC	Dissolved Inorganic Carbon
DOC	Dissolved Organic Carbon
EDX	Energy-Dispersive X-ray analysis
ESD	Energy-Dispersive spectroscopy
Eh	Redox potential (usually expressed in mV)
Fe(II)	Ferrous iron
Fe(III)	Ferric iron
FSM	Fracture domain Simpevarp model
GMWL	Global Meteoric Water Line
^{4}He	Helium-4 (heavy isotope of helium)
^{1}H	Hydrogen (stable isotope)
^{2}H	Deuterium (heavy stable isotope of hydrogen)
^{3}H	Tritium (radioactive hydrogen isotope, half-life = 12.43 years)
HCO_3^-	Bicarbonate
HRD	Hydraulic Rock Domain
HREE	Heavy Rare Earth Elements
HRL	(Äspö) Hard Rock Laboratory

IRB	Iron-Reducing Bacteria
^{39}K	Decay of argon, half-life ^{39}Ar = 269 y
^{40}K	Half-life = 1.3 Ga
Last deglaciation	Last phase of the ice sheet coverage
LIBD	Laser-induced Breakdown Detection
LREE	Light Rare Earth Elements
M3	Program for calculation of groundwater mixing proportions
m.a.s.l	Metres above sea level
MPN	Most Probable Number
MRB	Manganese-Reducing Bacteria
NASC	North American Shale Composite
NRB	Nitrate-Reducing Bacteria
^{16}O	Light stable isotope of oxygen
^{18}O	Heavy stable isotope of oxygen
PHREEQC	A Computer Program for Speciation, Batch-Reaction, One-Dimensional Transport, and Inverse Geochemical Calculations
PDB	Standard according to Pee Dee *Belemnitella* Formation (used for ^{13}C as well as for ^{18}O, especially for carbonates)
PLU	Platsundersökning
PmC	Percent modern carbon
PVB	Pressure Vacuum Beaker
^{87}Rb	Half-life = 48 Ga
REEs	Rare Earth Elements (La, Ce, Pr, Nd, Sm, Eu, Gd, Tb, Dy, Ho, Er, Tm, Yb and Lu)
Radioactive isotopes	Radioactive isotopes decay and produce isotopes (daughters) that can be either stable (radiogenic isotopes; see below) or radioactive (e.g. decay chains like the U-series). The decay rate for a specific isotope is constant and usually expressed as half-life
Radiogenic isotopes	Radiogenic isotopes are stable but formed by radioactive decay
RSM	Rock domain Simpevarp Model
^{87}Sr	Radiogenic strontium isotope, produced by decay of ^{87}Rb
^{86}Sr	Stable isotope of strontium
SDM	Site Descriptive Model
SEM	Scanning Electron Microscope
^{32}S	Light stable isotope of sulphur
^{34}S	Stable isotope of sulphur
$\delta^{34}S_{(SO4)}$	Stable sulphur isotope ratio in dissolved sulphate
SMOC	Standard Mean Ocean Chloride
SRB	Sulphate-Reducing Bacteria
TIC	Total Inorganic Carbon
TNC	Total Number of Cells
Tritium	Radioactive hydrogen isotope (^{3}H) half-life = 12.43 years
TU	Tritium Units
TDS	Total Dissolved Solids
USD	Uranium-Series Decay analyses
VSMOW	Vienna Standard Mean Ocean Water (Standard used for $^{18}O/^{16}O$ and $^{2}H/^{1}H$ ratios)

1.5 Conceptual mixing and reactions

The hydrogeochemical evolution of fracture groundwater results from advective mixing and water-rock interactions driven by past and present changes in the climate as evidenced by the extensive site investigations in, among other countries, Sweden and Finland (e.g. /Laaksoharju and Wallin 1997, Laaksoharju et al. 1999, Pitkänen et al. 1999/). Many of the evaluation and modelling steps used in the current site descriptive modelling are focused on differentiating these effects by using different modelling approaches such as mixing, reactions and transport modelling /Laaksoharju et al. 2008b/.

For modelling purposes, different approaches can be used leading to quite different descriptions of the system. For example, when applying end-member mixing models, the choices of end members

are crucial for the description of both mixing and reactions. This does not necessarily mean that some models are correct and some models are not. It is more a question of choosing the most suitable model available for describing the part of the system that is to be addressed, and also to focus on the time period of interest. All epochs and all parts of the system can never be described with high resolution using the same model; usually several models are required as well as different sets of end members and starting prerequisites.

Figure 1-2a-d illustrates the different approaches to model groundwater mixing and reactions, using sodium versus chloride as an example. The sodium content in groundwater can be altered by, for example, feldspar weathering or cation exchange, but chloride is regarded as a water conservative tracer not affected by reactions. The task is to model the reactions that have caused the measured sodium content. In Model 1 (Figure 1-2b), the water composition is the result of reactions, for example, the sample with about 0.85 mol/kg Cl, indicated with the arrow, has gained about 0.28 mol/kg Na due to reactions. There is no flux or mixing in the system since the system is closed. In Model 2 (Figure 1-2c) the water composition is the result of mixing of two end members (indicated with the dashed black line); here the sample has gained about 0.07 mol/kg Na. The water composition is described mainly as a result of two-component mixing with some gain of sodium by reactions. In Model 3 (Figure 1-2d) the water composition is described almost exclusively as the result of mixing of several end members. Here, the sample has not gained any sodium, since it plots on, or close to, the mixing line (black dashed line). The water composition is described as the result of multi-component mixing and the sodium content is the result of pure mixing/transport. Plots above the mixing line indicate a gain of sodium, whereas plots below the mixing line indicate a loss of sodium.

The example given above clearly shows that the description of the groundwater system depends on the model selected. Model 1 describes the total amount of reactions taking place to obtain the sodium content measured in the sample. However, it does not describe where and when the reactions took place.

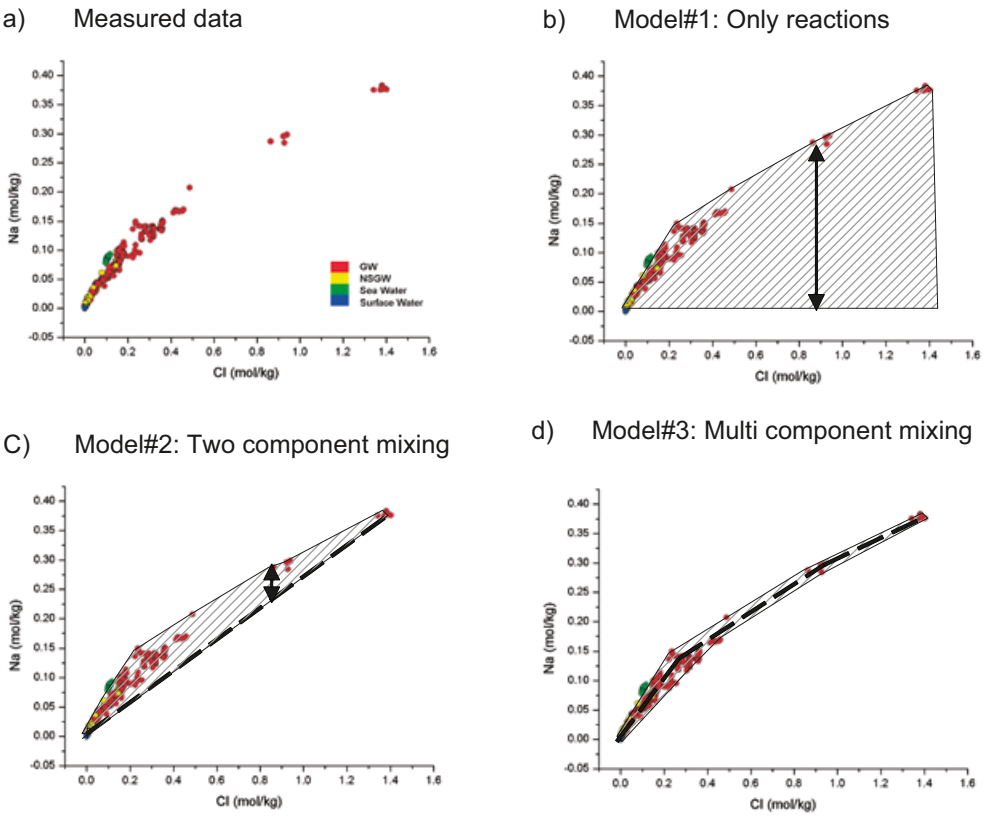

Figure 1-2. *Schematic presentation of how different models are used to describe the processes behind the measured Na content. The arrows indicate the amount of reactions taking place for a particular sample, the grey shaded area indicates samples affected by reactions and the black dashed line indicates the mixing line: a) Measured Na versus Cl, b) Model based on reactions, c) Model based on a mixture of two end members and, d) model based on several end members /Laaksoharju et al. 2008b/.*

Models 2 and 3 describe the water composition in relation to the end-member composition. Hence, these models can be used to calculate the mixing proportions of the end members. This, in turn, can be used not only to indicate the origin, but also to indicate the range of possible residence time in the bedrock. This is useful information when, for example, integrating the results with the hydrogeological modelling. Models 2 and 3 do not describe the evolution of the end-member composition, but assume that the processes responsible for this composition are implicitly considered (including all the reactions that ever took place).

It is generally a relatively easy task to construct Model 2, but with the risk that the system is oversimplified such that the effects from reactions are overestimated and the effects from transport underestimated. Model 3 can provide realistic descriptions of conservative and non-conservative compounds, but model uncertainties (such as uncertain end-member compositions and mathematical uncertainties in the model applied) can still lead to an erroneous conclusion concerning the gain/losses of element concentrations. The accuracy of Models 2 and 3 can be tested by, for example, plotting the model-predicted Cl and $\delta^{18}O$ contents versus the measured ones. The deviation from a perfect correlation will then indicate the model uncertainties /Laaksoharju 1999/. The uncertainties in the modelling are discussed in Section 4.14 and in /Laaksoharju et al. 2008a/ and /Gimeno et al. 2009/.

The importance of mixing becomes apparent under the following circumstances.

1. The palaeo- and present climate has a huge impact on the hydrogeology and, hence, on hydrochemistry in Fennoscandia /Laaksoharju et al. 2008b/. This facilitates different water types (i.e. glacial, sea water and meteoric water) to enter or to be flushed out from the bedrock.
2. The temperature in the rock is relatively low (at –200 m elevation = 11°C; the gradient is 1.6°C per 100 m) and therefore most water-rock interaction processes are slow.
3. Where groundwater flow is faster and more dominating than reaction times (i.e. for highly transmissive conditions), the origin of the water may still be distinguished.

The significance of reactions becomes apparent, particularly with respect to: a) redox conditions where microbiologically mediated reactions are rapid, and b) pH and alkalinity values buffered by kinetically fast calcite precipitation/dissolution reactions /Smellie et al. 2008, Gimeno et al. 2008, 2009/.

The exact quantification of the contribution from reactions versus mixing is complex, and at best semi-quantitative at the site scale. This requires different modelling approaches ranging from explorative analyses, mass-balance calculations, mixing calculations and coupled reactive transport modelling (e.g. /Gimeno et al. 2009/). The extensive testing of optimum models for mixing calculations /Gimeno et al. 2009/ has shown that indications of mixing contra reactions can be achieved by simplifying the system by using less end members and hence being able to use water conservative elements as tracers in the M3 model quantitatively (cf Section 4.2.2 and /Gimeno et al. 2009/).

2 Previous model versions and input from other disciplines

2.1 Previous conceptual model

Hydrogeochemical model versions 1.1 and 1.2 for the Simpevarp subarea /Laaksoharju et al. 2004, Laaksoharju 2004/ and subsequent hydrogeochemical model versions 1.2 and 2.1 for the Laxemar subarea, are reported in /SKB 2006ab/. No full SDM was produced for model step Laxemar 2.1 but it included feedback from the SR-Can study and Insite/Sierg reviews. Preliminary work based on data freezes Laxemar 2.2 and Laxemar 2.3 (August 31st, 2007), and partial information from the extended hydrogeochemical data freeze Laxemar 2.3 (November 30th, 2007), was carried out during 2007 and resulted in an updated category assessment of the analytical data delivered in early February, 2008.

The earlier Laxemar hydrogeochemical model versions 1.2 and 2.1 /SKB 2006ab/ concluded that the complex groundwater evolution and patterns observed in the Laxemar-Simpevarp regional area were a result of many integrated factors such as: a) the present day topography and proximity to the Baltic Sea, b) past changes in hydrogeology related to glaciation/deglaciation, land uplift and repeated marine/lake water regressions/transgressions, excluding the western part of the Laxemar subarea which was never completely submerged because of higher topography, and c) organic or inorganic alteration of the groundwater composition caused by water-rock interactions and microbial processes. The chemistry of the sampled groundwaters reflects to various degrees processes related to modern and ancient water/rock interactions and mixing.

The groundwater flow regimes in the Laxemar-Simpevarp regional area were considered local and believed to extend down to depths of approximately 600 to 1,000 m depending on local topography. Close to the Baltic Sea coastline in the Simpevarp subarea, where topographical variation is small, groundwater flow penetration to depth will be less marked. In contrast, the Laxemar subarea is characterised by higher topography resulting in a much more dynamic groundwater circulation which appears to extend to at least 500 to 600 m depth in most boreholes. The marked differences in the groundwater flow regimes between the Laxemar and Simpevarp subareas are reflected in the groundwater chemistry were four major hydrochemical groups of groundwaters (types A–D) have been identified /SKB 2006b/:

TYPE A: Present at shallow depths (< 200 m) at the Simpevarp subarea but deeper (to about 800 m) at the Laxemar subarea. Groundwaters are of low salinity, i.e. fresh to brackish in type (< 2,000 mg/L Cl; 0.5–3.5 g/L TDS) with $\delta^{18}O$ = –11 to –8‰ VSMOW, mainly meteoric and Na-HCO_3 in type.

TYPE B: Present at shallow to intermediate depths (150 to 600 m) at the Simpevarp subarea but deeper (about 500–950 m) at the Laxemar subarea. Groundwaters are brackish (2,000–10,000 mg/L Cl; 3.5–18.5 g/L TDS) with $\delta^{18}O$ = –14 to –11‰ VSMOW. Comprise: a) meteoric, mainly Na-Ca-Cl in type including non-marine glacial/deeper saline components, and b) meteoric, mainly Na-Ca-Cl in type but including marine Na-Ca(Mg)-Cl(Br) types (e.g. Littorina) and also glacial/deeper saline components.

TYPE C: Present at intermediate to greater depths (600 to 1,200 m) at the Simpevarp subarea but at even greater depths (900–1,200 m) at the Laxemar subarea. Groundwaters are saline (10,000 to 20,000 mg/L Cl; 18.5 to 30 g/L TDS) with $\delta^{18}O$ = ~ –13‰ VSMOW. They are dominantly Ca-Na-Cl in type at the Laxemar subarea but Na-Ca-Cl changing to Ca-Na-Cl only at the highest salinity levels at the Simpevarp subarea. Increasingly enhanced Br/Cl ratios and SO_4^{2-} contents with depth are observed at both the Simpevarp and Laxemar subareas, and components of glacial/deeper saline mixtures are often present.

TYPE D: Present at greatest depths (> 1,200 m) only at the Laxemar subarea. Groundwaters are highly saline (> 20,000 mg/L Cl; to a maximum of ~70 g/L TDS) with $\delta^{18}O$ = > –10‰ VSMOW. They are dominantly Ca-Na-Cl with high Br/Cl ratios and the stable isotope composition deviates from the GMWL when compared to Type C groundwaters. Mainly comprise a mixture of deep saline and brine groundwaters with diffusion being the dominant mixing process.

In /SKB 2006b/ the Laxemar 2.1 models and site understanding were consolidated. The models were updated and further understanding achieved concerning the spatial variability, origin, evolution and major reactions of the groundwaters, the microbial contents and their depth variation, and the contents of colloids and gases. In addition, porewater composition and its interaction with fracture groundwaters was further quantified and uncertainties in the mixing calculations identified (cf Section 4.2 and /SKB 2006b, Appendix 7/). Furthermore, studies of fracture fillings and especially the isotopic signatures in calcite have supported the conceptual understanding of the Laxemar subarea (cf Section 2.2.5 and Section 4.8 and /SKB 2006b, Appendix 1 therein/), and the detailed mineral investigations were used as direct input to the hydrogeochemical modelling /SKB 2006b/.

2.2 Geology model input

A fundamental understanding of the geology including the rock domains, fracture domains and deformations zones are important for the characterisation and interpretation of the hydrogeochemistry. The different water types identified in the bedrock display a complex mixing pattern governed by the palaeo and present hydrogeology and the structural geology in combination with water-rock interaction with dissolution and precipitation of minerals. All these processes and the character of the geology will affect the groundwater composition and over a long time period the chemical composition of the rock and fracture minerals will leave its distinguishing imprint in the groundwater. This is specifically observed in the diluted waters and the recharge waters in the upper part of the bedrock. Therefore, in order to get an overview of the geological situation at Laxemar the geological model is briefly described in this section.

The geology of the Laxemar subarea has been described in /Wahlgren et al. 2008/ and the bedrock evolution from the Palaeoproterozoic through to the Quaternary is described in /Söderbäck 2008/. Furthermore, the interplay between, for example, structural geological and hydrogeological features within the Laxemar subarea has been addressed in /Rhén et al. 2009/.

The Laxemar-Simpevarp area is located close to the proximity of the Baltic Sea coast some 30 km north of Oskarshamn (Figure 2-1). The bedrock in the area forms part of the ca 1.8 Ga generation of the Transscandinavian Igneous Belt (TIB) of Precambrian basement rocks. It is dominated by the so-called Ävrö granite, a collective name for reddish grey to greyish red, porphyritic rocks ranging in composition from granite to quartz monzodiorite, and equigranular, grey, medium-grained quartz monzodiorite. In the Laxemar area, an area/volume has been distinguished which is dominated by Ävrö quartz monzodiorite (Figure 2-2), i.e. a quartz poor variety of the Ävrö granite. Along the south-eastern part of the Laxemar subarea and at the Simpevarp peninsula, a grey, fine-grained dioritoid occurs. It is compositionally similar to the quartz monzodiorite and is inferred to constitute a high-level intrusion. A thin belt of this rock type is also identified in the central part of Ävrö island. Small amounts of aplitic (named fine-grained granite) and dioritic and gabbroic rock types also occur sporadically in smaller bodies. In particular, smaller bodies of diorite/gabbro are common in the Ävrö quartz monzodiorite, along the contact to the equigranular quartz monzodiorite, in the Laxemar subarea.

Transecting all above-named rock types are dykes characterised by fine- to medium-grained granite and pegmatites. In addition, N-S trending dolerite dykes have been identified along the western margin in the Laxemar subarea.

A characteristic feature of the region is magma mingling and mixing relationships between the different rock types. Geochemically, the most common rocks display similar and overlapping compositional variations such that the most important criteria employed in distinguishing between these rock types are texture and grain size. All rock types in the Laxemar subarea, and the larger Laxemar-Simpevarp area, display low contents of uranium (< 6 ppm), except for pegmatite in which the uranium content locally exceeds 16 ppm.

From a structural point of view, the bedrock at Laxemar is dominated by well-preserved intrusive rocks. However, a faint to weak foliation, which is not uniformly distributed in the bedrock, is present. The orientation of this foliation in the Laxemar local model volume is inferred to define an irregular anti-formal configuration with a sub-horizontal to gently west plunging fold axis /Wahlgren et al. 2008/.

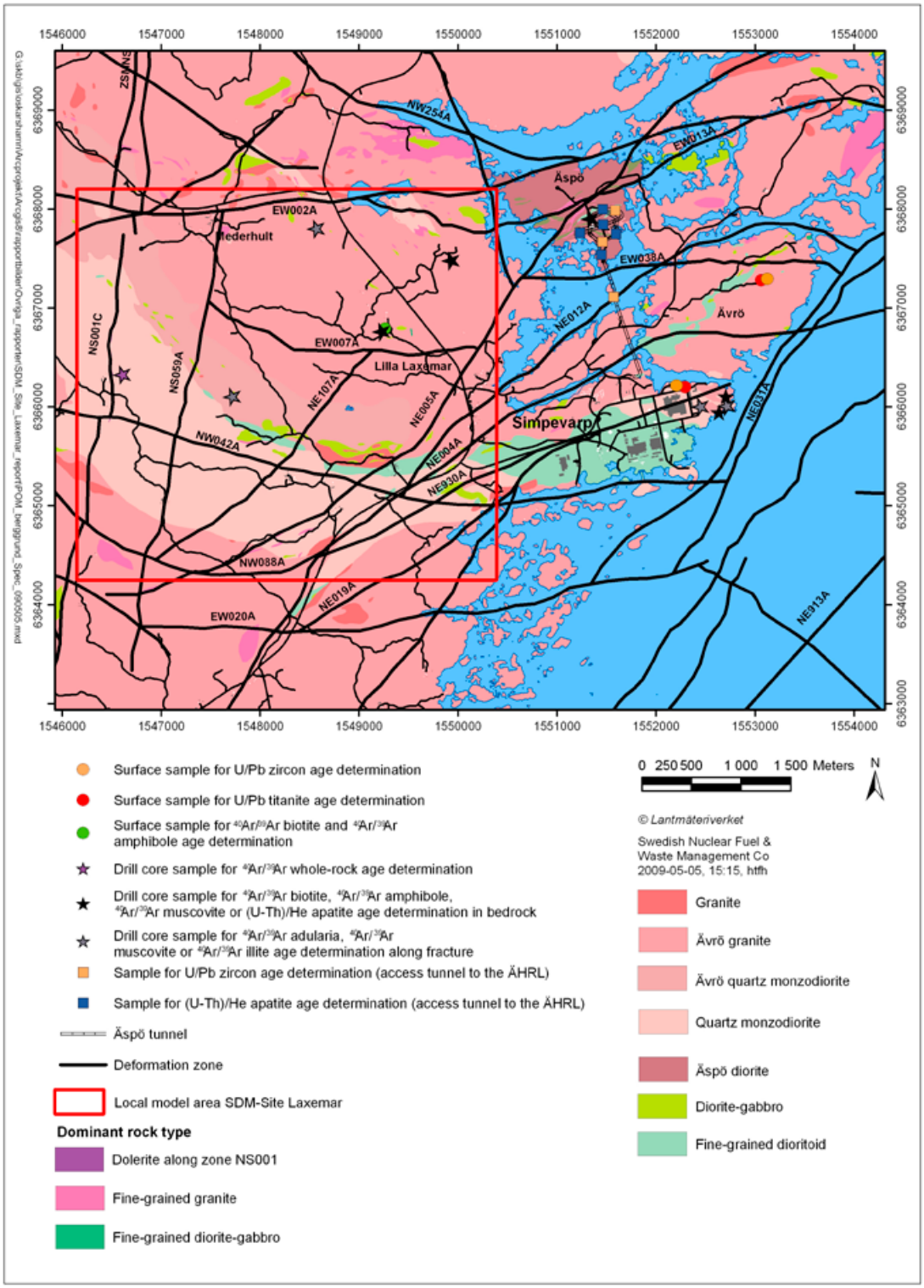

Figure 2-1. *Map showing the bedrock geology at the surface in the Laxemar-Simpevarp area.*

All rock-types have also been subjected to alteration (red staining caused by disseminated microcrystalline hematite, cf Section 2.2.5) largely due to post crystallisation penetration of hydrothermal fluids along pre-existing zones of weakness (e.g. fractures).

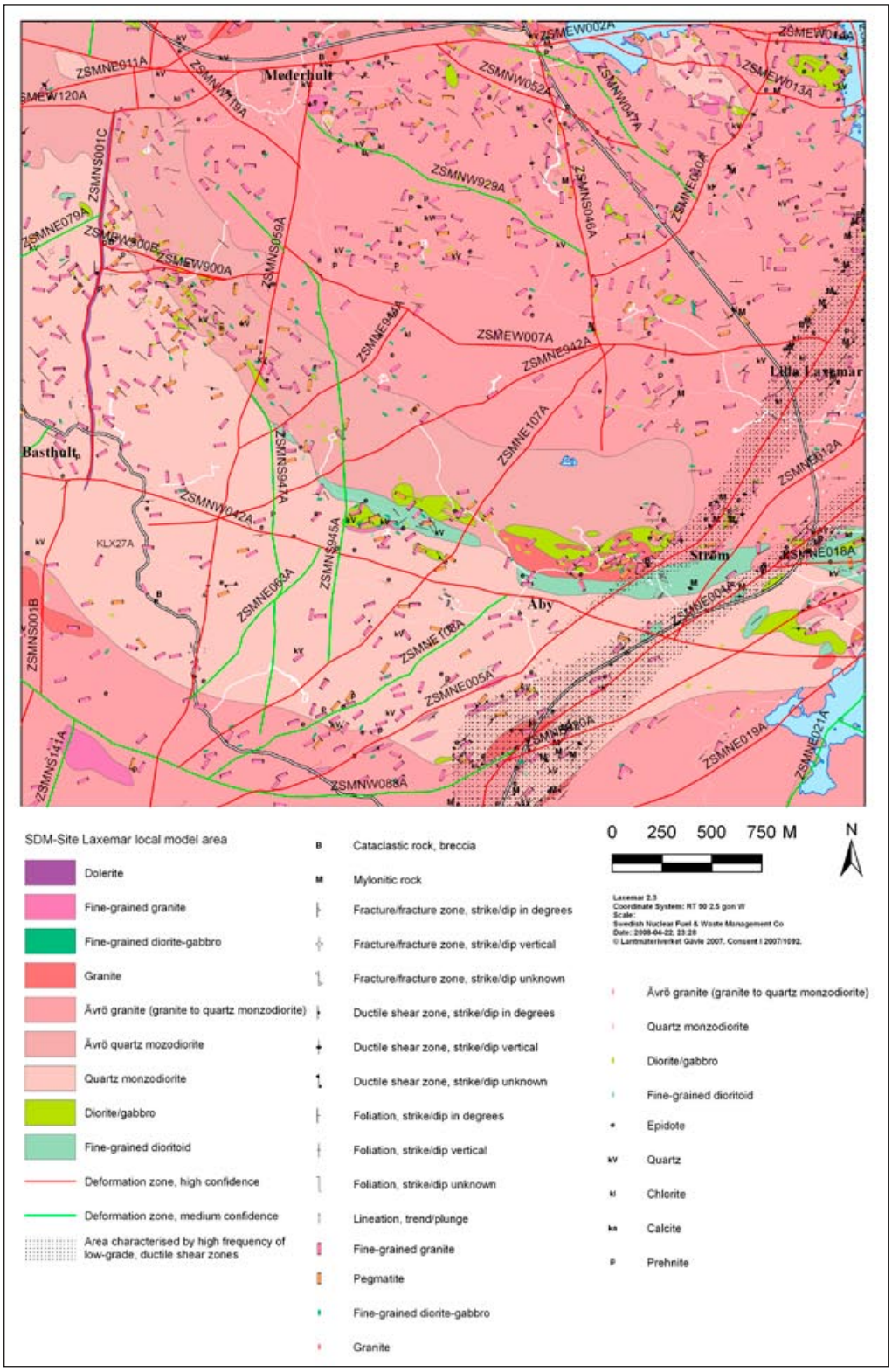

***Figure 2-2**. The bedrock geology of the Laxemar local model area /Wahlgren et al. 2008/.*

2.2.1 Rock domains

Rock domains refer to rock volumes where the bedrock shows similar composition, grain size, degree of bedrock homogeneity, and degree and style of ductile deformation. The dominant rock types at Laxemar are the porphyritic Ävrö granite and Ävrö quartz monzodiorite, and the equigranular quartz monzodiorite. The division into rock domains comprised two working stages, namely: a) definition of rock domains at the surface, and b) definition of rock domains in the cored boreholes. Based on the character of the rock types, nine different rock domains (RSM) are identified in the Laxemar-Simpevarp area, as listed below.

The rock domains have been designated with different codes; 1) RSM**A**-domain (Ävrö granite), 2) RSM**B**-domain (fine-grained dioritoid), 3) RSM**A01**-domain (mixture of Ävrö granite and fine-grained dioritoid), 4) RSM**C**-domain (mixture of Ävrö granite and quartz monzodiorite), 5) RSM**D**-domain (quartz monzodiorite), 6) RSM**E**-domain (diorite/gabbro), 7) RSM**G**-domain (Götemar type granite), 8) RSM**M**-domain (high frequency of minor bodies to small enclaves of diorite/gabbro in particularly Ävrö quartz monzodiorite), and 9) RSM**P**-domain (high frequency of low-grade ductile shear zones in the above mentioned rock types).

The three major domains are characterised as follows. The RSM**BA**-domain, Ävrö granite, is dominating in the northern and eastern area (named A01, rose colour in Figure 2-3 and in inserted block model in Figure 2-4) intersected by NE-SW striking ductile deformation zones (P-domain). The Ävrö granite is the dominant rock type in the RSMA01 domain and, if all boreholes are considered, it constitutes around 82% of the volume.

South of the Ävrö granite is the RSM**M01**-domain constituting a 'crest-type feature' in a NW-SE striking orientation; this is dominated by Ävrö quartz monzodiorite with abundant diorite/gabbro (i.e. denoted as M01 and green in colour in Figure 2-3). The RSMM01 domain is characterised by a much higher proportion of diorite/gabbro (mean value around 16%) than in the other rock domains. Further south is the RSM**D**-domain dominated by quartz monzodiorite striking in an E-W direction and dipping towards the north as seen in Figure 2-4 (denoted D01 and light rose in colour). The narrow RSMB-domains (B05 and B06 in Figure 2-3) between the RSMM01- and RSMD01-domains are characterised and dominated by fine-grained dioritoid.

2.2.2 Deformation zones

Deformation zones refer to parts of the bedrock along which there is a concentration of strain and damage. The deterministic deformation zones (of size > 1,000m) interpreted in Laxemar can be correlated from surface lineament expressions and from geological single-hole interpretation; the strike of the deformation zone is assumed to be the same as the trend of the matching lineament. The dip inferred from the borehole intercept is interpreted as the average dip angle of the deformation zone along its entire extent. Deformation zones observed only at the surface, which lack information on their subsurface extents and geometry, are assumed to be vertical. Furthermore, a limited number of deterministic deformation zones are interpreted solely on the basis of borehole intercepts and interpreted true thickness. Fractures and deformation zones of size < 1,000 m are described stochastically as part of the geological DFN model (cf Section 2.2.3).

The steeply dipping deformation zones are assumed to truncate, along their strike direction, other deformation zones as indicated by the lineament map. Gently dipping deformation zones have been detected by an integration of data from single boreholes together with the interpretation of seismic reflectors.

An overview of the deformation zones and rock domains modelled deterministically in the Laxemar-Simpevarp regional model area is presented in Figure 2-5. This is to provide an overview of the modelled deformation zones and a better understanding of the structural geological model.

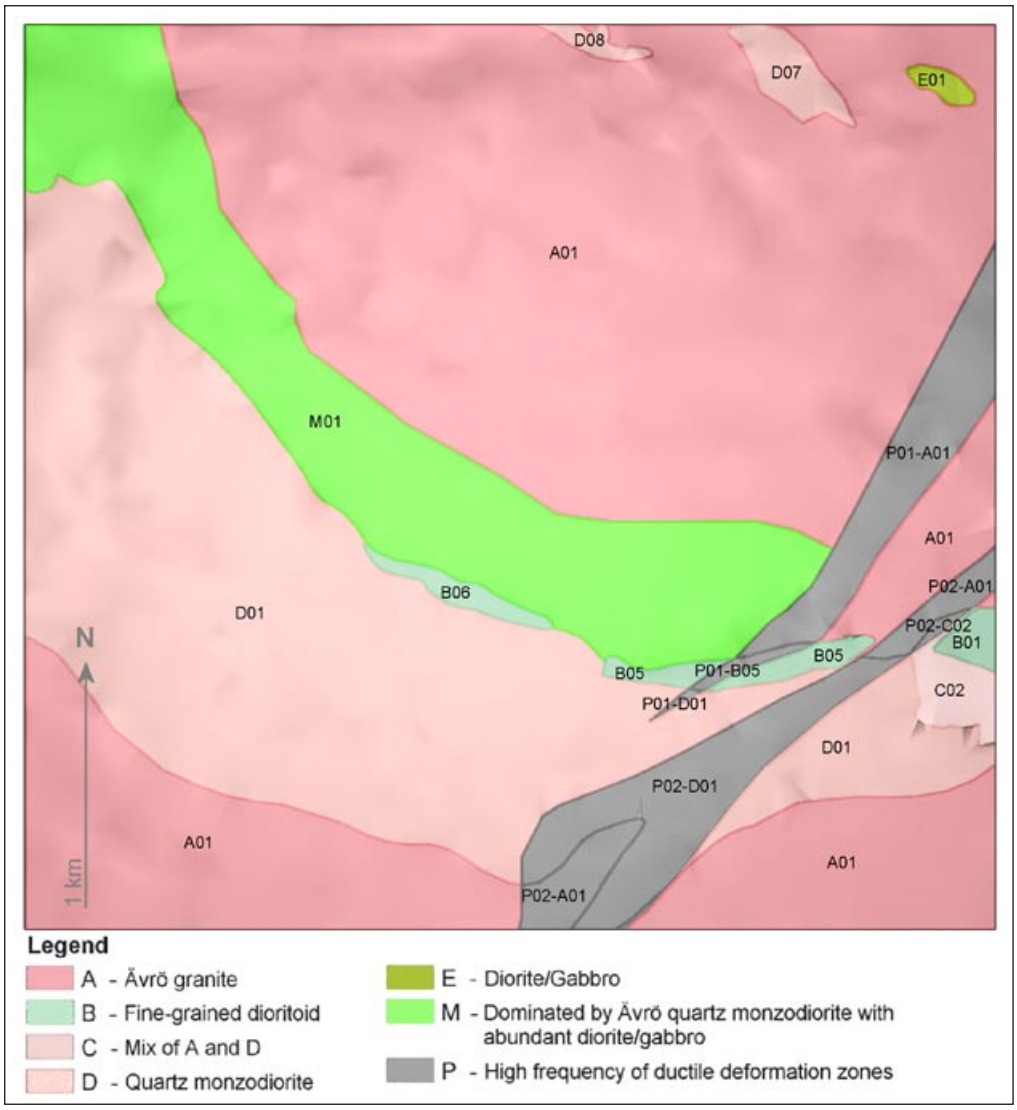

Figure 2-3. *Two dimensional model at the surface for rock domains in the Laxemar local model area (compare with Figure 2-1) /Wahlgren et al. 2008/. For reasons of simplicity, the prefix RSM has been excluded in the denomination of the rock domains.*

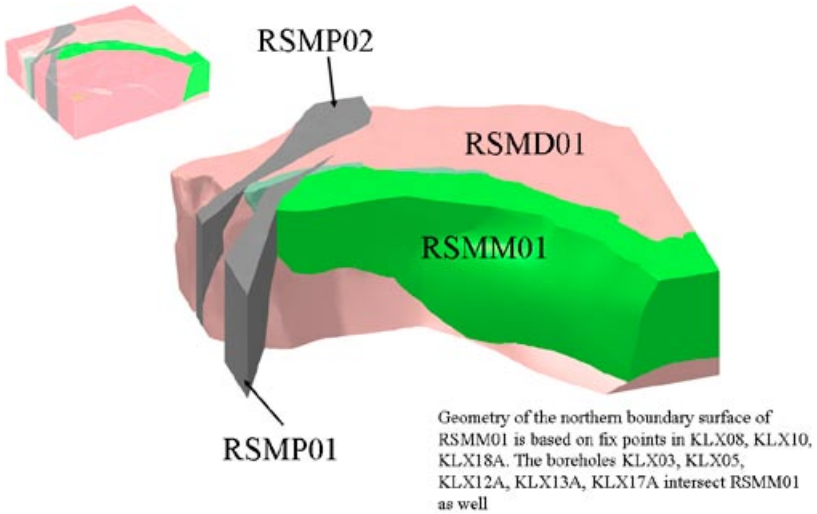

Figure 2-4. *View of the RSMM01 rock domain combined with RSMD01, RSMP01 and RSMP02. RSMA01 corresponds to the transparent parts surrounding the indicated rock domains. View to the south /Wahlgren et al. 2008/.*

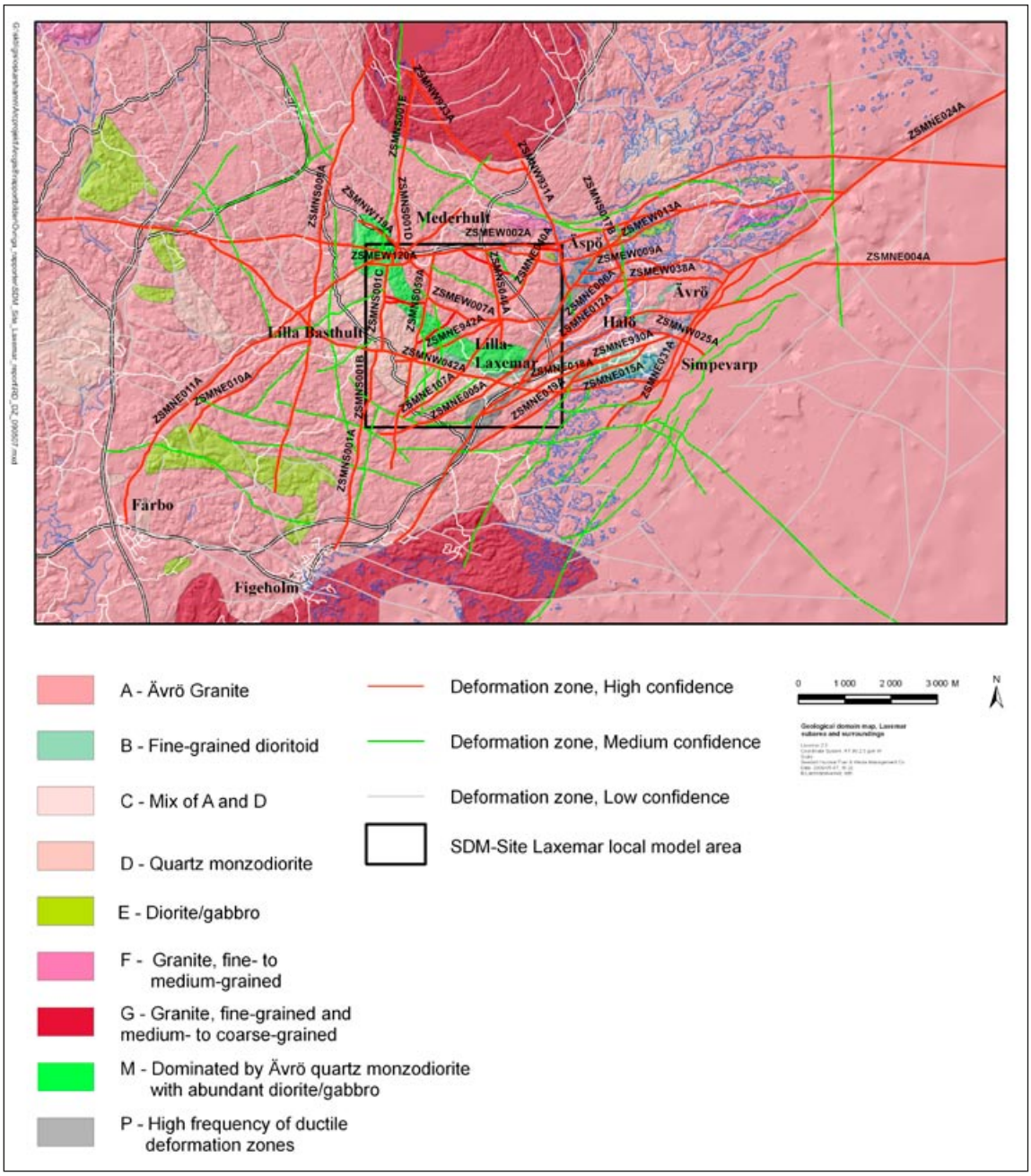

Figure 2-5. *An overview of the deformation zones and rock domains modelled deterministically in the Laxemar-Simpevarp regional model area /Wahlgren et al. 2008/.*

The identified deformation zones in the Laxemar-Simpevarp regional model area can be grouped as follows:

- Northeast-southwest striking, moderate to steeply dipping.
- North-south striking, moderate to steeply dipping.
- East-west to northwest-southeast striking, steep to moderate dip to the south.
- East-west to northwest-southeast striking moderate dip to the north.
- Gently dipping.

The first group of deformation zones is characterised by three regional deformation zones, ZSMNE011A, ZSMNE005A and ZSMNE004A, which roughly represent the outer NW and SE boundaries for the rock volume demarcated for a potential repository, respectively. All three deformation zones have a

ductile origin and complex internal geometry as evidenced by the numerous mylonite fabrics identified during the outcrop mapping campaign. Within this outer boundary three additional N-S striking deformation zones dominate: ZSMNE107A, ZSMNE942A and ZSMNE944A (Figure 2-6). These brittle-ductile to ductile shear zones vary in size and occur throughout the site investigation area. However, the area east of ZSMNE005A is more affected by ductile deformation zones (shown as a grey raster in Figure 2-7) relative to the Laxemar subarea.

The north-south striking local major and regional deformation zones are dominated by ZSMNS001A-E and ZSMNS059A in the local model area (cf Figure 2-8). Both deformation zones have parallel strikes and dip 80–90° W. They are steeply dipping with a tendency towards the west.

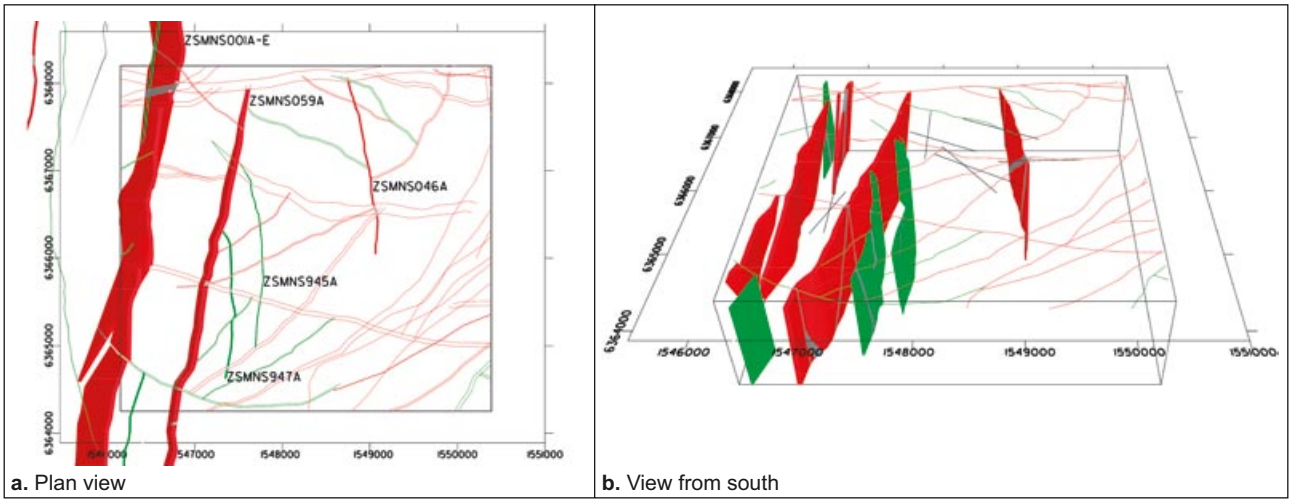

Figure 2-6. *All N-S striking local major and regional deformation zones which are associated with surface lineaments in the local model area /Wahlgren et al. 2008/.*

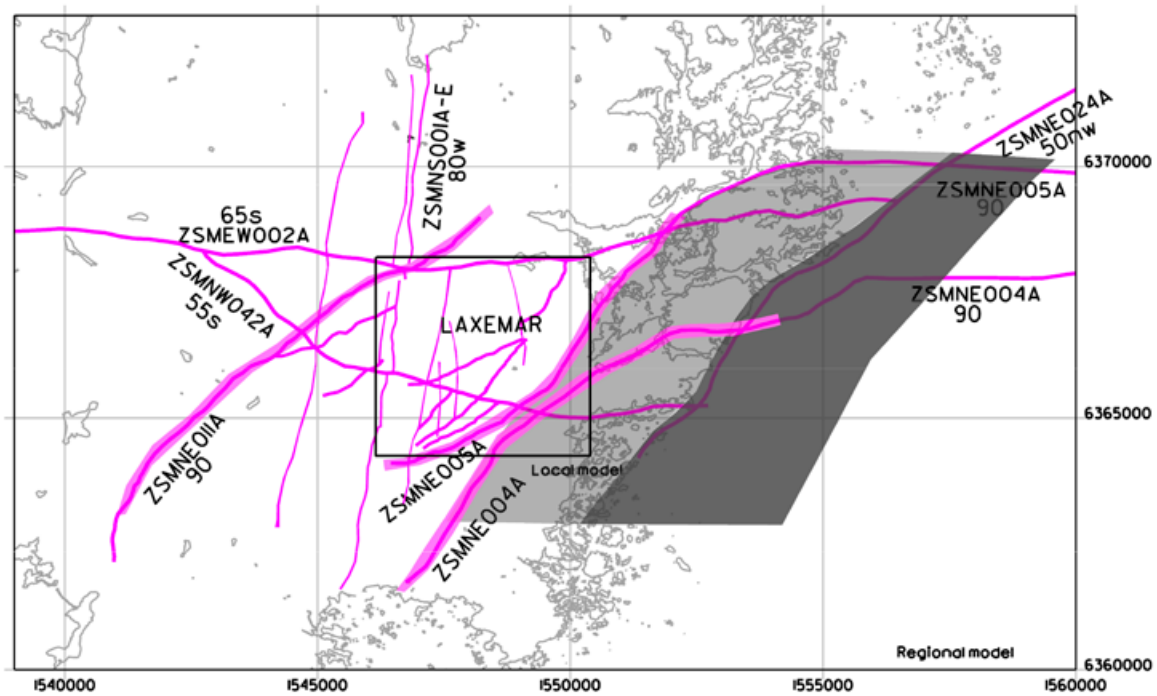

Figure 2-7. *Overall pattern of ductile deformation zones across Laxemar /Wahlgren et al. 2008/.*

The E-W and NW-SE striking zones include steep to moderately southward dipping deformation zones. This set of structures is dominated by ZSMEW007A, ZSMEW002A, ZSMEW120A, ZSMEW900A-B and ZSMNW042A. Zone ZSMNW042A is included in this group, which is otherwise dominated by the E-W structures, since it has a similar character, size and inferred relationship with the regionally dominant Mederhult zone ZSMEW002A. The Mederhult zone is by far the largest deformation zone in this group and is more or less parallel with the northern boundary of the local model area.

The last group comprises the gently dipping deformation zones ZSMEW946A (080/23°) and ZSMNW928A (120/28°). It is not a straightforward matter to identify the lateral extent of this group of deformation zones since often they do not have a clearly identifiable intercept with the ground surface. In addition, if such deformation zones are segmented and later offset by movements along steeply dipping deformation zones, which is considered highly likely, then the interpretation and estimation of their effective extents and 'size' becomes extremely difficult.

2.2.3 Fracture domains and hydraulic rock domains

The fracture domains defined by geology (cf /Wahlgren et al. 2008/, Figure 2-9) have been used as base geometrical models to analyse the spatial variation of hydraulic properties and to define the hydraulic rock domains (HRD) (cf /Rhén et al. 2008/, Figure 2-10). The individual hydraulic rock domains equate to the corresponding fracture domains with the exception of HRD_C which is made up of a combination of FSM_C, FSM_NE005 and FSM_S. Furthermore, these hydraulic rock domains may also be demarcated by observed differences in hydrochemistry (cf discussion in Section 4.1.1).

2.2.4 Two dimensional cross-sections

The major geological structural characteristic features of the Laxemar subarea and the Laxemar-Simpevarp area are further detailed in a series of strategically selected cross-sections that in an appropriate way best integrate the geological and hydrogeological understanding with the available hydrochemical data. Five sections have been extracted from the SDM-Site Laxemar regional geological models and the location of the profile lines are shown in Figure 2-11.

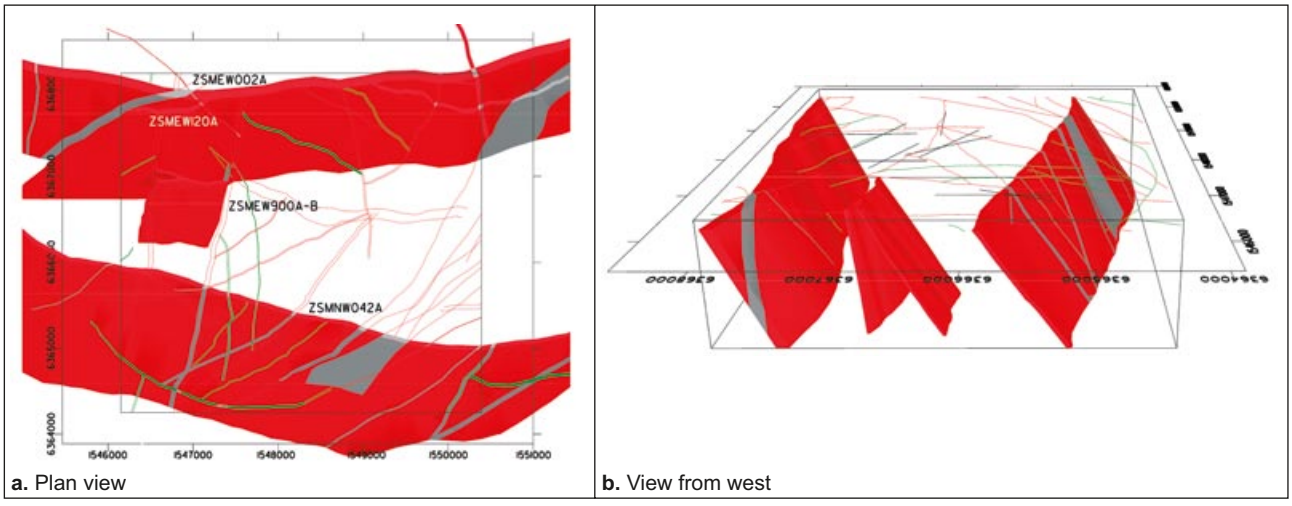

a. Plan view **b.** View from west

Figure 2-8. *The main members of the E-W and NW-SE, steep to moderately southward dipping deformation zones /Wahlgren et al. 2008/.*

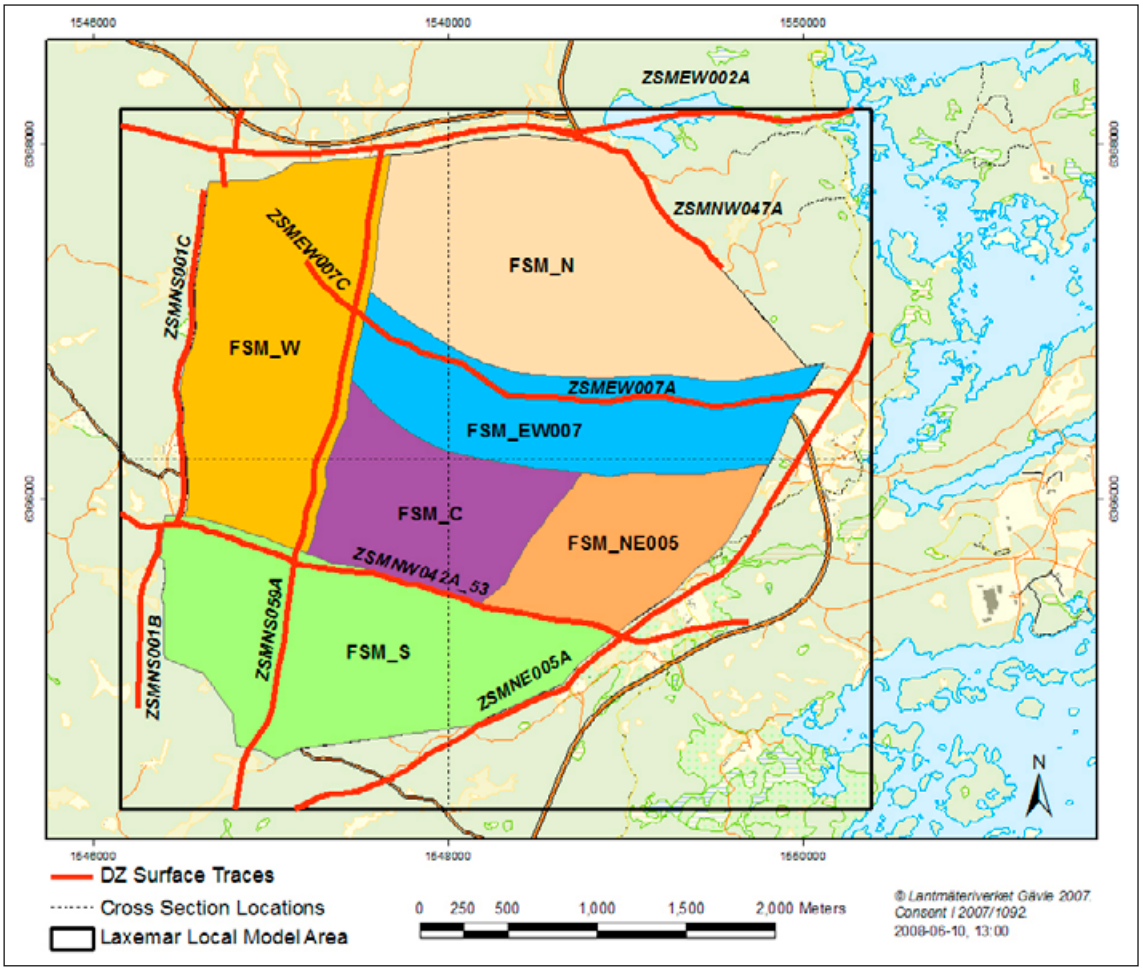

Figure 2-9. *Fracture domain model for the Laxemar subarea /Wahlgren et al. 2008/.*

The five sections are:

- **Section 1:** Approximately NE-SW in orientation to intercept sampled cored boreholes KLX01, KLX02/KLX07A/KLX7B, KLX10 and KLX15A.
- **Section 2:** Approximately NNE-SSW/NE-SW in orientation to intercept cored boreholes KLX05, KLX04/KLX08, KLX18A, KLX03, KLX19A, KLX14A and KLX27A.
- **Section 3:** Approximately NW-SE/W-E in orientation to intercept cored boreholes KLX13A, KLX04/KLX08, KLX02/KLX07A/KLX07B, KSH02, KSH01A/KSH01B and KSH03A.
- **Section 4:** Approximately N-S in orientation to intercept cored boreholes KLX13A, KLX17A, KLX11A and KLX27A.
- **Section 5:** Approximately NNW-SSE/W-E in orientation to intercept cored boreholes KLX17A, KLX03, KLX15A and KLX05/KLX12A.

NOTE: In each case the closest percussion boreholes have been projected onto the cross-sections. In addition, the regular E-W and N-S grid lines covering the Laxemar subarea constructed for the hydrogeological modelling, proved to be unsuitable for hydrochemical considerations because of the distribution of the sampled boreholes. However, despite having to choose alternative sections, the above five sections were orientated to follow a general N-S and E-W coverage to facilitate as much as possible comparison with the hydrogeological simulation results.

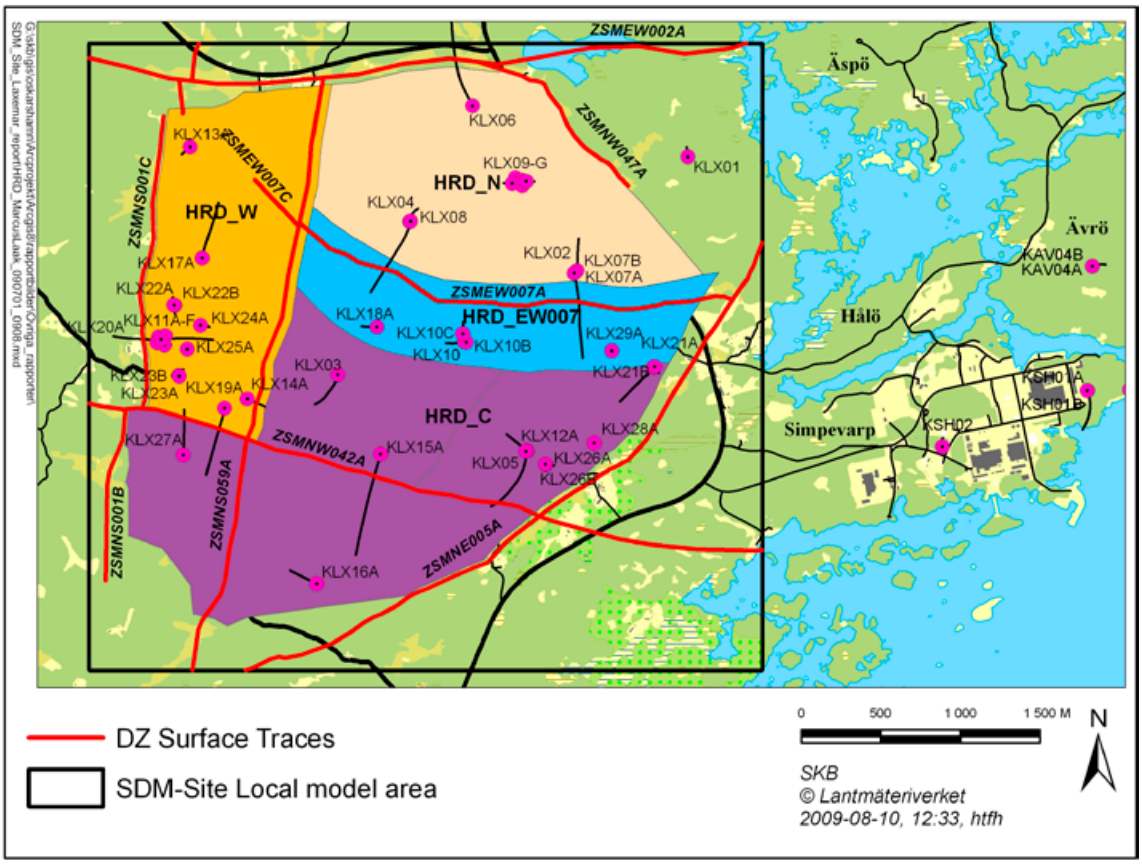

Figure 2-10. *Illustration of the SDM Site Laxemar Hydraulic Rock Domain Model as superimposed on the geological Rock Domain Model. Modified after /Rhén et al. 2008/.*

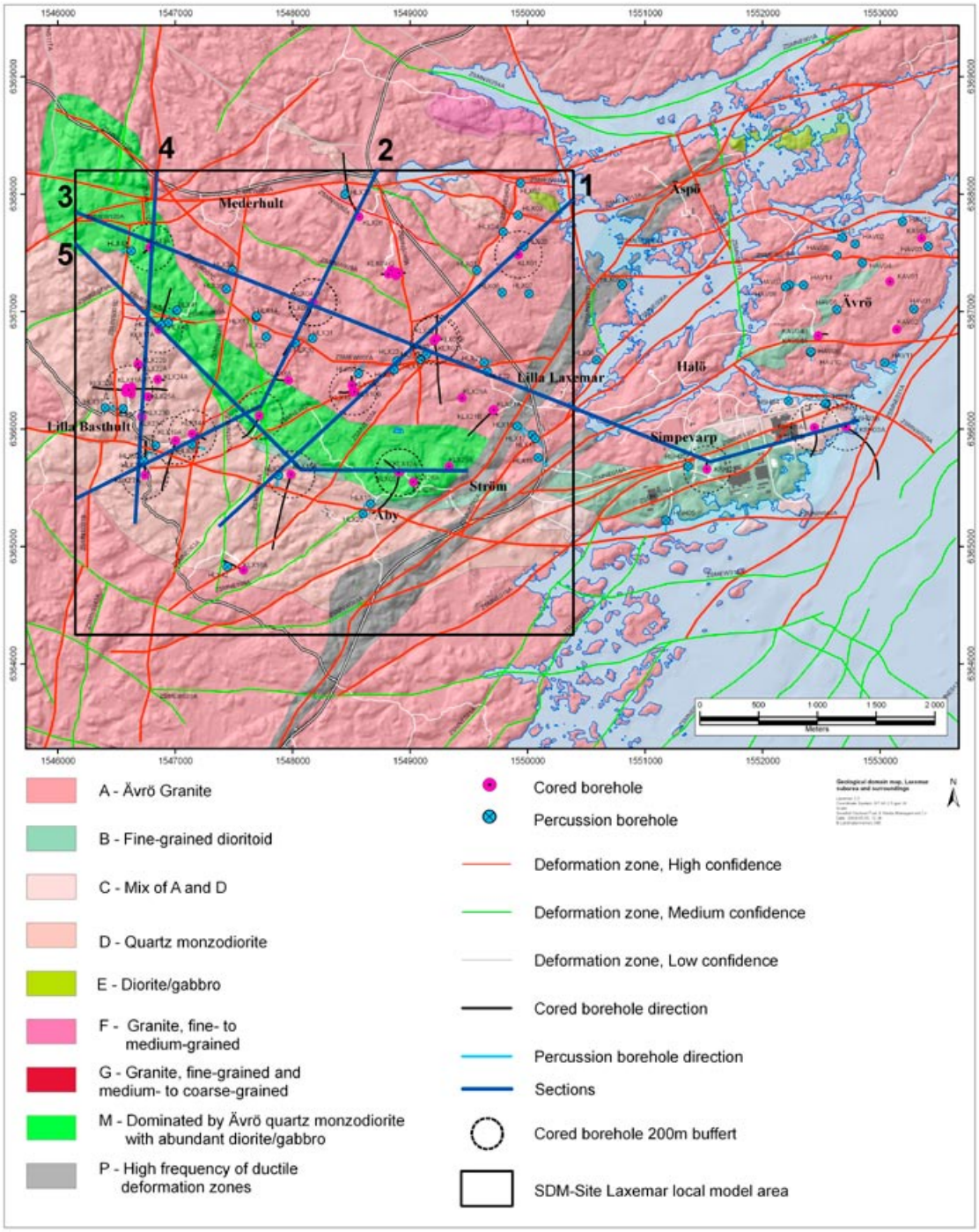

Figure 2-11. *Location of cross-sections #2, #3 and #5 used quantitatively to visualise the hydrochemistry of the Laxemar-Simpevarp area (cf Chapter 6). Cross-sections #1 and #4 were used qualitatively.*

The basic geological information compiled in the cross-sections to provide the framework for constructing the SDM-Site Laxemar conceptual descriptive model for the Laxemar subarea is illustrated below for cross-sections #3 and #5 in Figure 2-12 and Figure 2-13 respectively. Section #3 has already featured in the Laxemar 1.2 and Laxemar 2.1 hydrogeochemical model versions because its orientation is essentially parallel to the approximate west to east regional groundwater flow direction, and because it also includes the Simpevarp subarea. This provides the opportunity to visualise the changes in groundwater chemistry from recharge conditions to the west to discharge conditions in the coastal margin to the east (cf Chapter 6).

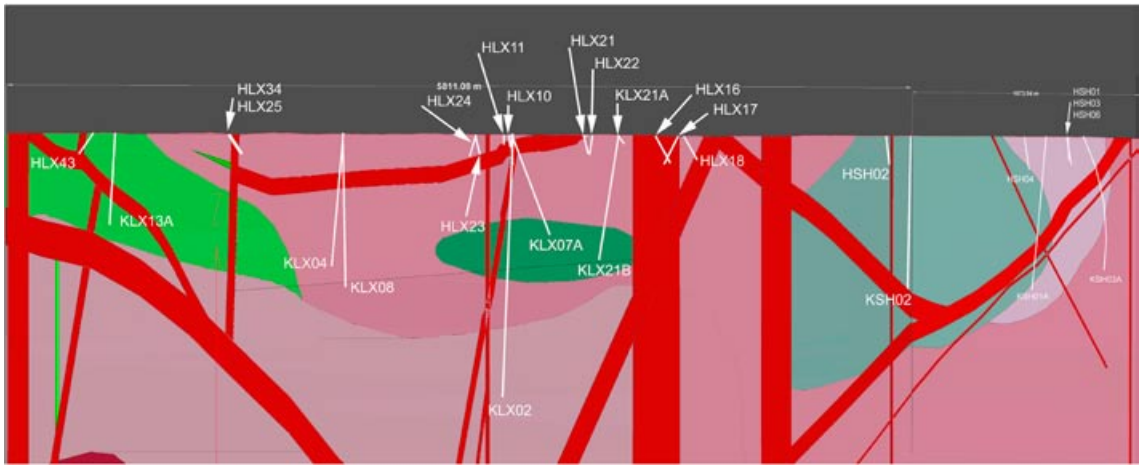

Figure 2-12. *NW-SE/W-E 2D cross-section through the central part of the Laxemar subarea to the Simpevarp subarea to the east (cross-section #3 in Figure 2-11). Indicated are the major rock domains, the major deformation zones and the projected positions of the cored and percussion boreholes. The varying widths of the deformation zones reflect their orientation relative to the cross-sectional cut, (cross-section length = 7,385 metres; vertical thickness of section = 2,000 metres).*

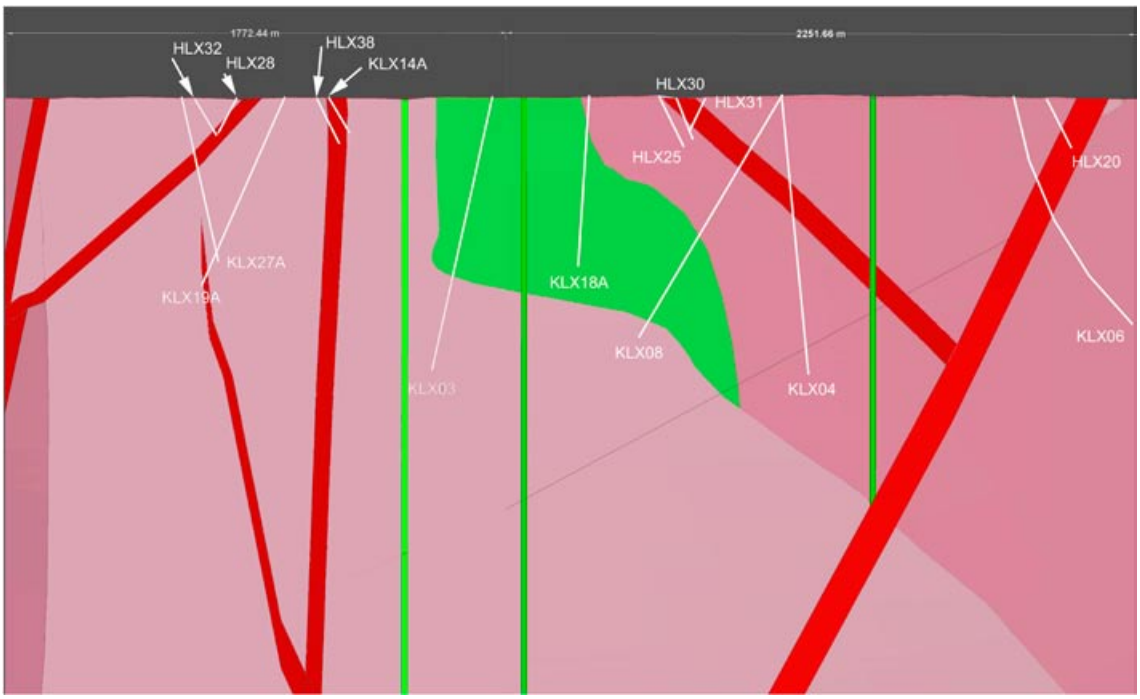

Figure 2-13. *NW-SSE/W-E 2D cross-section from the western margin of the Laxemar subarea, through the central part and towards the eastern margin in the direction of (but not including) the Simpevarp subarea (cross-section #5 in Figure 2-11). Indicated are the major rock domains, the major deformation zones and the projected positions of the cored and percussion boreholes. The varying widths of the deformation zones reflect their orientation relative to the cross-sectional cut, (cross-section length = 4,024 metres; vertical thickness of section = 2,000 metres).*

2.2.5 Fracture mineralogy input

Detailed investigations of the fracture mineralogy and altered wall rock have been carried out as part of the Laxemar site characterisation programme and these investigations are summarised and evaluated in /Drake and Tullborg 2009a/. Presented below are descriptions of the identified fracture minerals; their chemical composition, stable isotope composition and parageneses, important palaeo-hydrogeological indications and the sequence of fracture mineralisations. Chemical analyses of bulk fracture fillings have been used to identify possible sinks for certain elements and also to identify minor mineral phases potentially overlooked by X-ray diffraction (XRD). Included in the report is also information derived from the extensive drill core mapping carried out within the programme.

General characteristics

The occurrence and frequency of the different fracture minerals have been evaluated based on drill core mapping (Boremap) data combined with supporting analyses (SEM-EDS, stereomicroscope, XRD, and geochemistry). The frequency of different fracture minerals shows large variation and the relative frequency of occurrence can be summarised as follows: calcite and chlorite >> epidote, quartz and clay minerals > pyrite > hematite, adularia and prehnite >> zeolites. Other minerals have only been found as minor occurrences but can be more frequent in certain intervals (e.g. gypsum, muscovite, amphibole, talc, fluorite and goethite). For instance gypsum is mainly found in certain intervals at greater depths than 360 m and only in a few of the boreholes (mainly KLX03, KLX06, KLX08, KLX10, KLX12A and KLX17A). Pyrite is by far the most common sulphide. Other sulphides identified include chalcopyrite, galena and sphalerite. Sulphates identified in addition to gypsum are barite and very rarely celestine. Zeolites identified are laumontite (Ca-zeolite), harmotome (Ba-zeolite) and less commonly analcime (Na-zeolite). However, the absolute volumes of each mineral in the specific fractures vary widely.

The main clay mineral phases are corrensite (or similar mixed-layer clay) > illite > mixed layered illite/smectite (cf Figure 2-14). Only a few samples with pure smectite, pure vermiculite and kaolinite have been identified.

Potential differences in fracture mineralogy between the different fracture domains and rock domains have been studied and it was concluded in /Drake and Tullborg 2009a/ that:

- The differences are very small between different domains.
- The small mineralogical differences observed can normally be attributed to varying wall rock chemistry; for example, slightly higher frequency of chlorite, calcite, clay minerals and epidote and smaller amounts of quartz and K-feldspar in fractures in domains dominated by quartz monzodiorite and Ävrö quartz monzodiorite (rock domains RSMM01 and D01) compared to RSMA01, which is dominated by Ävrö granodiorite.
- The difference in mineralogy between different rock domains is more pronounced than the difference between fracture domains. This may be explained by less data for each fracture domain.

Most minerals occur in similar frequencies at all depths investigated, however, notable deviations occur in the uppermost approximately 20 metres and at depths greater than about 800 m.

- Dissolution of pyrite due to percolation of oxidising water is almost complete in the water-conducting fractures in the upper 20 metres of the bedrock. In the same depth interval goethite is formed. This change is accompanied by lower frequency of calcite to the same depth (about 20 m) probably related to near surface dissolution caused by descending diluted waters unsaturated with respect of calcite. In more fractured parts of the bedrock, goethite and pyrite oxidation is found to greater depths (usually less than 60 metres). The fracture mineral frequency together with chemical analyses has been used to describe the redox front (cf for detailed description, Section 4.8).
- At depths below about 800 m, the frequency of calcite, chlorite and pyrite is lower than above about 800 m, whereas hydrothermal minerals such as quartz, prehnite and epidote are more frequent. This marks the shift to a less hydraulically conductive interval at depths below approximately 800 m, where Palaeozoic to recent calcite precipitation has been limited.

The dominating fracture minerals in the hydraulically conductive fractures are chlorite, calcite and clay minerals but pyrite, quartz, feldspars, and hematite also occur frequently.

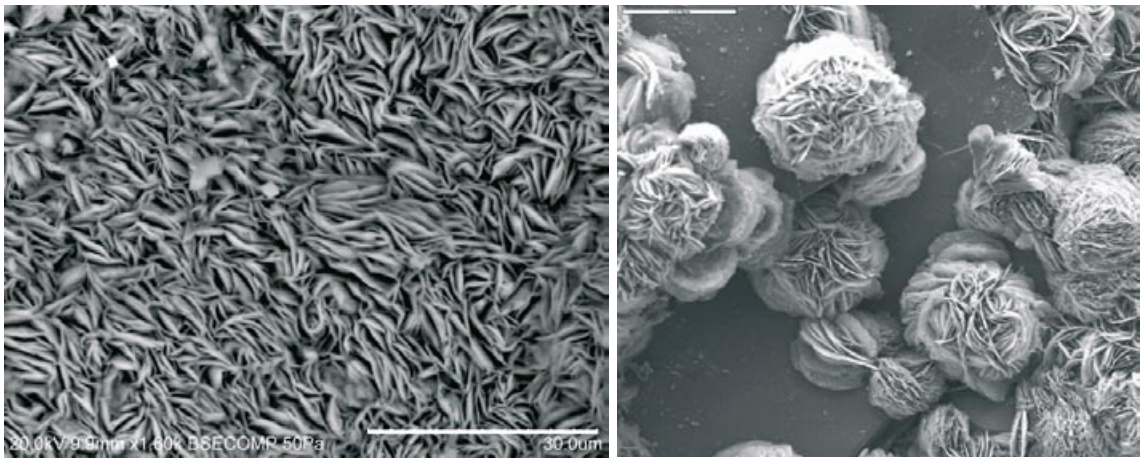

Figure 2-14. *Back scattered electron images of mixed-layer clay. The left image shows mixed-layer clay on a fracture surface from KLX08 (approximately 108 m borehole length). Scale bar is 30 µm. The right image is spherulitic corrensite aggregates on a fracture surface from borehole KLX06 (approximately 831 m borehole length). Scale bar is 200 µm.*

Sequence of fracture mineralisation events

The detailed studies of fracture mineralisations have resulted in the recognition of six different events (fracture mineral generations) /Drake and Tullborg 2004, 2006, 2007, 2008/.

Generation 1 is represents an epidote- and quartz-rich mylonite formed during the early geological history of the area. The mylonites are mainly associated with deformation zones and are often accompanied by wall rock alteration. These mylonites have a minimum age close to ca 1,773 Ma, when the rock cooled below about 500°C (based on formation temperature estimates). The shear zones are clearly older than the ca 1,450 Ma Götemar granite.

Generation 2 represents a cataclasite which occurs in at least two different varieties, sometimes with semi-ductile features. Both varieties were formed during the early geological history of the area, although both have experienced later re-activation. The cataclasites are mainly associated with deformation zones and the older ductile shear zones have influenced the orientation of many Generation 2 structures. The observed semi-ductile features suggest formation close to 300 to 350°C. The formation temperatures suggest either: 1) formation prior to 1,620 Ma when the rock initially cooled below 300°C and/or 2) formation related to the intrusions at Götemar and Uthammar or at a slightly earlier thermal event.

Generation 3 represents a sequence with at least three different mineral parageneses in sealed fractures, and occasionally of greisen. Major minerals are calcite, quartz, chlorite, fluorite, pyrite, muscovite, epidote, prehnite and laumontite. The latter three replace or cut each other in chronological order. This generation is interpreted to be related to the intrusions of the Götemar and Uthammar granites but some of the fillings are probably older. These granites have been interpreted to be associated with the Danopolonian orogeny to the south and consequently the Generation 3 fillings would also have been formed as a result of the far field effect of this orogeny. $^{40}Ar/^{39}Ar$ plateau ages of the greisen and the characteristically altered and red-stained wall rock indicate about 1,424 to 1,417 Ma, which confirms the association of a major part of this generation to the nearby intrusions.

Generation 4 mainly includes calcite, adularia, laumontite, chlorite, quartz, illite and hematite. These minerals are found in thin sealed fractures cross-cutting Generation 3 fillings but are difficult to distinguish due to similar mineralogy and appearance. However, they have slightly different stable isotope and fluid inclusion signatures, as well as chlorite chemistry, and are interpreted to be formed later than ca 1,400 Ma, but prior to 710±78 Ma. Generation 4 may be Sveconorwegian in age as indicated by a $^{40}Ar/^{39}Ar$ adularia age of ca 989 Ma. Furthermore, the intrusion of N-S oriented ca 900 Ma dolerites in the westernmost part of Laxemar subarea indicates an E-W directed late Sveconorwegian extension. Although Generation 4 may be largely Sveconorwegian, it is not very distinct and not as widespread as Generations 3 and 5.

The oldest **Generation 5** fillings were probably formed in relation to the Caledonian orogeny. These calcite dominated fillings were formed from warm brine fluids (about 80 to 145°C) at ca 440 to 400 Ma. Other minerals include adularia, fluorite, pyrite, gypsum (possibly originally anhydrite), barite, zeolites, hematite, clay minerals, chlorite, chalcopyrite, galena, sphalerite and REE-carbonate. These fillings precipitated from organic-rich fluids, probably influenced by descending waters from overlying sediments. The relatively high formation temperatures may also be influenced by subsidence due to thick overlying sediments. Younger fillings of Generation 5 precipitated during gradually lower temperatures as the overlying sedimentary successions were successively eroded, shown by the changing stable isotope compositions and chemical compositions, which grade into Generation 6 signatures.

Generation 6 consists of low-temperature fracture coatings which might be precipitated recently, i.e. during the Quaternary. These include clay minerals, calcite and goethite above the redox front and pyrite below. Generation 6 minerals are not easily distinguished from the youngest Generation 5 fillings, which have overlapping stable isotope signatures and trace element compositions. The stable isotope composition of these minerals (mainly calcite) shows that they may have been precipitated from groundwaters with similar signatures as the present day groundwater at the site.

Minerals from Generation 5 and especially Generation 6 are of interest for palaeohydrogeological studies and the results of stable isotope analyses and trace element analyses of, for example, calcite, pyrite and gypsum, are discussed in Section 4.8 where also water/fracture mineral interaction processes and the redox buffer capacity of the fracture system are addressed.

Wall rock alteration

Red staining is the most noticeable wall rock alteration feature in the Laxemar-Simpevarp area (Figure 2-15). This staining is due to hematite dissemination and is associated with fractures sealed with mineralisations of generations 1, 2 and 3. The alteration is strongly associated with single fractures and sealed networks of generation 3 fractures within the fracture domains, but they also shows spatial association with deformation zones. The characteristics and properties of the red-stained rock have been described in detail in /Drake et al. 2008, Drake and Tullborg 2009a/. A summary of the main features associated with this altered red-stained rock is given in Section 4.8.3. The red-stained rock displays major changes in mineralogy compared to fresh rock; biotite, plagioclase and magnetite have been altered and chlorite, K-feldspar, albite, sericite, prehnite, epidote and hematite have been formed. Moderate alteration in the macroscopically fresh reference rock shows that the hydrothermal alteration, especially alteration of plagioclase and biotite, extends further from the fracture into the adjacent wall rock than the red staining. Consequently, the amount of red-stained rock mapped should be seen as a minimum value of the amount of altered rock.

2.2.6 Concluding remarks

The Laxemar-Simpevarp area is dominated by Precambrian basement granitoids (dated to around 1,800 Ma) which comprise porphyritic and even-grained rocks ranging from red/grey granites to quartz monzodiorite. The porphyritic granitoids are referred to as the Ävrö granites and the grey, medium-grained monzodiorites which are dominantly quartz monzodioritic in composition, are simply referred

Figure 2-15. *Red stained, hydrothermally altered rock adjacent to a fracture filled with prehnite. Sample KSH03A:128.08–123.23 m borehole length. Drill core diameter is approximately 5 cm.*

to as quartz monzodiorite. All rock-types have been subjected to alteration (red staining caused by disseminated micrograins of hematite) largely due to post-crystallisation penetration of hydrothermal fluids along pre-existing zones of weakness (e.g. fractures).

The rock types have been subdivided into rock domains, i.e. rock volumes where the bedrock shows similar composition, grain size, degree of bedrock homogeneity, and degree and style of ductile deformation. Three main rock domains are recognised: RSMA01 to the north and east characterised by Ävrö granite, RSMM01 characterised by Ävrö quartz monzodiorite with abundant diorite/gabbro, and RSMD01 characterised by quartz monzodiorite. These rock domains are intersected by RSMP-domains (RSMP01 and RSMP02) which are characterised by a high frequency of low-grade ductile shear zones.

Deformation zones in the area are mostly steeply dipping and are assumed to truncate, along their strike direction, other deformation zones. Gently dipping deformation zones do occur but their extent and importance are not fully understood. The identified deformation zones in the Laxemar regional model area can be grouped as follows:

- NE-SW striking, moderate to steeply dipping deformation zones characterised by ZSMNE011A, ZSMNE005A and ZSMNE004A which all have a ductile origin and complex internal geometry as evidenced by the numerous mylonite fabrics.
- N-S striking, moderate to steeply dipping zones represented by ZSMNS001A-E and ZSMNS059A characterised by parallel strikes.
- E-W to NW-SE striking zones, steep to moderate dip to the south with a few zones moderately dipping to the north. This group is dominated by south-dipping ZSMEW002A (regionally dominant Mederhult zone), ZSMEW120A, ZSMEW900A,B and ZSMNW042A, as well as the north-dipping ZSMEW007A.The last group comprises the gently dipping deformation zones ZSMEW946A (080/23°) and ZSMNW928A (120/28°).

Fracture mineral phases characteristic of the Laxemar-Simpevarp area show large variations in occurrence and frequency which can be summarised as: calcite and chlorite >> epidote, quartz and clay minerals > pyrite > hematite, adularia and prehnite >> zeolites. Other minerals have only been found as minor occurrences but can be more frequent in certain intervals (e.g. gypsum, muscovite, amphibole, talc, fluorite and goethite). Six different fracture mineralisation generations have been documented extending in age from ca 1,700 Ma to possibly Quaternary.

Red staining, due to hematite dissemination, is the most noticeable wall rock alteration feature in the area and is associated with fractures sealed by mineralisations of generations 1, 2 and 3 representing a geological time span from ca 1,800 to 1,400 Ma. This alteration is strongly associated with single fractures and sealed networks within the fracture domains, but also shows spatial association with deformation zones.

2.3 Hydrogeology input

2.3.1 General character of the regional hydrogeology

According to /Larsson-McCann et al. 2002/, evaluation of data prior to the site investigations for a large region around Laxemar-Simpevarp, the average (corrected) precipitation *P* in the region where the Laxemar-Simpevarp area is located is about 600 to 700 mm/y, and the average specific discharge R was estimated to be in the interval 150 to 180 mm/y. Hence, /Larsson-McCann et al. 2002/ estimated the evapotranspiration *E* to be in the interval 420 to 550 mm/y. The SDM-Site Laxemar modelling shows differences in the specific discharge *R* between seasons, years and catchment areas. This is due to seasonal and inter-annual variability of the meteorological conditions, and also differences in land use, fraction of open water and other properties between catchment areas. According to the SDM-Site Laxemar evaluation of meteorological and hydrological data /Werner et al. 2008/, the site-average annual precipitation can be estimated to about 600 mm/y, whereas the site-average specific discharge of 165 mm/y is within the interval estimated by /Larsson-McCann et al. 2002/.

Groundwater recharge is generally associated with high altitude areas, whereas groundwater discharge is located in low altitude areas (valleys, watercourses and depressions). The degree of surface runoff (overland flow) may be large, as there are extensive areas with exposed or very shallow bedrock /Werner et al. 2008/. However, there is often a thin layer of Quaternary deposits and/or vegetation present also in the areas mapped as exposed bedrock, which may act to reduce the degree of surface runoff. The impact of these thin deposits and vegetation layers on the surface runoff is still somewhat unclear, even though there is yet no field evidence to support the assumption that precipitation and snow melt are the only sources of groundwater recharge.

The SDM-Site Laxemar modelling, which includes, for example, the evaluation of groundwater level data below Lake Frisksjön and a near-shore area at Lake Jämsen, indicates that the central parts of the lakes and the watercourses do not contribute to groundwater recharge even during dry periods when groundwater levels are low. According to the data evaluation, interaction between lakes and groundwater in the underlying Quaternary deposits mainly occurs in near-shore areas of the lakes /Werner 2008/. The small watercourses in the areas are dry during long time periods. As the groundwater table is generally located close to the ground surface, evapotranspiration and precipitation cycles have a strong effect on the groundwater level in Quaternary deposits /Werner et al. 2008/.

The regional groundwater flow in the Laxemar subarea is driven by topography with a general gradient from the high elevated areas in the west to the Baltic Sea in the east. The flow pattern is largely governed by the mutual connections of the deformation zones which characterise the region. The topography also results in localised areas of recharge/discharge which represent groundwater circulation cells of varying depth and extent, and therefore of varying groundwater ages. There is a diminishing effect of groundwater circulation down to a depth about 1,000 m, and below about 1,200 m the groundwater is effectively stagnant /Rhén et al. 2009/.

Based on modelled particle tracking used to trace potential groundwater flow paths, Figure 2-16 shows the recharge (red) and discharge (blue) for particles released within the local scale area for the base case. All the major islands (Äspö, Ävrö and Hålö) together with the Simpevarp peninsula act as recharge

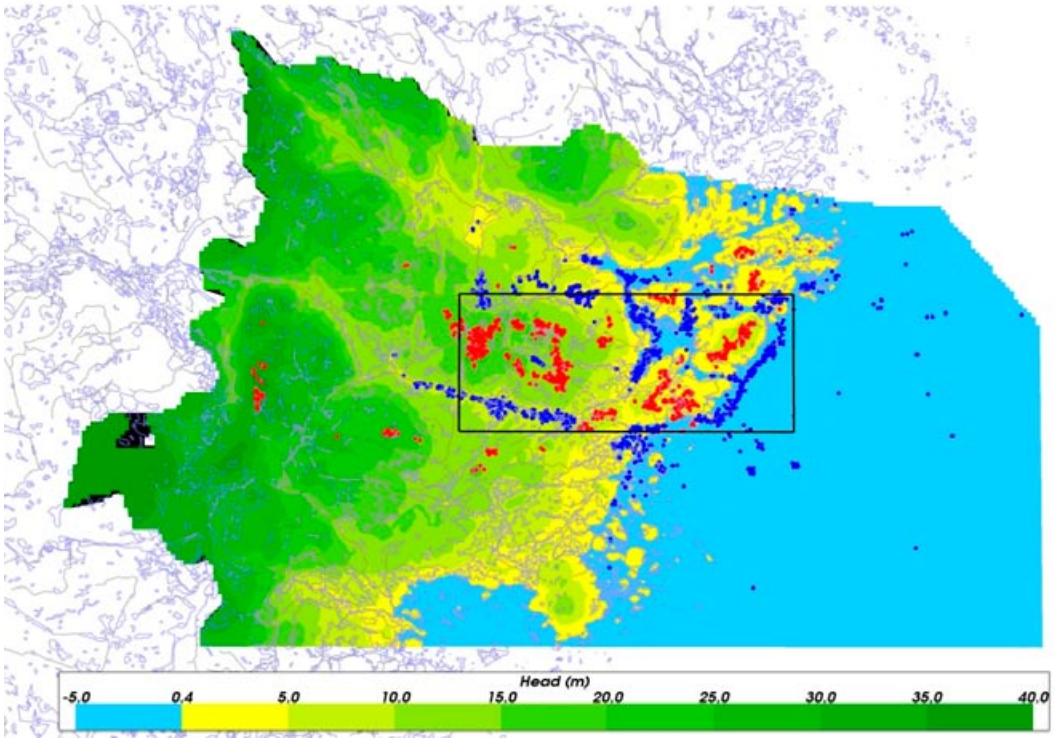

Figure 2-16. *Recharge (red) and discharge (dark blue) locations for particles released in the local scale area for the reference case. The local scale release area (black rectangle) is shown for geographical reference. The recharge points are the upstream start points on the model surface for flow paths through the release area. The discharge points are the equivalent downstream exit points /Rhén et al. 2009/.*

areas, as does the central parts of the Laxemar subarea. A few recharge areas that influence the Laxemar subarea are located at hills several kilometres to the west and southwest. Generally, the discharge areas for groundwaters from deeper levels in the bedrock are located mainly in valleys to the south and north of Laxemar and along the shoreline, especially south of the Äspö island. Hydrochemically, the most convincing discharge point is situated in the centrally located outflow area of Ävrö. There is also a minor discharge area associated with a small stream in the centre of the Laxemar subarea.

The input from hydrogeological modelling is important not only for understanding the interplay between surface water, near surface groundwater and deep groundwater, but also for providing greater understanding of the palaeohydrogeochemical evolution of the site. For example, input from the hydrogeology model can be in the form of conceptual model support and testing, and in the form of descriptions of flow directions and flow properties. Furthermore, it is important to bear in mind that the anisotropy in the structural geological model effectively governs the pathways for flow at all depths.

2.3.2 Surface features

Conceptual and geometrical models of the overburden in the Laxemar-Simpevarp area are presented by /Sohlenius and Hedenström 2008, Nyman et al. 2008/, whereas /Werner 2008/ present an evaluation of hydrogeological properties data of the overburden. Generally, glacial sand to gravel till overlies the bedrock, whereas glacial clay and post glacial sediments (i.e. gravel, gyttja clay/clay gyttja, gyttja, and peat) are deposited in many low-altitude areas (Figure 2-17). The horizontal sequence of hydraulic properties of these 'Hydraulic Soil Domains (HSD') from the top of the overburden to the bedrock interface range in hydraulic conductivity from 10^{-6} to 10^{-8} m/s for the post glacial sediments, about 10^{-5} m/s for the till, and the highest value of 10^{-4} m/s for the glacial-fluvial sediments which are in contact with the basement rock surface. These observed hydraulic conductivity values generally are higher than in the underlying bedrock which means, for example, that the till layers will not significantly reduce the infiltration or have a large effect on the deep bedrock hydrogeology, but also that a large part of the infiltrating water may flow in the overburden to the discharge areas.

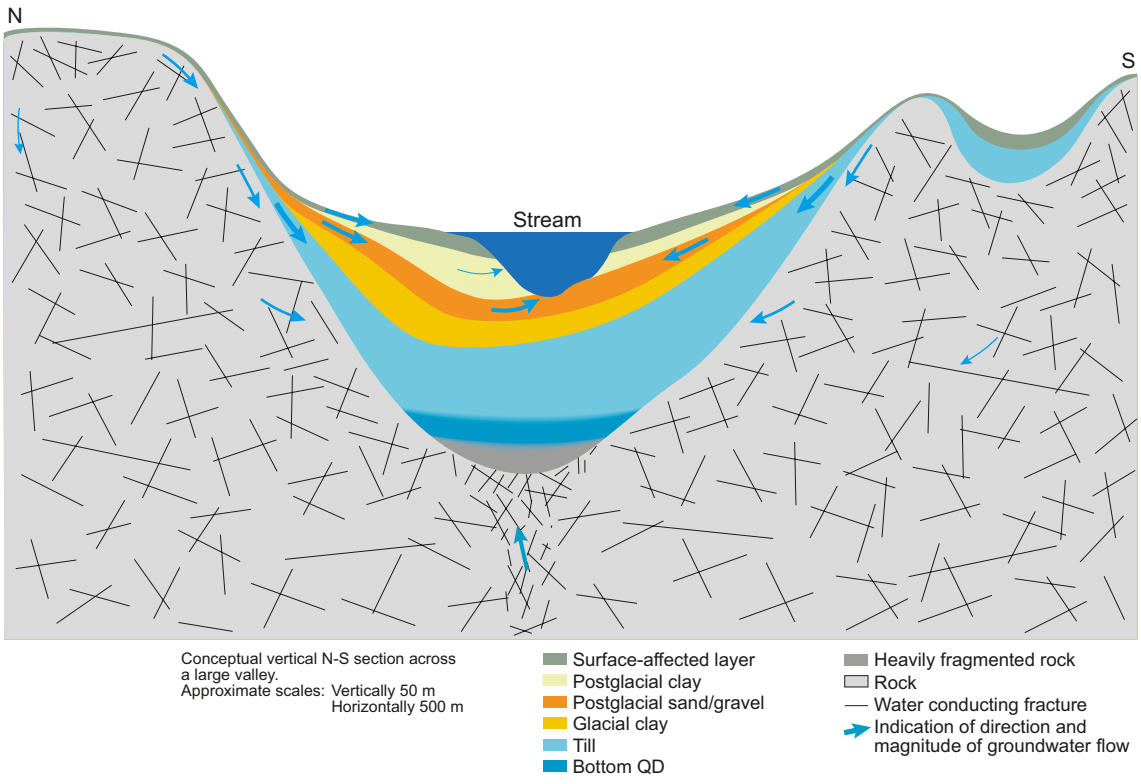

Figure 2-17. *Conceptual model of the overburden and near surface bedrock /Werner 2008/.*

The Laxemar 1.2 conceptual model of the overburden hydrogeology recognises three subdivisions: type areas, flow domains and interfaces between flow domains. Based on /Werner et al. 2005/, the type areas are described as: a) '*high altitude areas'* (dominated by exposed or very shallow bedrock), b) '*valleys'* (with thicker Quaternary deposits, and post glacial sediments at the surface), c) '*glacio-fluvial deposits'* (of which the Tuna esker in the western part of the regional model area is the largest), and d) '*hummocky moraine areas'* (primarily existing in the southwestern part of the regional model area and in the central part of the Laxemar subarea). Groundwater flow in the large Tuna esker and other eskers can, in its most simple form, be conceptualised as channel flow, taking place parallel to the esker orientation /Lindborg 2006/. Depending on their hydraulic interactions with their surroundings (and the differences in groundwater levels between the eskers and their surroundings) the eskers can discharge groundwater to the surroundings, or groundwater recharge can take place from the surroundings into the eskers.

2.3.3 Bedrock features

In common with the surface environment, topography appears to control much of the groundwater flow pattern in the upper part of the rock mass, and probably to much greater depths until decreasing transmissivity and increasing salinity will reduce the flow rates (Figure 2-18). As mentioned above, discharge areas are located at the extreme east of the Simpevarp area along the Baltic Sea coastline and also onshore in conjunction with deformation zones. Results from the Simpevarp 1.2 modelling /SKB 2004a/ and the Laxemar 1.2 modelling /SKB 2006b/ indicate that regionally the Laxemar subarea is predominantly subjected to recharge conditions and that the Simpevarp subarea is an area of mainly groundwater discharge.

Variations in bedrock hydraulic conductivity

Lateral and vertical groundwater flow through the bedrock of the Laxemar subarea is dependent on the hydraulic properties of the water conductive open connected fractures and deformation zones in combination with the differences in hydraulic gradient which exert the driving force for flow.

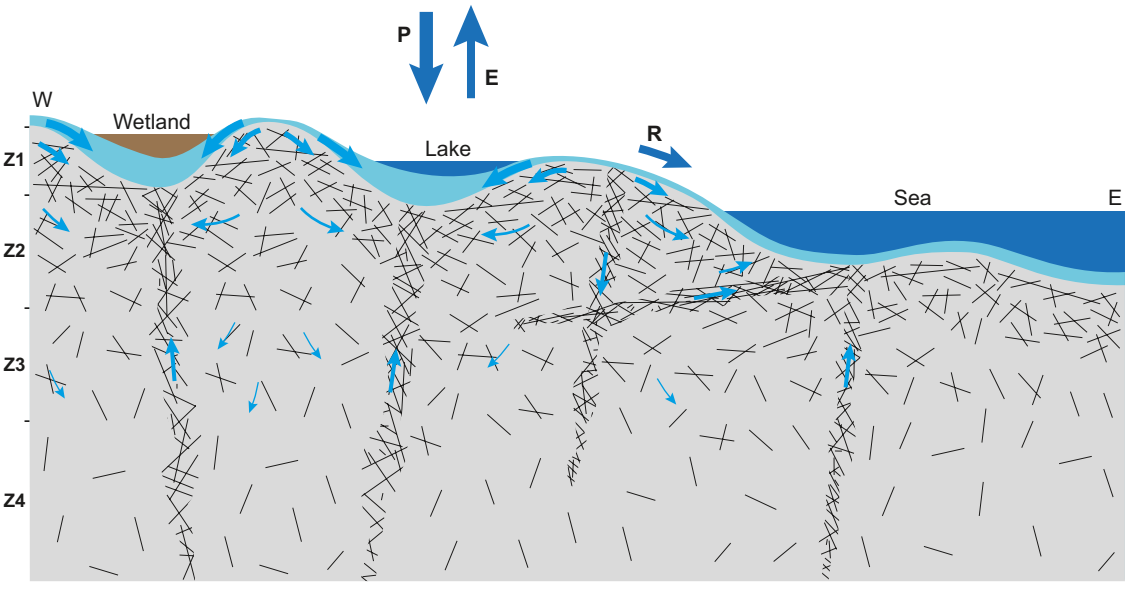

Figure 2-18. *Conceptual model of the main water flow in the overburden and in the near surface to intermediate bedrock to maximum depths of about 650 m. P = precipitation, E = evaporation and R = runoff /Werner 2008/.*

Advective flow is greatest in the upper bedrock, less at intermediate levels, and least at greater depths. This is illustrated by compilations of hydraulic tests in boreholes /Rhén et al. 2008/ which compare data (at 100 m test scale) from test sections in the bedrock between deterministic deformation zones to test sections containing one or more hydraulically conducting deformation zones, representing hydraulic conductor domains, HCD (Figure 2-19). These data show a clear decrease in hydraulic conductivity with elevation below surface.

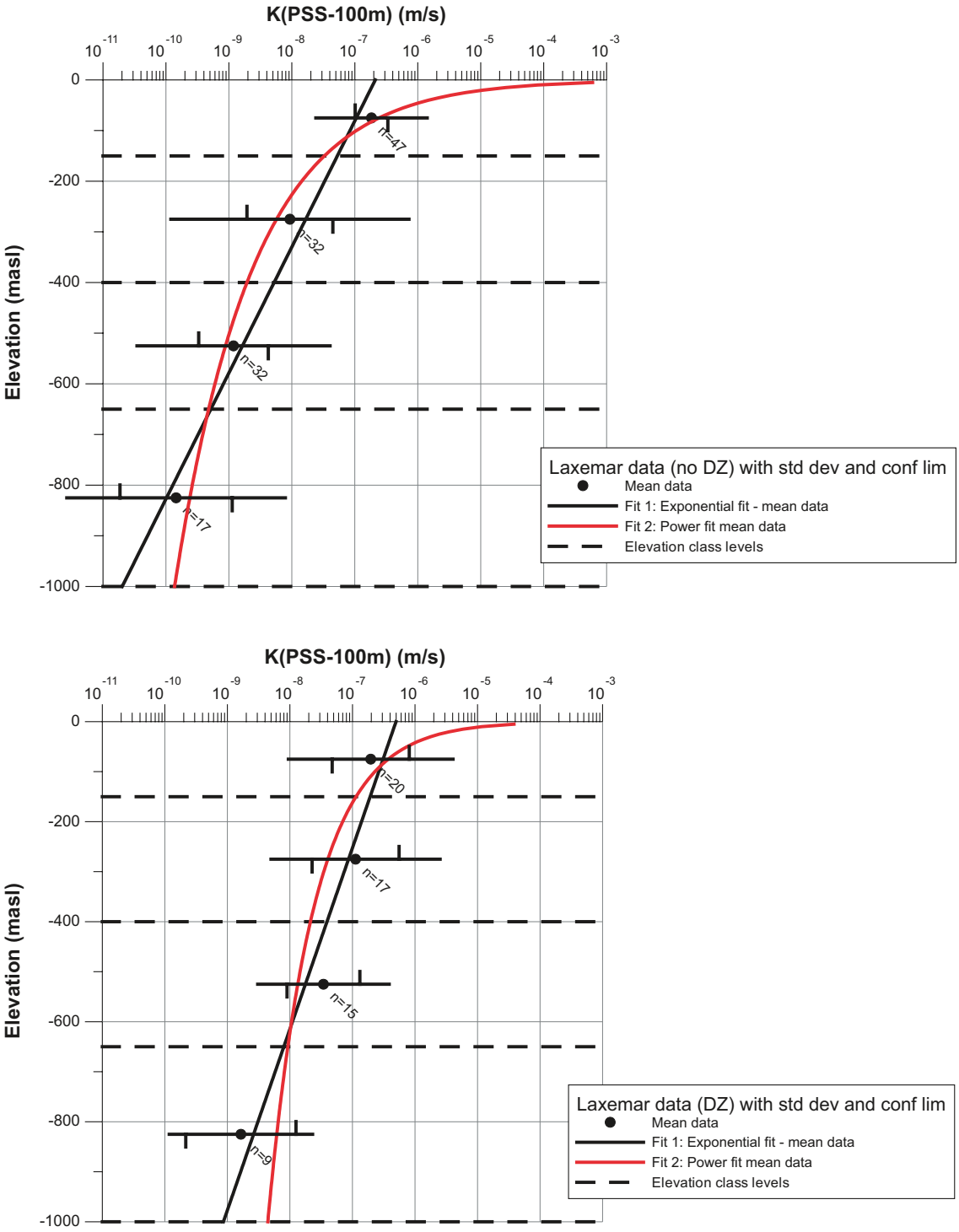

Figure 2-19. *Hydraulic conductivity (K) for 100 m test scales versus elevation. Top plot: Data from test sections in between deterministic deformation zones (DZ). Bottom plot: Data from test sections including one or more hydraulically conducting domains (HCD) /Rhén et al. 2008/.*

The frequency of open flowing fractures with transmissivities greater than 1×10^{-9} m^2/s also decreases with depth, particularly below –50 to –150 m elevation. It has also been shown that horizontal water-conducting fractures have a slightly higher intensity than vertical water-conducting fractures above –150 m elevation as compared to deeper levels. Combining these observations with relatively low stress levels close to the surface (smaller rock load) at shallow depths, probably results in changes in hydraulic anisotropy with depth. In such cases the horizontal conductive fractures are significant or dominant in the near surface rock, but at deeper levels they generally become less hydraulically significant compared to the vertical sets. The WNW vertical fracture set is hydraulically important at all depths compared to other vertical sets. Furthermore, at these shallow bedrock levels it has also been suggested that the uppermost part of the rock at around 5 to 10 m depth may be more fractured and permeable due to influence of the latest glaciation, particularly so on the southeastern slopes of the bedrock surface.

Rock-type variations in hydraulic conductivity

Data are available that describe the distributions of hydraulic conductivity for the different rock types between the deterministically defined deformation zones /Rhén et al. 2008/. This has important implications for the matrix porewater studies, cf Section 4.9. According to tests with a test scale of 5 m (thus including flowing fractures), the most conductive rock type is generally the fine- to intermediate-grained granite with the Ävrö granite (granite to quartz monzodiorite, normally porphyritic) generally showing a geometric mean hydraulic conductivity that is 3-8 times less than the fine-grained granite, with an even greater difference seen below 650 m depth. Unfortunately, there are rather few test sections with the medium- to coarse-grained equigranular granite, but it appears to have similar properties as the Ävrö granite. Fewer data exist for the pegmatite so that its hydraulic properties cannot be judged with certainty.

The most low-conductive rock types are dolerites (present as highly fractured dykes), followed by fine-grained dioritoid (metavolcanite, volcanite) and quartz monzonite (quartz monzonite to monzodiorite, equigranular to weakly porphyritic).

Intact rock matrix hydraulic conductivity on samples from the Ävrö granite and quartz monzodiorite has been measured in the laboratory indicating a range from 10^{-16} to 10^{-12} m/s.

Fracture intensity

Determination of the intensity of open fractures formed part of the hydraulic DFN modelling phase /Rhén et al. 2008/ and Figure 2-20 shows all the fractures on a vertical slice (left-hand picture) and the effect of removing isolated and dead-end fractures (the right hand picture). This demonstrates how small fractures tend not to contribute to connectivity and are far less likely to form potential flow paths, leaving areas of rock through which there is little or no flow. This effect becomes more widespread for parts of the rock with low intensity of open fractures, as found at greater depth /Rhén et al. 2008/. Importantly, this depth subdivision of connected fractures coupled with the hydraulic conductivity data described above provides an important framework for hydrochemical understanding and visualisation.

General groundwater flow characteristics

In general, groundwater flow is considered to be controlled by anisotropic conditions, as described for the HRDs and conductive fractures above. Of the major deformation zones, the NW-SE, N-S and NE-SW trending types are less transmissive than the E-W trending deformation zones, certainly at the regional scale, although such differences may not exist at the local scale (except for the dominating ZSMEW007 deformation zone). Deformation zones ZSMEW002A (Mederhult zone) and ZSMNW042 (along the Laxemar river) are considered as areas of discharge whilst the other major deformation zones show both a recharge and discharge character (Rhén pers.comm. 2008). More difficult to evaluate is the nature of the gently dipping deformation zones which are not directly linked to surface lineaments (cf Section 2.2.2, Figure 2-9).

Dolerite is present as highly fractured dykes, and three of the deformation zones have been modelled as such: ZSMNS001 (30±10 m thick), ZSMNS059A 5±5 m thick) and KLX19_dz5-8 (possibly

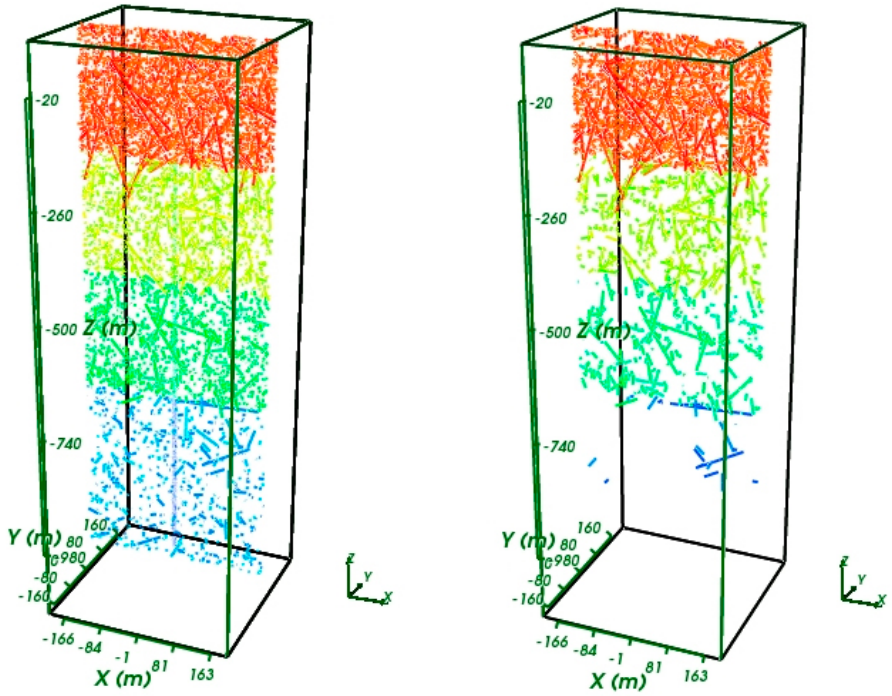

Figure 2-20. *Example of connectivity analysis shown on a vertical (E-W) slice through a DFN simulation of OPO-CP fractures in HRD_C. On the left is a slice through the OPO-CP fractures with all fracture types included. On the right is the network after isolated fractures and fracture dead-ends are removed. The fractures are coloured according to the depth zone in which their centres are generated. /Rhén et al. 2008/.*

5±5 m thick but has no surface expression). Because of its extent and thickness, deformation zone ZSMNS001, located in the west central part of the Laxemar subarea, is of particular interest as it may act as a potential hydraulic barrier; this is supported by interference pump tests carried out in nearby percussion and cored borehole locations (Figure 2-21, /Rhén et al. 2008/).

Although widely believed to be fractured, these dolerite dykes have an impermeable core and permeable contacts to the surrounding wall rock that sustain the groundwater flow. However, the continuity of these impermeable cores and conductive flanks is uncertain.

2.3.4 Palaeohydrogeological issues

A central part of the hydrogeochemical interpretation is the understanding of past climatic events that have influenced the present day groundwater chemistry. In this respect, palaeohydrogeological modelling input, integrated with observed hydrochemical signatures, has helped considerably to recognise and constrain the different climatic scenarios and also to indicate their probable extent within the Laxemar bedrock. In turn, this can help to interpret the hydrochemistry of individual boreholes. These issues are identified and discussed in Chapter 5.

2.4 Surface and shallow model input

The surface and near surface groundwater system in the Laxemar-Simpevarp area has been investigated in detail by the SurfaceNet modelling team /Tröjbom et al. 2008/. This work has been based on a mathematical/statistical approach, involving a large number of visualisations and models to reflect the hydrochemistry in the near surface groundwater system. Models used to explain the geochemical patterns and trends observed include M3 and other multivariate analyses, ion source models and mixing models. The results reveal that the present situation in the surface system reflects the palaeohydrogeology, and these observations have been used to strengthen the overall conceptual model for the Laxemar-Simpevarp area which is described below.

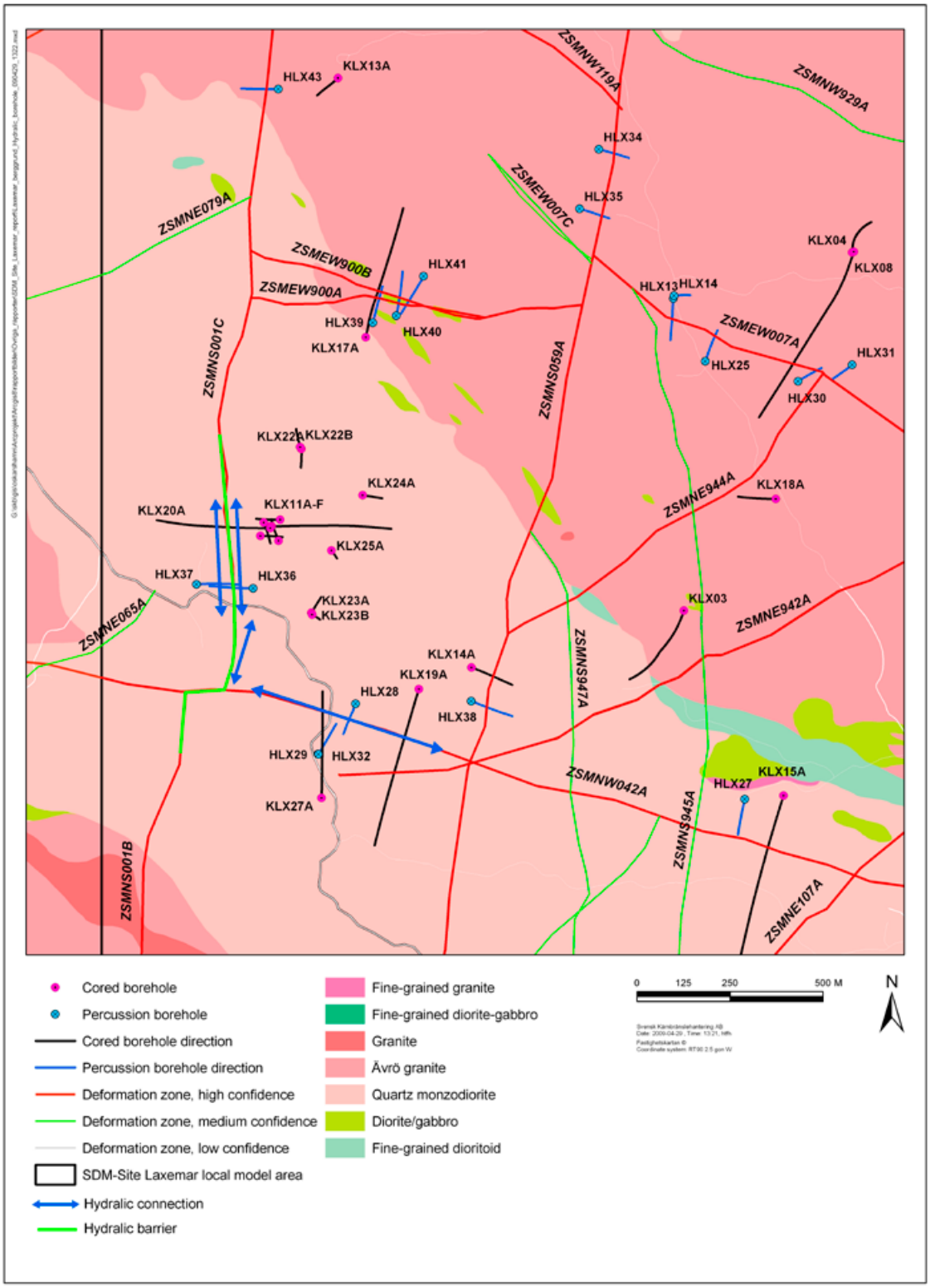

Figure 2-21. *Location of the ZSMNS001 dolerite dyke in the west central part of the Laxemar subarea showing interpreted hydraulic connections and hydraulic barriers /Rhén et al. 2008/.*

The conceptual model suggests that the hydrochemistry observed in the surface system today is partly a consequence of the palaeohydrogeological past. Areas at low elevation close to the coast, which contain marine remnants in the Quaternary deposits, have a significant influence on the hydrochemistry, whereas areas situated at higher altitudes are mostly influenced by atmospheric deposition and weathering processes. In these higher elevated areas, meteoric recharge has a considerable influence on the observed hydrochemistry which is usually characterised by dilute fresh water of low ionic strength. The vegetation cover has also a great hydrochemical impact on the surface system, where degradation of biogenic carbon generates large amounts of H^+ ions which drive weathering processes and ion exchange processes in the Quaternary deposits, as well as in the upper parts of the bedrock. Microbial sulphate reduction is ongoing in the sediments, although this also takes place in the deeper parts of the groundwater system. These conditions, together with inorganic processes and the groundwater flow pattern in the upper part of the bedrock, is responsible for the development of the redox front (maximum penetration depth of oxygen) as exemplified in Figure 2-22.

The meteoric recharge in the western parts of the Laxemar–Simpevarp area gives rise to two different flow systems: a) a shallow young groundwater system which partly discharges towards the east, and b) a deeper/older groundwater pathway which merges with an overall regional flow at greater depth (at about 250 m depth) discharging further east. Recharge into the deeper parts the bedrock takes place close to deformation zones in the higher elevated parts of the central Laxemar-Simpevarp

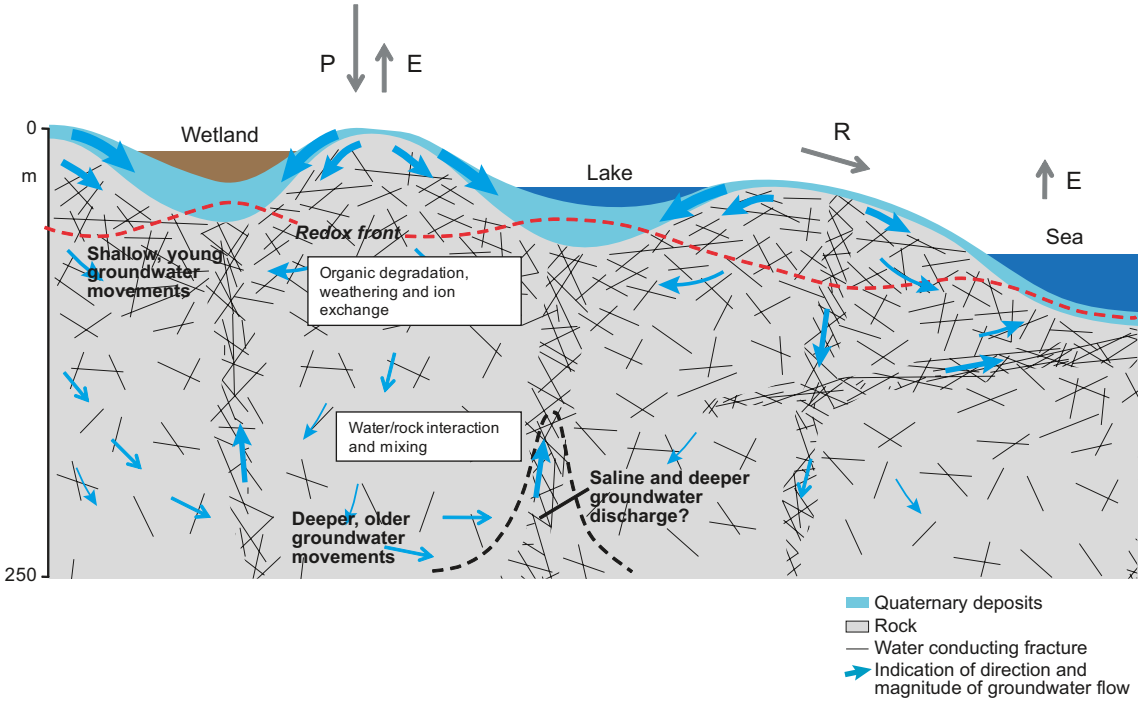

Figure 2-22. *Simplified W-E cross-section of the Laxemar-Simpevarp area illustrating the groundwater recharge and discharge pattern and flow properties from surface Quaternary overburden sediments to the approximately upper 250 m of the bedrock. P = precipitation, E = evapotranspiration, R = runoff. The meteoric recharge in the western area gives rise to two different flow pathways: a) a shallow young groundwater system which partly discharges towards the east, and b) a deeper/older groundwater movement which has an overall regional flow at greater depth (at about 250 m depth). A transition zone, coinciding with a change to lower hydraulic conductivity, is developed at depths of about 200 to 250 m, indicated by the mixing of different groundwater types (old glacial/old meteoric water and brackish water types). Saline waters, together with relict marine waters, possibly mixed with Littorina water, are discharging in the east. (Note that the vertical and horizontal scale for some of the objects in the figure is exaggerated and therefore some observations may not be placed at the correct depth). The redox front indicates the maximum depth of oxygen penetration. Modified after /Werner et al. 2008/.*

area. In low elevated areas in the eastern part, the regional flow is reversed and groundwater discharge from deeper levels is associated with deformation zones located below lakes and brackish basins. The depth variation of the redox front shown in Figure 2-22 is due to the varying recharge/discharge conditions (i.e. the groundwater flow direction along deformation zones), as well as the varying redox capacity of the bedrock and fracture minerals. The figure also shows that oxygenated water tends to go deeper in the fracture zones where the flow is directed downwards, resulting in a lowering of the redox front. This condition is reversed at deformation zones subject to regional discharge.

The interaction between the shallow and deeper groundwaters results in complex mixtures, for example, at greater depths recharged meteoric water is mixed with old glacial/old meteoric water. In addition, along this groundwater flow pathway water-rock interaction processes also take place, adding yet another chemical imprint to these waters. A transition zone is developed at a depth of about 200 m below ground surface over a large part of the Laxemar-Simpevarp area, indicated by different brackish groundwater types. This transition corresponds to a change in hydraulic conductivity at increasing depths whereupon these brackish groundwaters are then mixed with more saline, relict marine waters in areas of discharge to the east within the Simpevarp subarea. Here, local recharge/discharge and development of smaller circulation cells is confirmed by tritium free shallow groundwaters.

In areas of lower topography close to the coast, there are indications of ongoing out-flushing of relict marine waters which have remained in the groundwater since the area was covered by sea water. However, at most locations in the Laxemar-Simpevarp area, this flushing is more or less completed and observed concentrations of marine ions can be explained mainly by wind-blown sea spray deposition and anthropogenic sources, such as road salt /Tröjbom et al. 2008/.

On a regional scale, representing a west-east profile through the Laxemar-Simpevarp area based on a modified version of Figure 2-18 after /Werner 2008/, the following conceptual model may explain the surface and shallow hydrochemistry:

- Meteoric recharge in the area gives rise to two different flow pathways: a) a shallow young groundwater system extending to depths of about 100 m which partly discharges towards the east, and b) a deeper/older groundwater system extending to depths of about 250 m which has an overall regional flow at greater depth and discharges further to the east. The interaction between the shallow and deeper groundwaters results in a complex mixture of different water types, such as mixing with old glacial/old meteoric water in the west and a relict marine component observed in a few percussion boreholes.
- In areas at slightly higher altitudes, which should also have been covered by sea water after the latest glaciation, meteoric isotope signatures and low chloride concentrations indicate that marine influences have been flushed out due to the meteoric recharge.
- In low altitude areas close to the coast, relict marine water prevails in the deeper parts of the deposits and in the upper parts of the bedrock. The high salinity of these relict waters, compared with present Baltic Sea water, in combination with negative values of deuterium excess observed in two soil pipes, indicates that this relict sea water is probably remnant portions of the Littorina Sea stage when sea water with a chloride concentration of approximately 6,500 mg/L infiltrated the overburden deposits and the bedrock.
- In deposits closer to the ground surface in low topography areas, increased chloride concentrations, in combination with meteoric $\delta^{18}O$ isotope signatures, indicate ongoing flushing of the relict marine water (e.g. Littorina).
- In areas located above the highest coastline of the Littorina Sea, there are no indications of relict marine water. Chloride concentrations in these areas can be fully explained by deposition and anthropogenic point sources such as road salt.

Deep saline signatures observed in two soil tubes located in till below thick lake and sea sediments may possibly be explained by the influence of deep groundwater discharge. Both these sites are located in the vicinity of major deformation zones in the area, which have been proposed as potential areas for deep groundwater discharge.

2.5 Evolutionary effects

2.5.1 Background

Palaeohydrogeochemical and palaeoclimatological reconstruction has been a key element and integral part of the SKB site investigation programme since the early 1980s. Considerable advances have been made since then based on a greater geological understanding of Quaternary field evidence and on improved laboratory techniques. Such techniques have led to more quantitative isotopic and major and trace element geochemical evidence of palaeo-indicators from different sources, including groundwaters, rock matrix porewaters and mineral coatings from water-conducting deformation zones. In addition, isotopic systematics have helped determine the residence times of key groundwaters and, indirectly, matrix porewater types, providing a time frame to more quantitatively conceptualise the hydrochemical evolution of the Laxemar subarea. Furthermore, there has been the recognition of an old, dilute meteoric water of a warmer climate origin present before the last glaciation, possibly dating as far back as Tertiary times.

2.5.2 Quaternary evidence

Permafrost

In general, but not always, glaciation is preceded by tundra and then permafrost. Permafrost formation is governed by cold and dry climates where an annual ground temperature of between –5 and –2°C is defined as the boundary for extensive discontinuous permafrost (50–90% of landscape covered by permafrost) and –5°C and colder as the boundary for continuous permafrost (90–100%) /Heginbottom et al. 1995/. However, it is also stated that a large part of the area with continuous permafrost has a ground temperature warmer than –5°C. Sporadic permafrost (less than 50% of landscape covered), may exist when the annual mean temperature is between 0 and –2°C.

As indicated by present day occurrences of permafrost in Greenland and Canada, depths of penetration can reach at least 500 m /Ruskeeniemi et al. 2004/ and take several thousand years to form. In Siberia permafrost extends to 1,500 m depth and more (e.g. /Alexeev and Alexeeva 2003/), but this is considered to represent a very old cumulative effect incorporating input from several glacial periods far back in time. Furthermore, some discontinuous remnants of permafrost from the Weichselian glaciation and the Holocene are believed to exist in northern Fennoscandia /Kukkonen and Safanda 2001/.

Prior to phases of ice sheet coverage at Laxemar, the Weichselian ice sheet had a more restricted configuration. Ice free periods may have occurred several times at Laxemar during the last glacial cycle, for example at 60,000 years before present and between ca 50,000 and 30,000 years before present /SKB 2006d, Näslund et al. 2008, Wohlfarth 2009/. It is therefore likely that the Laxemar site has been subject to permafrost conditions for significant periods of time prior to phases of Weichselian ice sheet coverage /SKB 2006d/.

The impact of permafrost on groundwaters is largely unknown as most evidence has been removed/modified either during permafrost decay coeval with the advancement of the ice cover, and/or subsequently flushed out during deglaciation (cf /Smellie et al. 2008/ and Section 4.11 for discussion). However, the possibility of preservation of such evidence in the matrix porewaters cannot be ruled out (cf /Waber et al. 2009/).

After the last deglaciation

Quaternary climate variations resulted in a number of glaciations in the Northern Hemisphere, including Northern Europe. The last glacial period in northwestern Europe was the Weichselian glaciation and during and after this event an interplay between ice sheet variations and isostatic- and eustatic changes resulted in local changes in shore level displacement /cf Påsse 1997, SKB 2006d/. A detailed description of the development at Laxemar after the last deglaciation, including shoreline displacement and the development of the Baltic Sea, is given in /Söderbäck 2008/, Table 2-1 and summarised below.

Table 2-1. Evolution of the Baltic Sea basin since the last deglaciation /Söderbäck 2008, Follin et al. 2008/.

Baltic stage	Calender year BC	Salinity	Environment in Laxemar
Baltic Ice Lake	13,000 to 9500	Glacio-lacustrine	Covered by ice sheet.
Yoldia Sea	9500 to 8800	Lacustrine/Brackish /Lacustrine	At the rim of the retreating ice sheet.
Ancylus Lake	8800 to 7500	Lacustrine	Regressive shoreline
Littorina Sea (→ Baltic Sea)	7500 to present	Brackish	Regressive shoreline. Most saline period 4500–3 000 BC. Present day Baltic Sea conditions have prevailed during the last ca 2,000 years.

In association with the Last Glacial Maximum (LGM), the Weichselian ice sheet depressed the Scandinavian Shield up to 800 m below its present altitude along the Swedish northern Baltic Sea coast. This was followed by a marked climatic change at about 18,000 years ago, when the ice started to retreat, a process that was completed after some 10,000 years. During this period a major standstill and in some areas the ice front advanced again during the cold Younger Dryas period, ca

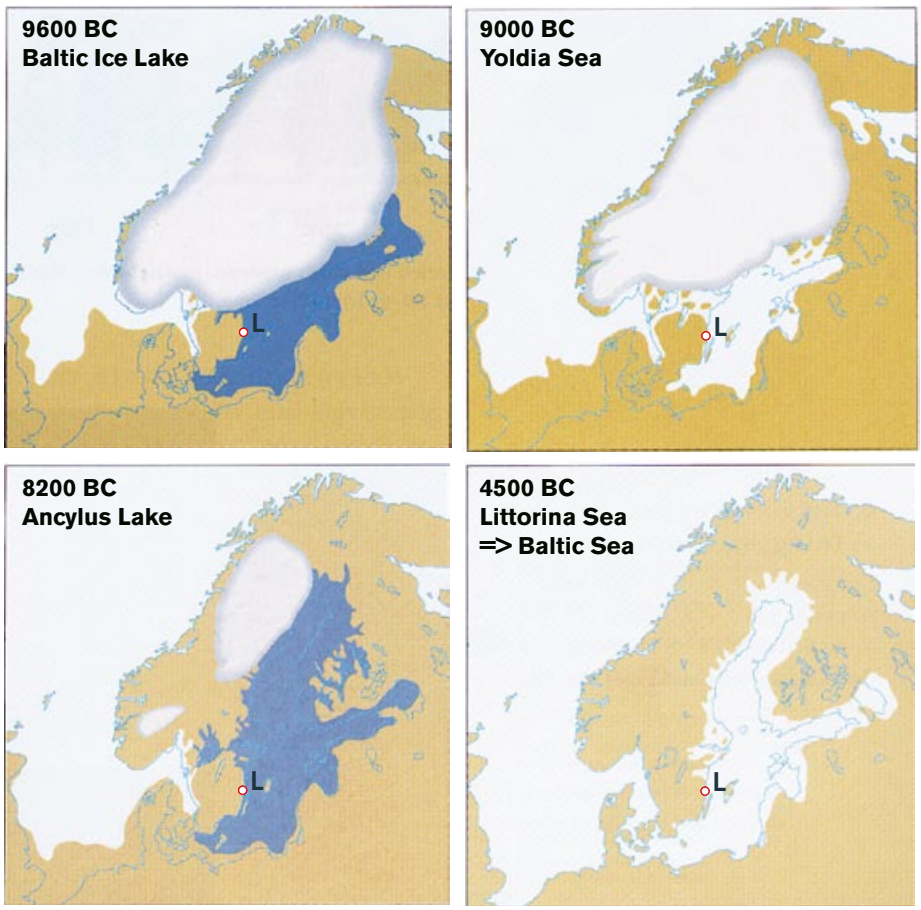

Figure 2-23. *Map of Fennoscandia with some important stages during the Holocene period based on /Follin et al. 2008/. Four main stages characterise the development of the aquatic systems in the Baltic basin since the last deglaciation: the Baltic Ice Lake (13,000 to 9500 BC), the Yoldia Sea (9500 to 8800 BC), the Ancylus Lake (8800 to 7500 BC) and the Littorina Sea 7500 BC–present (the figure shows the maximum salinity at 4500 BC during the Littorina Sea stage). Fresh water is symbolised with dark blue and marine/brackish water with light blue. Laxemar (notated L) was already situated in an ice free area during the Baltic Ice Lake stage.*

13,000 to 11,500 years ago The end of this cold period marked the onset of the present interglacial, the Holocene, whereupon the ice retreated more or less continuously during the early part.

As soon as the vertical stress decreased after the ice recession, the basement and crustal rocks started to slowly rise (isostatic land uplift). This uplift started before the final deglaciation and, importantly, is still an active process in most of Sweden where the current rate of uplift is around 6 to 7 mm per year.

Figure 2-23 shows the aquatic evolution in the Baltic basin since the last deglaciation characterised by a series of brackish and fresh water stages, which are related to changes in sea level. This evolution has been divided into four main stages: the Baltic Ice Lake, the Yoldia Sea, the Ancylus Lake, and the Littorina Sea /Björck 1995, Fredén 2002/. The most saline period during the Holocene occurred approximately 4500 to 3000 BC, when the surface water salinity in the Littorina Sea was 9 to 14‰ compared with approximately 5‰ today in the Baltic Sea /Westman et al. 1999/.

The following sequence of events following the melting and retreat of the ice sheet and conceptualised in Figure 2-24 (compare with Figure 2-23), are thought to have influenced the Laxemar-Simpevarp area.

When the continental ice melted and retreated (i.e. deglaciation stage approximately 18,000 to 12,000 BC), glacial meltwater was hydraulically injected under considerable head pressure into the bedrock close to the ice margin. This is in line with the notion of having wet based ice sheet conditions, i.e. conditions for sub-glacial groundwater recharge, during the last glacial maximum and during the deglaciation /SKB 2006d/. The exact penetration depth of the meltwaters is still unknown, but depths exceeding several hundred metres are possible according to hydrodynamic modelling /e.g. Svensson 1996/. Any permafrost groundwater signatures may have been disturbed or destroyed during this stage, but also may have been preserved in some of the matrix porewaters.

A series of alternating non-saline and brackish lake/sea stages then transgressed the Laxemar-Simpevarp area during the period ca 12,000 to 1500 BC. Of these, two periods with brackish water can be recognised; Yoldia Sea (from 9500-8800 BC), Littorina Sea (from 7500 BC to 3000 BC continuing to the present), and the Baltic Sea (from 2000 BC continuing to the present). The Yoldia Sea, which was present during a relatively short period, is considered to contribute only minor portions of the subsurface groundwater since the water was very dilute to brackish in type from the large volumes of glacial meltwater it contained.

The Littorina Sea period in contrast to the Yoldia Sea transgression had a salinity maximum which prevailed at least from 4500 to 3000 BC; during the last 2,000 years the salinity has remained almost equal to the present Baltic Sea values (/Westman et al. 1999/ and references therein). There are signatures of Littorina water present in the basement groundwaters at Laxemar, although in minor portions as should be expected. Most likely this is due to the fact that: a) the Laxemar subarea was not totally submerged by the Littorina Sea transgression, b) there was restricted access of the Littorina Sea to the Laxemar subarea along the valley systems and this persisted for a relatively short time, and c) the Littorina Sea water in the valleys was diluted continuously by meteoric recharge run-off waters. This resulted in a diluted Littorina end-member water, especially in the inner part of the bays, which limited the density induced intrusion of the brackish marine water into the bedrock. Mixing with the brackish glacial groundwater already present in the bedrock was therefore either non-existent, (i.e. where the land had not been submerged), or at the most weak.

The central and western part of the Laxemar subarea therefore has been dominated by meteoric water recharge during the entire post glacial period. In contrast, the Simpevarp subarea of low topography was only raised above the sea level at about 2000 BC, and therefore has retained a much stronger Littorina Sea component. Many of the natural events described above may be repeated during the lifespan of a repository (thousands to hundreds of thousands of years). As a result of the described sequence of events, brine, glacial, marine and meteoric waters are expected to be mixed in a complex manner at various levels in the bedrock, depending on the hydraulic character of the deformation zones, groundwater density variations and borehole activities prior to groundwater sampling.

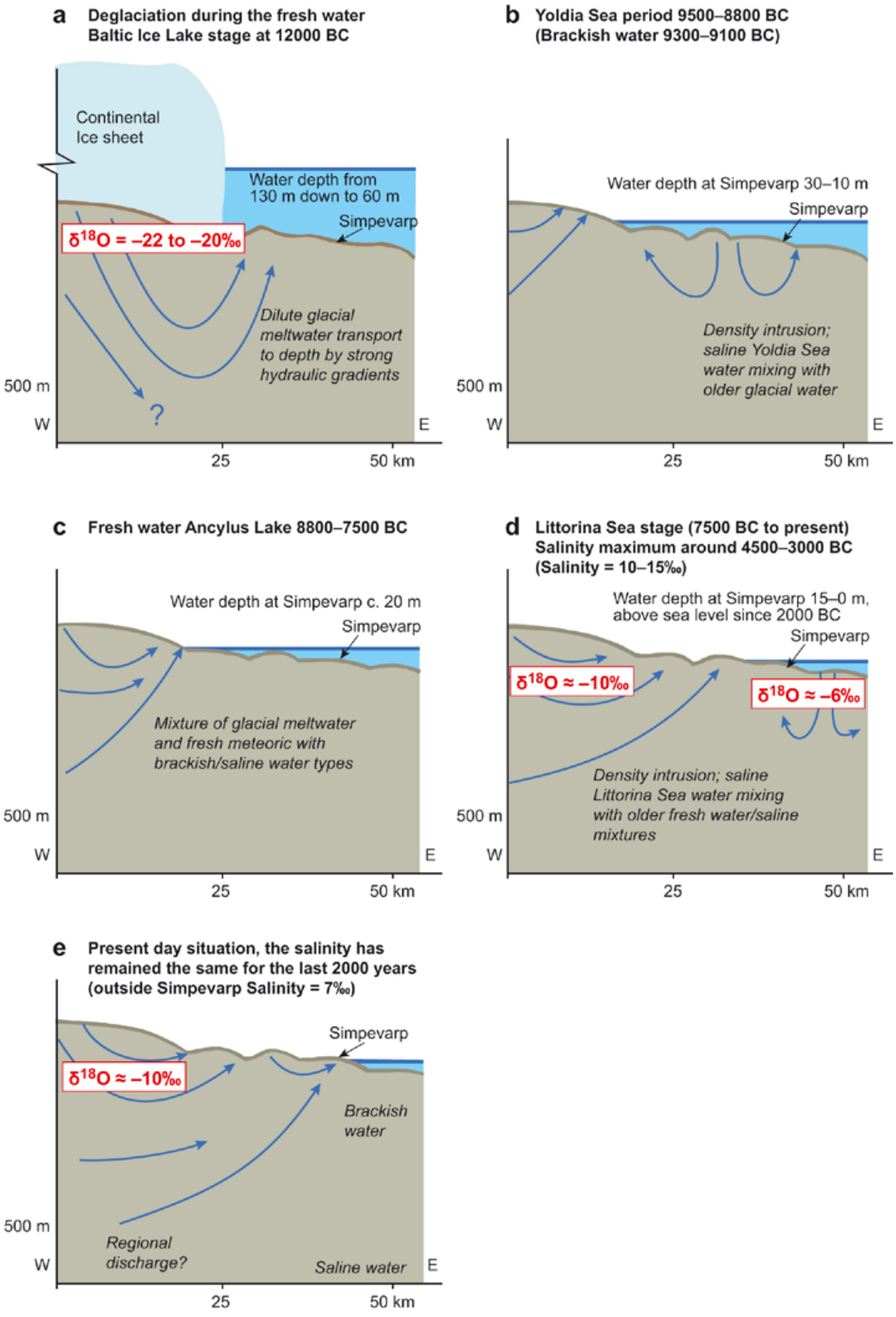

Figure 2-24. *Conceptual model of the period since the last deglaciationl for the Laxemar-Simpevarp area. The different stages are: a) deglaciation and the development of the Baltic Ice Lake (> 12,000 BC), b) the Yoldia Sea stage (9500 to 8800 BC), c) freshwater Ancylus Lake between 8800 to 6500 BC, d) minor portions of Littorina Sea water introduced by density intrusion between 7500 BC to 0 AD, and e) the present day situation. Blue arrows indicate possible groundwater flow pattern.*

2.5.3 Conceptual understanding

Background

The infiltrating water can be glacial meltwater, precipitation, or sea water depending on the prevailing climatic conditions. The hydraulic driving forces, or the density of these water types, together with hydrogeological properties of the bedrock, determine where and how deep the waters can penentrate. Climate change, as well as climate-related phenomena such as permafrost and ice sheets, typically occur as cyclic processes (e.g. /SKB 2006d and references therein/). The result of this is that earlier water types typically are washed out. However, the driving forces and conditions can vary, and residual water types originating from earlier climate periods may be preserved. Extreme conditions, such as the maximum melting of the ice sheet, the most saline sea water, or the longest wet period, provide the best possibility to leave an imprint on the bedrock groundwater. These palaeohydrogeochemical events therefore provide an important framework to understand the hydrogeochemical evolution of the bedrock groundwaters. To only consider scenarios occurring after the last deglaciation, however, can be seriously misleading, especially considering hydrochemical input data to establish boundary conditions for hydrodynamic modelling of the Laxemar subarea. Geochemical data imply that remnants of old glacial water are still residing in low conductive areas at Laxemar. In other words, there is an important groundwater component from before the last deglaciation that has influenced to varying degrees the present day hydrochemistry of the Laxemar-Simpevarp area.

Working hypothesis

In the initial hypothesis for the Laxemar-Simpevarp area /SKB 2004a, SKB 2006b/, the older component from before the last deglaciation was not considered and modelling was based on the post glacial scenario (cf Figure 2-23) which illustrates the most important post glacial phases (cf /Söderbäck 2008/). The post glacial hydrochemical conceptualisation was supported broadly by hydrogeological studies and subsequently integrated into the hydrodynamic models.

The conceptual model at that time considered four key water types that contributed to the Laxemar groundwater system and chronologically comprised: *Deep Saline Water (oldest) > Glacial Meltwater > Littorina Sea Water* (→ *Baltic Sea Water*) > *Present day Meteoric Water (most recent)*. Figure 2-24 illustrates the most important post glacial climatic phases (cf also /Söderbäck 2008/).

This early conceptual model was much improved upon during model version SDM-Site Laxemar, and now includes the recognition of older groundwater components from before the last deglaciation. The four key water types listed above, whilst simplified, essentially still reflect much of the present day understanding although the following major groundwater types, in chronological order, are now recognised: *Highly Saline Water > Saline Water > Brackish Non-marine Water > Last Deglaciation Meltwater > Brackish Marine (Littorina/Baltic) Water > Fresh Water* /Gimeno et al. 2009/ (Note that Last Deglaciation, i.e. the final stage of the last phase of ice sheet coverage, refers to the period 18,000 to 12,000 BC).

The present working hypothesis for the hydrogeochemical site conceptual model therefore recognises that Quaternary evolution has influenced the groundwater chemistry, especially in the most conductive parts of the bedrock. This is not restricted to post glacial time as there is groundwater and porewater evidence that indicates an old, warm climate derived meteoric water component. The age of this component is unknown, but possibilities include certainly pre-Holocene and perhaps pre-Pleistocene or even further back in time. However, irrespective of age the hydrochemistry of the Laxemar area cannot be explained without recognising this older component. The present groundwaters, therefore, are a result of complex mixing and reactions over a long period of geological time. Mixing will be more important in those parts of the bedrock with highly variable hydrogeological properties (and groundwater flow). In other less dynamic parts, the groundwater chemistry will be more influenced by water-rock interaction processes and probably also porewater diffusion exchange.

Conceptual model

The upper part of the basement rocks are dominated by a fresh water (< 200 mg/L Cl) which is found to a depth of about 200 m, although local variations in depth occur over the entire area. The groundwaters found directly below the fresh water are characterised by a mixed water ($\delta^{18}O > -13‰$

VSMOW) with a variation in salinity between 200 to 2,000 mg/L Cl, most likely influenced by mixing, reactions and porewater diffusion exchange with the rock matrix. At greater depths a brackish to saline non-marine groundwater is found, often containing a portion of glacial meltwater which may be partly from the last deglaciation phase, but equally well may be from previous phases of the Weichselian glaciation or even from previous glaciations.

Figure 2-25 and Figure 2-26 illustrate the conceptualisation of the Laxemar-Simpevarp area groundwater system from before the last deglaciation to the present day. In the context of geological time scales, fluid inclusions in calcite of Palaeozoic origin show the presence of very saline (approximately 20 wt%) mainly Ca-Cl fluids /Drake and Tullborg 2009a/. It can be assumed, therefore, that during the Late Palaeozoic several kilometre thick piles of marine and terrestrial sediments covered the Precambrian Shield area of south-east Sweden, including a series of sandstones, limestones and shales. During this period, brine solutions were most likely formed due to leaching of salt inclusions and possibly evaporties, allowing very highly saline waters to slowly penetrate and saturate both the fractures and eventually the interconnected pore spaces in the underlying crystalline bedrock (Figure 2-25).

Figure 2-26 shows a tentative distribution of groundwater types and salinity gradients in the Laxemar-Simpevarp area before the intrusion of the last deglaciation meltwater just prior to the Holocene. Based on an understanding of the climatic changes that have occurred since the last deglaciation, it is logical to presume that there must have been at this time old meteoric waters comprising components derived from both temperate and cold climate events. These waters would have intruded the bedrock and have had long times to interact with the minerals and porefluids. Assuming there were favourable gradients, old meteoric waters could have been partially mixed with deeper, more saline groundwaters, but the high density contrast would have prevented further mixing. What can be said with confidence is that the residual old brackish waters present today in Laxemar do not have a marine signature. In the early post glacial secenario, glacial meltwaters initially penetrated the basement rock, possibly mixing with remnant old Glacial (and Old marine) waters. This was followed by an intrusion of minor portions of brackish marine waters during the subsequent Littorina Sea stage. Finally, during the last 4500 to 2000 BC the basement rock was exposed to meteoric water recharge, as exemplified in the upper part of Figure 2-26.

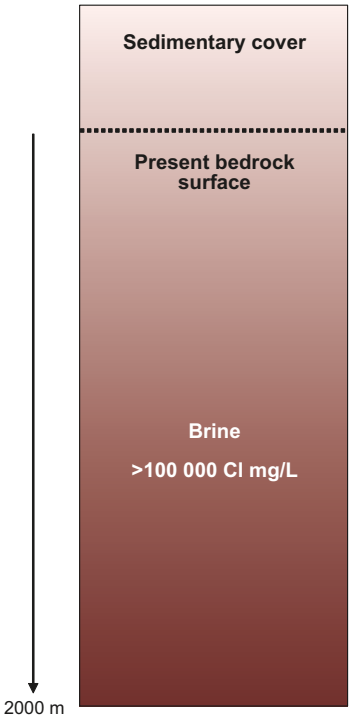

Figure 2-25. *A simplified sketch of the groundwater situation during the Late Palaeozoic (250 Ma) when the Laxemar-Simpevarp area was covered by large thicknesses of marine and terrestrial sediments. The brine component increases with depth /Cederbom et al. 2000/ and the sedimentary thickness in this illustration is underrepresented to emphasise the groundwaters*

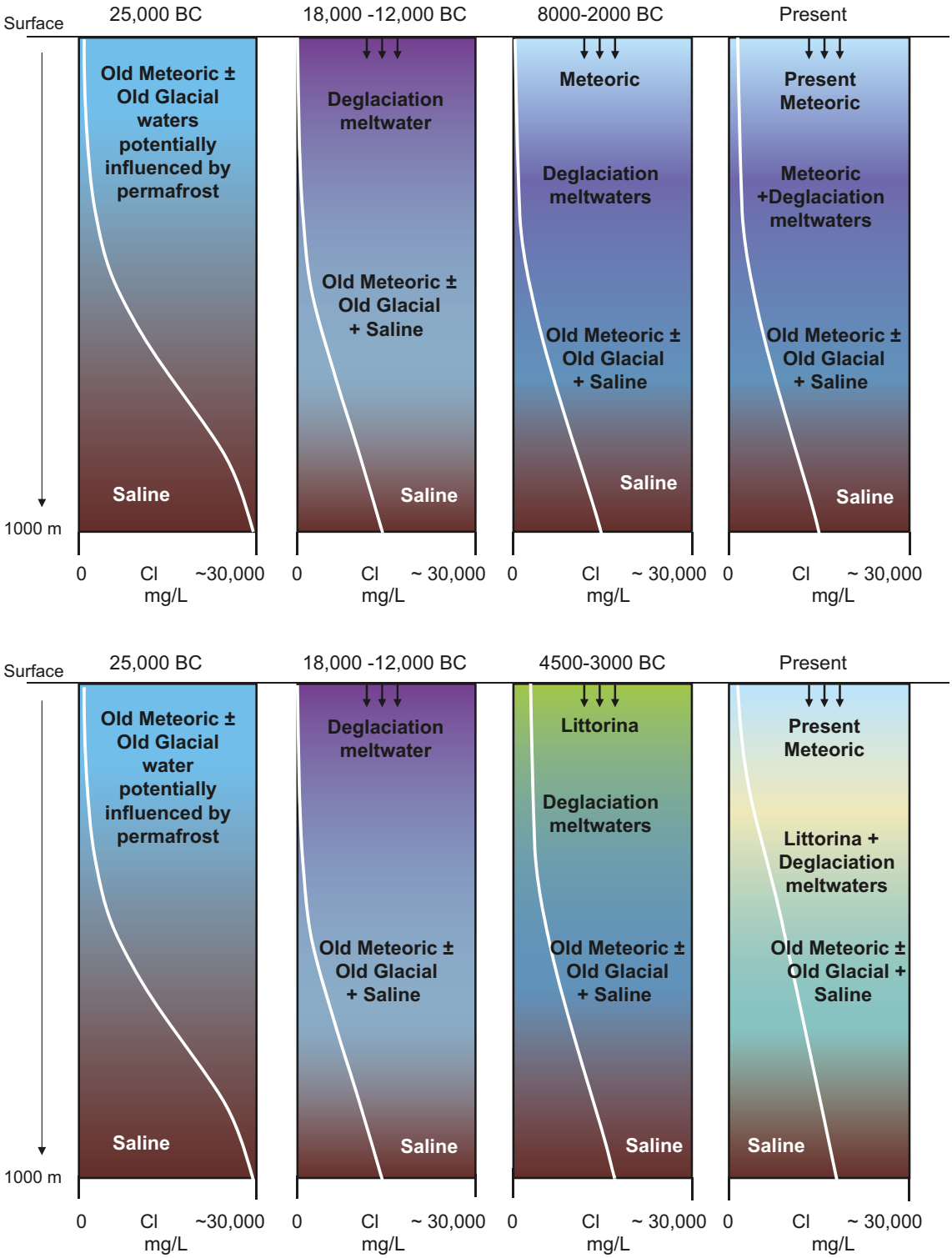

Figure 2-26. *Sketch showing tentative salinities and groundwater-type distributions versus depth for the transmissive zones in the Laxemar subarea. Two different scenarios are outlined; the upper series representing areas not covered by the Littorina Sea, and the lower series representing areas submerged by the Littorina Sea for a period long enough to influence the groundwater. The upper series shows from left to right: 1) the situation prior to the last deglaciation, 2) last deglaciation and intrusion of Late Weichelian meltwater, 3) meteoric recharge, and 4) the present situation. The lower series shows: 1) the situation prior to the last deglaciation, 2) last deglaciation and intrusion of Late Weichelian meltwater, 3) intrusion of brackish marine (Littorina Sea) water, and 4) the present situation.*

The present situation is shown in Figure 2-26, where recharge and subsequent mixing of the groundwaters took place during the deglaciation and the post glacial period. At the Laxemar subarea two different scenarios are applicable depending on whether or not the actual surface was covered by the Littorina Sea. The time period of submergence below sea level and the variation in salinity of the brackish sea water during post glacial time are important factors controlling the intrusion of the brackish marine (Littorina) waters. Subsequent flushing of meteoric waters commenced during land uplift above sea level which established hydraulic gradients and is continuing to the present day. Today, part of the recent glacial water can be identified as a minor component in the bedrock. Further conceptual development of the Laxemar-Simpevarp area, for example, the land uplift processes, are described in /Söderbäck 2008, Tröjbom et al. 2008/.

3 Hydrogeochemical data

3.1 Databases

The SDM-Site Laxemar hydrochemistry evaluation is based on the 'Extended data freeze Laxemar 2.3' of December 4th, 2007. These data were compiled and their quality checked in February 2008, and the resulting 'internal' dataset was used both for the hydrogeochemical modelling and for delivery to HydroNet. Minor edits and updates were carried out in May 2008 and this version represents the final 'Extended data freeze Laxemar 2.3' dataset used in the SDM-Site Laxemar hydrogeochemistry modelling. Additional data, for example from borehole KLX27A, were compiled in October 2008 but only used for comparison purposes and as partial support in the construction of the conceptual visualisations. All datasets are stored in the Simon database.

The datasets used in the SDM-Site Laxemar hydrochemistry evaluation include all relevant data in the Simpevarp and Laxemar subareas together with available information from Äspö (before tunnel construction). The Sicada database contains complete hydrogeochemical analyses including microbes, colloids and gas analysis, and porewater analyses from bedrock samples. Quality assessment of the Laxemar-Simpevarp data is documented in /Smellie and Tullborg 2009/ together with reference to earlier evaluated Äspö and Ävrö data. Groundwater data from other Nordic sites and SFR (Final Repository for Radioactive Operational Waste) have been used on occasions for comparison (e.g. /Gimeno et al. 2009/).

3.2 Borehole groundwater chemistry data

The locations of the percussion and cored boreholes in the Laxemar subarea are shown in Figure 3-1; a total of 46 cored and 43 percussion boreholes have been drilled. Twenty cored boreholes and 19 percussion boreholes were sampled for hydrochemical evaluation, and of the cored boreholes 6 were sampled also for gases, 5 for microbes and 4 for colloids.

Table 3-1 summarises the type and number of samples included in the dataset for the Laxemar and Simpevarp subareas and the data freeze at which they were delivered /Gimeno et al. 2009/.

Table 3-1. Number of sampling points and types of sample categories included in the final 'Extended data freeze Laxemar 2.3' for the Laxemar-Simpevarp area. The different rows indicate the number of new samples delivered at each data freeze (2.1, 2.2 and 2.3) or updated existing samples between one data freeze and the next (2.1–2.2 and 2.2–2.3). No supplementary data from existing samples in Laxemar 2.1 and 2.2 were added after the final 'Extended data freeze Laxemar 2.3'. The numbers in the table indicate the total number of sampling points and then after the slash, the number of these samples which have category 1, 2, 3, or 4. (Perc. Bhs: percussion boreholes; Cored Bhs: cored boreholes; NSGW: near surface groundwaters; Precip: precipitation).

		Perc Bhs.	Cored Bhs	Tube sampling	NSGW	Sea Water	Lake Water	Stream Water	PRECIP.
Laxemar 2.1	Äspö	14/5	137/21						
	Ävrö		61/3						
	Laxemar	15/5	122/12	35/2	45/39				
	Simpevarp	10/2	15/3	10/0	53/38	54/31	230/186	553/335	
Laxemar 2.1 –2.2	Ävrö	9/4	4/0						
	Laxemar	5/3	39/7	64/0	4/4				
	Simpevarp		11/5	20/0	37/22	289/124	17/15	38/32	2/2
Laxemar 2.2.	Ävrö		3/0						
	Laxemar	14/6	49/4	46/5					
	Simpevarp		10/2		68/60	67/29	34/34	64/63	3/3
Laxemar 2.2–2.3	Laxemar	3/3	26/6	17/2					
	Simpevarp		2/2		8/6	4/2	2/2	6/6	3/3
L.axemar 2.3	Laxemar	1/1	46/9	4/0					
	Simpevarp				27/21	24/11	13/13	33/31	1/1
Total		71/29	525/74	196/9	242/190	438/197	296/250	694/467	9/9

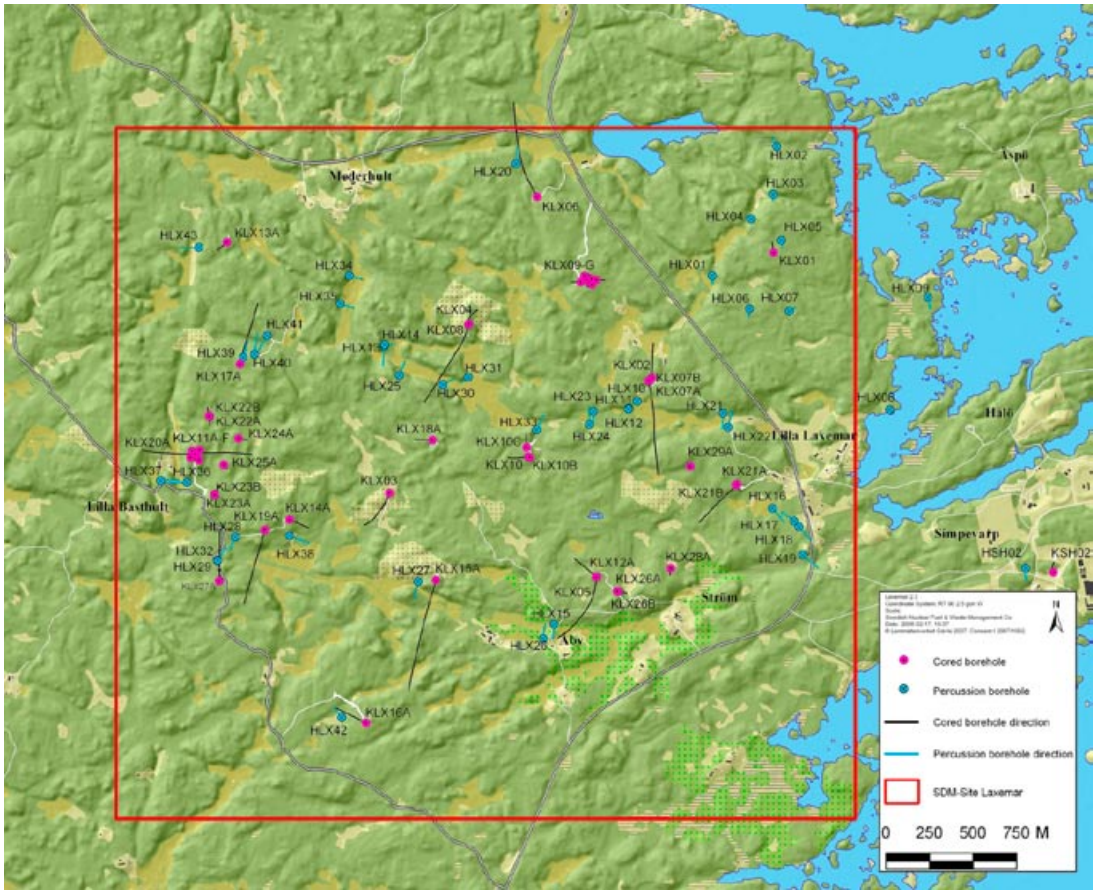

***Figure 3-1**. Location of the drill sites and boreholes within the Laxemar subarea.*

3.3 Quality assured data

3.3.1 Hydrochemical data

The 'Extended data freeze Laxemar 2.3' groundwater dataset has been evaluated systematically with respect to quality, and an assignment of different categories made regarding their value for further hydrogeochemical interpretational work /Smellie and Tullborg 2009/. This was based on an integrated geological, hydrogeological and hydrochemical approach. A separate small-scale feasibility study of some selected borehole sections was made to determine the possibility of further quantifying the effects from drilling and pumping /Gascoyne and Gurban 2009/, but this did not affect the categorisation of the dataset. Of the five categories chosen, Categories 1–3 primarily meet the requirements of hydrogeochemical (but also hydrogeological) modelling, Category 4 primarily meets hydrogeological requirements (but may also be of use for more qualitative hydrogeochemical modelling with caution), while Category 5 generally needs to be used with great caution in the context of both hydrogeochemistry and hydrogeology, in particular the tube sample data. A colour code was introduced to quickly distinguish between sample quality when, for example, data are presented in spread-sheet tables or as symbols in scatter plots. In the database, the classification category is indicated numerically in a separate column in addition to the colour coding. An outline of the classification into the various categories for the cored boreholes is presented in Table 3-2. The number of samples and the allocated category are listed in Table 3-3 and the complete tables are stored in the SKB model database Simon.

Table 3-2 lists the most important criteria used to categorise the groundwater samples. For example, a Category 1 sample has < 1% drilling water, adequate time-series data to assess groundwater chemical stability when sampled, an adequate section length based on the hydraulic properties of the borehole, a charge balance within ± 5%, complete major ion and isotope data, a good coverage of trace elements and, finally, no evidence of short circuiting either within the borehole around the packed-off section or between different fracture systems in the surrounding bedrock. Ideally, these Category 1 groundwaters should also cover microbes, colloids, organics and gases, but these have not been routinely sampled at all occasions and also require different evaluation criteria. In comparison, a Category 3 sample may have some of the Category 1 criteria but will differ in failing

Table 3-2. Classification criteria for cored boreholes /Smellie et al. 2008, Smellie and Tullborg 2009/.

Cored boreholes	Category				
Aspects/conditions	1	2	3	4	5
Drilling water (≤ 1%)	x	x	x	x	x
Drilling water (≤ 5%)		x	x	x	x
Drilling water (≤ 10%)			x	x	x
Drilling water (> 10%)				x	x
Time series (adequate)	x	x	x	x	x
Time series (inadequate)			x	x	x
Time series (absent)				x	x
Suitable section length	x	x	x	x	x
Sampling during drilling				x	x
Sampling using PLU hydraulic testing equipment			x	x	x
Tube sampling					x
Charge balance ± 5% (± 10% for < 50 mg/L Cl)	x	x	x	x	x
Major ions (complete)	x	x	x	x	x
Major ions (incomplete)			x	x	x
Environmental isotopes (complete)	x	x	x	x	x
Environmental isotopes (incomplete)		x	x	x	x
Hydraulic effects (short circuiting)					x

to satisfy all the criteria. For example, the sample may be characterised by inadequate time series data and/or > 5% drilling water. At the other extreme, a Category 5 sample may still record < 1% drilling water and have a complete set of analytical data, but fail to meet several or all of the other criteria, for example, long sampled section, inadequate time-series data and influenced by short circuiting effects etc. Type samples in this category include those collected during drilling and using the PLU hydraulic testing equipment. Almost all samples of tube sample origin also fall within this category because of open hole mixing effects.

It should be noted that the amount of uranine spiked water used for drilling is based on an average value of the uranine. This introduces a degree of uncertainty which may influence the calculated percentage of drilling water for any one borehole section sampled for groundwater. However, this is not considered to be at a level to negatively influence the categorisation procedure.

The main criteria used to categorise the groundwaters sampled from percussion and cored boreholes are:

Category 1 Samples: Characterised by adequate time-series data (i.e. stable chemistry recorded over a suitable time period of days to weeks) and accompanied by complete analytical data (i.e. particularly all major ions and environmental isotopes), a charge balance of ±5%, and less or close to 1% drilling water. In addition, reliable redox values, a good coverage of trace elements (including U, Th and REEs) and, if possible, microbe, organic and dissolved gas data, is also recommended. Note, however, that the quality of these parameters is not considered in the categorisation process because they require a different set of criteria.

Category 2 Samples: Of similar quality to Category 1 but marked by incomplete analytical data (usually restricted to an absence of ^{14}C and $\delta^{13}C$ and less trace element, microbe, organic and gas data) and/or with elevated concentrations of drilling water (1 to 5%).

Category 3 Samples: This category differs from Categories 1 and 2 in terms of inadequate time-series data, time-series data that indicate instability during sampling, incomplete analytical data (such as absence of some isotopic and trace element data, microbe, organic and gas data, and redox values), and elevated drilling water concentrations (5 to 10%).

Category 4 Samples: Analyses are mostly restricted to Cl, Br, $\delta^{18}O$, Mg, HCO_3, Na, Ca and SO_4, elevated drilling water concentrations (> 10%), and absence or very incomplete time-series data. Type samples are often of an exploratory nature, i.e. mostly taken to see if there is adequate water volume and to check strategic indicators such as drilling water content, salinity (electrical conductivity) ± pH ± major ions (Cl, Br, SO_4, HCO_3) ± $\delta^{18}O$. Some samples taken during drilling and those sampled using PLU hydraulic testing equipment also fall within this category.

Category 5 Samples: Samples with some major ions or $\delta^{18}O$ missing, no charge balance values, elevated drilling water concentrations (> 10%) and absence or very incomplete time-series data. Type samples in this category include those collected during drilling and sampled using the PLU hydraulic testing equipment. Almost all samples of tube sample origin also fall within this category because of open hole mixing effects. Note, however, that in some cases the uppermost tube sample (usually near surface groundwater from zones of high hydraulic conductivity) and the deepest sample (usually the most saline accumulation due to density constraints) may be quite representative.

The highest quality data are required, for example, for geochemical equilibrium calculations, modelling of redox conditions, and reliability for specialised studies involving microbes, organics and colloids. On the other hand, overall site understanding (e.g. groundwater distribution, origin and evolution and its integration with hydrogeology) is adequately addressed by a combination of all categories with the obvious proviso that the higher the category number of data used, the more caution is required in their interpretation.

As a general rule, samples classified as category 1 to 4 data have been used mainly in the presentation and interpretation of the SDM-Site Laxemar modelling. However, there are occasions where it can be very helpful to plot initially all data, for example, for ^{18}O and tritium, to obtain a general impression of site behaviour and follow this up using only category 1 to 3 or 1 to 4 data to quantify interpretation and description. On other occasions, it is important to trace the evolution of a specific analysis over the set time period of sampling, and for this the whole time series of measurements have been used to derive, for example, field measurements of pH and Eh which may not be available for the actual sample selected as being most representative hydrochemically. The lack of such field data has reduced very much the available set of samples for speciation-solubility calculations.

Analysed data include the same parameters chosen in the previous Laxemar.2.1 hydrogeochemical model version. The pH, Eh, temperature and electrical conductivity values used in this report are those determined in the field when available (from Chemmac logs). In the remaining cases, laboratory determinations have been included in the table but not used for modelling purposes.

In order to observe the effects or consequences of using a selected set of category 1 to 3 or 1 to 4 samples instead of all samples, a comparative analysis has been made. Figure 3-2 plots all the samples, i.e. including samples from category 5 and also time-series samples. The main conclusions from this comparison are that:

- In most cases, the absence of category 5 samples greatly enhances the general trends derived from the category 1 to 4 samples. In some cases, however, the presence of category 5 samples serves to cover the gaps when there is a shortage of higher quality category 1–4 samples.
- Samples corresponding to the time-series measurements (open symbols in Figure 3-2) usually plot at the same position as the samples selected as representative for the sampled section. For example, in the case of chloride or sodium (Figure 3-2a and b), i.e. indicative for the major ions, the differences found related to different samples taken from the same depths are negligible.
- For ferrous iron and sulphide and including trace elements in general, samples based on time-series measurements (and the monitoring programme) usually show a range of variation which could be expected as they are very sensitive to sampling procedures.
- Samples categorised as 5 include tube samples, samples collected during drilling and samples generally with high drilling water content.

Table 3-3. Number of samples from percussion and cored boreholes allocated to each category up to and including the 'Extended data freeze Laxemar 2.3'.

Category	1	2	3	4	5
Percussion boreholes	0	0	6	12	3
Cored boreholes	2	3	18	23	242

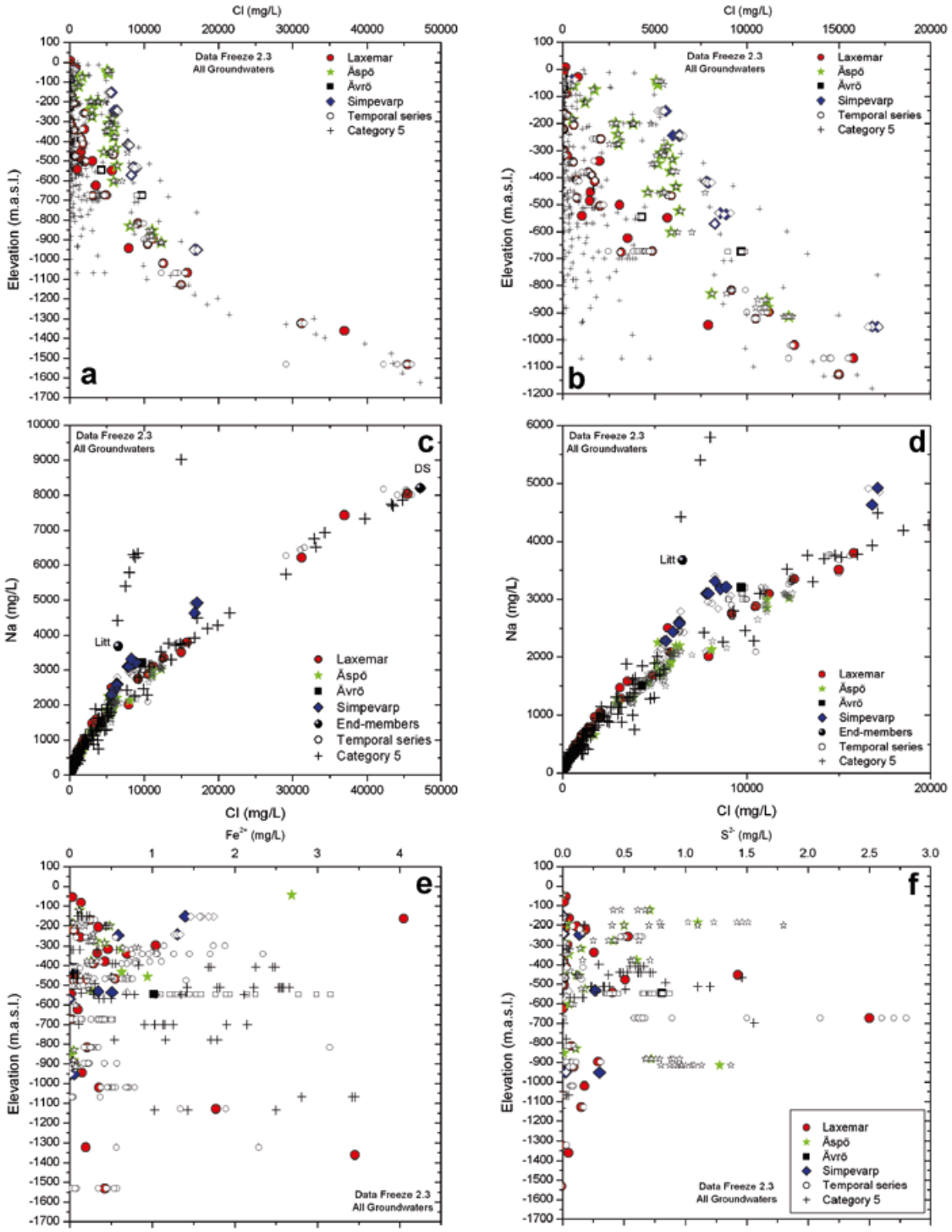

Figure 3-2. *Examples of trends shown by groundwaters representing all sample categories (1 to 4 are colour coded) and including time-series variations. Plots (b) and (d) are the same as (a) and (c) respectively, but with the x-axis scale enlarged to better visualise the shallow to intermediate depths /Gimeno et al. 2009/.*

3.3.2 Microbiological data

For microbiological field investigations, in common with colloids (cf Section 3.3.3), gases (cf Section 3.3.4) and generally with most trace components, the sampling of good quality groundwaters has been overshadowed to a degree by their sensitivity to drilling and sampling activities. In cases this has resulted in uncertainties due to suspected contamination caused by, for example, pumping rates, artefacts from drilling, insufficient sampling time, short circuiting during sampling etc.

During the drilling of boreholes used for microbiological sampling a thorough cleaning and sterilisation programme was applied /Pedersen 2005/.The effectiveness of this programme was tested during each drilling operation in the Forsmark site investigation studies. This was conducted by analysing the TNC, ATP and the number of cultivable aerobic heterotrophic bacteria (CHAB) in the drilling water. It has previously been demonstrated at the Äspö Hard Rock Laboratory (HRL) that contamination of groundwater by drilling water does not create a sustained contamination of the intersected aquifers /Pedersen et al. 1997/. In line with these results, a correlation could not be demonstrated between the amount of drilling water in the samples and any of the microbiology parameters measured in the Forsmark site investigation samples /Hallbeck and Pedersen 2008b/. The quality and reproducibility of the applied methods for microbiological analyses were tested and are discussed in detail by /Hallbeck and Pedersen 2008b/. The reproducibility of all analyses was found to be within the standard deviation of the methods used. The analysis of TNC and ATP has been demonstrated to agree and to give reliable results on numbers and biomass in Fennoscandian shield groundwaters /Eydal and Pedersen 2007/. The analysis of TNC, ATP, CHAB and MPN as conducted on the Forsmark groundwater samples was applied in parallel on 60 independent groundwater samples from between 3.9 and 450 m depth in Olkiluoto, Finland /Pedersen et al. 2008/. Significant correlations were found between groundwater chemistry and borehole conditions with cultivable numbers, diversity and biomass, suggesting a mutual dependency between microbiological processes and the groundwater geochemistry. In conclusion, the analysis of microbiology in the Laxemar subarea was based on a solid scientific basis with methods that were well established, quality assured and published in peer-reviewed scientific journals.

3.3.3 Colloid data

The primary silicon data were excluded for borehole KLX15A:–467 m elevation because of likely sampling artefacts. The groundwater from this section was also analysed by fractionation which indicated a high aluminium content, but no filtration had been done. The high numbers of colloids found in this sample were also most likely due to sampling artefacts. All other available data were used in the evaluation.

With respect to calcite and sulphur, the calcite values were subtracted from the total amount of colloids, while the sulphur values were not recalculated as pyrite because this phase could not be confirmed. Sulphur is therefore represented as that recorded in Sicada. Calcium and sulphur colloids are commonly regarded as pressure-drop related and their actual concentrations in the sampled groundwater can not be safely inferred from the data.

3.3.4 Gases

The sampling of gas was performed using a PVB pressure vessel which has occasionally been linked with some leakage problems of pressure gas into the sample. This elevates the argon or nitrogen concentration of the sample being collected /Hallbeck and Pedersen 2008b/. There are two possibilities to track such effects which were tested during the Forsmark investigations. One way is to use two PVB samplers, one with nitrogen and the other argon. The result from this sampling showed that the volume of argon was higher in the argon filled sampler and the nitrogen was higher in the sampler filled with nitrogen because of leakage in the sampler equipment. By using the two corrections the volume and the gas composition in the groundwater could be calculated. This contamination effect becomes almost impossible to compensate for in the calculations of gas concentrations unless two samples are taken every time (not done in the present study), because the degree of contamination for one of the two gases will remain unknown. Presently, the best possible way is to judge a sample result in relation to several other results for samples from similar depths. A large discrepancy between a particular sample result and the average result for samples from the same depth region

indicates a sampling artefact. These samples contain more nitrogen, and also more total gas, than do all other samples in relation to depth, which may suggest leaking PVB vessels. Consequently, all other gases in these potentially contaminated samples were diluted resulting in an underestimate of the actual values. Stable isotope data concerning nitrogen (and the other gases) would have helped to confirm or reject whether nitrogen contamination from the pressure vessel was a problem.

During the extraction process there were problems with air entering the sample, subsequently confirmed by the presence of oxygen. Data reported in Sicada are not corrected for this air leakage into the samples; the data used, however, are corrected for such leakages using the dissolved content of oxygen as an indicator. The oxygen could originate either from the sampling vessel or from gas extraction and analysis in the laboratory. As deep groundwaters generally contain ferrous iron and sometimes sulphide, oxygen should not be present because these two ions are not stable in oxidised water.

The analytical precision around 20% was established on samples from Forsmark. The same precision is assumed to be valid for Laxemar gas samples.

3.3.5 Questionable data

Some data appear to be reasonably representative but they may still reflect a wide range of possible influences on groundwater flow conditions. These include; a) limited hydraulic short circuiting effects during sampling, b) small scale contamination from different borehole activities, and c) induced mixing over large distances by long term draw-down hydraulic pumping tests and dilution and tracer tests. Some issues of concern were identified, which included:

- The hydraulic tracer test programme from 2003 to 2007 involved at different stages the injection of uranine (and additionally caesium and rubidium in six tests). In some of the sampled groundwaters, especially from monitoring sections, this has resulted in an increase of uranine, which may be incorrectly interpreted as an artefact of the introduced uranine during initial drilling of the boreholes. Furthermore, in some of the monitoring samples there were anomalous increases in caesium. This was investigated and the tested borehole sections identified and documented /Smellie and Tullborg 2009/.
- Low but detectable tritium contents (around one or a few TU) have been detected at varying depths in the Laxemar subarea, in many cases where it would not otherwise be expected. In cases where contamination due to excess drilling water or normal tritiated shallow formation groundwaters could be excluded, the risk of artificial contamination, therefore, had to be addressed. The problem was subsequently found to have originated from a leakage of tritium from the down-hole pumping equipment where high tritium in deionised water is occasionally used during routine Complete Chemical Characterisation (CCC) sampling. *In situ* production of tritium in the bedrock and laboratory contamination were considered less probable.
- During sampling, fracture networks intersecting the boreholes may lead to short circuiting of the groundwater flow in the surrounding bedrock and also to bypassing the packer systems used to isolate the borehole sections being sampled. This effectively means that the section sampled may have been supplied by mixed groundwaters from higher or lower levels in the bedrock, and/or mixed borehole waters above or below the packer systems. In both cases, the sampled groundwaters when interpreted in isolation may be evaluated erroneously as being of high quality.

Each of these issues was addressed in detail during the quality evaluation of the data and appropriate action taken in the categorisation process /Smellie et al. 2008, Smellie and Tullborg 2009/.

4 Explorative analysis and modelling

Explorative analysis involves an initial general examination of the groundwater data using traditional geochemical approaches to describe the data and provide an early insight and understanding of the site, i.e. the construction of a preliminary conceptual model for the area (cf Section 2.5.3). Based on this hydrochemical framework, selected data are further evaluated using different modelling approaches such as data evaluation and visualisation, mixing modelling, geochemical equilibrium modelling, redox modelling and evaluation of microbes, colloids and gases.

The computer codes that were used in the hydrogeochemical evaluation are listed below.

- PHREEQC: Code for calculations of chemical equilibrium, reaction, advective transport and inverse modelling /Parkhurst and Appelo 1999/. Thermodynamic data base: WATEQ4F /Ball and Nordstrom 2001/, distributed with the PHREEQC code, with some modifications (cf details in /Gimeno et al 2009/).
- M3: Mixing and mass balance calculation program /Laaksoharju et al. 1999, Gómez et al. 2006, Gómez et al. 2009/.
- CORE^{2D}: Coupled hydrochemical/hydrogeological modelling code /Samper et al. 2000/.
- OpenDX: 3D visualisation (IBM Open Visual environment, OpenDX) free code available over the Internet.

Studies of fracture fillings, composition of the porewaters in the bedrock and groundwater residence times also provide important information for the site description /Drake and Tullborg 2009a, Waber et al. 2009/. The background data, the explorative analysis and the modelling of the hydrochemical data are detailed in the sections below and in /Gimeno et al. 2009, Hallbeck and Pedersen 2009, Kalinowski 2009/.

During the explorative analyses of the groundwaters explorative analyses it became apparent that a subdivision of the sampled groundwaters into six major groundwater types would facilitate the description and interpretation of the figures and diagrams. Based on the conceptual understanding of the Laxemar-Simpevarp area, this subdvision has been based on three of the most important hydrochemical signatures i.e. Cl, Mg and $\delta^{18}O$. The major groundwater types distinguished are; *Fresh*, *Brackish Glacial*, *Brackish Marine*, *Brackish Non-marine*, *Saline* and *Highly Saline*. In addition, two groundwater types were included to accommodate important mixing processes resulting from anthropogenic and/or natural processes: a) a shallow near surface '*Mixed Brackish*' type mainly comprising fresh and brackish glacial (sometimes with a weak marine component) groundwaters, and b) a deeper '*Transition'* water type mainly comprising degrees of mixing between brackish glacial or brackish non-marine groundwaters with a brackish marine water component. This subdivision into different groundwater types corresponds to that used in the conceptual visualisation (cf Chapter 6). The main chemical and isotopic character of each groundwater type, and their respective colour coding used for plotting and in the site descriptive visualisations, can be summarised as follows:

Fresh

Water type: Fresh (< 200 mg/L Cl; < 1.0 g/L TDS); Mainly meteoric in origin, i.e. Na(Ca)-$HCO_3(SO_4)$ in type, $\delta^{18}O$ = –11.5 to –9.8‰ VSMOW.

Mixed Brackish (Not a specific groundwater type)

Waters of mixed Fresh ± Brackish Glacial (± Brackish Marine) origin (200–2,000 mg/L Cl; 1.0–3.5 g/L TDS); it is usually sampled at 20–150 m depth and may be the result of natural and/or anthropogenic mixing during drilling activities and sampling.

Brackish Glacial

Water type: Brackish Glacial (200–10,000 mg/L Cl; < 1.0–18 g/L TDS); $\delta^{18}O \leq$ –13.0‰ VSMOW). Last Deglaciation meltwater + Brackish Non-marine to Saline component; Ca-Na-Cl (SO_4); Mg < 25 mg/L; $\delta^{18}O$ < –13.0‰ VSMOW.

(It may also occur with a weak marine (Littorina) component in the Simpevarp subarea; Na-Ca-Cl (SO_4); Mg > 25 mg/L; $\delta^{18}O$ < –13.0‰ VSMOW).

Brackish Marine

Water type: Brackish Marine (2,000–6,000 mg/L Cl; 3.5–10 g/L TDS; Mg > 100 mg/L); variable Littorina Sea component (± modern Baltic Sea) + Last Deglaciation meltwater ± Brackish Non-marine to Saline component; Na-Ca-Mg-Cl-SO_4; $\delta^{18}O$ > –13.0‰ VSMOW.

Transition zone (Not a specific groundwater type)

Transition type representing a mixture of Brackish Glacial and/or Brackish Non-marine groundwaters with a variable component of Brackish Marine. These waters range from 2,000–10,000 mg/L Cl and from 25–100 mg/L Mg; $\delta^{18}O$ > –13.0‰ VSMOW. They may be the result of natural and/or anthropogenic mixing during drilling activities and sampling.

Brackish Non-marine

Water type: Brackish Non-marine (3,000–10,000 mg/L Cl; 5–18 g/L TDS; Mg < 25 mg/L); Old Meteoric ± Old Glacial ± Last Deglaciation meltwater ± Saline component, i.e. Na-Ca-Cl (SO_4) in type, $\delta^{18}O$ > –13.0‰ VSMOW.

Saline

Water type: Saline (10,000–20,000 mg/L Cl; 18–35 g/L TDS; Old Meteoric ± Old Glacial ± Last Deglaciation meltwater ± Highly saline component, i.e. Ca-Na-Cl (SO_4) in type, $\delta^{18}O$ = –13.0 to –10.0‰ VSMOW.

Highly Saline

Water type: Highly Saline (> 20,000 mg/L Cl; > 35 g/L TDS); Ca-Na-Cl (SO_4) in type; $\delta^{18}O$ > –10.0‰ VSMOW.

4.1 Initial data evaluation and visualisation

Contributions to this section include that of /Gimeno et al. 2009, Hallbeck and Pedersen 2009/. Addressed are the primary major ions and isotopes for site understanding; some minor ions of relevance to the repository safety case (e.g. phosphate) and the trace elements (including REEs, uranium and radium) are briefly presented and discussed. The redox sensitive elements are discussed in Section 4.3 under ‘The redox system’.

For visualisation and interpretation of primary data widespread use has been made of scatter plots: a) to separate the different groundwater groups, b) to demonstrate depth variations of the major ions and also their relationship to fracture domains, hydraulic domains and deformation zones, and c) to help derive the origin and major ion evolution trends of the different groundwater systems. Three dimensional visualisations of the same data also have been used to quickly locate and orient the boreholes to achieve a better understanding of the lateral distribution of the different groundwater types.

Strictly, the scatter plots should be presented always showing the analytical error bars on each sample point and, in the case of elevation, an error bar relating to the uncertainty of the depth measurement. This has not been routinely done (except for the porewaters which require microanalytical techniques and are therefore more sensitive to analytical error) because in many cases the error bars interfere with the main illustrative objectives of the plots. For specific, more exotic constituents plotted (e.g. ^{37}Cl), the analytical uncertainties are given in the text or figure text.

4.1.1 Fracture domains and hydraulic rock domains

Based on earlier experience from the Forsmark site investigations, the Laxemar subarea has been subdivided into rock domains and fracture domains (cf Sections 2.2.1 and 2.2.2). In turn, these rock and fracture domains have been used as base geometrical models to study the spatial variation of hydraulic properties for definition of the hydraulic rock domains (HRD). Analysis has shown that with only a slight modification of the fracture domains, they can correlate closely with the hydraulic rock domains. To determine whether these two domains can be demarcated by differences in hydrochemistry, both fracture domains and hydraulic rock domains have been compared using chloride, magnesium and oxygen-18. These are considered the most important hydrochemical signatures to describe the groundwaters based on the conceptual understanding of the Laxemar-Simpevarp area.

Comparing the groundwater chemistry (Cl, Mg and $\delta^{18}O$) in the fracture domains with that in the hydraulic rock domains, shows essentially identical patterns (i.e. Cl in Figure 4-1a and b). Consequently, for Mg and $\delta^{18}O$ only plots from the hydraulic rock domains are illustrated in Figure 4-1c and d. Figure 4-1b indicates that there is some difference in the chloride trends between the different hydraulic rock domains with domain HRD_C indicating somewhat higher salinity than domains HRD_W and HRD_EW0007 at depths greater than about 200 m. Magnesium (Figure 4-1c) shows the greatest increase in domain HRD_C at about 500 to 550 m depth, and weaker increases in domains HRD_EW0007 and particularly HRD_W at about 200 to 400 m depth respectively. Oxygen-18 shows most depletion at about 400 m depth in domains HRDW_W and HRD_EW0007, whilst domain HRD_C, in comparison, shows a small peak of more enriched oxygen-18 values at about 600 m depth.

The observed differences between the hydraulic rock domains may warrant some consideration when describing the hydrochemistry of the Laxemar subarea. More important, however, is the relation of the hydrochemistry to the deformation zones which have provided the majority of the hydrochemical data. These zones often demarcate the boundaries between the different hydraulic domains, in addition to representing a groundwater archive of past climatic events. To further assess the potential of these deformation zones, data from each major deformation zone were examined to determine changes in groundwater composition at different elevation levels within the same zone. However, no such changes were observed, possibly due to the limited available data.

4.1.2 Depth trends of selected major ions and chemical parameters

Chloride, magnesium and oxygen-18

The major ions of chloride, magnesium and $\delta^{18}O$ are plotted against elevation showing the variation in composition with depth of the different groundwater types. Also presented in each plot are the near surface soil pipe groundwater samples (NSGW) to provide a reference to the hydrochemical end-member composition entering the upper bedrock system. Two sets of plots are used to visualise groundwater compositions. One set initially presents the wider regional picture involving all the groundwater samples from the regional scale Laxemar-Simpevarp area, including the representative near surface soil pipe groundwaters (category 3) and the shallow and deep groundwaters (categories 1 to 3). Each category group is distinguished with different symbols and colour codes and maximum elevation and chloride scales are used. The second set shows only the samples from the Laxemar subarea were the 'x' and 'y' scales are reduced to –1,200 m elevation and 20,000 mg/L Cl respectively to increase resolution at shallow and intermediate depths were most data plot.

Figure 4-2a, c and e presents chloride, magnesium and $\delta^{18}O$ groundwater data representing the Laxemar-Simpevarp area, and Figure 4-2b, d and f represents similar compositional data from just the Laxemar subarea for comparison. Figure 4-2a shows a range of chloride from less than 200 mg/L to about 8,000 mg/L, which generally characterises the upper approximately 600 m depth. With

increasing depth there is a rapid and systematic increase to a maximum of around 45,000 mg/L at about 1,500 m depth sampled from borehole KLX02 in the Laxemar subarea. For magnesium (Figure 4-2c) a decrease ranging from about 250 to 50 mg/L is observed from close to the bedrock surface to about 600 m depth, and this can be directly correlated to variable amounts of brackish marine (Littorina) type groundwaters when present (this is particularly clear from the Äspö data). From 600 to 900 m depth there is a further decrease in magnesium to well below 25 mg/L with the exception of the Äspö data which still show groundwaters with around 50 mg/L Mg to depths just below 900 m. Below 1,000 m depth magnesium is less than 5 mg/L.

The $\delta^{18}O$ data (Figure 4-2e) is influenced in the upper approximately 600 m on the one hand by depleted values associated with the brackish glacial groundwaters ($\delta^{18}O \leq -13.0$‰ VSMOW), and on the other hand by enriched values associated especially with brackish marine groundwaters, but also with recharge meteoric groundwaters ($\delta^{18}O \geq -13.0$‰ VSMOW). This results in a wide variation in $\delta^{18}O$ from within 50 m of the bedrock surface ($\delta^{18}O = -13.5$ to -7‰ VSMOW) and this variation further broadens with increasing depth to about 550 m to include more depleted values of about $\delta^{18}O = -16$‰ VSMOW. At about 600 m the range in $\delta^{18}O$ decreases dramatically and from here there is a gradual enrichment with increasing depth to about $\delta^{18}O = -9$‰ VSMOW at the maximum depths sampled.

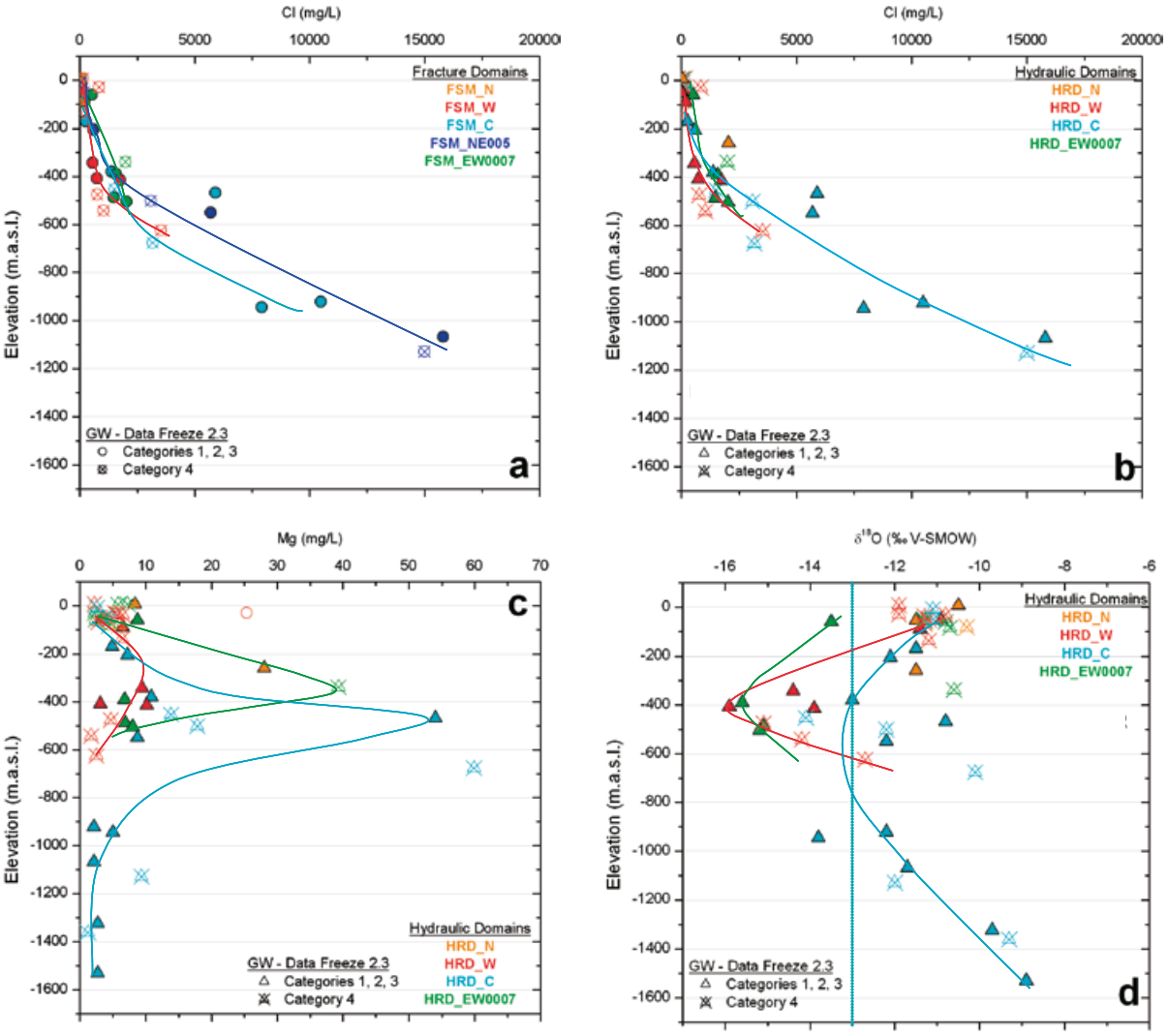

Figure 4-1. *Laxemar subarea: Comparison of Cl between fracture domains (a) and hydraulic rock domains (b), and comparison of Mg (c) and $\delta^{18}O$ (d) between the different hydraulic rock domains. Note the red open circle in plot (c) at around 25 mg/L Mg; this is an anomalous outlier and has not been included in the curve representing HRD_N. The hand drawn curves are based mostly on category 1 to 3 data.*

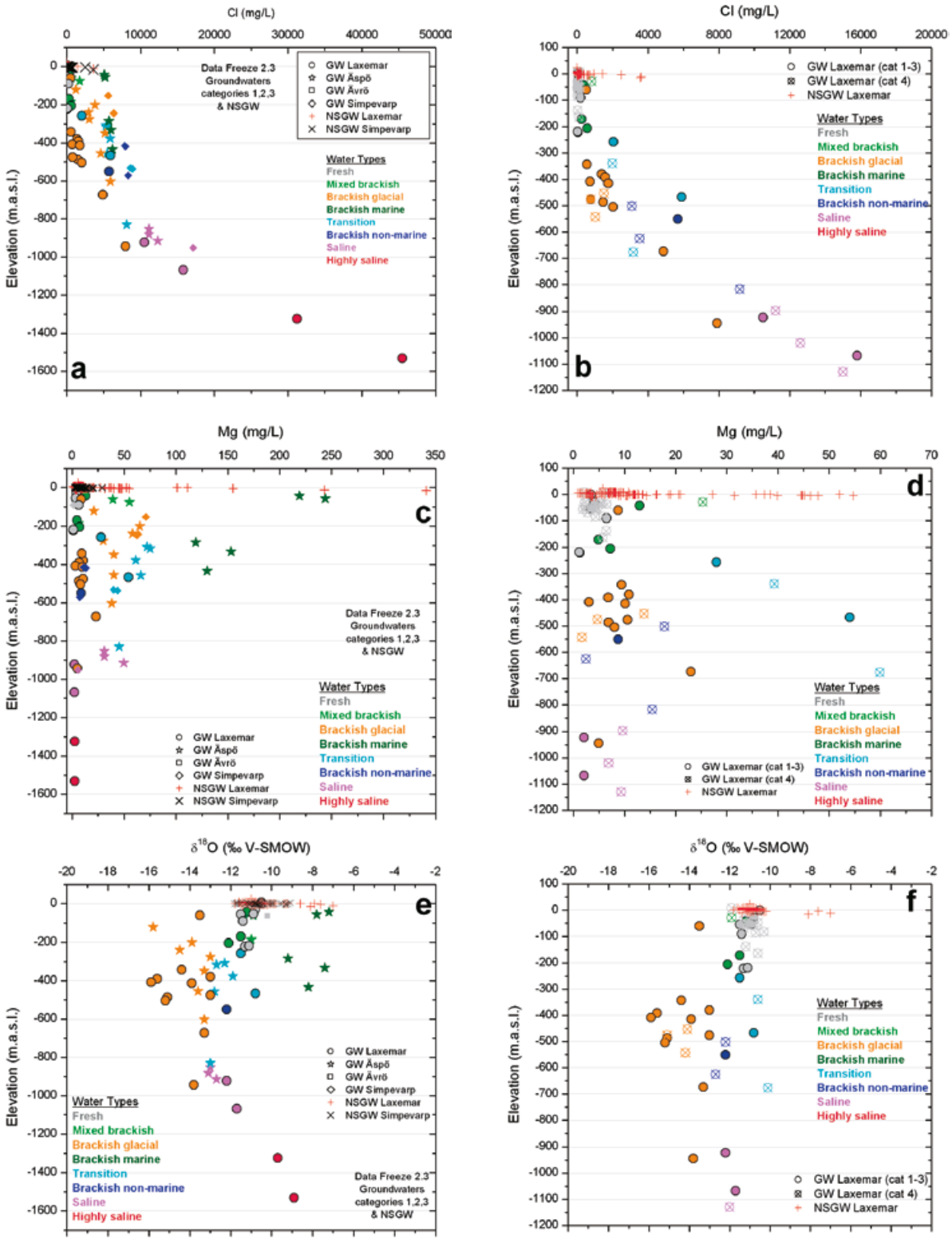

Figure 4-2. *Distributions of chloride (a, b), magnesium (c, d) and $\delta^{18}O$ (e, f) in the Laxemar-Simpevarp area (left-hand figures) and the Laxemar subarea (right-hand figures), respectively. The scales along the chloride, magnesium and depth axes have been increased in the Laxemar subarea plots to better visualise the groundwaters at shallow to intermediate depths.*

In more detail, the **upper 250 m** in the Laxemar subarea (Figure 4-2b, d and f) are characterised by fresh recharge groundwaters (< 200 mg/L Cl) of Na-HCO_3 type and a narrow range of $\delta^{18}O$ values which correspond closely to the overburden soil pipe waters. Also indicated is the presence of sporadic brackish glacial groundwaters (200–10,000 mg/L Cl). One shallow sample (HLX30: –60.4 m elevation) has an upper bedrock Na-Cl-HCO_3 (SO_4) composition with a chloride content of around 500 mg/L and a depleted glacial signature ($\delta^{18}O$ = –13.5‰ VSMOW; Figure 4-2f), This groundwater also shows a tritium free pre-bomb test signature and a carbon-14 content of around 35 pmC which infers an age of decades to several thousands of years (cf Section 4.9). Such an occurrence may indicate preserved 'pockets' or 'lenses' associated with dead-end fractures or bedrock volumes of low transmissivity.

Also included in the upper 200 m are groundwaters of mixed brackish origin which range generally in type from Na-HCO_3 to Na-Cl-HCO_3 (SO_4) with chloride contents of 260 to 840 mg/L, carbon-14 ranging from 30 to 50 pmC, low tritium (below detection to < 3 TU), and $\delta^{18}O$ values largely similar to those of modern recharge waters (–12.1 to –10.9‰ VSMOW; Figure 4-2f). Magnesium is low, from 5 to 25 mg/L (Figure 4-2d), and the higher values may indicate a weak marine component, for example, borehole HLX38 with 25.3 mg/L Mg lies on the cut-off value of 25 mg/L Mg used to discriminate between a weak Littorina or non-Littorina component. Note that several of the overburden soil pipe groundwaters have significant magnesium (> 25 mg/L). All of these occurrences (five sampling points) are situated close to or beneath the present Baltic Sea coast line. The groundwaters are not pure Baltic Sea water but they possibly represent mixing between brackish and fresh waters which may have occurred under natural flow or percolation conditions and/or due to anthropogenic activities such as drilling and sampling. Some of the groundwaters may also represent pockets of old Littorina Sea water.

Within the **250 to 600 m** depth interval the Laxemar groundwaters are characterised mainly by brackish glacial types with some examples of brackish non-marine and transition types. In addition, some mixed brackish types are included in the upper approximately 200–300 m of bedrock. The brackish glacial types cluster within the approximately 350 to 550 m depth interval, and are distinguished from the shallower example described above by higher chloride contents (up to 2,500 mg/L) and much more depleted glacial signatures ($\delta^{18}O$ = –16 to –13‰ VSMOW). Three transition samples occur within this depth interval showing a progressive increase in chloride content (2,000 to 5,900 mg/L) with increasing depth, but also showing a significant range of magnesium (28–54 mg/L, cf Figure 4-2d) exceeding the 25 mg/L cut-off for a weak brackish marine (Littorina) component. This component is also reflected in the $\delta^{18}O$ values ($\delta^{18}O$ = –11.5 to –10.6‰ VSMOW) (Figure 4-2f) which are more enriched than the brackish glacial groundwaters. The mixed brackish marine (Littorina) component in these otherwise brackish glacial to brackish non-marine groundwaters has resulted in them being referred to as 'Transition' types.

Three brackish non-marine groundwaters are present at this depth interval with lower confidence given to the two category 4 samples with chloride values ranging from 3,000 to 3,500 mg/L compared to the category 3 samples at 5,700 mg/L Cl. All indicate low magnesium (< 20 mg/L) with two under 10 mg/L. The $\delta^{18}O$ values all lie around or just below $\delta^{18}O$ = –12‰ VSMOW which suggest some glacial component.

The approximate depth interval **600 to 1,200 m** marks the transition from brackish non-marine to saline groundwater type, characterised by a steady increase in chloride to about 16,000 mg/L (Figure 4-1b), and at greater depths the transition to highly saline groundwaters at a maximum of 45,000 mg/L measured at an elevation of –1,530 m in borehole KLX02 (Figure 4-2a). The saline and highly saline groundwaters are typically Ca-Na-Cl in type with low magnesium, i.e. < 10 mg/L for the saline and < 5 mg/L for the highly saline groundwaters. The $\delta^{18}O$ values for the saline groundwaters range from –12.2 to –11.7‰ VSMOW suggesting a small glacial content, while the highly saline water show more enriched $\delta^{18}O$ values (Figure 4-2f).

Attempts have also been made to visualise these groundwater data in three dimensions to obtain a feel for the spatial distribution of the chemical species laterally across the Laxemar-Simpevarp area. Figure 4-3 shows the location of the Laxemar-Simpevarp area, the orientation of the visualisation, and the two marked horizontal levels representing the expected range of repository depths in the Laxemar subarea, i.e. between –400 to –700 m elevation. Figure 4-6, which shows the vertical chloride distributions mirrors that described in Figure 4-2a and b, except in the former case it is possible

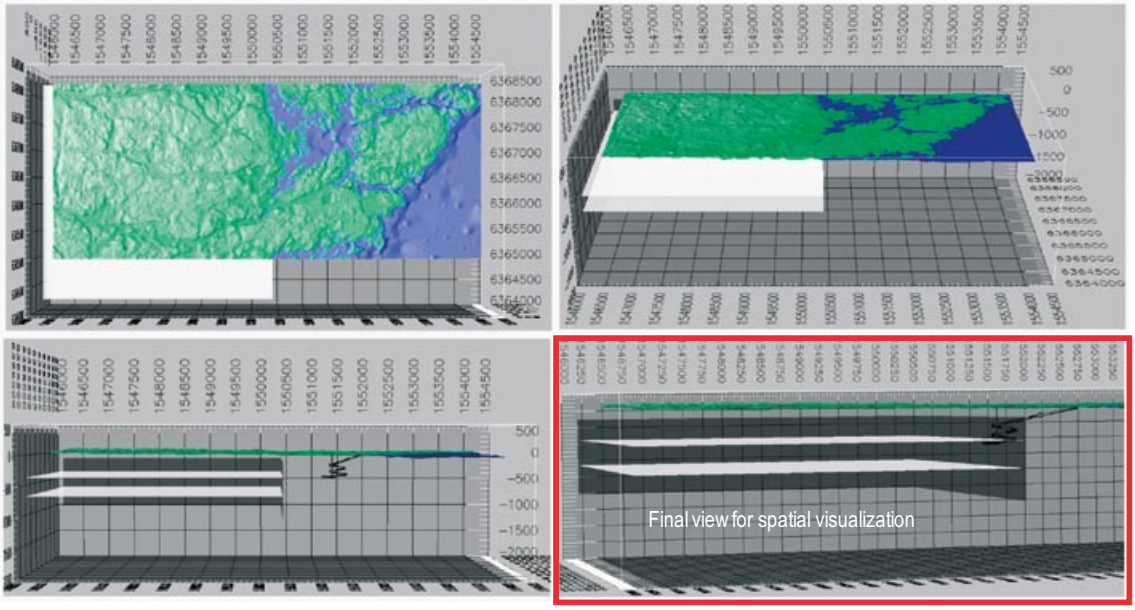

Figure 4-3. *Laxemar-Simpevarp area showing orientation of the three dimensional visualisation and the two marked horizontal levels (in white) representing expected repository depths in the Laxemar subarea, i.e. –400 to –700 m elevation (boxed in red). (Note also the position of the Äspö HRL spiral tunnel at the top right-hand corner of the section).*

not only to see how many salinity data there are at potential repository depth in the Laxemar subarea, but also the higher levels of salinity further to the east illustrating the large scale discharge features exemplified in the Simpevarp subarea. The salinity profile shown in KLX02 provides the only deep groundwater input to site understanding, and may well reflect the deep groundwater chemistry within the Laxemar-Simpevarp area as a whole.

Figure 4-5 shows the vertical distribution of $\delta^{18}O$, emphasising in particular more depleted values at intermediate depths in the Laxemar subarea. The main contrast towards the discharge area to the east is that these depleted values are sampled closer to the surface. Borehole KLX02 shows the most enriched $\delta^{18}O$ values at greatest depth which represents the lower end of a trend which at greater enrichments is a common observation in very deep groundwaters in the Canadian Shield subjected to water-rock interaction under stagnant conditions /Frape and Fritz 1987/.

Sodium, calcium, potassium and sulphate

Figures 4-6a and b show the distribution of sodium and calcium in the Laxemar subarea. Sodium indicates little change within the first 250 m depth interval, remaining below 500 mg/L and associated with groundwater types ranging from fresh, mixed brackish and brackish glacial. Towards greater depth there is a steady increase to 3,750 mg/L at about 1,100 m depth, and although not shown in the plot the sodium concentration increases to 8,000 mg/L at about 1,500 m depth. Two possible sodium trends may be indicated (Figure 4-6b); one lower concentration trend associated with the brackish glacial groundwaters, and a higher concentration trend associated with the brackish to saline non-marine groundwaters (and also transition waters).

Calcium, in common with sodium, shows a weak increase to about 500 mg/L in the upper bedrock, but in this case extending to greater depths of about 450 m (Figure 4-6b). Furthermore, from about 500 m to greater depth calcium exhibits a similar trend to sodium where higher calcium concentrations link up with transition and brackish to saline non-marine groundwaters, and a lower compositional range which links up with the brackish glacial types. Figure 4-7a shows the maximum calcium values measured in the Laxemar subarea at around 19,000 mg/L.

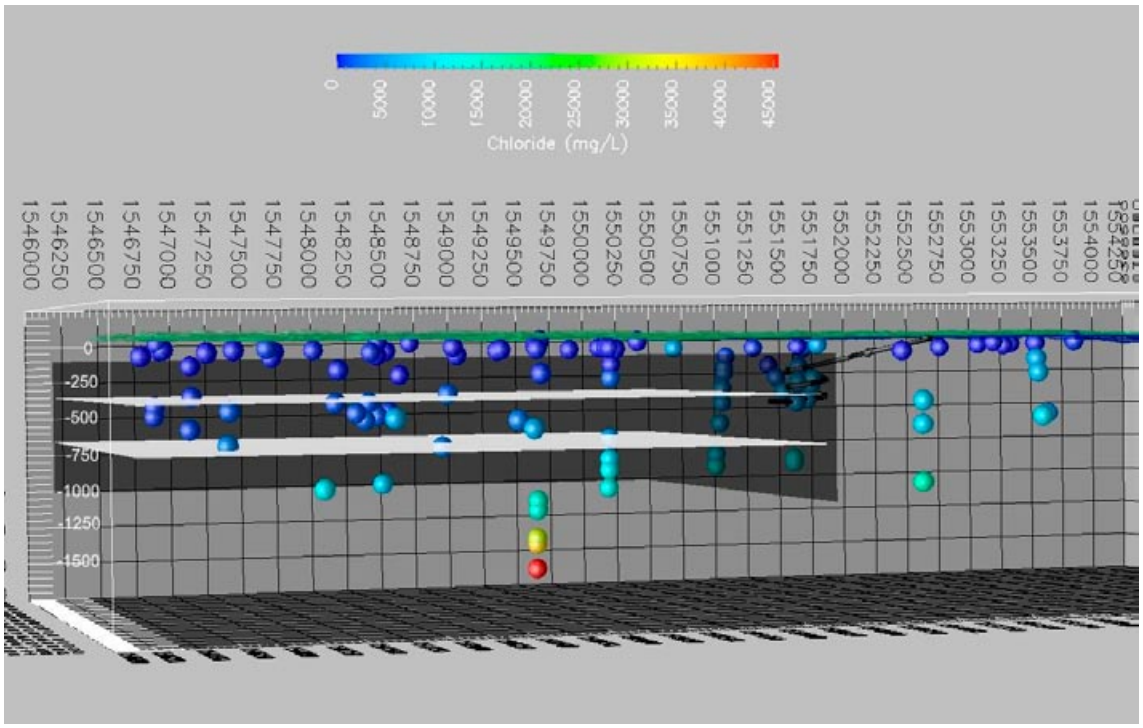

Figure 4-4. *Three dimensional visualisation of chloride concentrations and their lateral and vertical distribution across the Laxemar-Simpevarp area. The deepest borehole corresponds to KLX02.*

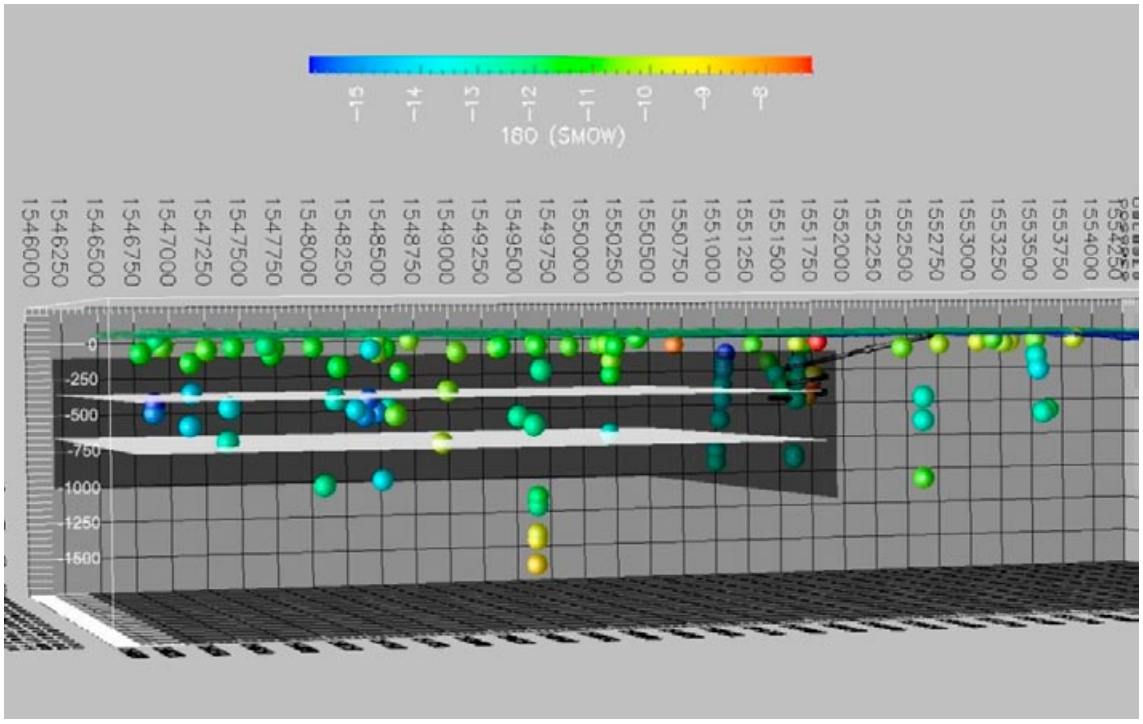

Figure 4-5. *Three dimensional visualisation of $\delta^{18}O$ concentrations and their lateral and vertical distribution across the Laxemar-Simpevarp area. The deepest borehole corresponds to KLX02.*

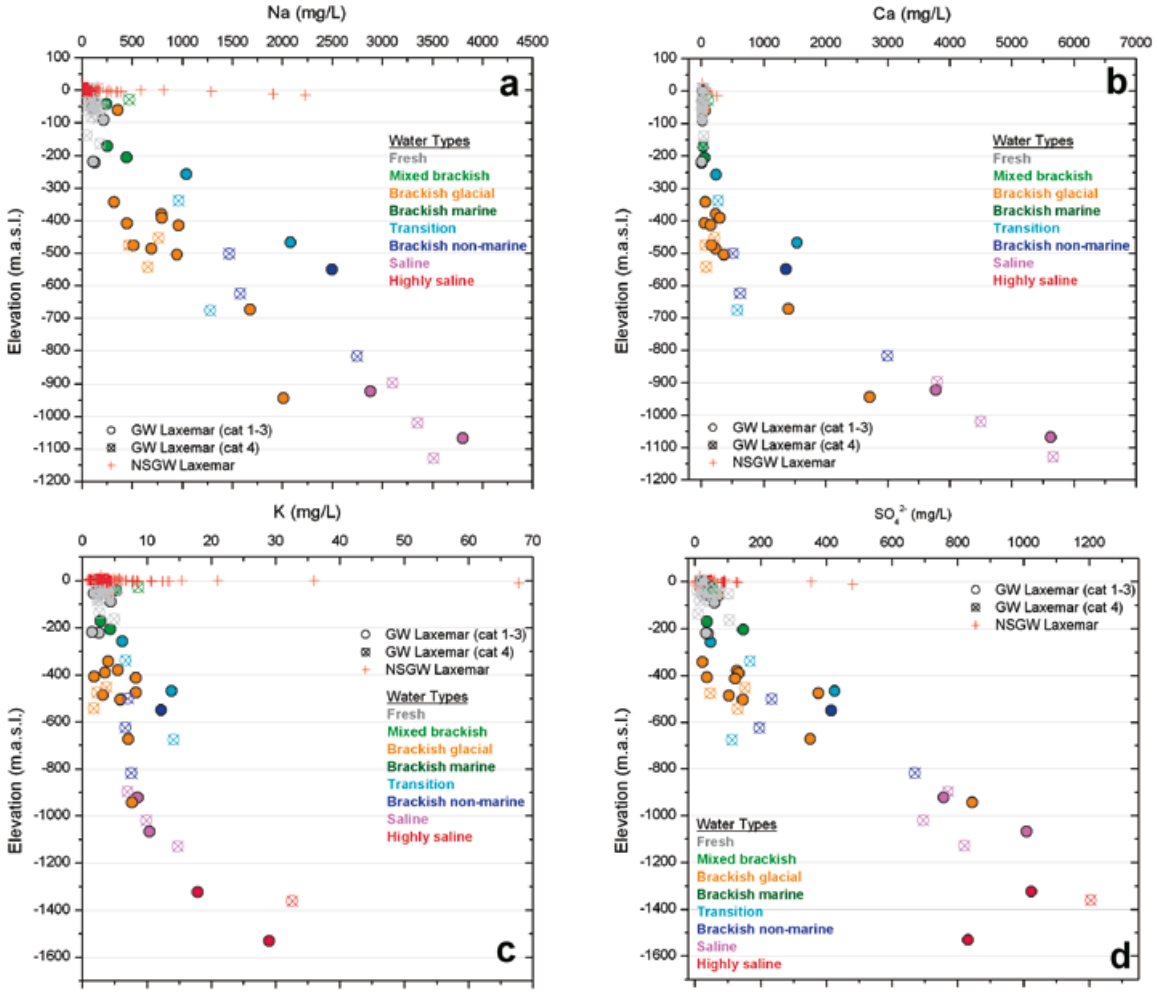

Figure 4-6. *Depth distributions in the Laxemar subarea of sodium (a), calcium (b), potassium (c) and sulphate (d). Different depth scales have been used where appropriate to better visualise and describe the ions in question.*

Not evident from these sodium and calcium plots but indicated in Figure 4-10 and described in /SKB 2006b, Gimeno et al. 2009/, is the transition at around 600 m from a Na-Ca Cl type groundwater to a deeper and more evolved Ca-Na Cl type groundwater, accompanied by a decrease to very low magnesium values. In the Simpevarp subarea this transition is also evident, but occurs at deeper levels in the bedrock, perhaps due to the greater density penetration of a marine water component (i.e. sodium source) at this low topographic coastal location during the Littorina Sea transgression.

Potassium contents associated with the fresh and mixed brackish groundwaters are < 6mg/L in the uppermost 250 m (Figure 4-6c), and variable up to a maximum of 15 mg/L in the approximate depth interval 250 to 500 m characterised by brackish glacial, brackish non-marine and transition groundwater types. Potassium and magnesium both increase in the brackish groundwaters with a marine component. Below 550 m to the maximum depths sampled, there is a gradual and steady increase in potassium from about 7 mg/L to a maximum of about 30 mg/L corresponding to increasing chloride.

Most of the sulphate contents appear to be uniformly under 100 mg/L in the upper 200 m and under 200 mg/L down to about 450 m depth (Figure 4-6d). A marked increase to just over 400 mg/L occurs from 450 to 550 m, and from here continues to increase steadily to about 1,000 to 1,200 m depth, where a maximum value of just over 1,000 mg/L SO_4 is reached. At this point the sulphate levels out down to around 1,300 m depth, and then it appears to decrease to around 830 mg/L at the maximum depth sampled. It is not certain that this decrease is reliable as the borehole section sampled is almost 280 m long and mixing from different sources has probably occurred, but the decrease does conform to the hypothesis that these groundwaters are at equilibrium with gypsum, as suggested by the model calculations (cf /Gimeno et al. 2009/ and discussion in Section 4.1.6).

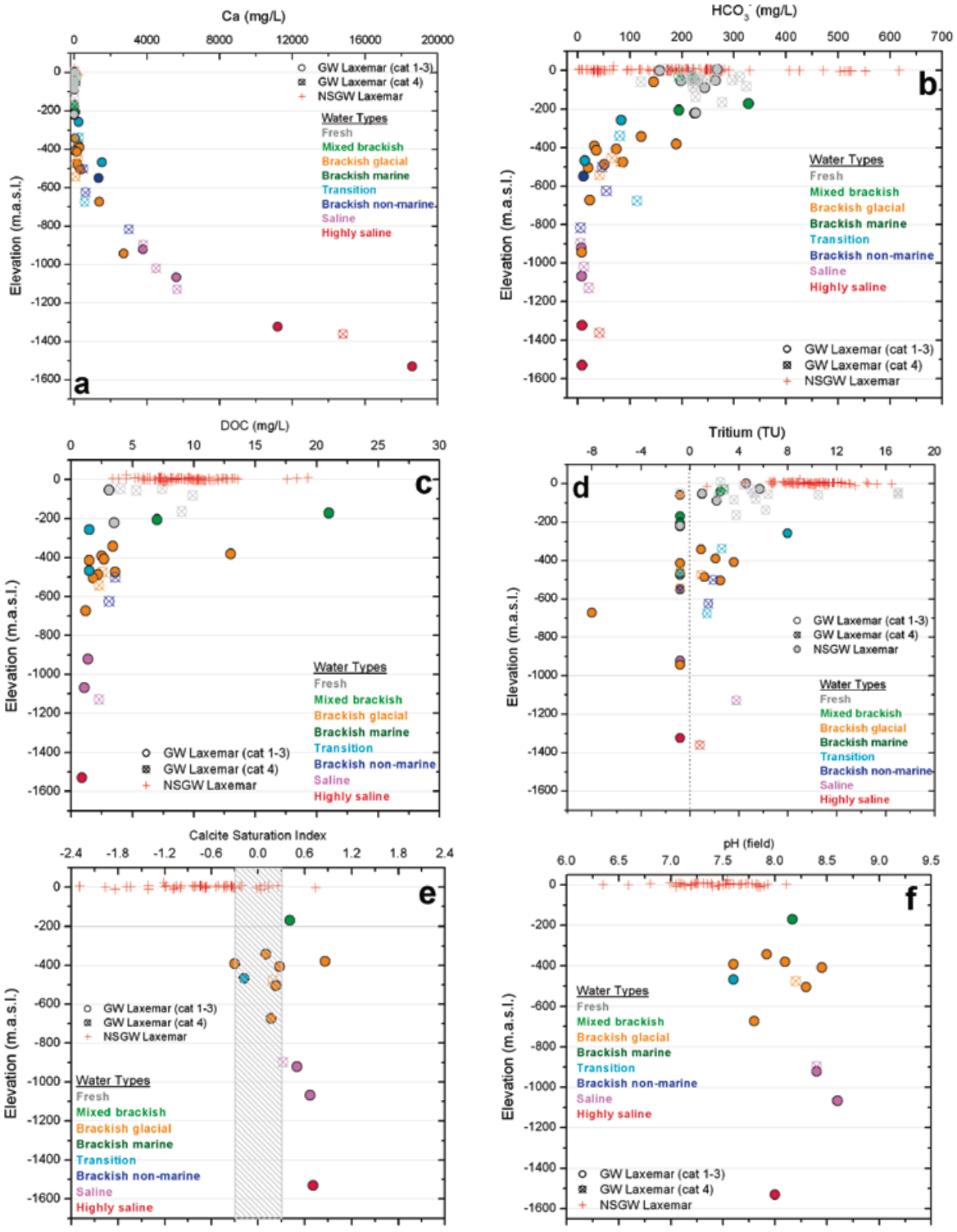

Figure 4-7. *Depth distributions in the Laxemar subarea of calcium (a), bicarbonate (b), dissolved organic carbon (DOC) (c), tritium (values under detection limit are negative) (d), calcite SI calculations (uncertainty area of ± –0.3 is shaded) (e), and pH (f).*

Bicarbonate, DOC, tritium, calcite saturation index and pH

Bicarbonate contents (Figure 4-7b) are variable from around 150 to 320 mg/L HCO_3 in the first approximately 250 m of the bedrock, and even more so in the overburden sediments which show extreme ranges in composition from close to zero to just over 600 mg/L HCO_3. In both cases, this illustrates environments where the carbonate system and the microbial production of CO_2 are very active /Gimeno et al. 2008b/. Concentrations and variability then decrease from 200 to 600 m after which very low values (< 10 mg/L HCO_3) continue to the maximum depths sampled. These observations are consistent with highest microbial breakdown of organic material in the dilute near surface groundwaters, and significant in the brackish glacial groundwaters probably due to the presence of a post glacial meteoric component. This is in contrast with the brackish to saline non-marine groundwaters which show values ranging from about 60 to < 10 mg/L HCO_3 with increasing depth. Unfortunately, these low HCO_3 values preclude the possibility of ^{14}C dating some of these groundwaters.

The DOC values (Figure 4-7c) in the upper, more hydraulically active recharge bedrock horizons, show significant variations and high values up to around 20 mg/L, similar in range to the overburden groundwaters. However, because the highest value represents a mixed brackish type groundwater it may have been infuenced by anthropogenic activities. Otherwise, the content of DOC appears to be within the 1 to 7 mg/L range. From about 250 to 600 m the DOC, with one exception, consistently lies within the range of about 1.5 to 3.5 mg/L, and at greater depths to about 1.0 to 1.5 mg/L. In Figure 4-7d, showing tritium against depth, there is a trend (with one exception of a transition groundwater) of less than 4 TU at depths greater than 100 m, indicating in most cases little or no influence of modern water. However, this range is higher than expected and appears to be most prevalent at depths of about 350 to 550 m where anthropogenic artefacts during drilling (e.g. short circuiting) and especially reported contamination during sampling has been recorded /Smellie et al. 2008/. Uncertainties related to some of the tritium data are addressed in Sections 3.3.1 and 4.9.3.

With respect to pH (Figure 4-7f) all groundwaters lie within a range of 7.5 to 8.6. As expected, pCO_2 in equilibrium with these groundwaters decreases with depth due to water-rock interaction, and/or mixing with saline groundwaters, and most groundwaters are in equilibrium with calcite (Figure 4-7e) /Gimeno et al. 2009/. However, groundwaters mostly of brackish glacial water type show variable pH, but essentially at equilibrium with calcite apart from one exception with higher pH and pCO_2. Studies of fracture filling calcites /Drake and Tullborg 2009a/ indicate only minor recent changes (either precipitation or dissolution), in accordance with the recorded close to equilibrium conditions.

Summary of general depth trends

The depth trends show that:

a) Groundwaters of fresh and mixed brackish origin dominate the upper approximately 250 m of the bedrock; some isolated occurrences of brackish glacial groundwaters also occur.

b) From about 250 m to 600 m the presence of transition type groundwaters and brackish non-marine groundwaters of variable composition represent relicts of groundwaters prior to the last deglaciation; Na/Ca > 1 is characteristic of this depth interval.

c) Within the same 250 to 600 m depth interval, but tending to cluster from about 300 to 600 m, are the brackish glacial groundwaters also of variable composition which have been superimposed on the earlier system (point (b) above) during the last deglaciation; this interval can also show a weak Littorina groundwater component.

d) From about 600 m to the maximum depth sampled at approximately 1,500 m there occurs an increase in all major ions (apart from Mg and HCO_3) and a change in ratio to Ca/Na > 1.

e) From about 600 to 1,000 m there is evidence of a superimposition of a deeper glacial groundwater component on the earlier relict groundwater system, although this may not necessarily originate always from the last deglaciation.

f) Borehole KLX02 indicates a more rapid increase in salinity at and above approximately 1,200 m, which also appears to be a maximum depth affected by surface-influenced groundwater circulation and mixing.

The depth intervals described above are largely supported by the hydrogeological studies (cf Section 2.3.3) which basically indicate a systematic decrease in hydraulic conductivity with depth to about 1,000 m, and thereafter characterised by low flow and stagnant groundwater conditions.

4.1.3 Major ion-ion/isotope plots

Relationship to chloride

At low concentrations sodium shows a positive correlation with chloride (Figure 4-8a) close to that of the Sea Water Mixing Line (SWML) suggesting some mixing with a marine groundwater end member. Possible sources are the near surface soil pipe groundwaters which contain high amounts of sodium /Tröjbom et al. 2008, Gimeno et al. 2009/). At greater concentrations this is followed by a marked deviation at about 1,500 mg/L Na and 3,000 mg/L Cl which continues to maximum concentrations (i.e. to maximum depths). This deviation slope clearly shows increasing mixing of sodium, initially with the brackish non-marine groundwater, and then with the deeper saline and highly saline groundwaters. This near conservative behaviour of sodium is supported by the modelling results which confirm that mixing is the main processes controlling the sodium concentrations for most of the saline groundwaters /Gimeno et al. 2009/.

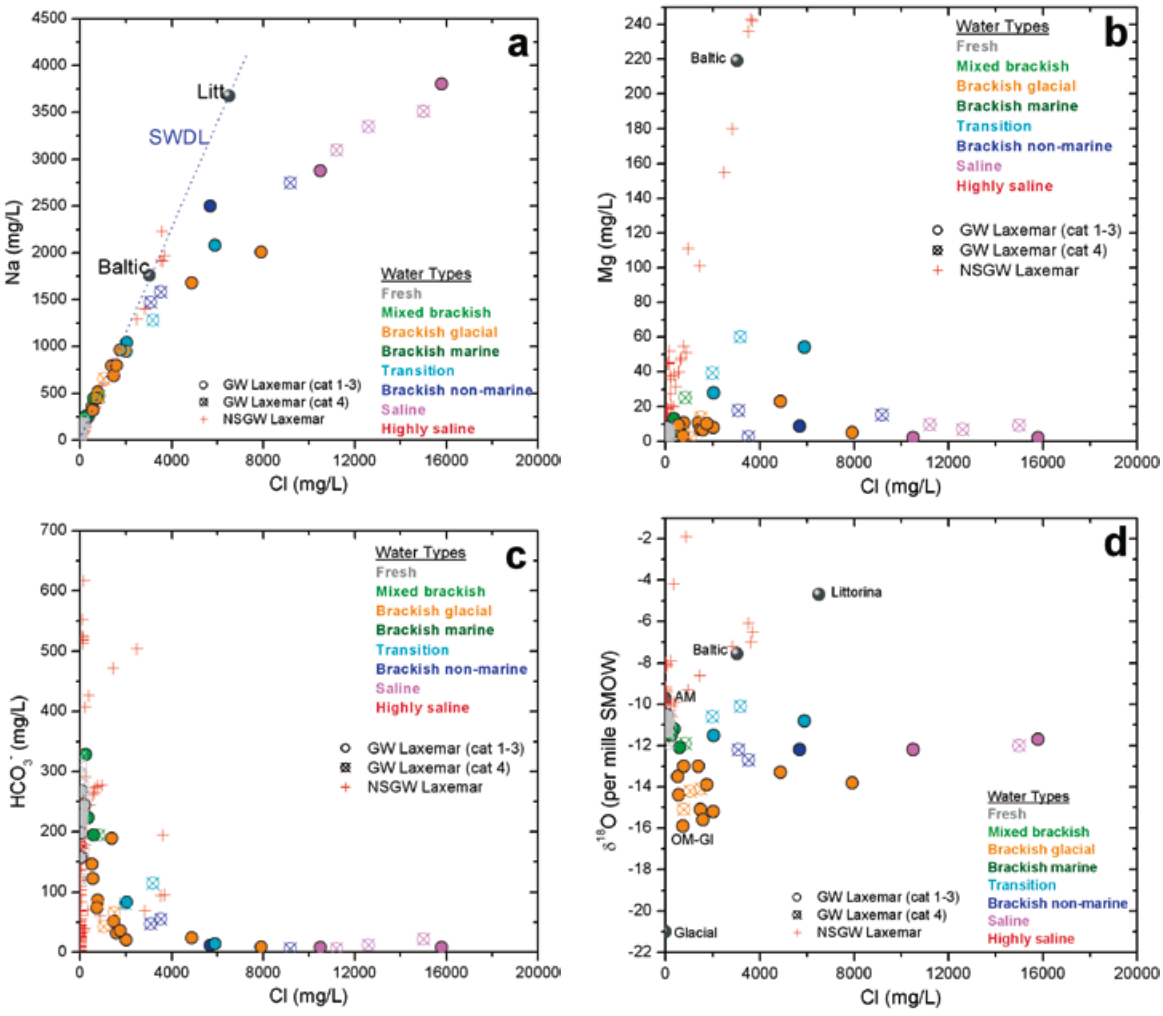

Figure 4-8. *Plots of sodium (a), magnesium (b), bicarbonate (c) and $\delta^{18}O$ (d) versus chloride related to the Laxemar subarea. Also indicated when appropriate are the end members of the Baltic and Littorina (Litt.) Sea waters, Glacial and Old meteoric+Glacial (OM-Gl) waters, Altered Marine water (AM), and the Sea Water Dilution Line (SWDL). Note that the chloride concentrations are restricted to 20,000 mg/L (i.e. absence of highly saline groundwaters) for increased resolution at lower concentrations (i.e. at shallower depths).*

Magnesium (Figure 4-8b) is present in significant amounts (to about 240 mg/L) in several of the near surface soil pipe groundwaters close to the present Baltic Sea coast line or even below the Baltic Sea. Consequently, magnesium generally shows a correlation with chloride along the SWDL indicating residual Baltic Sea type waters. In the bedrock groundwaters magnesium is present only in small amounts (mostly less than 20 mg/L) and shows no correlation with chloride apart from the possibility of the two transition samples which have been influenced by a weak Littorina component (to around 55 mg/L Mg). Cation exchange also needs to be considered as it may have contributed to an underestimation of the brackish marine component; however, its effects have not been intense enough to remove the marine (i.e. Littorina) signatures (cf similar discussion concerning Forsmark /Gimeno et al. 2009/).

Bicarbonate (Figure 4-8c) generally shows the expected trend with a rapid reduction associated with increasing chloride contents (i.e. increasing depth) signifying the sharp decline in the carbonate system and decrease in active microbial production of CO_2. In common with magnesium, some small increases in bicarbonate at low concentrations associated with transition-type groundwaters may reflect the weak marine component.

The $\delta^{18}O$ versus Cl in Figure 4-8d clearly demarcates: a) the brackish glacial group of groundwaters, including the two deeper, more saline varieties, b) the shift to slightly more enriched $\delta^{18}O$ values of the transition groundwaters (categories 1–3 and 4) with a weak Litttorina component, c) the fairly consistent saline groundwater signatures ($\delta^{18}O \approx -12$‰ VSMOW) becoming more enriched ($\delta^{18}O = -9.7$ to -8.9‰ VSMOW) at high chloride compositions (i.e. depths greater than 1,200 m; cf Figure 4-2a and e), and d) the presence of some Baltic Sea type (and possibly even Littorina Sea type) groundwaters in the overburden.

Calcium shows a positive correlation with chloride (Figure 4-9a). Once again, this can be explained by mixing processes although cation exchange may play a more important role in this case /Gimeno et al. 2009/. In addition, plotting molar concentration of Ca against Na (Figure 4-10a) shows a shift from Na-Ca-Cl to Ca-Na-Cl type groundwaters with increasing depth and salinity (around 600 m), where the older and deeper Ca-Na-Cl groundwaters reside. The bedrock environment in which these older groundwaters occur represents low flow or stagnant hydraulic conditions, where mixing is driven by upward molecular diffusion rather than advection. Such conditions are also conducive to water-rock interaction processes and porewater diffusion exchange. Increased calcium with depth in granitic domains normally results from increased albitisation of plagioclase and alteration of hornblende when in contact with sodium-rich groundwaters. Over long time periods these processes will result in the removal of sodium from solution and release calcium to the groundwaters.

Sulphate in Figure 4-9b (essentially reflecting Figure 4-6d) correlates with chloride up to about 1,000 mg/L SO_4, after which there is a levelling off at this maximum value followed by a decrease to about 900 mg/L SO_4 associated with the deepest, highest chloride groundwaters. As mentioned above (cf Section 4.1.2), this decrease conforms to modelled predictions which show that gypsum equilibrium is controlling the sulphate in these deepest groundwaters /Gimeno et al. 2009/. This limitation of sulphate content in deep saline groundwaters and the presence of fracture gypsum was noted earlier by /Gascoyne 2004/ at the URL site in Canada, and attributed to similar causes.

Figure 4-9c plotting bromide against chloride provides some understanding of the groundwater system as bromide and chloride are considered generally to be the two most conservative tracers (exceptions not relevant to Laxemar are discussed in /Gimeno et al. 2009/). Comparing the groundwater distributions to the SWDL shows that bromide relative to the chloride is too enriched and suggests therefore an alternative source(s) of salinity. Enriched bromide may be explained by long term water-rock reactions in magmatic (and metamorphic) rocks which normally contain much more bromide than sea water (e.g. in fluid inclusions, along mineral grain boundaries, in crystal lattices etc) giving Cl/Br weight ratios of around 100 or less /Stober and Bucher 1999/. Bromide enrichment can result also from sea water evaporation processes, for example, when a TDS value of around 100 g/L is achieved through evaporation, halite (NaCl) crystals begin to form thus removing chloride from the evaporating sea water and thereby enriching bromide in the residual sea water. However, other parameters would appear to lend more support to water-rock interaction processes at depths greater than around 1,100 m at Laxemar (cf discussion in /Smellie et al. 2008/ and Section 4.13.2).

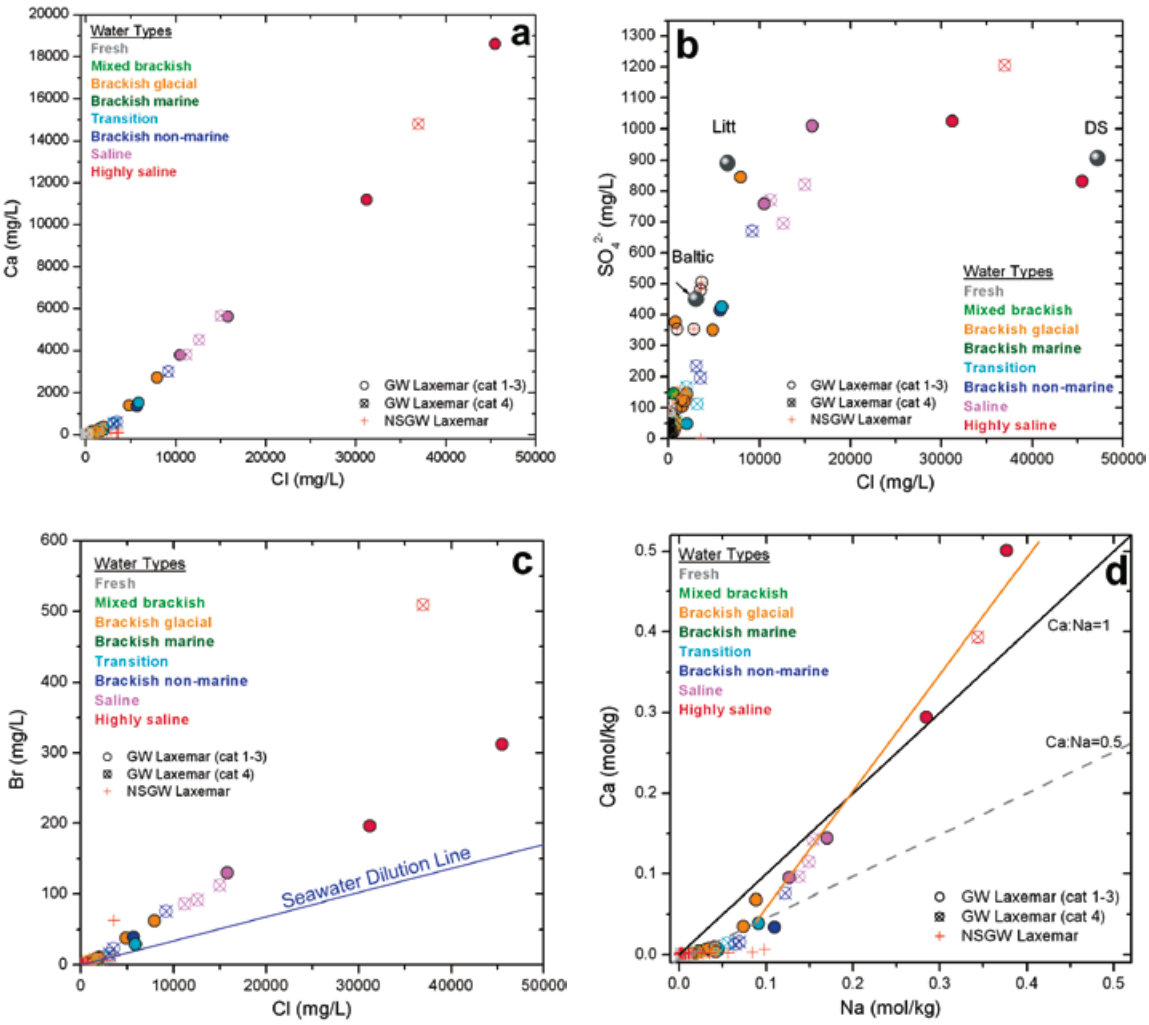

Figure 4-9. *Plots of calcium (a), sulphate (b) and bromide (c) versus chloride, and (d) calcium versus sodium showing a shift from Na-Ca-Cl to Ca-Na-Cl type groundwaters with increasing depth and salinity, in the Laxemar subarea.*

Stable isotopes of δ^2H and $\delta^{18}O$

The stable isotopes of δ^2H and $\delta^{18}O$ for the Laxemar subarea are plotted in Figure 4-10 together with the various identified groundwater end members. Generally, the groundwaters lie on or close to the Global Meteoric Water Line (GMWL). Exceptions are the deep, evolved, highly saline groundwaters which show a deviation coeval with increased salinity and enriched deuterium (^2H), and the near surface soil pipe groundwaters characterised by residual marine (Baltic) waters which plot below the GMWL. The former are usually explained by very intensive water-rock interactions under long periods of residence time /Frape and Fritz 1987/ and therefore characteristic of groundwaters of a very old age. The latter Baltic type groundwaters relate to evaporation processes resulting in ^{18}O enrichment.

Plotting along the GMWL and clearly distinguished are the fresh groundwaters (and those of mixed brackish type) which tend to cluster around typical modern recharge values ($\delta^{18}O \sim -11$‰ VSMOW). The brackish glacial groundwater types exhibit a wide range of depleted values ($\delta^{18}O = -16$ to -13‰ VSMOW) reflecting the heterogeneity of the mixing processes during and following their introduction into the bedrock at the last deglaciation. In addition, the transition and some of the saline non-marine samples contain a glacial component and plot at slightly depleted $\delta^{18}O$ values.

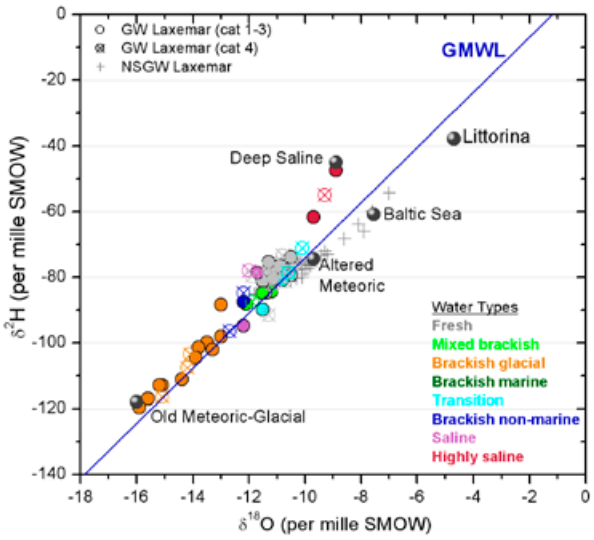

Figure 4-10. *Relationship between δ^2H and $\delta^{18}O$ for the Laxemar subarea groundwaters. End members are shown as dark grey spheres.*

4.1.4 Major ion ratio plots

Br/Cl versus elevation

The Br/Cl percentage weight ratio versus elevation (Figure 4-11a) shows a wide range of Br/Cl values in the overburden soil pipes (0.002 to 0.012). In the upper bedrock, a narrow range of Br/Cl values (about 0.0035 to 0.005 wt.%) occur within this more dynamic hydraulic system down to about 250 m. This is followed by a steady increase in the Br/Cl percentage weight ratio from 0.0045 to 0.008 at about 400 to 800 m, which represents a gradual decrease in hydraulic conductivity (and therefore groundwater flow). Following this, the Br/Cl weight ratio maintains similar values to about 1,200 m before decreasing to about 0.007 at greater depths characterised by very low flow and stagnant groundwater conditions. This decrease helps to underline the uniqueness of these deep, highly saline evolved groundwaters at depths greater than about 1,200 m, suggesting closed system conditions.

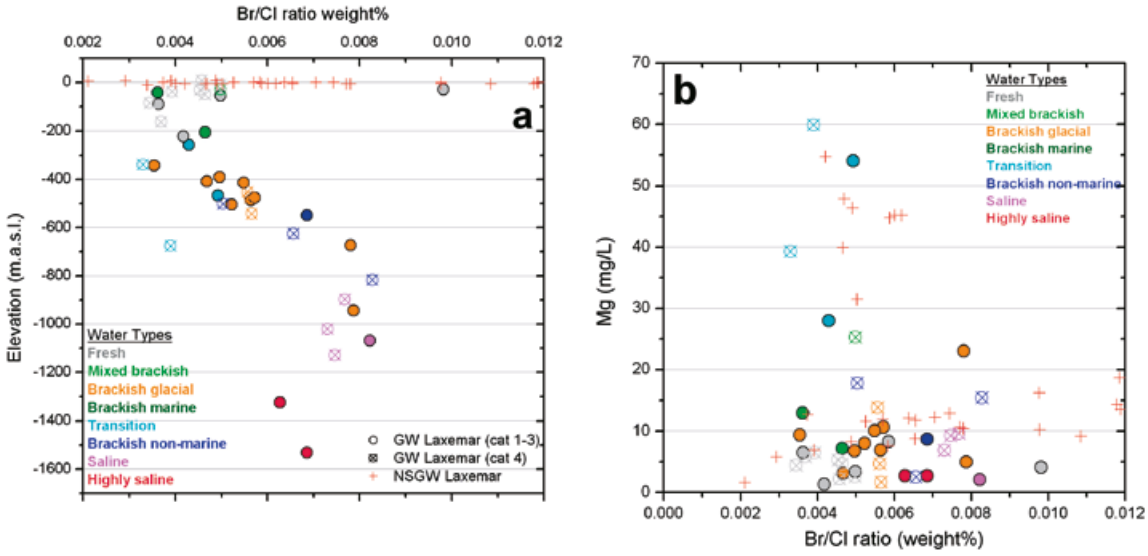

Figure 4-11. *Plot of Br/Cl versus elevation (a), and Mg versus Br/Cl (b) for groundwaters in the Laxemar subarea.*

The brackish glacial groundwaters do not deviate from the overall trend to about 1,000 m which is not unexpected as these glacial waters would have been highly diluted (i.e. insignificant bromide and chloride compared to the pre-existing bedrock groundwaters) when introduced during the last deglaciation.

Magnesium versus Br/Cl

Most of the magnesium data (Figure 4-11b) fall within the Br/Cl percentage weight ratio of 0.003 to 0.008 apart from high values associated with some of the soil pipe groundwaters and an anomalous fresh groundwater sample. Within the main group there is a weak subdivision between the more saline groundwaters with higher Br/Cl values and generally lower magnesium (< 10 mg/L), and lower Br/Cl values linked to higher magnesium, represented by one of the mixed brackish and both transition type groundwaters which contain a small marine (Littorina) component.

Ca/Mg versus Br/Cl

Figure 4-12, plotting Ca/Mg versus Br/Cl, provides an opportunity to interpret further the nature of the Laxemar groundwaters. The figure differentiates: a) a small group of residual modern marine waters (Baltic Sea) in the overburden, b) most of the fresh groundwaters circled in grey, c) most of the brackish glacial groundwaters circled in orange, d) the deepest most highly saline groundwaters circled in red, and e) the position of the two transition samples influenced by a weak Littorina Sea component. The red arrow shows a potential evolution pathway in the deeper bedrock groundwaters (i.e. > 600 m depth) via brackish to saline non-marine groundwater types. Much of the data along this pathway (i.e. to depths of about 1,000 m) represent groundwaters that contain an increasing component of the highly saline non-marine (or mixed non-marine/old marine) groundwater type. However, this highly saline groundwater deviates significantly from the evolutionary trend indicated, reflecting the rapid change from low flow conditions (i.e. saline groundwaters to about 1,000 m depth) to very low flow and stagnant conditions (i.e. highly saline groundwaters to at least 1,500 m depth) indicated in KLX02 to occur at depths greater than about 1,200 m /Ekman 2001/. Accompanying this overall increase in salinity to about 1,000 m depth is the change from a Na-Ca-Cl groundwater at shallower depths, to a Ca-Na-Cl groundwater at greater depths. This is clearly shown above in Figure 4-9d and by plotting Na/Cl versus Br/Cl (cf Figure 4-67).

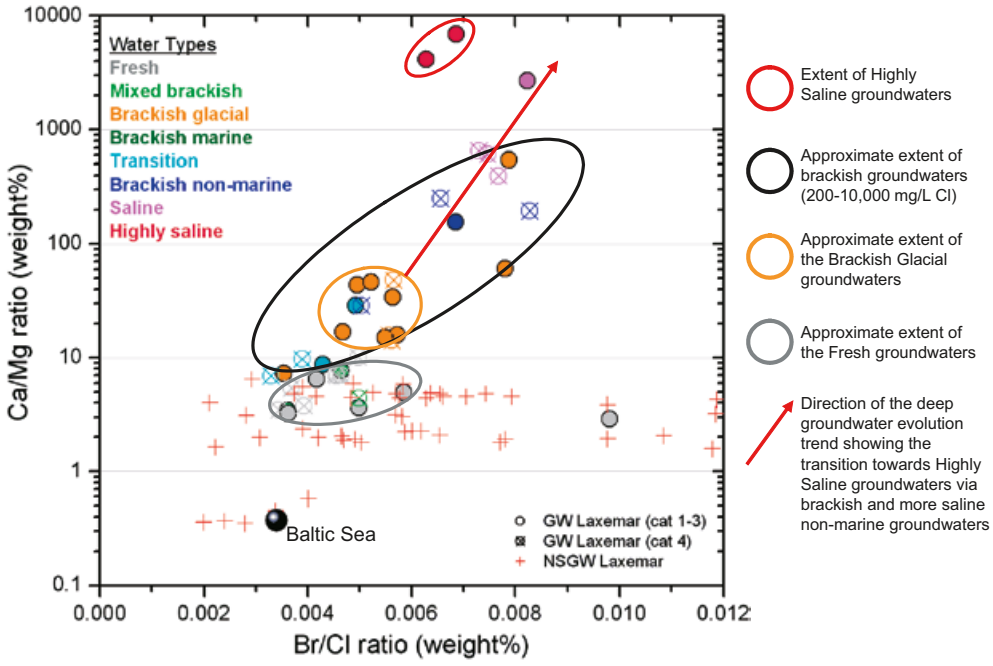

Figure 4-12. *Plot of Ca/Mg versus Br/Cl for the Laxemar subarea showing a potential evolutionary trend in the deeper bedrock groundwaters (i.e. > 600 m depth) from brackish to saline non-marine groundwaters to highly saline groundwater types.*

Na/Cl versus Br/Cl

The relation between the Na/Cl and Br/Cl ratios has been used to illustrate the potential effect of freezing processes versus evaporation (cf Section 4.11 and Figure 4-67). This further emphasises two of the evolutionary trends already derived from simpler plots and the Ca/Mg versus Br/Cl plot above, namely: a) the relative decrease in sodium with increasing salinity (i.e. depth), and b) the increase in the Br/Cl values associated with the deepest and most saline groundwaters with the lowest Na/Cl ratios.

4.1.5 Depth trends of selected trace elements and REEs

This section refers mostly to the heavy trace elements Mo, As, Cr, Co, Cu, Pb and Ni; other trace elements such as Li, Sr, Rb, Cs etc are addressed under other specific headings in this report, for example, cf Section 4.1.7 and Section 4.12 on deep saline groundwater signatures.

In general, different trends in trace element concentration may be expected in normal groundwater systems, for example: a) some trace element concentrations, irrespective of their source, will be expected to decrease as they are transported through the bedrock groundwater system with increasing depth; adsorption by manganese and iron oxides is one of the main uptake processes, and b) other trace elements will increase with depth due to their release from water-rock interactions involving the solubility of phases containing the elements as major constituents (e.g. oxides/hydroxides, carbonates or sulphides); these phases will provide an upper limit to the element's concentration. At Laxemar, however, this simplistic pattern is complicated by the periodic introduction of differing groundwater compositions, particularly since the last deglaciation.

In the Forsmark studies /Smellie et al. 2008/ the general conclusions reached with respect to the heavy trace element data and the difficulties surrounding their evaluation included:

- Incursion and mixing of different groundwater types at different stages in the past, particularly since the last deglaciation.
- Contamination resulting from borehole activities which may have affected mainly low hydraulically conducting fracture zones. Subsequent pumping when sampling may have served to mobilise many of these residual elements resulting in enhanced values. This further underlines the importance of adequate pumping prior to sampling to help remove excess trace metal contamination.
- Periodic monitoring of borehole sections where high pump rates are used to prepare the section for sampling, i.e. by removing three section volumes of water followed by immediate sampling. This activity may also have served to mobilise many of these elements, both residual types from drilling activities and those naturally occurring elements from mixed sources loosely bound along the fracture systems.
- In some cases a groundwater sample characterised as being of good quality, based on major ions and isotopes etc (i.e. Categories 1–3), was sampled when the trace element contents had stabilised. There are other cases, however, when the chosen groundwater sample had not achieved trace element stability and therefore not representative.

In the Laxemar subarea there is the additional possibility that short circuiting during pump testing and sampling may have resulted in the mixing of trace element compositions from different sources.

Compared with Forsmark there exist very few data in Laxemar relating to the heavy trace elements in question, i.e. Mo, As, Cr, Co, Cu, Pb and Ni. In fact, only arsenic is analysed in any detail and this is shown in Figure 4-13 for the Laxemar subarea which also includes the negative below detection values. The Laxemar subarea plot includes the temporal series data (small open coloured circles) and the sample (if available) actually chosen as being representative based on the major ion quality evaluation (infilled coloured circles; cf Section 3.3.1). Samples from category 5 are also included as small black open circles.

Figure 4-13 generally shows a fairly restricted range of arsenic content with increasing depth (< 0.5 µg/L), and several of the individual sample values show good stability during the time series measurements forming a tight cluster of open circles. However, there are three anomalously high

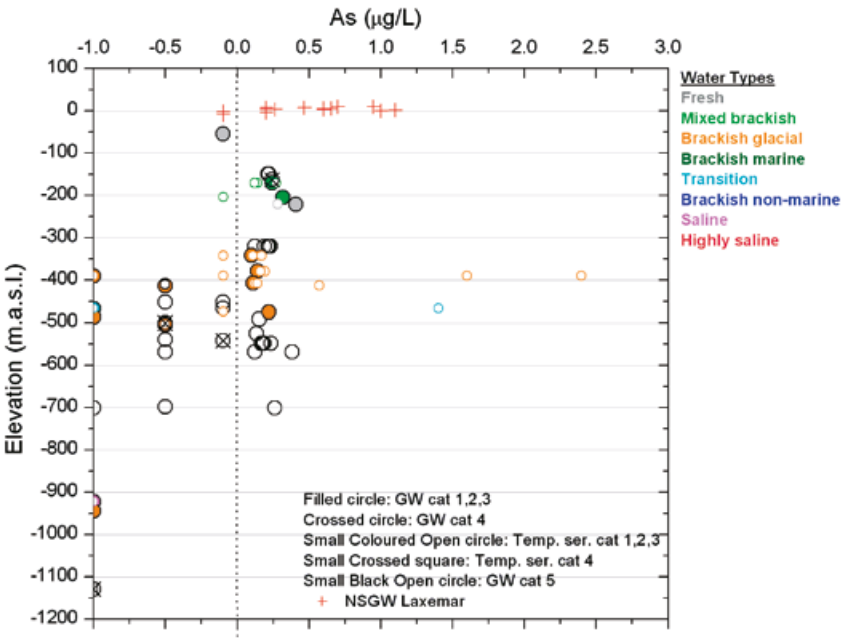

Figure 4-13. *Distribution of As with elevation in the Laxemar subarea discriminating the temporal series samples (open coloured circles) from the sample selected as being representative (infilled coloured circles). Negative values indicate contents below detection limit for different analytical methods thereby underlining the analytical uncertainties.*

groundwaters, KLX08:–391 m, KLX13A: –408 m and KLX15A: –467 m, where values up to 1.25 to 2.50 µg/L are measured; the first two also show instability during the time series measurements. The KLX08:–391 m sample shows a systematic decrease in As from 2.4 µg/L to under detection during 2 to 3 weeks, and KLX13A: –408 m a decrease from 0.14 to 0.11 µg/L in one week, but then increased again during the following six days. The representative sample selected from this borehole depth coincides with the lowest arsenic content. The anomalously high value of 1.4 µg/L As in KLX15A: 467.22 m represents the only value measured over a 39 day period, the rest being under the detection limit of 0.1 µg/L.

In conclusion, there are too few data available to make a proper evaluation of the instability/ contamination or otherwise of these heavy trace elements at Laxemar that may have arisen during borehole activities (drilling; logging, sampling etc.). However, minor ions such as sulphide do show a disturbing fluctuation of values recorded during the monitoring programme.

Rare earth elements

Rare earth elements (REEs) are usually evaluated collectively due to their similar chemical behaviour. In general, the total REE concentrations in the Laxemar groundwaters vary from below the detection limit to 4.5 µg/L, and most of the groundwaters analysed for REEs lack data above the detection limit for the complete series.

In only nineteen cored borehole sections, representing sampling depths from approximately 160 to 1,300 m, was it possible to analyse an almost complete REE series. The REE-chondrite normalised curves for these samples are shown in Figure 4-14 (chondrite values used are from /Evansen et al. 1978/). The majority of the analysed samples consist of brackish glacial waters sampled mainly between about 300 and 600 m depth together with: a) two shallower samples (~25 to 330 m depth) of fresh and mixed-brackish water composition (Cl < 250 mg/L), and b) two of the deepest samples corresponding to a transition to saline non-marine (~700 m), and highly saline groundwaters (~1,300 m). The total REE concentrations in these samples range from 0.3 to 4.45 µg/L except for the highly saline type which shows the lowest REE contents (ΣREE = 0.06 µg/L).

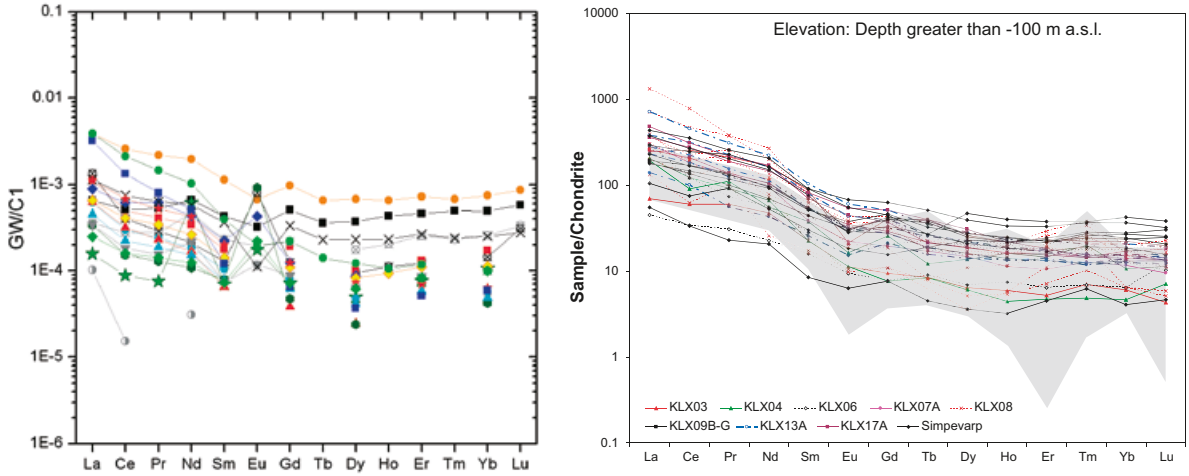

Figure 4-14. *Chondrite normalised groundwater REE curves from cored boreholes (left figure). Chondrite normalised REE patterns for fracture fillings from below 100 m depth (right figure). The grey shaded area represents the composition of the main rock types (Ävrö quartz monzodiorite, Ävrö granodiorite and quartz monzodiorite; taken from /Drake and Tullborg 2008/.*

In general, all the samples largely exhibit similar uniform REE patterns normalised to chondrite, i.e. light REE-enriched patterns. This pattern is very similar to REE patterns found in the contact fracture fillings and wall rock /Drake and Tullborg 2008/, i.e. when normalised to NASC (North American Shale Composite) or local granites, dissolved REE patterns tend to exhibit flat or slightly heavy REE-enriched trends. This suggests that the REEs are not strongly fractionated by water-rock interaction or, in some cases, the HREEs are leached preferentially. Preferential leaching of HREEs would be consistent with the greater stability of their aqueous complexes compared to those of the LREEs for all inorganic ligands except Cl^- and SO_4^{2-} /Wood 1990ab/ and it is normally associated with dominantly carbonate complexation.

Speciation calculations have been performed to confirm these results using the PHREEQC and the WATEQ4F databases with REE data from /Luo and Byrne 2001, 2004/ for carbonate and chloride complexes, /Schijf and Byrne 2004/ for sulphate complexes, /Klungness and Byrne 2000/ for hydrolised species, /Luo and Millero 2004/ for fluoride complexes, /Millero 1985/ for nitrate complexes, and /Byrne et al. 1991, 1996/ for phosphate complexes. The REE speciation results indicate that in most groundwaters carbonate complexes are by far the most important species; only when alkalinity contents are very low and chloride or sulphate very high, do REE-Cl and REE-SO_4^{2-} complexes, together with the free ions, comprise a significant percentage of the total REEs. The transition between the two extremes is represented by the brackish glacial groundwaters in which carbonate is the main ligand, but some traces of sulphate or even the free species can be important for the LREEs.

In general, the dissolved REE patterns show the same distribution as the fracture filling minerals and the wall rock, indicating that the REEs are mainly derived from these phases and that the leaching has been fairly equal for all of the REEs. For instance, the slightly negative Eu-anomalies found in the fracture fillings have been inherited from the wall rock signatures /cf Drake et al. 2006/ and the less common positive Eu-anomalies, and some LREE enrichments, could be derived from some calcites /Drake and Tullborg 2008/. However, slight HREE-enrichment can be found in some groundwaters as a result of speciation with carbonate complexes. Other fractionation effects due to the complexation with organic matter have not been analysed here but they should be considered in future studies.

4.1.6 Origin of sulphate

The available $\delta^{34}S$ and SO_4^{2-} data in the Laxemar-Simpevarp area groundwaters have been plotted in Figure 4-15a where the measured $\delta^{34}S$ values for category 1 to 3 samples range between +9.1 to +37.2‰ CDT /Gimeno et al. 2009/. Most of the Simpevarp subarea samples show values in the range of +15 to +25‰ CDT, whereas Laxemar groundwaters show both higher and lower values

/Smellie et al. 2006/. Values higher than marine (~ 21‰ CDT) are found in groundwaters with chloride contents < 6,500 mg/L (Figure 4-15b) and at depths down to about 400 m (Figure 4-15c). The highest $\delta^{34}S$ values correspond to samples of low dissolved sulphate concentrations (Figure 4-15a), and can thereby be interpreted as being produced *in situ* by sulphate-reducing bacteria.

The highest value (+37.2‰ CDT) is detected in the Laxemar subarea groundwaters with chloride contents less than 500 mg/L and with SO_4^{2-} about 30 mg/L in borehole KLX03 (–171 m elevation). Such an extreme $\delta^{34}S$ value is a strong indicator of sulphate reduction in closed conditions. Furthermore, all but two of the Laxemar groundwater sections sampled down to about 350 m depth show $\delta^{34}S$ values higher than +25‰ CDT, and all but one of these sections show sulphate contents below 100 mg/L. This supports the microbial data that show the presence and activities of sulphate reducers at these depths (cf Section 4.4.1). Below about 350 m a switch towards lower $\delta^{34}S$ values and correspondingly higher sulphate contents can be seen, although some high $\delta^{34}S$ values (> +29‰ CDT) are present down to about 400 m.

Generally, groundwaters with SO_4^{2-} contents higher than 250 mg/L show decreasing $\delta^{34}S$ with increasing sulphate content (Figure 4-15a), consistent with a lower (if any) sulphate reduction activity. This is shown by the samples from depths greater than about 400 m. Lowering of the $\delta^{34}S$ signature by oxidation of sulphides seems to be less probable for the groundwater samples and is not supported by fracture mineral investigations /Drake and Tullborg 2009b/. However, recent sulphur isotope analyses in fracture gypsum samples from boreholes KLX03 (from +5.9 to +6.6‰ CDT at –533 and –590 m elevation) and KLX08 (from +3.7 to +12.1‰ CDT at –795 to –919 m elevation) support that gypsum dissolution may lower the $\delta^{34}S$ to the observed values in the deeper groundwaters (cf Figure 4-15c).

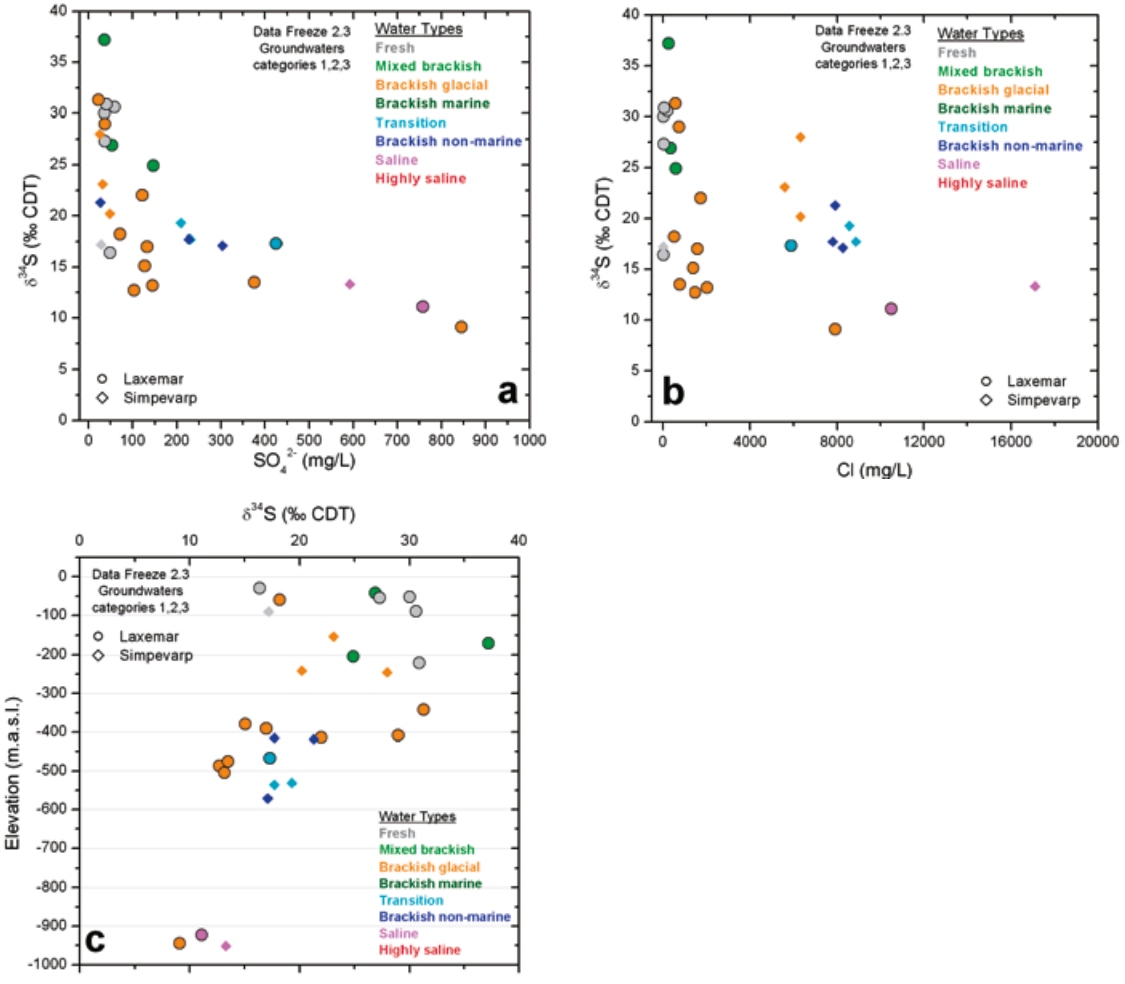

Figure 4-15. *$\delta^{34}S$ versus sulphate (a), chloride (b), and elevation (c) in the groundwaters from the Laxemar-Simpevarp area.*

In conclusion, the origin of the sulphate in the shallow groundwaters may be of a quite different origin in common with the surface and near surface waters (including atmospheric deposition, oxidation of sulphides, leaching of marine clays etc.), but the original isotopic signature is significantly modified by microbial sulphate reduction. This is most prominent down to depths between about 300 to 400 m depending on location. At greater depth the sulphate content increases and the origin of this sulphate can be attributed mostly to dissolution of sulphate minerals (gypsum), although some of marine origin may still be present.

4.1.7 Strontium and barium

The distribution of strontium with increasing depth and salinity is closely similar to that of calcium (Figure 4-16 a-d). However, the Ca/Sr ratio is not constant and shows a wide and variable range in the shallow groundwaters as a result of weathering of the different rocks and minerals. At greater depth the ratio seems to stabilise to almost constant values in groundwaters with salinities higher than approximately 4,000 mg/L, an observation shared also at Forsmark and Olkilouto /Gimeno et al. 2009/. A further observation is that these ratios agree with those characterising the respective brine end members. This may suggest that in the more saline groundwaters calcium and strontium are mostly inherited from the saline end member and controlled by mixing /cf Gimeno et al. 2008, 2009/, despite the fact that both elements, especially calcium, have undergone clear heterogeneous processes (e.g. gypsum dissolution or surface processes).

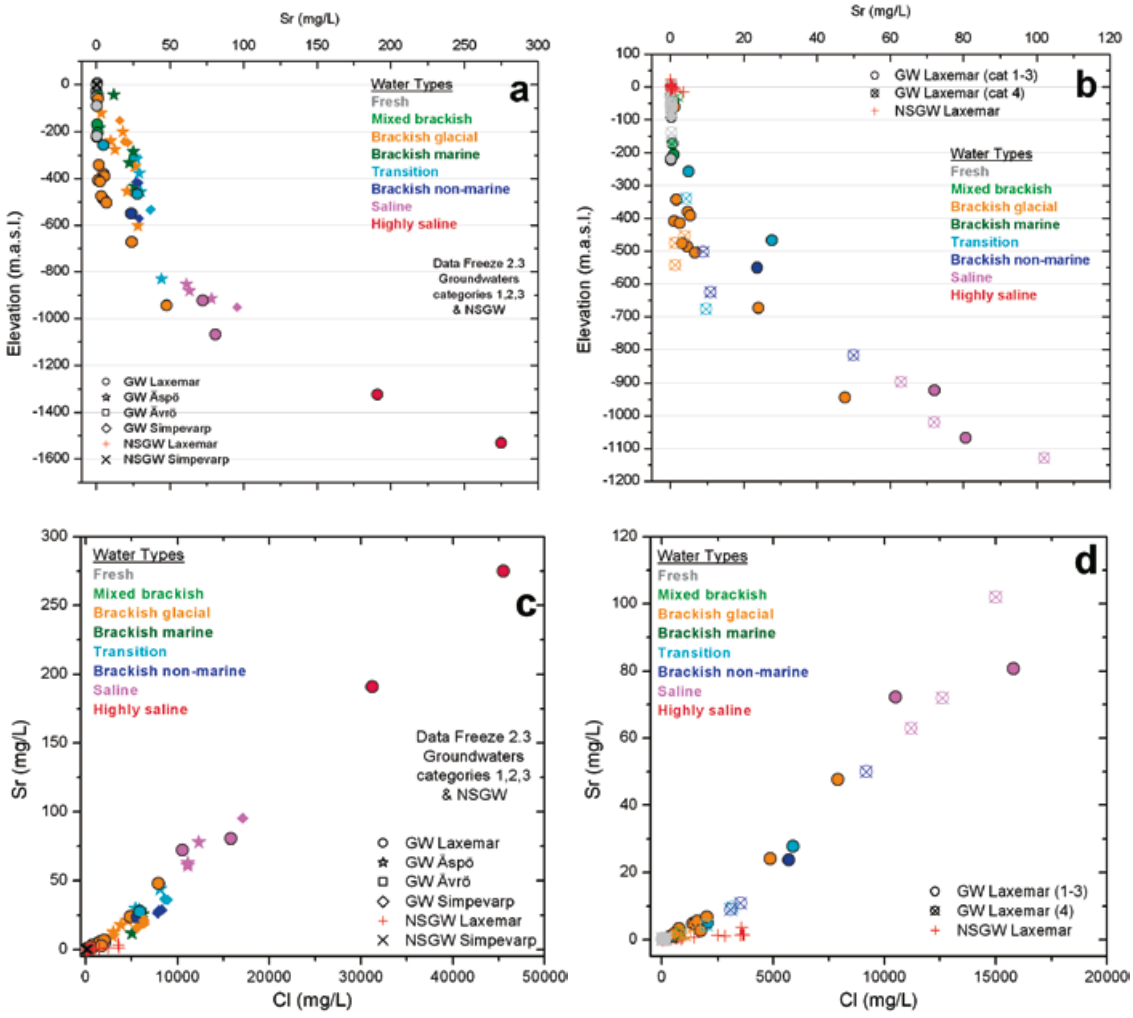

Figure 4-16. *Strontium concentrations versus elevation (a, b) and chloride (c, d). The Laxemar-Simpevarp area in a) and c) are based on categories 1–3 groundwaters and near surface groundwaters, and in b) and d) based on categories 1–4 groundwaters in the Laxemar subarea, including the near surface groundwaters. Note that the scales are different for the Laxemar-Simpevarp area and for the Laxemar subarea, for increased resolution at shallower depths in the latter.*

Strontium isotope ratios ($^{87}Sr/^{86}Sr$) have been measured in groundwater samples from cored and percussion boreholes in the Laxemar-Simpevarp area and are plotted against 1/Sr content in Figure 4-17 in order to reveal possible mixing trends. The isotope ratios show a large variation in the near surface groundwaters (0.711 to 0.732), especially high ratios in samples with low strontium contents which support the influence of different weathering processes noted above, whereas low ratios in samples with higher strontium contents indicate possible marine sources. For groundwaters at depths below 50 m the range is, with a few exceptions, much narrower (0.715 to 0.717) and overlaps with the values measured in the host rock /Drake and Tullborg 2009a/. There is no evident mixing trend when plotting the 1/Sr versus strontium isotope ratio, although the deepest sample analysed shows the highest ratio and the highest strontium content. The samples with a small marine component show no indication of a marine strontium isotope ratio (~ 0.7092) which means that water-rock interaction processes have erased a possible Littorina Sea signature. It can therefore be argued that: a) not only mixing but also water-rock interaction is important for the understanding of the strontium system, and b) the strontium istotopes show no significant variation with strontium content or with depth. In fact, all the Laxemar groundwater types show fairly similar strontium isotope ratios and this is interpreted as the result of homogenisation due to water-rock interaction, mainly ion exchange processes /Peterman and Wallin 1999/.

Barium, in contrast to strontium, does not show a clear trend with depth or salinity; most values fall within the 0–200 µg/L range with a small increase to about 400 µg/L at about 500 m depth (Figure 4-18a–b). The lack of any marked trend suggests some type of mineralogical control in the behaviour of barium (cf Section 3.4.3 in /Gimeno et al. 2009/). Two different barium minerals have been detected in fracture coatings in the area; barite (barium sulphate) and harmotome (a Ba-zeolite). The anomalously high barium concentrations measured in a few samples from Simpevarp at depths of about 200–400 m could be related to analytical problems, but alternatively can be explained by the presence of harmotome locally present in fractures down to about 300 to 400 m /Drake and Tullborg 2009a/ (cf Section 4.8.2).

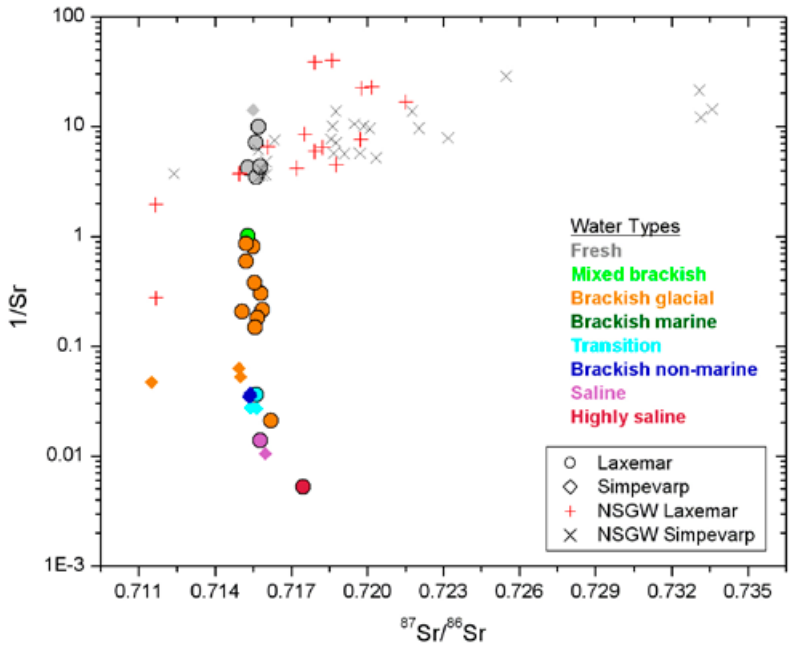

Figure 4-17. *Plot of $^{87}Sr/^{86}Sr$ versus 1/Sr in groundwaters from the Laxemar-Simpevarp area.*

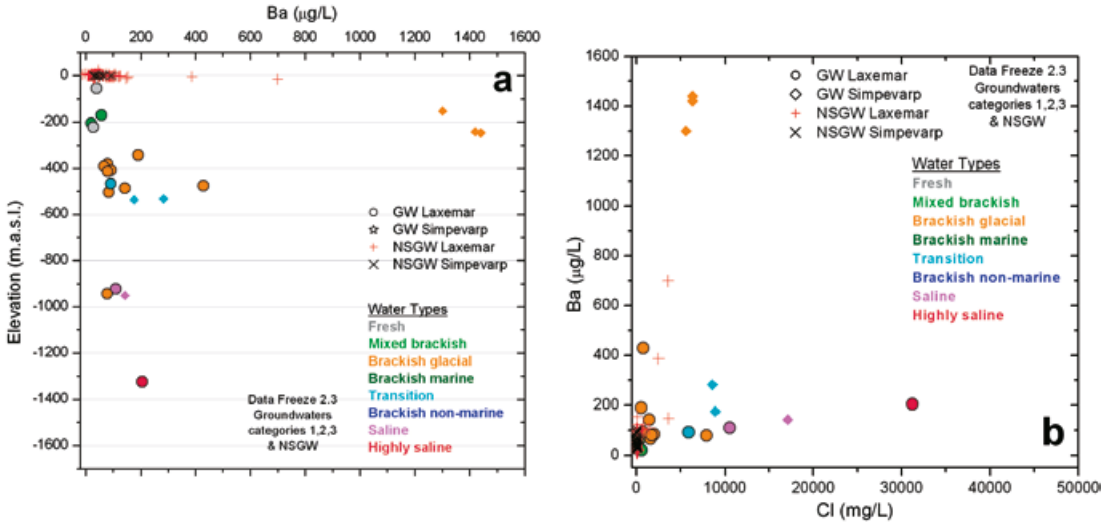

Figure 4-18. *Barium versus (a) elevation, and (b) chloride, in the Laxemar-Simpevarp area groundwaters (including near surface groundwaters – NSGW).*

4.1.8 Phosphate

Phosphate concentrations (PO_4^{3-}) in the Laxemar-Simpevarp groundwaters are low (Figure 4-19) compared with, for example, those recorded at Forsmark /Smellie et al. 2008/, Olkiluoto, Finland /Pitkänen et al. 2004/ or the Lac du Bonnet Batholith, Canada /Gascoyne 2004/. The highest variability and contents of dissolved phosphate in the Laxemar-Simpevarp area (and also in the Forsmark area) are associated with the near surface groundwaters (with maximum values near 30 mg/L) and some fresh shallow groundwaters (up to 0.1 mg/L; Figure 4-19). Concentrations in deeper groundwaters are mostly below 0.05 mg/L or even below the detection limit.

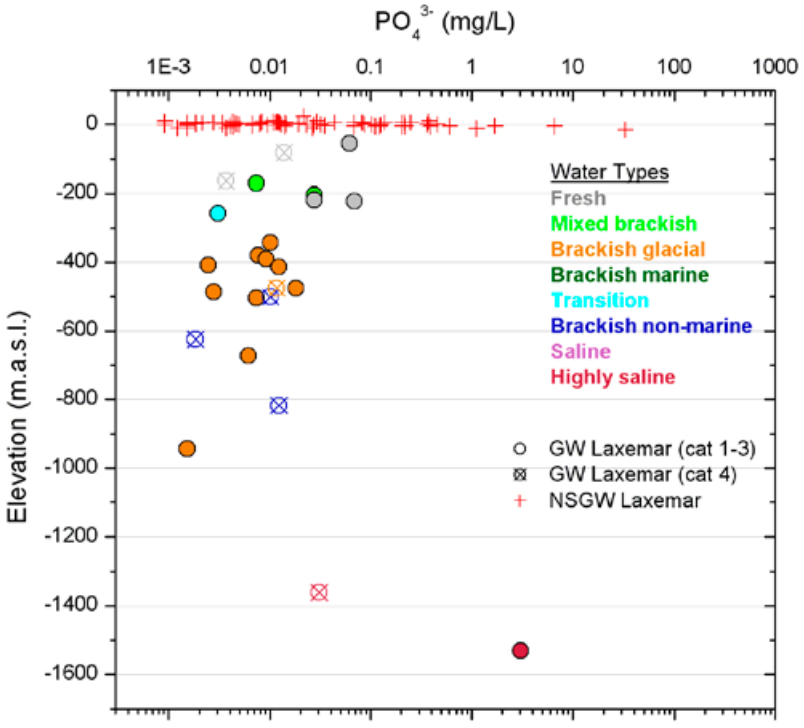

Figure 4-19. *Distribution of phosphate versus elevation in the Laxemar subarea groundwaters.*

4.1.9 Supplementary data from borehole KLX27A

Supplementary groundwater data from cored borehole KLX27A became available after the 'Extended data freeze Laxemar 2.3'. This borehole drilled in the southwestern part of the Laxemar subarea is 650 m long, inclined 65° to the north, and represents the last drilled borehole within the Oskarshamn site investigation programme (cf Figure 4-20). The intercepted bedrock consists of quartz monzodiorite with subordinate occurrences of fine-grained granite and mafic rocks. Eight deformation zones are identified in the geological single borehole interpretation of which six are classified as minor. Two major brittle deformation zones are located at 168 to 176 m and 208 to 255 m borehole length /Carlsten et al. 2008/.

Groundwater sampling for complete chemical characterisation (CCC) was performed at section 641.50 to 646.03 m borehole length (elevation –559 to –567 m). Sampling and analyses were carried out during the summer and autumn of 2008, and therefore the results are not included in the dataset used in the SDM_Site Laxemar hydrogeochemical interpretation and modelling studies. Because the section sampled falls within the intended repository depth interval (i.e. –400 to –700 m elevation), the results are of great importance for the site description. The time-series data recorded during the sampling campaign (from March 14 to June 6 2008) indicate stability and, together with a low drilling fluid content (< 0.1%), the sampled section is regarded as representative. Considerable effort was made to obtain high quality Eh measurements but this was unfortunately not successful due to equipment failure and extreme weather conditions (thunderstorms). Nevertheless, reducing conditions were indicated even though stable Eh values were not achieved.

The groundwater sampled is brackish glacial (Na-Ca-Cl-SO_4) in type (Cl = 1,700 mg/L, Na = 973 mg/L, Ca = 125 mg/L, SO_4 = 106 mg/L). Bicarbonate is low (13 mg/L) which excludes carbon-14 analyses of the inorganic carbon. Tritium is, as expected, below detection (< 0.8 TU) and stable isotope analyses show depleted $\delta^{18}O$ (–14.7‰ VSMOW). Figure 4-20 plots $\delta^{18}O$ versus chloride using category 1 to 4 groundwater samples from the Laxemar subarea, together with KLX27A:–563 m elevation. The plot shows that the groundwater composition of KLX27A is typical for the deeper, brackish glacial waters and therefore in agreement with the present understanding of the site.

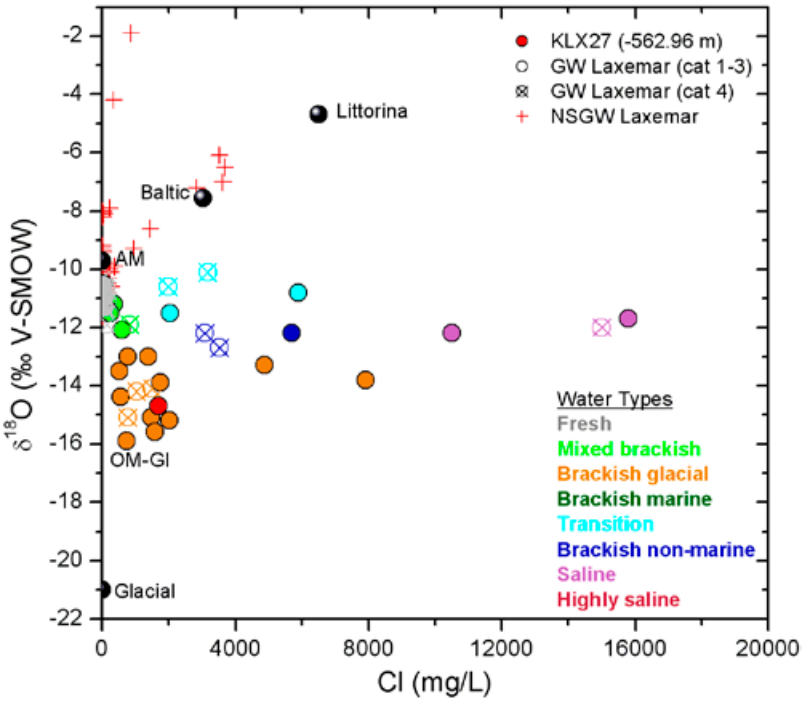

Figure 4-20. *$\delta^{18}O$ versus chloride for category 1–4 groundwaters (including near surface groundwaters) from the Laxemar subarea plotted together with KLX27A:–563 m elevation (red infilled circle). End members are shown as dark grey spheres.*

4.2 Mixing calculations

4.2.1 Background and predictions compared to groundwaters

Multivariate Mixing and Mass-balance Modelling (M3) /Laaksoharju et al. 1999, Gómez et al. 2006/ uses the Principal Component Analysis (PCA) method to analyse variations in groundwater compositions so that the mixing components, their proportions, and chemical reactions can be identified. The PCA method is statistical and identifies the principal components in terms of linear combinations of the concentrations of those species analysed that best explain the spread in data. The method quantifies the contribution to hydrochemical variations by mixing of groundwater masses in a flow system by comparing groundwater compositions with identified end-member waters. The choice of end members is crucial for modelling the mixing proportions and considerable effort has been made to select the more suitable ones and to assess the uncertainties associated with their compositions /Gimeno et al. 2008, 2009, Gurban 2009/.

The hydrogeochemical study of the Laxemar-Simpevarp and Forsmark groundwaters has confirmed that the measured groundwaters are a result of mixtures of (at least) four end-member waters; an old deep saline water (Deep Saline), an old marine water (Littorina Sea), a modern meteoric water (Altered Meteoric), and a glacial meltwater (Glacial). As a result, mixing can be considered the prime irreversible process responsible for the chemical evolution of the Laxemar-Simpevarp (and Forsmark) groundwater systems. The successive disequilibrium states resulting from mixing have conditioned the subsequent water-rock interaction processes and, hence, the re-equilibration pathways of the mixed groundwaters. These reaction processes are especially important in the Laxemar subarea.

In this section, the distribution of the mixing proportions with depth is shown in different plots (2D and 3D). Samples are colour coded to the type of groundwater to observe if the different groundwaters agree with the dominant end member as calculated by M3. These calculations have been carried out using the 'standard' simulation procedure which consists of four end members (composition given in /Gimeno et al. 2008, 2009, Gurban 2009/) and a large set of elements (i.e. Na, K, Ca, Mg, HCO_3^-, Cl, SO_4^{2-}, δ^2H, and $\delta^{18}O$).

Figure 4-21 shows the mixing proportions of Deep Saline water. Taking the different subareas separately, the first general conclusion that can be drawn is that the different groundwater types are very well correlated with the M3 mixing proportions for this end member (also observed for the remaining end-member distributions, cf Figures 4-22 to 4-24). The depth trend of the Deep Saline end member is clearly represented by the Laxemar subarea groundwaters. Here, the different

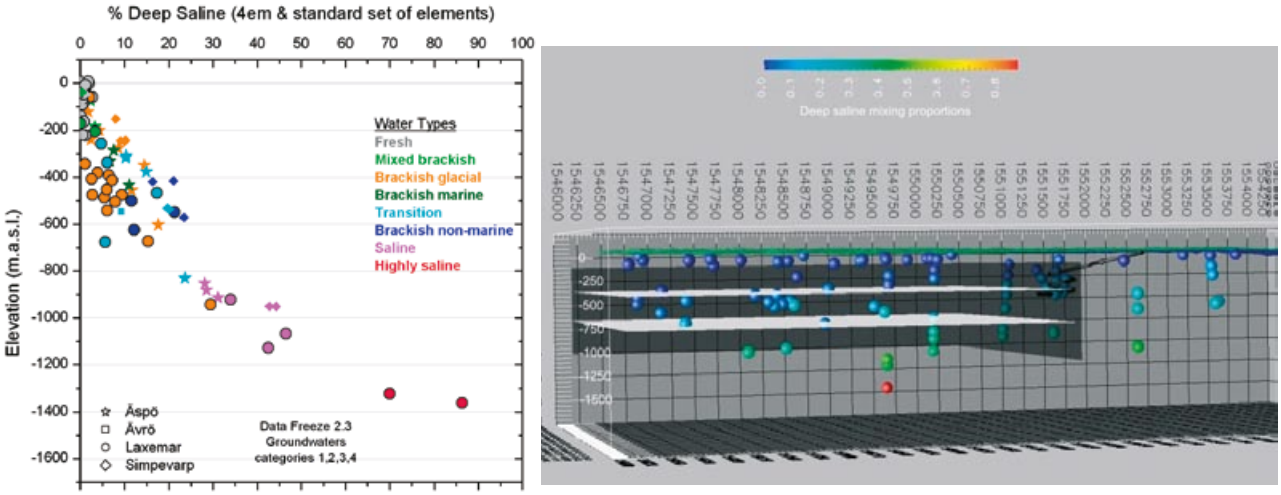

Figure 4-21. *Computed M3 mixing proportions (using 4 end members) of the Deep Saline end member compared with the resulting groundwater types (figure to the left) and shown in 3D in relation to the repository depth (–400 to –700 m elevation) and the Äspö HRL (spiral). Four end members and the standard set of elements have been used in the mixing modelling (this refers to Model 1 in the right hand figure).*

groundwater types evolve towards the saline and highly saline waters with increasing depth by an increased percentage of the Deep Saline end member from proportions > 35% up to almost 100% (deepest samples taken from borehole KLX02). These saline and highly saline waters are found below repository depths (–400 to –700 m elevation) in the focused volume. The other locations also show a percentage increase of Deep Saline with depth, but only up to a maximum of 30% in Äspö and 40% in the Simpevarp subarea. The slightly higher Deep Saline percentage for the same depth (about 1,000 m) in Simpevarp (40%) compared to Äspö and Laxemar (30–35%) is an interesting observation, reflecting the discharge nature of the groundwaters near the coast.

In Figure 4-22 the Glacial end member corresponds to the depleted $\delta^{18}O$ signatures indicative of an influx of cold climate water such as glacial meltwater from the last deglaciation. This glacial signature is clearly seen in the plots of the different areas and the agreement with the groundwater types defined is also good. Orange coded samples, which correspond to the brackish glacial groundwater type, have the highest glacial contribution (up to 55%) followed by the transition waters (turquoise code), and both are mainly found at repository depths in the focused volume. The rest of the groundwater types have Glacial mixing proportions of less than 30%.

Groundwaters with important Littorina Sea water end-member signatures (Figure 4-23) are only detected in a few samples from Äspö and Simpevarp. The percentage of Littorina in the Laxemar groundwaters is very low and close to the detection limit of the M3 method (0.1 mixing units). Only boreholes KLX01, KLX10 and KLX15A show slight influences of brackish marine water, with less than 15% of Littorina component in the focused volume and at repository depths. Independent evaluation of Littorina signatures based on chloride and bromide support this low marine water signature in the system. This may reflect that the penetration of Littorina Sea water has been less important at Laxemar due to the palaeogeographical history of the area /Smellie and Tullborg 2005/, or that it has already been flushed out (cf Section 2.5).

Figure 4-24 shows the mixing proportions of the recent Altered Meteoric end member. The groundwater samples with an Altered Meteoric end-member portion > 80% correspond generally to groundwaters with measurable tritium contents (restricted to the first 100 to 200 m). As expected, the resulting 'fresh' and 'mixed brackish' waters show large proportions of the Altered Meteoric end member. There is an important amount of Altered Meteoric end member at the repository level in the Laxemar subarea between 30 to 60% for most of the samples.

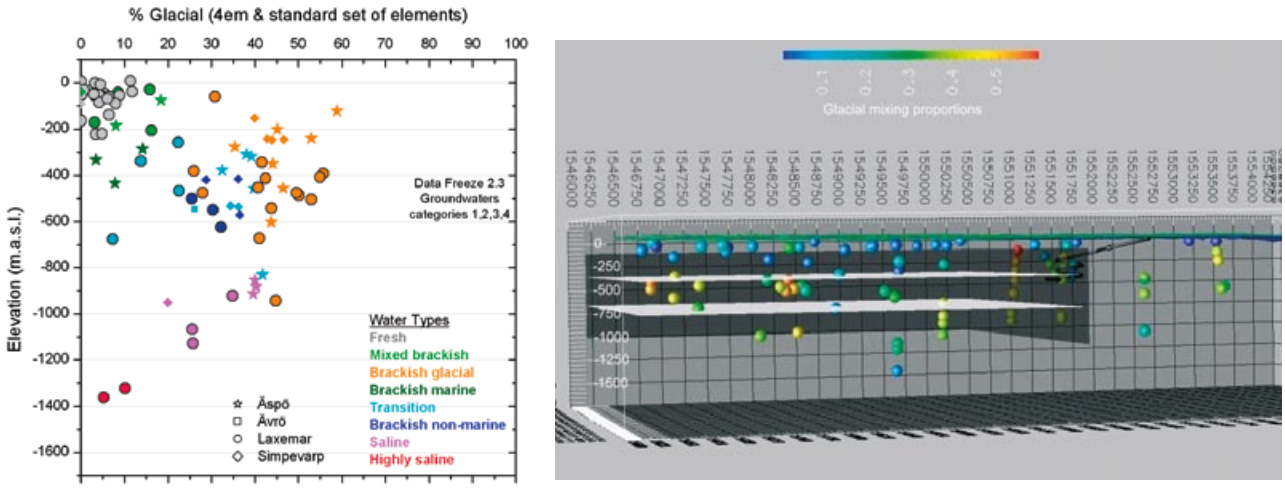

Figure 4-22. *Computed M3 mixing proportions of the Glacial end member compared with the resulting groundwater types (left-hand figure) and shown in 3D in relation to the repository depth (–400 to –700 m elevation) and the Äspö HRL (spiral).*

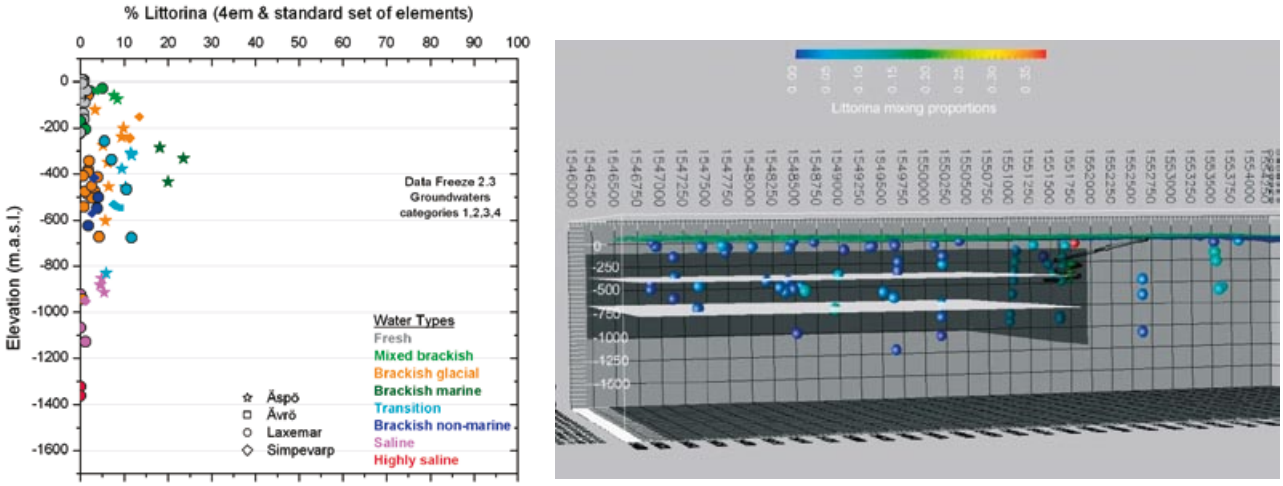

Figure 4-23. *Computed M3 mixing proportions of the Littorina end member compared with the resulting goundwater types (left-hand figure) and shown in 3D in relation to the repository depth (–400 to –700 m elevation) and the Äspö HRL (spiral).*

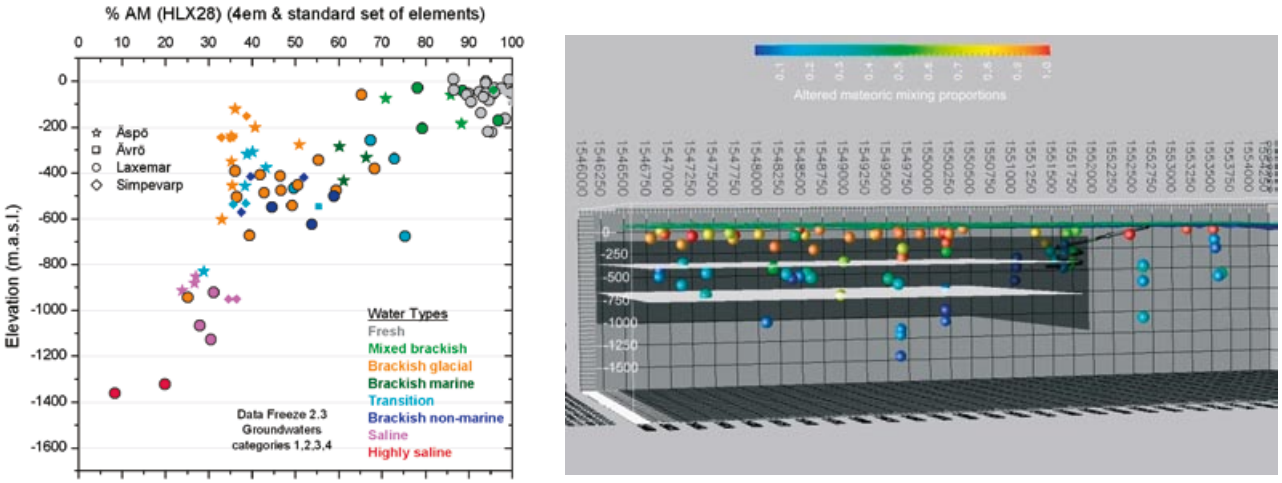

Figure 4-24. *Computed M3 mixing proportions of the recent Altered Meteoric end member compared with the resulting groundwater types (left-hand figure) and shown in 3D in relation to repository depth (–400 to –700 m elevation) and the Äspö HRL (spiral).*

4.2.2 Predictions related to conservative elements

The uncertainty analysis performed by /Gómez et al. 2008/ concluded that the scatter introduced by the reactions (unknown *a priori*) in any study with real groundwaters may produce important effects on the calculated mixing proportions and, therefore, M3 mixing proportions should not be used without first checking their ability to predict conservative elements (that is, elements not involved in chemical reactions). This analysis (mass balance analysis) was made on the M3 results described above (four end members and the standard set of elements) and on the results of an alternative approach suggested by /Gómez et al. 2008/ and reported in /Gimeno et al. 2009/ in which only those elements that behave conservatively in each system are used. The analysis compares the concentrations of conservative elements found in the groundwater systems and the concentrations obtained from the mixing proportions obtained with M3. As the conservative elements are not affected by reactions, the calculated values should be identical to the values measured in the real groundwater samples /Gimeno et al. 2009/.

Laxemar groundwaters represent a good set of samples to apply this present approach because the Littorina Sea influence is either weak or lacking, therefore enabling the use of only three groundwater end members, namely: Deep Saline, Glacial and Altered Meteoric. Consequently, the three independent conservative elements (Cl, Br and $\delta^{18}O$) provide an adequate basis on which to perform the principal component analysis. Using just the conservative elements is the only way to avoid the effects of reactions on the calculated mixing proportions.

The results of this mass balance analysis indicate that with the standard approach (four end members and the large set of elements) the mean deviation for chloride (differences between the measured groundwater concentrations and the values calculated from the mixing proportions obtained with M3) reaches values up to 1,000 mg/L, whereas the deviation between the calculated and measured chloride when using only conservative elements and three end members, is only 50 mg/L /Gimeno et al. 2009/. The main limitation of this latter approach is that the coverage is lower (90% vs. the 94% obtained with the standard procedure) as the samples with a Littorina contribution can not be explained. However, for the rest of the samples, the confidence in the calculated mixing proportions is clearly greater since the use of conservative elements reflects only pure mixing processes /Gimeno et al. 2009/.

Once the mixing proportions have been checked by means of the concentrations of the conservative elements, the concentrations of the remaining elements can also be evaluated by the mass balance analysis by comparing their real contents with those obtained with the calculated mixing proportions. The differences between the measured and the calculated concentrations can be a good indication of the main kind of chemical reactions taking place in the system.

Figures 4-25 and 4-26 show the measured concentrations of a particular element in the horizontal axis and the computed concentration (by using the mixing proportions) on the vertical axis. If all the samples plot, for a particular element, near the red diagonal line, it means that the measured and computed concentrations are identical and, thus, the content of that particular element is controlled only by mixing. If, on the other hand, the samples deviate from the diagonal line, this indicates that reactions have modified the concentration of the element. If the calculated concentration of an element is larger than the measured one, a process that depletes the real sample in that particular element must be accounted for. If the calculated concentration is lower than the measured one, a process that enriches that element is required.

The conservative elements Cl and $\delta^{18}O$ (Figure 4-25a and b) plot near the red diagonal line indicating that the measured and computed concentrations are generally well correlated and, thus, are controlled only by mixing.

Sodium and calcium (Figure 4-25c and d) plot very close to the diagonal line for the saline waters, but show slight deviations for the more diluted waters. This means that these elements, in spite of being controlled mainly by mixing (especially for the saline samples), are also affected by reactions. Looking at the position of the samples, sodium is underestimated while calcium is overestimated, which could be interpreted as a result of cation exchange. This is consistent with what is expected in dilution scenarios of highly saline waters, where calcium replaces sodium in the exchangers /Appelo and Postma 2005/ and also with what has been obtained by the thermodynamic simulations /Gimeno et al. 2009/.

Potassium shows a fairly good match between the real and the calculated values, which is surprising considering its reactivity in these systems (Figure 4-26a). However, the calculated contents for the more saline waters are overestimated while, in general, the less saline waters are underestimated. Therefore, exchange reactions and aluminosilicate dissolution processes appear to have affected this element (cf /Gimeno et al. 2009/).

The sulphate content is fairly well reproduced for some of the groundwaters (Figure 4-26b), although for the majority the calculated values underestimate the real ones, except for some dilute samples in the Laxemar subarea and some more saline waters in the Simpevarp subarea where the calculated values are higher than the measured ones. In general, dissolved sulphate is affected by the input of additional amounts originating from the dissolution of gypsum or by depletion related to the presence of sulphate reduction activity (cf /Gimeno et al. 2009/).

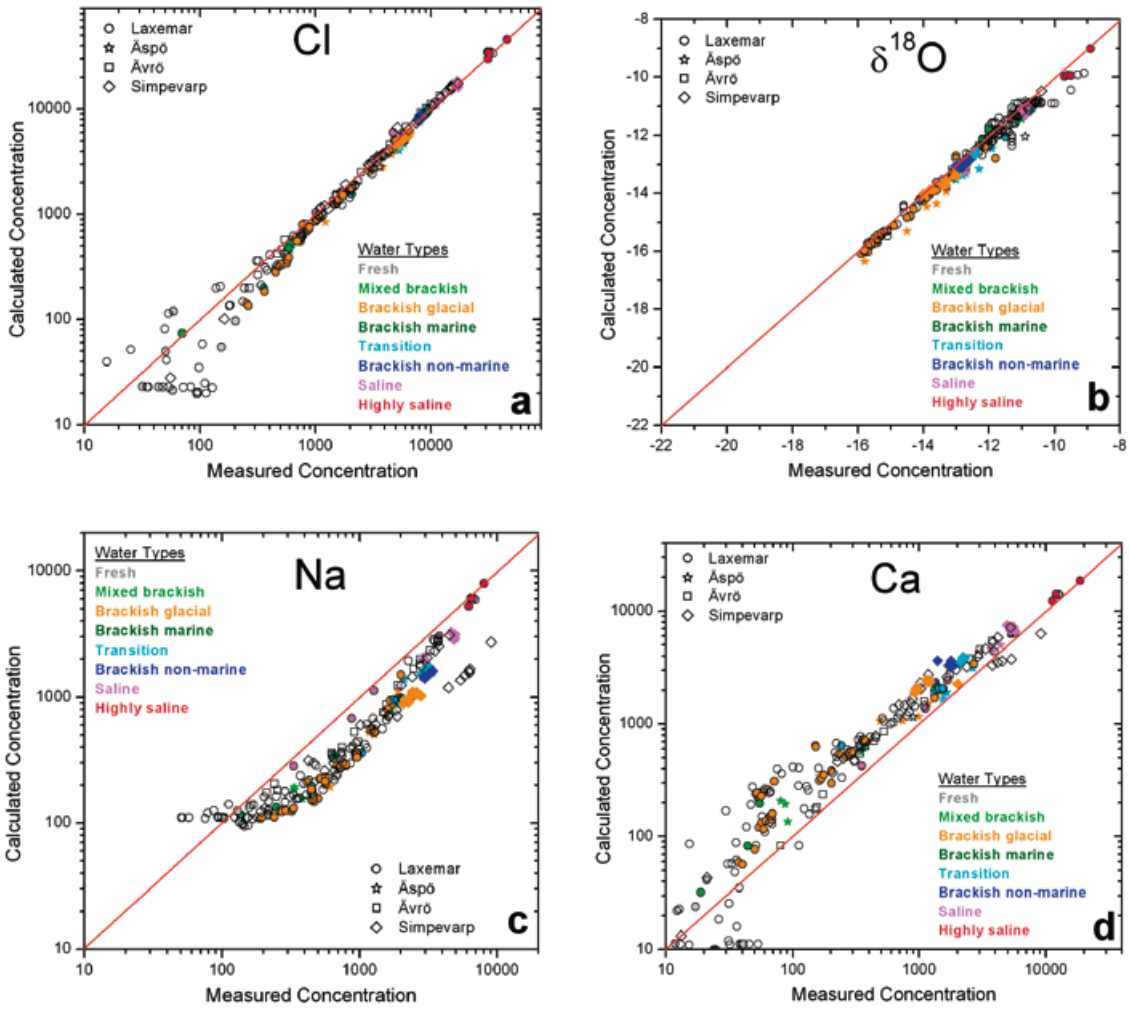

Figure 4-25. *M3 predicted concentrations versus measured concentrations of Cl (a), $\delta^{18}O$ (b), Na (c), and Ca (d) in the Laxemar-Simpevarp area groundwaters. The samples are colour coded based on, when possible, the groundwater type they represent, otherwise the symbols are uncoloured.*

Magnesium and bicarbonate are clearly affected by reactions (Figure 4-26c and d). The calculated values are very similar irrespective of the salinity of the sample, and they are lower than the measured values in the case of magnesium and higher in the case of bicarbonate. For bicarbonate, this fact is mainly related to the generalised presence of calcite reequilibrium which controls the bicarbonate (cf /Gimeno et al. 2009/). For magnesium the explanation is different as the results are partially affected by the exclusion of the Littorina end member in the calculations. The constant values obtained by M3 are the result of mixing three end members with very low and similar magnesium contents. Waters with greater deviations and higher measured values are those containing some Littorina proportion in the standard M3 calculation. For the remaining groundwaters, the highest measured concentrations of magnesium indicate the existence of reactions affecting Mg-bearing minerals (aluminosilicates).

In summary, when chemical reactions only produce slight variations with respect to the chemical composition of the conservative mixing, the reconstruction of chemical compositions from the mixing proportions calculated with M3 are in very good agreement with the measured ones. When chemical reactions produce an important compositional change, the M3 mixing proportions do not reproduce the measured values, and the departure depends on the chemical reaction and/or the type of groundwater. However, this methodology is very useful to obtain the part of the concentration which can be due to mixing and then, to infer what kind of chemical reactions must have occurred to modify (increase or decrease) the final contents. The scatter produced by the non-conservative elements in this kind of statistical analysis influences directly the mixing proportions calculated by the code and their values should be used with caution.

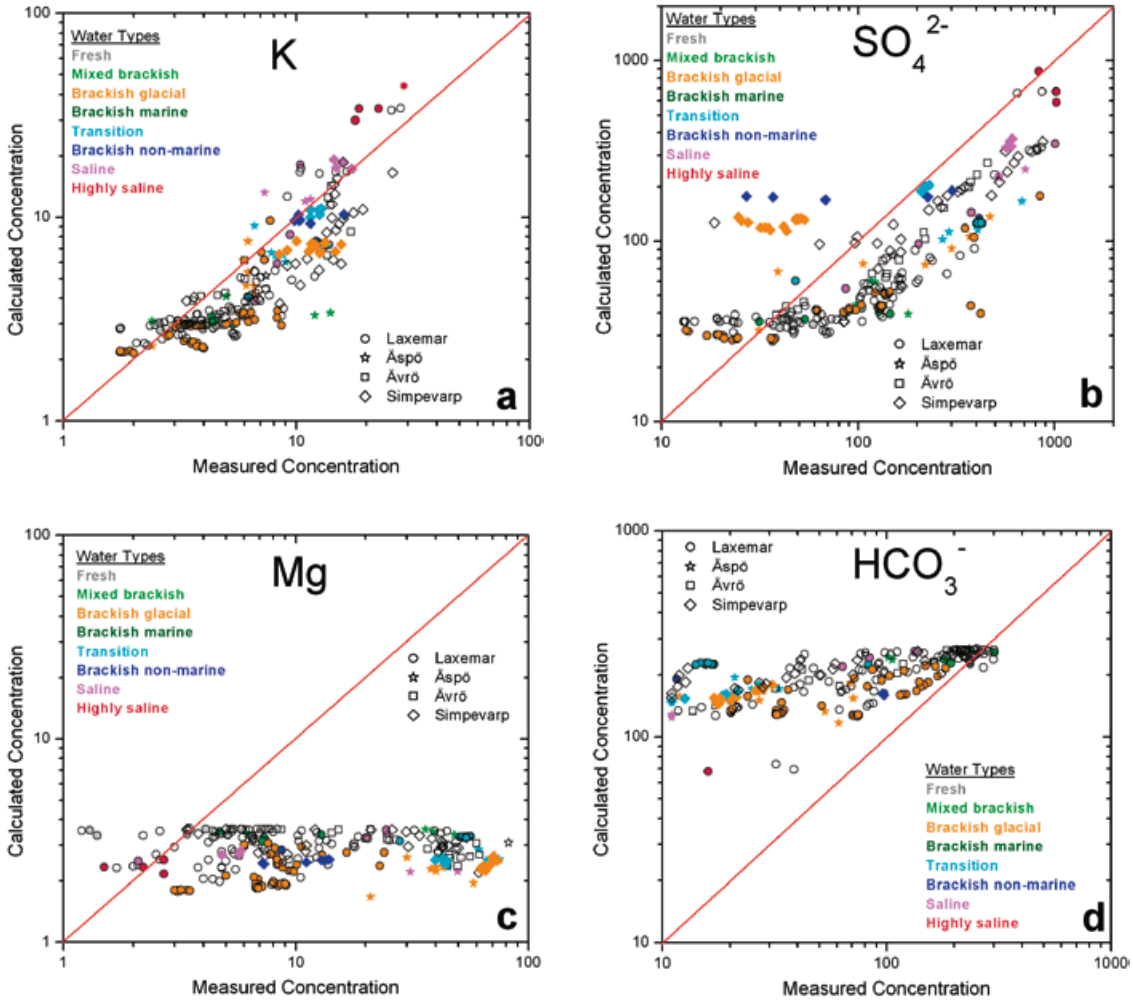

Figure 4-26. *M3 predicted concentrations versus measured concentrations for K (a), SO_4^{2-} (b), Mg (c), and HCO_3^- (d) in the Laxemar-Simpevarp area groundwaters. The samples are colour coded based on, when possible, the groundwater type they represent, otherwise the symbols are colourless.*

Therefore, in spite of the important qualitative information obtained when using all the elements in the M3 calculations, the quantitative values of mixing proportions must be calculated only with the conservative elements when reactions are important in the system. This procedure offers the possibility of obtaining quantitative and reliable mixing proportions and it is very useful when combined with additional methodologies (e.g. classical mass balance and inverse modelling using PHREEQC or similar codes) as the differences between the real and the calculated values for the non conservative elements can be a good indication of the main kind of chemical reactions affecting their contents.

4.3 The redox system

To evaluate the groundwater redox system in the Laxemar-Simpevarp area an integrated modelling approach has been applied by combining hydrogeochemical, mineralogical and microbiological information /Gimeno et al. 2009/. The major aim has been to: a) confirm or support the redox potential field measurements, and b) confirm the redox pair(s) believed to control the redox conditions in the groundwater.

In this section the results from the actual measurements of Eh and redox sensitive elements (i.e. manganese, iron, sulphur and nitrogen systems) initially are discussed. Subsequently, these results have been integrated with the results obtained from redox pair calculations, speciation-solubility cal-

culations and microbiological and mineralogical analysis to identify the main controls of the redox state in groundwaters. Uranium, which is also one of the redox sensitive elements but present in very low amounts in the Laxemar groundwaters, is presented in Section 4.7 together with radium and radon.

The number of samples with representative and complete data for the analysis of the redox system (Eh values, Fe^{2+}, S^{2-}, Mn, NO_3–NO_2–NH_4, microbial and mineralogical data) is scarce, especially the potentiometric Eh measurements at depths exceeding 500 m. Small amounts of oxygen, and possibly other oxidants, incorporated with the drilling water or by direct contamination with air, can produce important changes in the groundwater redox system without being detected during the Chemmac logging. As a trade-off between quality and quantity, only samples with less than 10% of drilling water have been used, in common with the previous model version. The selected waters (40 samples) cover a wide range of depths (from 120 to 1,500 m) but reliable data are restricted to 100 and 900 m representing different groundwater types, i.e. fresh, mixed brackish, brackish glacial, transition and saline groundwaters.

4.3.1 Potentiometrically measured Eh and redox sensitive elements

Potentiometric Eh measurements have been performed in most of the borehole sections sampled for Complete Chemical Characterisation (CCC), but such measurements can be sensitive to both technical and interpretative problems. Over the last 25 years SKB has developed methodologies for the measurement of this parameter /Auqué et al. 2008/ and the results obtained provide, at the very least, useful information for the study of the complex redox system /Gimeno et al. 2009/.

In the Laxemar-Simpevarp area Eh values are between –200 and –310 mV (Figure 4-27*a*), and most of the selected values plotted correspond to the range defined by /Drever 1997/ for groundwaters buffered by sulphate reduction (only some of the most reducing values, less than –300 mV, would be below this range). The distribution of Eh with depth (Figure 4-27b) does not show any evident trend even when individual subareas are considered, or when specific sections in each borehole are analysed. This behaviour was already noticed by /Nordstrom and Puigdomenech 1986/ in Swedish groundwaters down to 600 m depth, and in Forsmark by /Gimeno et al. 2009/. However, this contrasts with other crystalline systems (e.g. in Palmottu, where a similar methodology for Eh measurements was used) and in most aquifers elsewhere, where a marked decrease of redox potential is observed as the residence time and depth of the groundwaters increase (e.g. /Drever 1997, Blomqvist et al. 2000/). The sparseness and heterogeneous distribution of the Eh data with depth is illustrated in Figure 4-28 which represents a simplified 3D visualisation of the site.

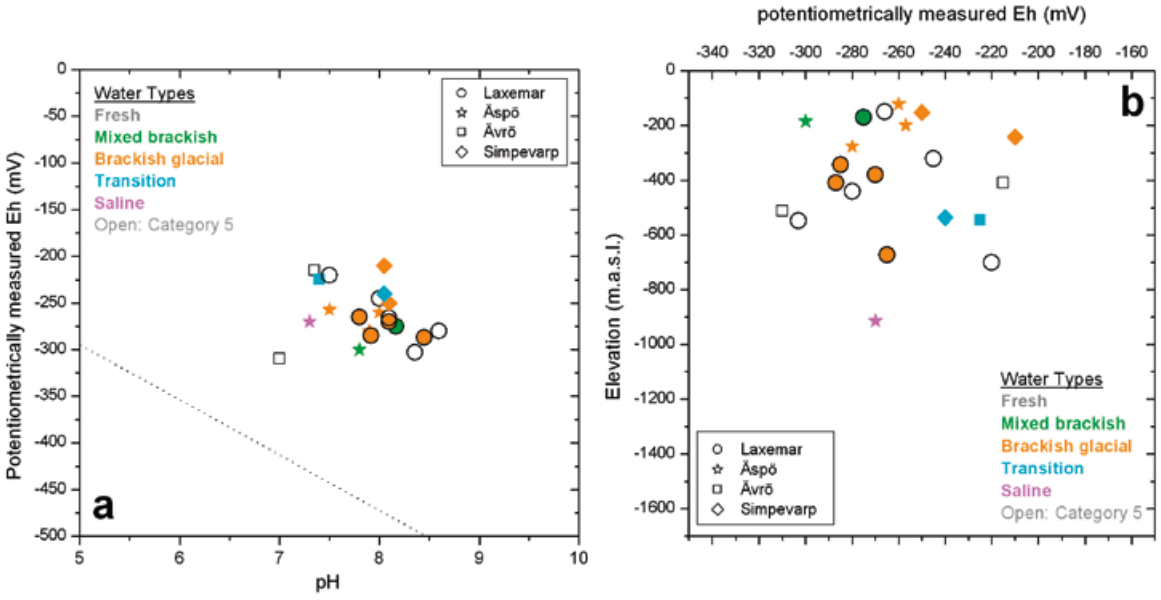

Figure 4-27. *(a) pH-Eh plot, and (b) Eh distribution with depth, for groundwaters from the Laxemar-Simpevarp area.*

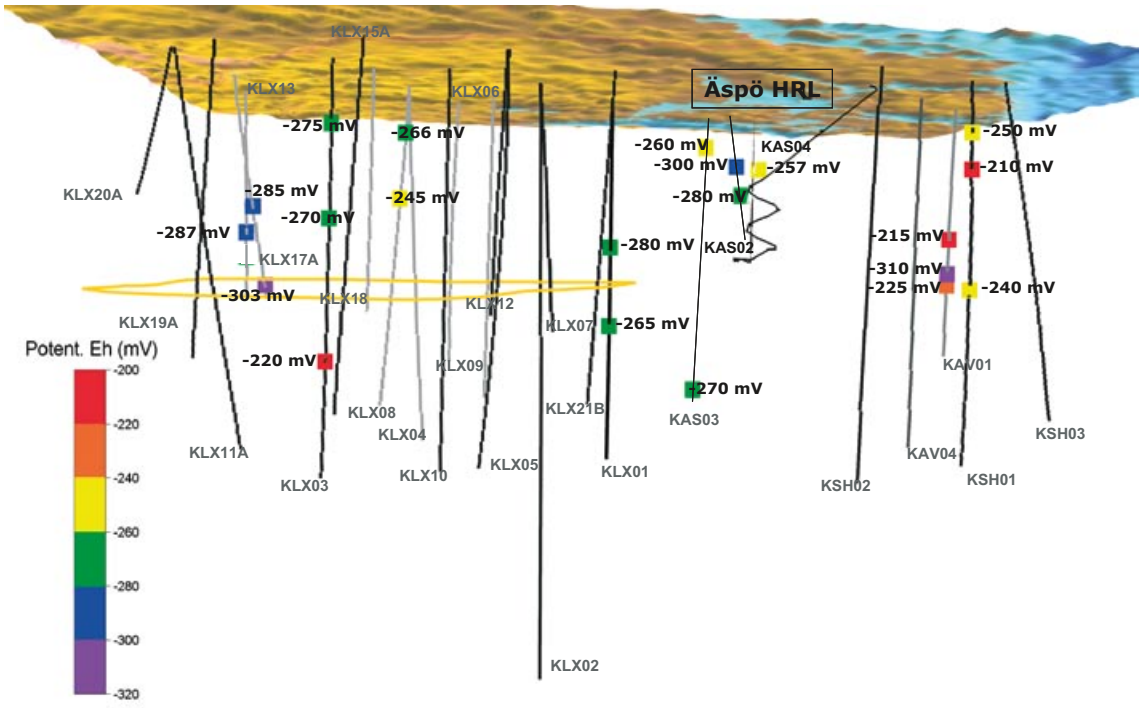

Figure 4-28. *3D distribution of the available potentiometrically measured Eh values illustrated on a simplified sketch of the Laxemar-Simpevarp area showing the position of the boreholes. Vertical scale is exaggerated and therefore some observations may not be placed at the exact depth. For visual reference, a preliminary selected repository candidate area is marked in yellow (Laxemar) and corresponds to 500 m depth.*

All the redox potentials at Laxemar-Simpevarp are clearly reducing even taking into account the possible perturbations of the original redox environment during the measurements, the shallow and dilute groundwaters which are barely affected by mixing, or even for some short-circuited groundwaters with very short residence times. This indicates the ability of microbial and water-rock interaction processes to create very reducing conditions even in the shallowest parts of the system.

With regard to the behaviour of redox sensitive elements, the general trends observed in the dissolved concentrations of iron, sulphur, manganese and nitrogen species are described below. Moreover, the controls of their dissolved contents are interpreted with the support of speciation-solubility calculations performed with the PHREEQC code /Parkhurst and Appelo 1999/ using the WATEQ4F database /Ball and Nordstrom 2001/ with modifications indicated in /Gimeno et al. 2009/.

The surface and near surface system

In the near surface groundwaters, dissolved $\mathbf{Fe^{2+}}$ and $\mathbf{S^{2-}}$ contents from the Laxemar-Simpevarp area do not deviate from the ranges found in similar groundwaters from other Fennoscandian sites. Dissolved Fe^{2+} in the soil pipe groundwaters (Figure 4-29a, b) display values in the range 0.1 to 9 mg/L, which are compatible to values in the near surface groundwaters from Forsmark and Olkiluoto (cf /Pitkänen et al. 2004/). Speciation-solubility calculations show that most of the near surface groundwaters are in equilibrium or oversaturated with respect to siderite ($FeCO_3$; Figure 4-29c, d). This suggests the effective precipitation of siderite and its involvement in the control of dissolved Fe^{2+}.

Table 4-1. Important chemical, physiochemical and microbiological parameters in the selected samples for redox modelling at the Laxemar-Simpevarp area. Cat: indicates the category of the sample. Depth: corresponds to the elevation of the mid part of the sampling interval (m.a.s.l.). DW: represents the percentage of drilling water. The pH and Eh data correspond to the field measurements. Ferrous iron, sulphide, uranium and manganese are expressed in mg/L and methane in mL/L. $\delta^{34}S$ is expressed in ‰ CDT. IRB, SRB and MRB (iron-, sulphate- and manganese-reducing bacteria, respectively) are expressed as ^{10}Log MPN (most probable number) in cells/mL.

Borehole	Sample	Cat	Depth (m)	DW (%)	pH	Eh (mV)	Fe^{2+}	S^{2-}	CH_4	U ($\times10^{-3}$)	Mn	$\delta^{34}S$ (‰CDT)	SRB ^{10}Log MPN	IRB	MRB
KAS02	1548	3	–199.8	0.81	7.5	–257	0.483	0.5	0.03	–	0.91	–	–	–	–
KAS02	1474	3	–317.2	0.71	7.6	–	0.624	0.15	–	–	0.67	–	–	–	–
KAS02	1428	3	–456.2	0.38	8.3	–	0.941	0.13	–	–	0.73	–	–	–	–
KAS02	1433	3	–523.0	0.28	8.35	–	0.24	0.18	–	–		–	–	–	–
KAS02	1560	3	–881.2	0.22	8.5	–	0.049	0.72	0.034	–	0.23	–	–	–	–
KAS03	1569	3	–121.8	0.06	8	–260	0.123	0.71	0.016	–	0.1	–	–	–	–
KAS03	1437	4	–198.7		7.65	–	–	0.05	–	–	0.39	–	–	–	–
KAS03	1448	3	–238.9	1.04	7.8	–	–	0.15	–	–	0.35	–	–	–	–
KAS03	1452	3	–602.4	2.23	8.05	–	–	0.05	–	–	0.24	–	–	–	–
KAS03	1455	3	–830.0	2.57	8.05	–	–	0.11	–	–	0.23	–	–	–	–
KAS03	1582	3	–914.0	0.13	7.3	–270	0.077	1.28	0.037	–	0.2	–	–	–	–
KAS04	1596	3	–185.1	0.16	7.8	–300	0.04	1.1	–	–		–	–	–	–
KAS04	1603	3	–275.6	0.52	7.9	–280	0.324	0.41	0.028	–	0.31	–	–	–	–
KAS04	1588	3	–376.7	0.08	8.04	–	0.256	0.6	0.004	–	0.44	–	–	–	–
KAV01	1384	5	–408.3	7.2	7.35	–215	2.49	0.55	–	–	2.8	–	–	–	–
KAV01	1383	5	–512.2	10	7	–310	2.23	1.2	–	–	2.4	–	–	–	–
KAV01	1374	4	–546.1	¿?	7.4	–225	1.02	0.81	–	–	1.7	–	–	–	–
KSH01A	5263	2	–152.7	2.39	8.1	–250	1.397	0.004	0.06	0.135	0.54	23.1	160	2.1	–0.2
KSH01A	5266	3	–241.7	7.54	8.05	–210	1.301	0.006	–	0.157	0.551	20.2	–	–	–
KSH01A	5288	3	–536.0	10.74	8.05	–240	0.511		0.04	0.148	0.484	17.7	35	3.3	–0.2
KLX01A	1517	5	–440.7	13	8.6	–280	0.027	0.73		–	0.14	–	–	–	–
KLX01	1516	3	–673.0	2.6	7.8	–265	0.029	2.5	0.22	–	0.2	–	–	–	–
KLX01	1773	4	–897.1	0.85	8.4	–	0.052	0.29	–	–	0.09	–	–	–	–
KLX02	2738	4	–298.6	0.22	8.1	–	1.04	0.04	–	–	0.15	–	–	–	–
KLX02	2705	4	–318.1	0.24	8.05	–	0.464	–0.01	–	–	0.14	–	–	–	–
KLX02	2731	3	–1531.0	0.14	8	–	0.426	–0.01	–	–	0.14	–	–	–	–
KLX03	7953	1	–170.8	0.24	8.17	–275	0.251	–0.002	0.87	0.631	0.0618	37.2	–0.2	3.4	1.1
KLX03	10091	3	–379.9	1.88	8.1	–270	0.429	0.007	0.62	0.421	0.107	15.1	220	2.3	280
KLX03	10188	5	–700.6	6.8	7.5	–220	1.0	0.005	–	–	0.27	–	–	–	–
KLX03	10076	1	–922.5	0.04	8.4	–	–	–	0.059	–0.01	0.0164	11.1	–0.2	–0.2	2.3
KLX08	10649	5	–150.4	1.4	8.1	–266	0.112	0.004	–	0.928	0.0854	39.4	2.3	13	0.4
KLX08	10747	5	–320.0	1.15	8	–245	1.02	0.037	–	0.397	0.053	32.7	130	30	17
KLX08	11159	2	–390.7	5.71	7.6	–	0.288	–0.002	–	0.0289	0.0877	17	–	–	–
KLX08	11228	3	–504.5	10.7	8.3	–	–0.005	0.01	0.025	0.028	0.0893	13.2	–	–	–
KLX13A	11607	3	–408.0	10.2	8.45	–287	–0.006	0.004	–	–	–	29	–	–	–
KLX15A	15008	2	–467.2	4.43	7.6	–	–	–	0.021	0.144	0.549	17.3	130	140	900
KLX17A	11809	3	–342.3	1.8	7.92	–285	0.69	0.028	–	–	–	31.3	–	–	–
KLX17A	11692	5	–548.0	0.21	8.36	–303	0.682	–0.006	0.145	0.22	0.025	18.6	3000	280	300

S2–< 0.01 below detection limit

F2+`< 0.05 below detection limit

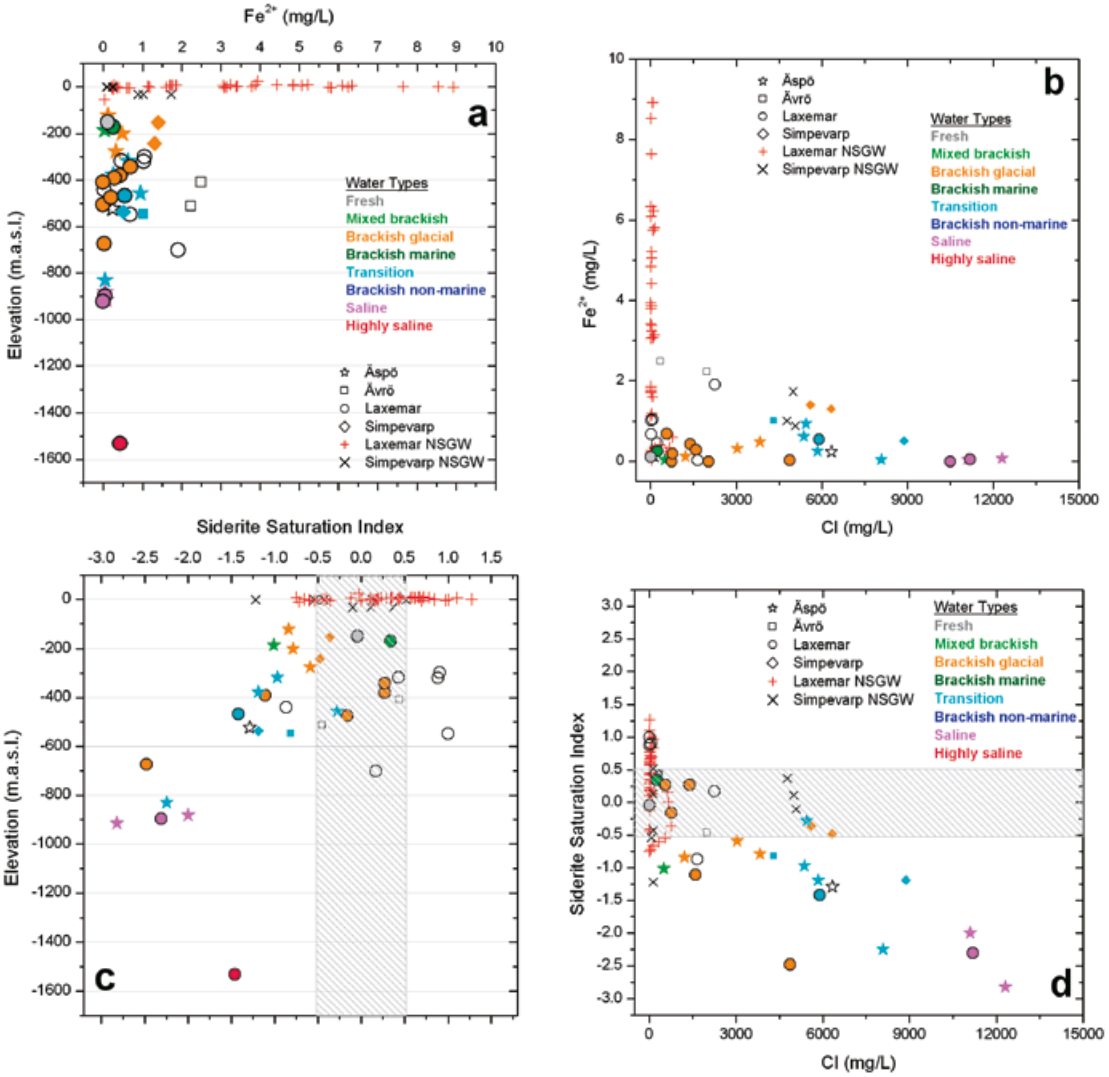

Figure 4-29. *Distribution of ferrous iron (a, b) and siderite saturation index (c, d) with respect to depth (a, c) and chloride contents (b, d) in the Laxemar-Simpevarp area groundwaters. Chloride scale in plots (b) and (d) is reduced to 15,000 mg/L to increase the resolution of the shallow to intermediate groundwaters and therefore the highly saline sample is not indicated.*

Maximum contents of dissolved **sulphide** are close to 1 mg/L (Figure 4-30a, b) and most values are less than < 0.2 mg/L. For the majority of groundwaters with sulphide contents greater than 0.04 mg/L, the speciation-solubility calculations indicate equilibrium with respect to 'amorphous' FeS (Figure 4-30c, d). This underlines its effective precipitation in the presence of microbial sulphate reduction in these groundwaters, as also deduced from $\delta^{34}S$ values by /Tröjbom et al. 2008/.

Dissolved **manganese** contents in the near surface groundwaters (Figure 4-31a, b) range from < 0.1 to 2 mg/L. The higher concentrations are consistent with the existence at very shallow levels of reducing environments with effective Mn(II) mobilisation due both to inorganic processes (e.g. weathering of amphiboles, biotites or chlorites) and to manganese reduction of organic matter by MRB (Manganese Reducing Bacteria) using the manganese sources in the soil minerals. The dissolved manganese concentrations in near surface groundwaters seem to be mainly limited by the precipitation of rhodochrosite ($MnCO_3$), which is the only manganese mineral reaching equilibrium in these groundwaters. Although rhodochrosite has not been detected so far in the overburden, its

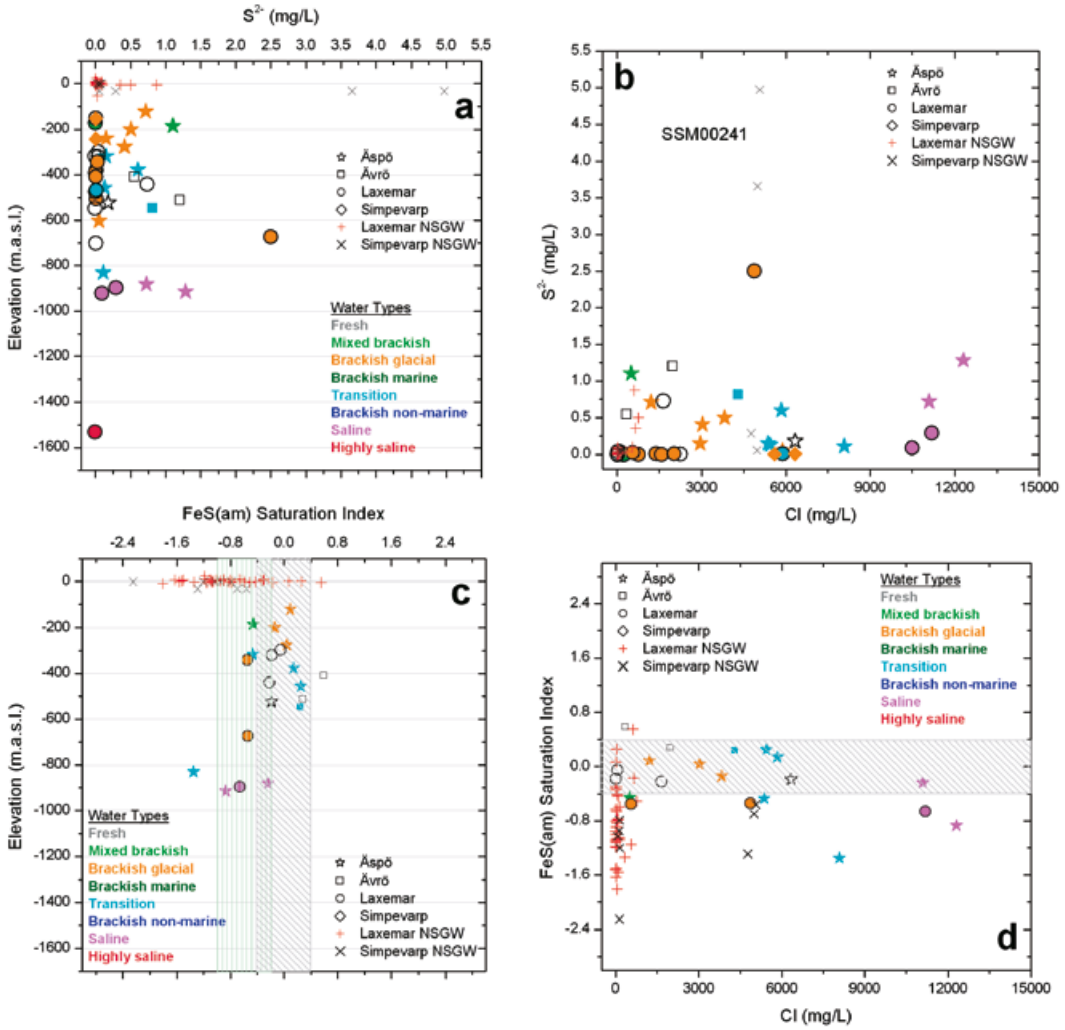

Figure 4-30. *Dissolved sulphide (a, b) and FeS(am) saturation index (c, d) distribution with respect to elevation (a, c), and chloride contents (b, d) in the Laxemar-Simpevarp area groundwaters. Chloride scale in plots (b) and (d) is reduced to 15,000 mg/L to increase the resolution of the shallow to intermediate groundwaters and therefore the highly saline sample is not shown.*

control on dissolved manganese contents is feasible in this environment in which the biogenic CO_2 input and the aluminosilicates and calcite weathering reactions can produce an important increase in alkalinity. Other possibilities include manganese control by rhodocrosite-siderite solid-solutions or co-precipitation with calcite, but cation exchange or surface complexation can also play a role.

For dissolved **nitrogen**, available analytical data include values for nitrate, nitrite and ammonium (Figure 4-32). The concentrations of nitrate and nitrite show in common with ammonium the greatest variability and largest concentrations in the near surface groundwaters. This variability is associated with the oxic/anoxic transition.

Maximum nitrate contents reach 5.5 mg/L with most samples under 1 mg/L. For nitrite, with only one exception at 0.37 mg/L, all contents are clearly under 0.05 mg/L,and those of ammonium are generally below 3.5 mg/L; exceptions include two extreme soil pipe outliers associated with relict marine waters (200 to 600 mg/L in SSM000241 and SSM000242). The groundwaters from these two soil pipes also show extreme DOC values (about 100 mg/L) which may reflect bottom sediment contamination.

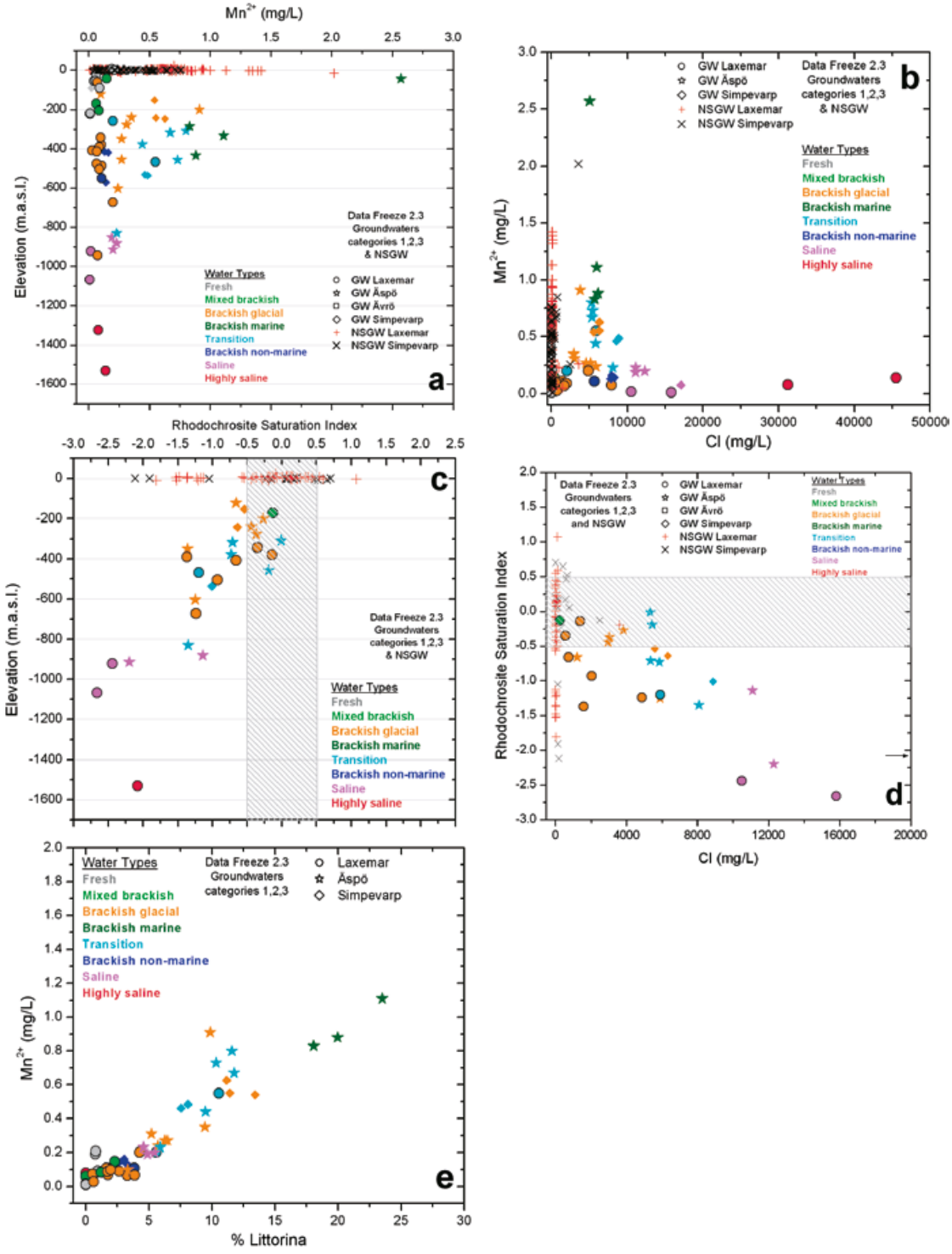

Figure 4-31. *Manganese content distribution (a, b) and rhodochrosite saturation index (c, d) with respect to elevation (a, c), and chloride (b, d) in the Laxemar-Simpevarp area groundwaters. Dissolved manganese content with respect to Littorina water percent (e) in the Laxemar-Simpevarp area groundwaters.*

The total dissolved nitrogen (N_{total}) contents in the near surface system are mainly derived from the atmospheric pool and from the degradation of organic matter /Tröjbom et al. 2008/, although some contribution from weathering of potassium-rich silicates containing ammonium is also possible. Moreover, cation exchange reactions involving NH_4^+ can participate in the behaviour of dissolved ammonium in the near surface groundwaters. Nitrogen contents show a large temporal variability possibly related to seasonal variation in the biological activity, where the main dissolved species are generally ammonium and/or dissolved organic nitrogen.

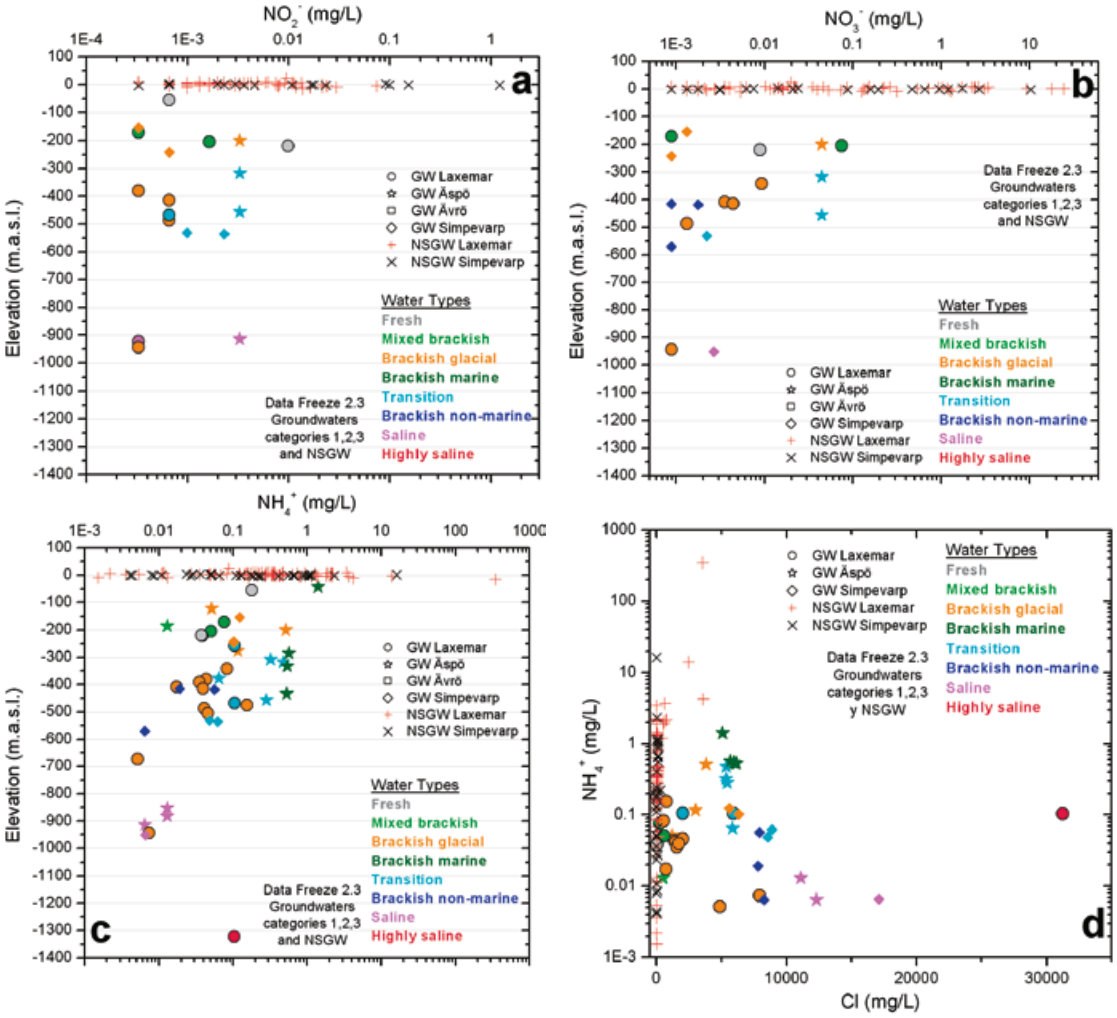

Figure 4-32. *Concentrations of NO_2^- (a), NO_3^- (b), and NH_4^+ (c) versus elevation and concentration of NH_4^+ versus.chloride (d) in groundwaters from the Laxemar-Simpevarp area.*

The deeper groundwater system

In the deeper groundwater system, dissolved **Ferrous iron** concentrations decrease roughly down to about 700 m depth (Figure 4-29). At greater depth, at least to about 1,000 m, the values are lower than 0.2 mg/L, after which the deepest, most highly saline samples reach Fe^{2+} values of 0.5 mg/L at 1,560 m depth (Figure 4-29). For dissolved $\mathbf{S^{2-}}$, there is a large number of samples with significant sulphide contents (e.g. > 0.2 mg/L), but no clear evolution trend with depth (Figure 4-30). As a general observation there are increased values (S^{2-} > 0.2 mg/L) mainly at Äspö and Ävrö compared to only a few at Laxemar. However, it is of outmost importance to keep in mind the potential problems involved in sampling sulphide (and other trace elements), and more specifically the large variation in sulphide values obtained from the original CCC sampling compared with later groundwater monitoring of selected borehole sections. Moreover, recent data show significant variation in sulphide during monitoring with some initially high values which makes representative values difficult or impossible to select. Initial drilling and pumping may have disturbed the system or may have facilitated sulphate reduction, but this issue remains to be resolved. However, ongoing sulphate reduction is occurring in groundwaters at shallow and intermediate depths (cf Section 4.4) and supported by enriched $\delta^{34}S$ values and decreased sulphate contents (cf Section 4.1.6).

Speciation-solubility calculations indicate that siderite saturation indices decrease with increasing depth and chloride content (Figure 4-29), indicating that this phase is not an important control on dissolved Fe^{2+} concentrations in this part of the system. With regard to Fe(II) monosulphides, equilibrium occurs down to about 600 m depth (Figure 4-30), mainly in groundwaters from Simpevarp and Äspö , but also in some groundwaters from Laxemar. It appears to be less frequent at depths

greater than 600 m, but is clearly reached at about 900 m by some groundwaters with very variable chloride contents from Äspö. This equilibrium, with respect to the amorphous and metastable iron monosulphides found in most Simpevarp groundwaters (including the near surface waters), indicates a presently continuous supply of H_2S produced by SRB (Sulphate Reducing Bacteria) activity combined with Fe(II) supplied by IRB (Iron Reducing Bacteria) activity (cf Section 4.4) or dissolution of Fe(II) minerals /cf Gimeno et al. 2009/. Pyrite of biogenic origin has also been identified in the bedrock fractures (cf Section 4.8).

Dissolved **Manganese** concentrations in the groundwaters from the Laxemar-Simpevarp area vary from below detection (< 3×10^{-3} mg/L /Nilsson 2008/) to more than 2.5 mg/L (Figure 4-31). Overall, its concentration with depth shows a similar pattern to that of the dissolved Fe^{2+} contents, with large and variable values in the brackish groundwaters in the upper 500 m bedrock, and very low values in the deeper, more saline waters. This roughly parallel behaviour could indicate the 'simultaneous' control of both elements by iron phases (i.e. oxyhydroxides, clays). The highest manganese contents found in the Simpevarp-Äspö subareas, for some deep brackish groundwaters between about 200 and 500 m depth, probably reflect residual input from recharged Littorina waters, in common with that described for the Forsmark, Olkiluoto and Finnsjön areas.

In most of the deep groundwaters, rhodochrosite saturation indices display a clear increased saturation trend with increasing depth and chloride content. The few groundwaters showing equilibrium correspond to dilute waters of meteoric origin at about 400 m depth in the Laxemar subarea, and to brackish groundwaters with a Littorina signature. Rhodochrosite equilibrium in these latter groundwaters (as stated for manganese above) may have been inherited during the infiltration of Littorina waters through marine sediments, as also proposed for the Forsmark groundwaters /Gimeno et al. 2006, 2008/.

The variability range and content of dissolved nitrogen species drastically decrease in the deeper groundwater system due to the general reducing conditions (Figure 4-32). Consequently, extremely low contents of nitrate and nitrite have been observed, comparable to other crystalline environments in the Canadian Shield /Gascoyne 2004/, Olkiluoto /Pitkänen et al. 2004/ and Forsmark /Gimeno et al. 2008/. Shallow groundwaters of meteoric origin at Laxemar-Simpevarp also show this character, indicating the development of an anoxic environment at an early stage in the groundwater evolution.

Ammonium contents also decrease in the deep groundwaters in the Laxemar-Simpevarp area with the largest variability occurring in the upper approximately 500 m of the bedrock where groundwaters with a clear Littorina component show the highest values (also recorded at Forsmark and Olkiluoto). Once again an inherited Littorina recharge component is proposed during which bacterial activity in the marine sediments transforms organic nitrogen compounds into NH_4^+ /Pitkänen et al. 2004/. The lower levels of dissolved NH_4^+ in Laxemar-Simpevarp compared to Forsmark probably reflect the weaker influence of the Littorina Sea transgression in the former. Significant NH_4^+ concentrations (around 0.1 mg/L) have also been observed in the saline groundwaters sampled between about 1,100 and 1,400 m depth at Laxemar. According to /Pitkänen et al. 2004/, enhanced NH_4^+ at great depth may be associated with large hydrocarbon contents; this has not been possible to confirm at Laxemar due to lack of information. Note that ammonium is not a conservative component and reaction processes (e.g. exchange reactions) can reduce the NH_4^+ concentrations during circulation of marine waters through the fractured bedrock. However, these reaction processes are not able to completely mask the Littorina marine signature in the Laxemar-Simpevarp area or in the Forsmark or Olkiluoto groundwaters. On one hand, this situation is supported by the stability of dissolved ammonium in reducing environments and, on the other hand, it supports the existence of reducing conditions in these groundwaters over a long time span.

4.3.2 Redox pair modelling

The redox pairs analysed here are similar to those used in previous modelling phases /e.g. SKB 2006ab/. They involve the dissolved SO_4^{2-}/HS^- and CO_2/CH_4 redox pairs, and the heterogeneous couples $Fe^{2+}/Fe(OH)_3$, $HS^-/S_{(c)}$, SO_4^{2-}/FeS_{am} and SO_4^{2-}/ pyrite. According to (/Gimeno et al. 2007/ and references therein), these are considered the most suitable redox pairs for the Laxemar-Simpevarp area groundwaters having been tested in similar systems elsewhere in the Fennoscandian Shield. In addition, they include those redox pairs that can be involved in controlling the potentiometrically measured reducing Eh values shown in Figure 4-27.

PHREEQC and the thermodynamic data included in the WATEQ4F database have been used for the calculations, except in the case of the heterogeneous $Fe^{2+}/Fe(OH)_3$ pair for which three different sets of log K values have been used for the solid phase. These are: a) the set of values proposed by /Nordstrom et al. 1990/ corresponding to amorphous to microcrystalline hydrous ferric oxides, HFOs, or ferrihydrites (log K = 3 to 5,), b) the value derived from the calibration proposed by /Grenthe et al. 1992/ for a wide spectrum of Swedish groundwaters (log K= −1.1 for a crystalline phase such as hematite or goethite), and c) the value of log K = 1.2 as defined by /Banwart 1999/ using the same methodology as /Grenthe et al. 1992/ but involving groundwaters from the Äspö HRL based on the 'Large-scale Redox Experiment' which represents an *in situ* system affected by a recent oxygen intrusion. The redox potential corresponding to the heterogeneous $Fe^{2+}/ Fe(OH)_3$ redox pair has been obtained in all these calculations using the already mentioned equilibrium constants and the Fe^{2+} activity calculated with PHREEQC. Results obtained with the aforementioned redox couples are summarised in Figure 4-28 and Figure 4-29.

As already reported in /Gimeno et al. 2007/, the Eh values obtained with the $Fe^{2+}/Fe(OH)_3$ redox pair considering an amorphous or microcrystalline $Fe(OH)_3$ solid phase, are more oxidising than the measured ones. The Eh values calculated with the same redox pair using the equilibrium constant proposed by /Grenthe et al. 1992/ are only in agreement with the Eh values measured in 6 samples (Figure 4-33a), i.e. those already used by /Grenthe et al. 1992/ when they proposed the calibration. In contrast, using the equilibrium constant proposed by /Banwart 1999/ good agreement with the measured values for nine samples was recorded (Figure 4-33b).

All these observations suggest that the measured Eh in these groundwaters could be controlled by different iron oxyhydroxides with different solubilities or degree of crystallinity. The redox potential measured in some brackish to saline groundwaters from Äspö, Ävrö and borehole KLX01 in Laxemar, appears to be controlled by the presence of a clearly crystalline iron oxyhydroxide, such as the ubiquitous hematite represented by Grenthe's constant (Figure 4-33a). This is in agreement with the long residence time of these groundwaters were poorly crystalline phases are not expected (/SKB 2004c/ and references therein). Other groundwaters, mainly in the Laxemar subarea show good agreement between their measured Eh values and those calculated with the Banwart solubility value; Figure 4-33b. Eh values in these groundwaters could be controlled by the occurrence of an iron phase of intermediate crystallinity, such as a recent poorly crystalline iron oxyhydroxide recrystallised from an amorphous one. For the studied system, characterised by reducing groundwaters with long residence times, this situation points towards a brief oxygen intrusion and precipitation of Fe(III) oxyhydroxides during the Eh measurements. For the rest of groundwaters considered, measured Eh values are consistent with situations intermediate between the calculations and calibrations carried out by /Grenthe et al. 1992/ and /Banwart 1999/.

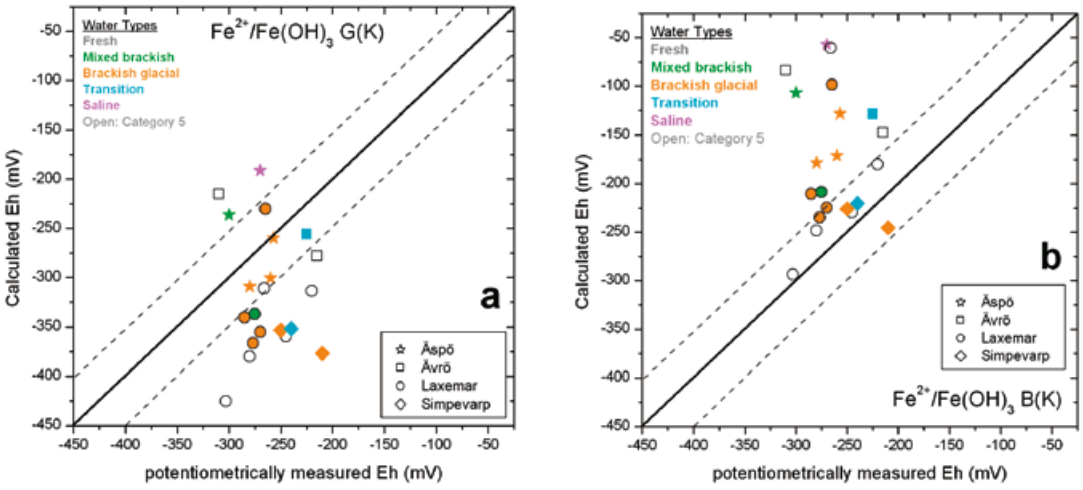

Figure 4-33. *Comparison of the potentiometrically measured Eh values with Chemmac and Eh values calculated with the $Fe^{2+}/Fe(OH)_3$ redox pairs using (a) the equilibrium constant for the hematites as defined by /Grenthe et al. 1992/, and (b) using the equilibrium constant for the solid phase as defined by /Banwart 1999/. The dashed lines indicate the accepted range of Eh variability of ±50mV.*

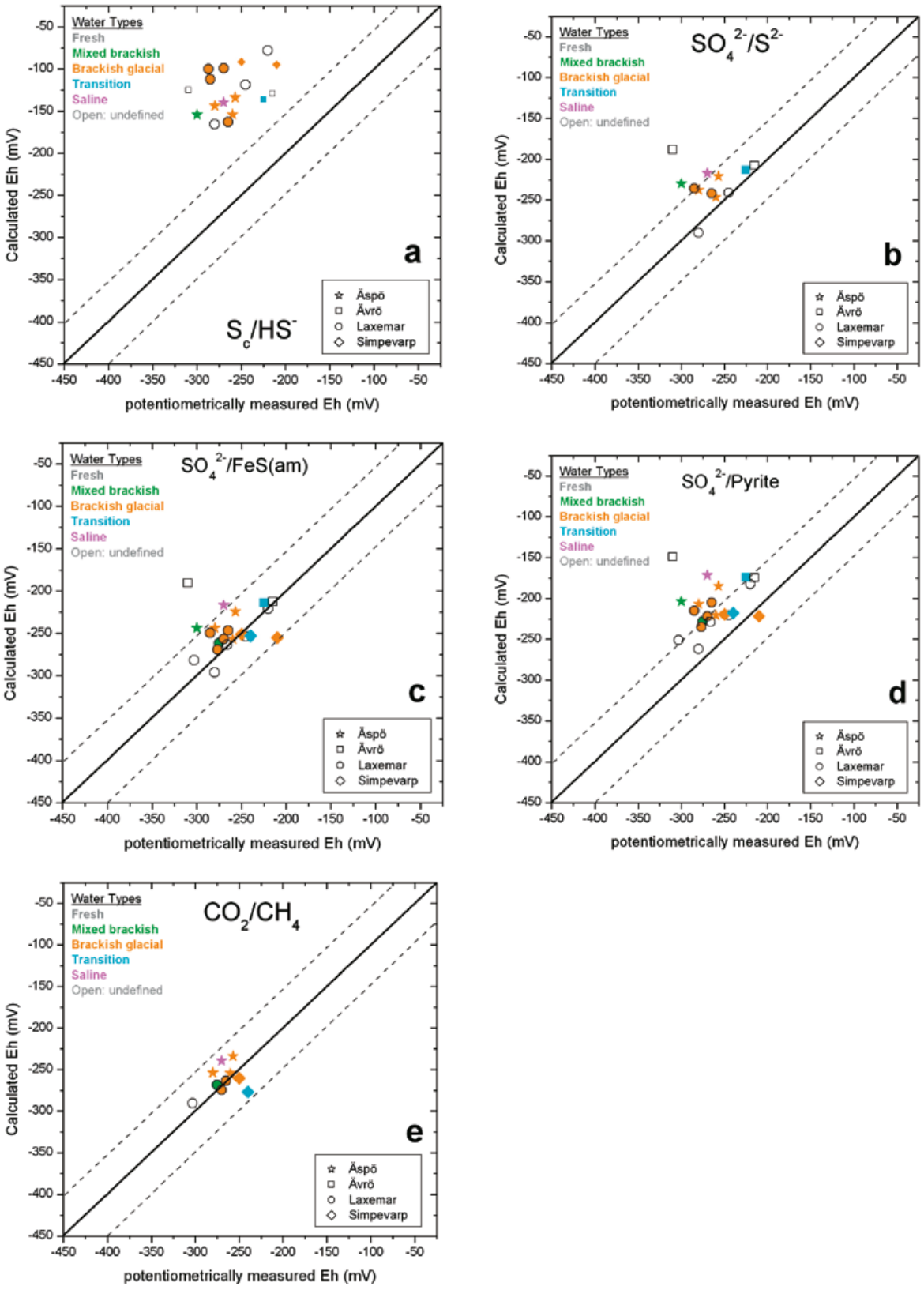

Figure 4-34. *Comparison of the potentiometrically measured Eh values with Chemmac and the Eh values calculated with the sulphur and methane redox pairs: (a) S_c/HS^-, (b) SO_4^{2-}/HS^-, (c) SO_4^{2-}/FeS_{am}, (d) SO_4^{2-}/Pyrite, and (e) CO_2/CH_4. The dashed lines indicate the accepted range of Eh variability of ±50mV.*

Eh values calculated using the electroactive $S_{(s)}/S^{2-}$ redox couple in the Laxemar-Simpevarp area and in the Forsmark groundwaters (Figure 4-34a), are invariably larger than the measured Eh values. Therefore, this couple seems not to be involved in the control of measured Eh in contrast with other Swedish groundwaters /Nordstrom and Puigdomenech 1986/. The rest of the studied sulphur redox couples (SO_4^{2-}/S^{2-}, SO_4^{2-}/FeS_{am} and SO_4^{2-}/pyrite) usually agree within a range of ± 50mV with the potentiometrically measured Eh values (Figure 4-34a, b, c and d) and the same case for the few Eh values obtained with the CO_2/CH_4 non-electroactive pair (Figure 4-34e).

The good agreement between the Eh values obtained for all these redox pairs is not unusual since the redox windows for these redox pairs are very close when not overlapping (e.g. /Kölling 2000/). However, this situation does not imply the existence of partial redox equilibrium between these couples. What is really interesting is that the potentiometric Eh values reach the potentials of these windows as CO_2/CH_4 and the sulphate/sulphur redox pairs are *non-electroactive*. As far as known, there is no experimental evidence on the achievement of reversible potentiometric Eh values from the SO_4^{2-} /pyrite and SO_4^{2-}/FeS(am) buffers. Furthermore, the mechanisms by which the electrodes could respond to sulphur or other electroactive species 'mediators' generated during sulphate-reduction is presently unknown. The agreement between the potentiometrically measured Eh and the potentials calculated from the SO_4^{2-}/FeS or SO_4^{2-} /pyrite redox buffers has rarely been found /Gimeno et al. 2009/. However, the important role of both the sulphur system and the microbially mediated sulphate reduction on the redox state of the groundwaters, has been supported by different criteria independent of the potentiometrically measured Eh (i.e. evaluation of the saturation state of sulphide minerals, microbiological data, etc.), and therefore their influence on the potentiometric determinations of Eh could be reasonable. In any case, this is a problem strictly related to the Eh measurements and not to the real importance of the sulphur or CO_2/CH_4 redox pairs as representing the effective processes which contribute to the redox state in many groundwaters in the Laxemar-Simpevarp area.

4.3.3 Integration with mineralogical and microbiological data

As indicated above, the ***iron and the sulphur systems*** are very important for the control of redox processes in the groundwaters at Laxemar-Simpevarp. Iron (II) and (III) minerals are widely distributed in the studied systems and the presence of IRB has been documented (cf Section 4.4). However, the bioenergetic calculations and the redox modelling approach performed from a partial equilibrium assumption for iron reduction and sulphate reduction processes (cf /Gimeno et al. 2009/) indicate that sulphate reduction is the thermodynamic favoured processes. It should be stressed again, however, that there is an uncertainty concerning the influence of pump rates, short circuiting and other perturbations induced by the drilling activities on the measured sulphide values (cf Sections 4.1.5 and 4.3.1).

The mineralogical and geochemical studies performed on the fracture fillings in the shallow bedrock /Drake et al. 2009/ indicate that the present redox front in the Laxemar subarea, deduced from the occurrence of recent, low temperature Fe-oxyhydroxides and the results of the uranium-series analyses, is located at about 15 to 20 m depth. These estimations are in agreement with the results of previous studies using different methodologies /Puigdoménech et al. 2001, Tullborg et al. 2003/. However, some scattered Fe-oxyhydroxide phases of low temperature origin have been found at greater depths (down to 120 m) /Drake et al. 2007/, although the most recent amorphous phases are only detected to about 50 m. The reason for this may be changing groundwater flow paths over time but most of all variation between fractures/fracture zones of different hydraulic conductivity. Importantly, the presence of Fe^{2+}-bearing minerals (mainly chlorite and pyrite) in the fracture fillings at all depths indicates that all these oxidising episodes have not exhausted the reducing capacity of the fracture minerals, even in the shallowest part of the system. Both chlorite and unaltered pyrite have been identified in the fractures at the Laxemar-Simpevarp area even in the uppermost approximately 100 m of the bedrock /Drake et al. 2008/.

All these data indicate that the system has retained a significant reducing capacity to the present day. The key role played by SRB in the stabilisation of these reducing conditions is supported by several lines of evidence, including the extremely negative $\delta^{34}S$ values found in pyrites from Äspö, the large positive $\delta^{34}S$ values in the Laxemar-Simpevarp area which characterise shallow to

intermediate depths, and the low $\delta^{13}C$ values found in calcites from fracture fillings from the same area. The importance of the SRB at very great depths (> ~700 m) in the Laxemar subarea remains unclear. They are not documented in the one existing sample from below 700 m depth (KLX03: –922 m elevation) and moreover no Eh measurements are available from these depths. At –1,160 m elevation in borehole KLX02 /Haveman and Pedersen 2002/ documented 330 cells/mL of SRB, but unfortunately the groundwater in this borehole has been very perturbed and it is not sure whether these data are representative for the actual sampled locality.

Regarding ***the manganese system,*** the concentration of this element in groundwaters is very variable and seems to be controlled by the precipitation of rhodochrosite in most near surface groundwaters, or by the association with iron phases, mainly oxyhydroxides and clays in the remaining deeper groundwaters.

Following the classification proposed by /Hallbeck 2006/, most groundwaters analysed for MRB have insufficient MPN numbers to influence their chemistry. Even with large MPN values, the active presence of MRB and their effect on the composition of deep groundwaters should be considered with caution since, as also observed in Forsmark, they are not correlated with the observed Mn^{2+} concentrations in groundwaters. Although manganese oxyhydroxides (that MRB may utilise) have been identified in the fracture fillings of the more superficial bedrock (down to about 10 m depth), they have not been found at greater depths in Laxemar-Simpevarp or in Forsmark. This is consistent with the existence of reducing conditions and with the presence of dissolved Fe^{2+} and S^{2-} which are known to diminish the stability of manganese oxyhydroxides /Appelo and Postma 2005/. Manganese-reducing bacteria are assumed to be most active in the upper part of the bedrock. However, manganese reducers have been identified at greater depths but it is not known whether their presence is a product of perturbation during drilling and sampling activities.

Finally, the behaviour of the ***nitrogen system*** is strongly affected by the existence of aerobic or anaerobic conditions. The observed evolution in the Laxemar-Simpevarp groundwaters shows a general depletion of nitrogen coupled to an increase in residence time and/or depth, a trend usually observed in anaerobic groundwater systems. The largest contents and variability in NO_2^-, NO_3^- and NH_4^+ concentrations are associated with the near surface groundwaters in the overburden were the oxic/anoxic transition appears to occur, whereas deep groundwaters show very low (if any) nitrate and nitrite concentrations in agreement with their reducing character.

4.4 Microorganisms

Microbial studies have included determination of the total number of cells (TNC) and concentration of adenosine-tri-phosphate (ATP). Cultivation methods consisted of aerobic plate counts for culturable heterotrophic aerobic microorganisms (CHAB), and most probable number (MPN) determinations of anaerobic microorganisms including nitrate-reducing bacteria (NRB), iron-reducing bacteria (IRB), manganese-reducing bacteria (MRB), sulphate-reducing bacteria (SRB), acetogenic bacteria (AA, HA) and methanogens (AM, HM) /Hallbeck and Pedersen 2008ab, 2009/. A degree of uncertainty in the data may have resulted from the effects of drilling and sampling that have not been possible to quantify; sampling techniques and uncertainties are presented in Section 3.3.

4.4.1 Characterisation of microorganisms

Size and activity of microbial populations

Investigations of the two different biomass parameters TNC and ATP in groundwaters from the Fennoscandian Shield have previously shown good agreement between these two parameters /Eydal and Pedersen 2007/. Similar data from the site investigation in Laxemar also showed very good agreement with a correlation at $p = 0.003$ /Hallbeck and Pedersen 2009/. When plotted, these data show one group that has high TNC and ATP values and another group with lower TNC and ATP values (Figure 4-35). The highest ATP and TNC values were found in borehole KLX17A at –548 m elevation (category 5), followed by the –342 m elevation section (category 3) in the same borehole (Figure 4-35). The high values from the –548 m elevation section could be interpreted as an effect of extensive inflow of shallow waters into the boreholes, but the data from the –342 m elevation

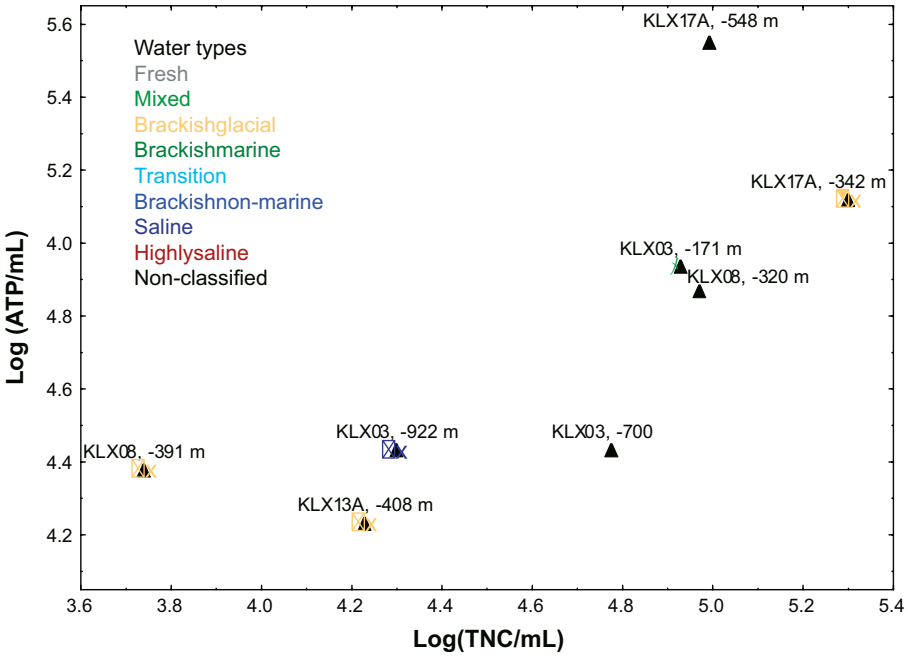

Figure 4-35. *Relationship between the total number of cells (TNC) and the concentration of ATP in groundwaters from the Laxemar subarea. Statistics: $^{10}Log(ATP) = 1.5 + 0.66 \times {}^{10}Log(TNC)$, $r = 0.75$, significant at $p = 0.003$, $n = 8$. Data from the 'Extended data freeze Laxemar 2.3'.*

section, considered representative, has almost similar values. There is no obvious explanation for these high numbers; data from KLX03:–171 m elevation is also quite high in comparison with the other data. This is probably explained by the shallow depth and the corresponding access to organic carbon from the ground surface. Comparing TNC and ATP in the Laxemar groundwaters shows no clear relation with the groundwater types. This is expected since the microbial population is regulated by the available energy, which is not directly related to the groundwater types found at depth.

Diversity and dominating microbial groups

There is no obvious trend with depth concerning the diversity of the microorganisms found in the groundwater in Laxemar. The highest stacked most probable number (MPN) values are found in borehole KLX03:–380 m elevation and in KLX15A and KLX17A at –467 and –548 m elevation respectively (Figure 4-36) /Hallbeck and Pedersen 2009/. The microbial populations consist of autotrophic and heterotrophic acetogens, and iron-, manganese- and sulphate-reducing bacteria. In KLX03:–380 m elevation both autotrophic and heterotrophic methanogens are found, and this diversity distribution is common to most of the samples but with different values. However, there are some exceptions to this pattern; the shallow samples in KLX08:–150 m, KSH01A:–153 and KLX03:–171 m elevation have no MRB and low MPN in general, and there are no SRB in the KLX03:–171 m and KLX03:–922 m elevations. The deepest sample at –922 m elevation has a very high salinity which could have been a problem in the culturing, so the presence of SRB at depth cannot be excluded. The dominating group of organisms in all sections is the acetogens which produce acetate, either from organic compounds in combination with production of hydrogen gas, or in an autotrophic way from carbon dioxide and hydrogen gas. Acetate is an excellent carbon and energy source for most microorganisms. Autotrophic production of acetate from hydrogen and carbon dioxide has been suggested as a base for subsurface ecosystems that are independent of organic material supply from photosynthesis /Pedersen 2001/.

Under anaerobic conditions, nitrate is the most thermodynamically favoured electron acceptor for the oxidation of organic substrates and it is used by nitrate-reducing bacteria (NRB) in respirative energy production. This nitrate reduction process (denitrification) occurs in different steps, each of which is catalysed by specific NRB which produce nitrite, nitrous oxide, and ammonium or nitrogen gas.

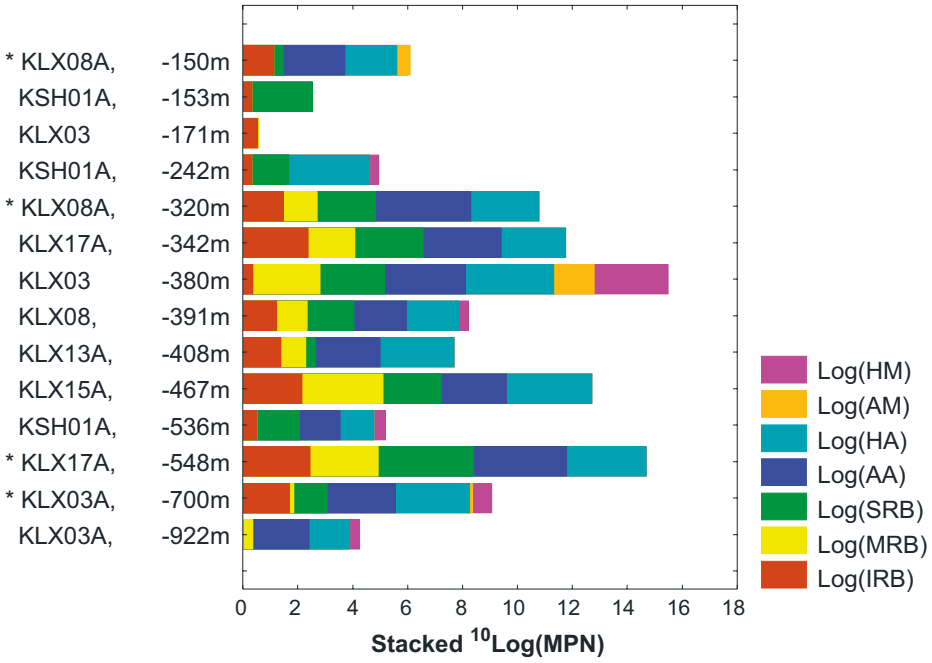

Figure 4-36. *Stacked log [10]MPN values showing the proportions of the different cultivable bacterias for samples from Laxemar and Simpevarp sorted by depth. IRB = iron-reducing bacteria, MRB = manganese-reducing bacteria, SRB = sulphate-reducing bacteria, AA = autotrophic acetogens, HA = heterotrophic acetogens, AM = autotrophic methanogens, HM = heterotrophic methanogens. * indicate that the groundwaters sampled were not representative for the sampled depth /Smellie and Tullborg 2009/.*

There is no major difference between the results from the MPN measurements for groundwater samples considered as disturbed and not representative, and the representative groundwater samples. It is therefore impossible to discuss microbial data in relation to the classification of the groundwater.

Sulphate-reducing bacteria, sulphide, sulphate and Eh

As discussed above, one of the main negative effects of microorganisms in the context of an HLW repository is the production of sulphide by SRB. The sulphide concentrations from groundwaters sampled at the same time for microbes were generally very low (from below detection up to about 0.1 mg/L). The possible influence of pumping during sampling on sulphate reduction and the concentration of sulphide was discussed by /Hallbeck and Pedersen 2009/. The increased flow rates in aquifers that pumping generates may lower the sulphate reducing activity of SRB and increase the ferrous iron production by IRB as observed in the Äspö HRL /Pedersen 2005/. A correlation matrix with the microbial parameters and chemical parameters possibly influenced by microbial activity is shown in /Hallbeck and Pedersen 2009/. The number of groundwaters with Eh measurements and available SRB data are relatively few (eight), and of these only five groundwaters were categorised as representative for the sampled depths. One of the most important and significant correlations found (at $p = 0.0006$) was the relation between E_h measured with Chemmac and the MPN of SRB (Figure 4-37). This correlation suggests that in some downhole environments the sulphide-producing activity of SRB may play an important part in controlling E_h as measured by the Chemmac probe.

The site investigations in Forsmark /Hallbeck and Pedersen 2008 ab/ showed that the concentration of sulphate in the groundwater decreased with depth and was very low at depths below about 600 m. A similar depth pattern was observed at Olkiluoto were the disappearance of sulphate coincided with a sharp increase in methane concentration at about 300 m depth /Pedersen et al. 2008/. At this depth, there was also an elevated sulphide peak in concentration which was attributed to microbial anaerobic oxidation of methane (AOM) with sulphate as the electron acceptor. Such a decrease in the sulphate concentration has not been seen in Laxemar were an increase with depth was found. However, the numbers of observations are too few in Laxemar to make any judgement to the presence or absence of AOM.

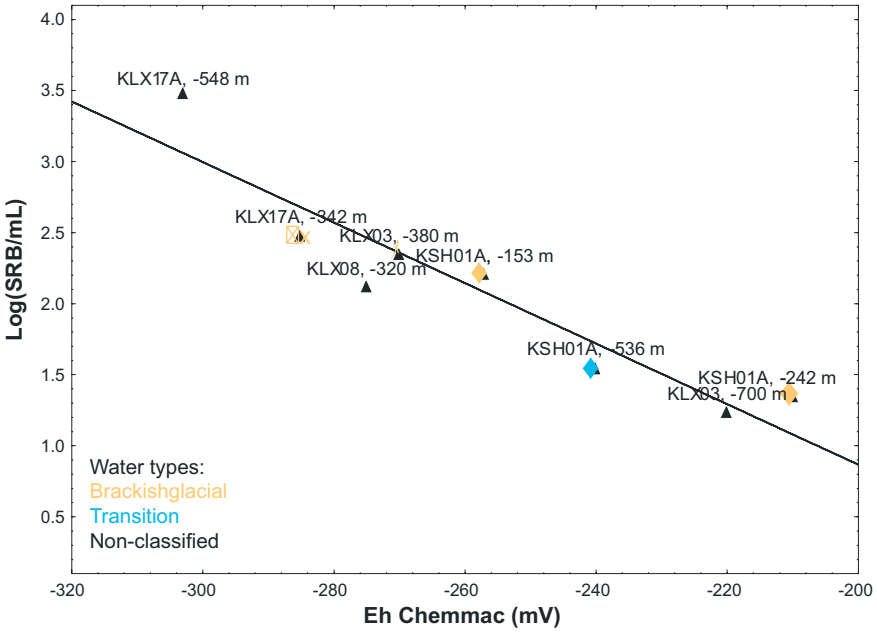

Figure 4-37. *Relationship between the number of sulphate-reducing bacteria and the measured Eh. Some data are excluded, i.e. KLX03:–171 m, KLX03:–922 m, KLX08:–150 m and KLX13A:–408 m elevation, where only very low numbers of SRB (if any) are identified, and KLX15A:–467m elevation were matching Eh values are not available. Statistics:* $^{10}Log(SRB) = –171$ *to* $–41 \times E_h$, $r = –0.94$, *significant at* $p = 0.0006$, $n = 8$. *Data from the 'Extended data freeze Laxemar 2.3'.*

4.4.2 Conclusions

The most important findings from the microbiological investigations in Laxemar are:

- Sulphate-reducing bacteria are present at all depths sampled, but show wide variations in population levels.
- Iron- and manganese-reducing bacteria are present at all depths, except for low population levels of manganese-reducers in samples from both the shallowest and deepest groundwaters.
- Acetogens are the dominating physiological group of microorganisms.
- Measured Eh correlates with the number of sulphate-reducing bacteria for a subset of samples from intermediate depths. This suggests that the SO_4^{2-}/S^{2-}system, catalysed by sulphate-reducing bacteria, plays an important role in determining the redox state of the system at these depths.

4.5 Colloids

4.5.1 Introduction

Suspended groundwater particles in the size range from 1 to 1×10^{-3} µm are regarded as colloids /Stumm and Morgan 1996/. Their small size prohibits them from settling which gives them the potential to transport radionuclides in groundwater, i.e. radionuclides can sorb (or adhere) or be incorporated in colloids and be transported or retarded with them. It is therefore important to estimate to what extent such colloids can occur or be formed in the groundwater, and over what time periods these colloids can be stable. The aim of the study of colloids in the Laxemar site investigation was to quantify and determine the composition of natural colloids in bedrock groundwater samples; sorption of radionuclides on colloids has not been analysed.

Different methods to characterise colloids were used during the site investigation: a) filtration method, b) laser-induced breakdown colloid detection (LIBD) /Berg et al. 2006/, used for some samples during the last sampling campaign in Laxemar, and d) colloid analysis by means of submicro-filtration plus scanning electron microscopy and energy-dispersive spectroscopy (SEM/EDS) /Nilsson and Degueldre 2007/.

Both inorganic and organic colloids exist and these types were measured at Laxemar; the results of the organic colloid analyses are presented in /Hallbeck and Pedersen 2009/. Microorganisms should also be considered as colloids as there are many groundwater examples ≤1 µm in size. In addition, a recent study of groundwater in the Äspö HRL tunnel identified a variety of viruses (i.e. phages) in the water; these are protein particles, approximately 200 nm in diameter that can infect microbial cells. Additional investigations are needed to assess the importance of these colloids considering that colloids have to be stable in order to facilitate transport to the biosphere /Hallbeck and Pedersen 2009/.

4.5.2 Concentration of colloids with depth

The range of measured colloid concentrations in the study is from approximately 5 to 90 µg/L with an average concentration 26.8 µg/L. This compares with the average concentrations for Forsmark (58.4 µg/L) and also similar range as reported from crystalline rock studies in Sweden, Switzerland and Canada (10 to 300 µg/L) /Laaksoharju et al. 1995, Degueldre 1994, Vilks et al. 1991/, where the same sampling approach was used. Plotting colloid concentration versus elevation (Figure 4-38) shows that the colloid concentration is greatest in groundwater from borehole KLX17A at –342 m elevation, although the concentration is also high in KLX08: –320 m, and KLX03: –171 m elevation. All other samples have colloid concentrations below 20 µg L^{-1}. A decrease in colloid contents versus depth is indicated and this was found also in Forsmark /Gimeno et al. 2009/.

4.5.3 Conclusions

The major conclusions from the colloid characterisation /Hallbeck and Pedersen 2009/ are:

- The number of colloids found in the Laxemar-Simpevarp groundwaters is approximately in the order of 10^6/mL and the measured concentrations are in agreement with measurements from other crystalline groundwater environments. Because the colloid samples come from a system which is disturbed following drilling and sampling which increase the colloid concentration, the measured populations can indicate maximum values.
- A decrease in colloid content versus depth is indicated.
- The filtration and fractionation method showed that the colloids are composed mostly of iron and sulphur. LIBD in combination with EDX on the other hand show that the colloids are composed mostly of aluminium, silica and iron; this may partly be due to contamination from drilling debris.
- Both inorganic and organic colloids exist at Laxemar and some colloids are probably microbes and potentially even viruses (phages).

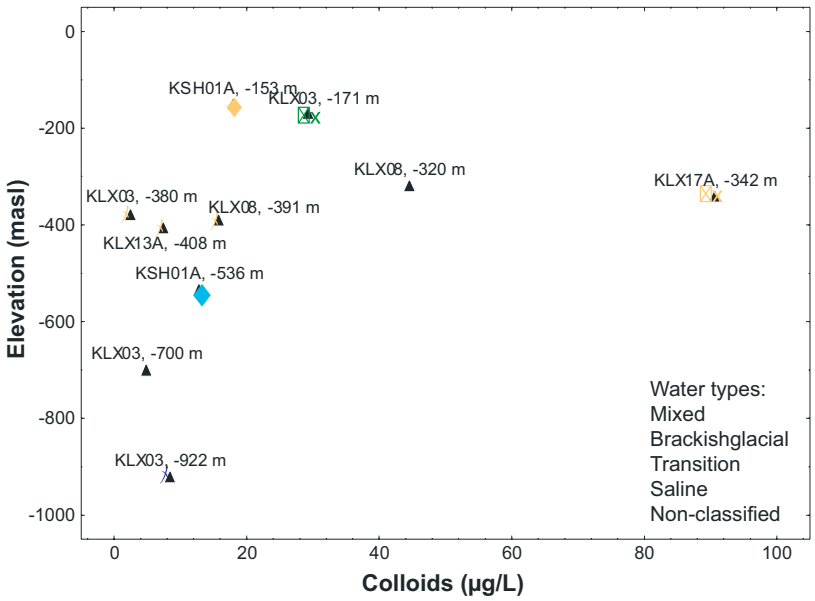

Figure 4-38. *Colloid concentration (µg/L) plotted against depth in the Laxemar-Simpevarp area; data from the 'Extended data freeze Laxemar 2.3'. Data from KLX15A: –467 m elevation are excluded because of sampling artefacts /Hallbeck and Pedersen 2008b/.*

4.6 Gases

4.6.1 Origin of gases and their properties

Gases in groundwater are of various origins, and gas is found in many Fennoscandian Shield groundwaters in concentrations which imply a deep mantle source for many gases (e.g. nitrogen, hydrogen and helium) /Apps and van de Kamp 1993/. Dissolved gases in groundwater contribute to the mass of dissolved species. The gases can be defined as chemically reactive (of which some participate in biological processes) or conservative. Chemically active species are, for example, oxygen, hydrogen sulphide with its anionic dissociation products HS^- and S^{2-}, carbon dioxide (with the dissolved species HCO_3^- and CO_3^{2-}), methane and hydrogen. Chemically inactive inert gases include the noble gases and to some extent nitrogen. Both argon and to an even greater extent helium are contributed from the mantle but are also produced by radioactive decay in the lithosphere; their different origin may be traced by isotope analyses. Nitrogen fixation and denitrification by microorganisms may possibly influence the reservoir of nitrogen gas in groundwater, making nitrogen a gas difficult to define as purely (bio) chemically active or inactive. Finally, gases such as ethane and propane and their reduced forms can be found in deep groundwaters.

4.6.2 Composition of dissolved gases

The major dissolved gases in groundwaters from the Fennoscandian Shield and the Laxemar-Simpevarp area are nitrogen, carbon dioxide, helium, methane and argon, with nitrogen followed by helium being present in greatest amounts. Other gases present are methane, argon, hydrogen and traces of higher hydrocarbons with up to three carbon atoms. The volume of total gas at Laxemar-Simpevarp is less than that measured at Forsmark /Hallbeck and Pedersen 2008b/. Saturation calculations from Forsmark showed that 1,200 mL of nitrogen gas could be dissolved in one kg of water at 700 m depth and at a temperature of 10°C /Hallbeck and Pedersen 2008b/. This indicates that the gas pressure in the Forsmark groundwater is far from saturation and the situation at Laxemar-Simpevarp is that the groundwaters are even less saturated in respect to dissolved gases. This indicates either an open, high out-flux system, or low in-flux of gases from below (geogases), or a combination of both depending on the depth sampled.

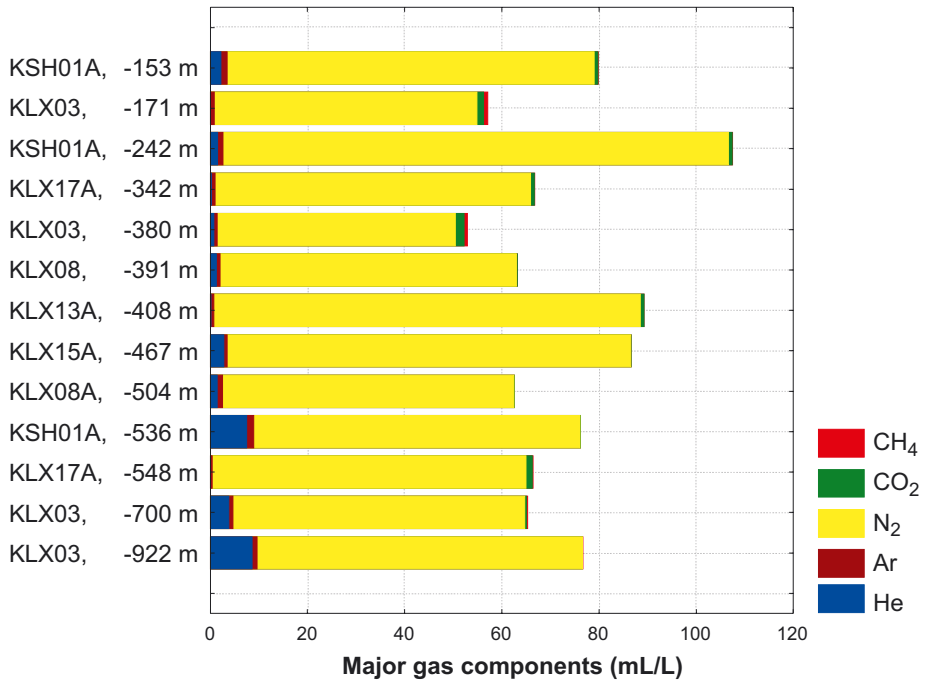

Figure 4-39. *Stacked values of the gas volume of major gas components in samples from the Laxemar-Simpevarp area. Note that the groundwaters sampled are not representative for the sampled depth /Smellie and Tullborg 2009/. Evaluation of the N_2/Ar and N_2/He ratios indicate the samples from KLX13: –408 m and KLX15A: –467 m elevation, together with the KLX17A: –548 m elevation sample, appear to be contaminated with nitrogen during sampling /Hallbeck and Pedersen 2009/.*

Because of the few available gas analyses and the complexities of sampling, obvious depth trends are uncertain. However, taking only the representative (category 1–3) samples into account there is an increase in helium with depth (Figure 4-40, also Section 4.10.3) and a generally higher carbon dioxide content is suggested in the upper 400 m compared with deeper levels.

4.6.3 Conclusions

The major dissolved gases in groundwaters from the Fennoscandian Shield and the Laxemar-Simpevarp area are nitrogen, carbon dioxide, helium, methane and argon. Nitrogen followed by helium are present in greatest amounts, with nitrogen and carbon dioxide being most common in the more shallow groundwaters and helium in the deeper parts of the system. Other gases present are methane, argon, hydrogen and traces of higher hydrocarbons with up to three carbon atoms. The available data indicate that the total gas content is less than would be expected in Fennoscandian Shield groundwaters. This indicates either an open, high out-flux system, or low in-flux of gases from below (geogases). Although their concentrations generally increase with depth, in particular helium, the gases are not oversaturated at the depths from which they were sampled. There are few samples taken for gas analyses and the isotopic composition of important gases like hydrogen and methane is missing. The description of the origin of gases should therefore be considered as preliminary.

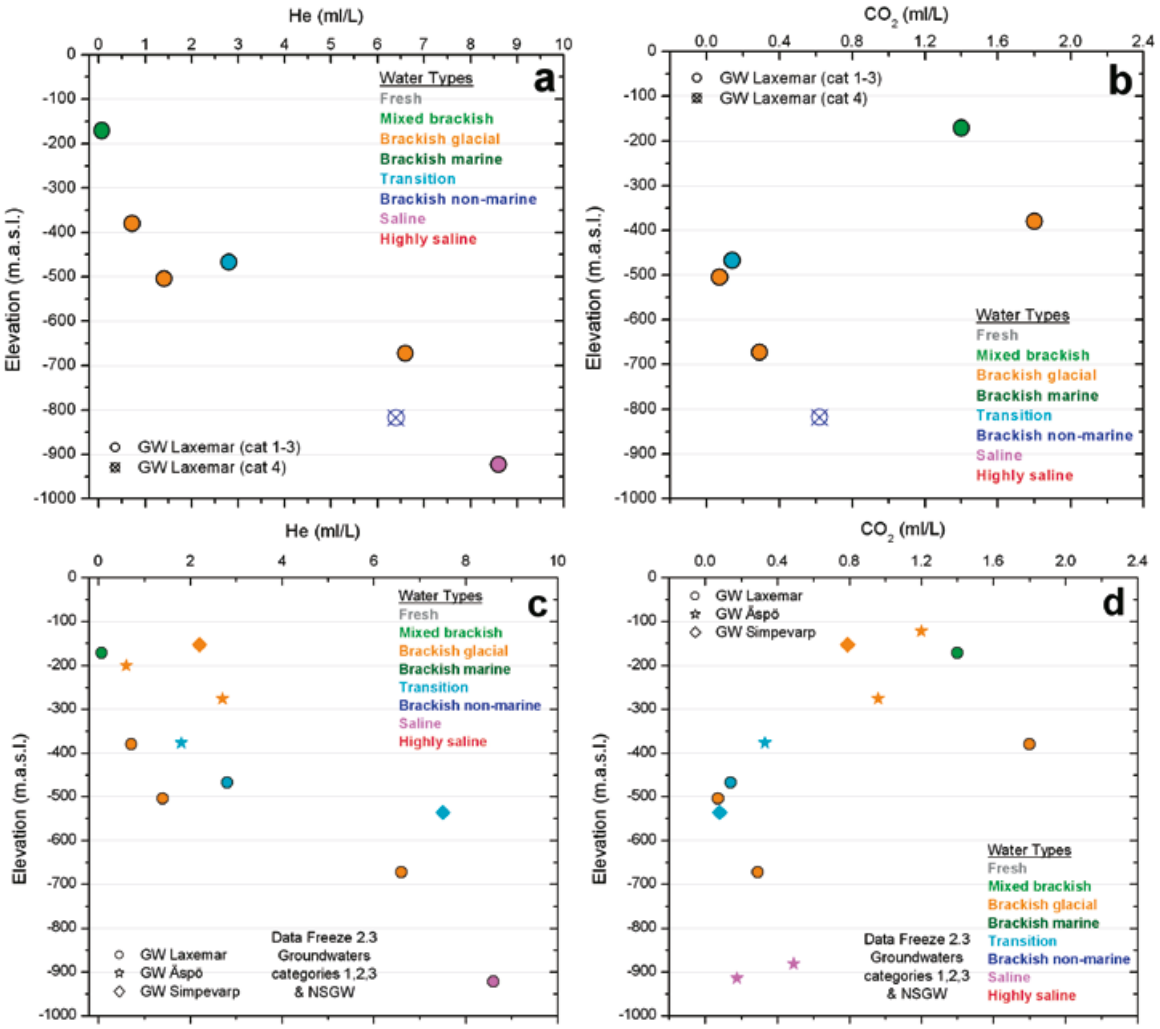

Figure 4-40. *The upper two diagrams show helium (left) and carbon dioxide (right) versus elevation for the Laxemar subarea. The lower two diagrams show the same plots for the entire Laxemar-Simpevarp area.*

4.7 Uranium, radium and radon

4.7.1 Background

This section documents and interprets measured data for uranium, radium and radon, given as contents (µg/L, only uranium) and activities (^{238}U, ^{234}U ^{226}Ra and ^{222}Rn) in near surface and bedrock groundwaters. Uranium is of special interest because of its redox sensitive character in groundwater and it has been measured as uranium-series isotopes on both groundwater and fracture mineral samples. The latter are presented in /Drake and Tullborg 2009a/ and describe the redistribution of uranium during the last 1 Ma. The isotope of ^{226}Ra (which largely accounts for the radium content) is the radioactive daughter of ^{230}Th in the ^{238}U decay chain (Figure 4-41). Knowledge of radium behaviour in undisturbed groundwater environments is important in that it may serve as a natural analogue to ^{226}Ra which in-grows from ^{238}U and especially from ^{238}Pu in spent fuel over the long term (> 10^5a). In the reducing groundwaters of the Fennoscandian shield, uranium concentrations are usually low and show a decreasing trend versus depth. This is explained by a decrease in Eh combined with decreasing bicarbonate content. Radium and radon, in contrast, behave quite differently.

In natural waters, radium has limited solubility and is readily removed from solution by absorption on clay minerals and other rock silicates and by coprecipitation with insoluble sulphates /Langmuir and Riese 1985/. Sorption of radium on fresh Fe-oxyhydroxide precipitates is common and has, for example, been identified on Fe-oxyhydroxides precipitated on the tunnel walls of the Äspö HRL /Landström and Tullborg 1995/. However, radium tends to be stabilised in solution by high concentrations of calcium, sodium and chloride /Langmuir and Melchior 1985/.

Radon (^{222}Rn), the radiogenic daughter of ^{226}Ra (Figure 4-41), is quite soluble in groundwater. Due to its short half-life of 3.82 days, it is only found in abundance near to a radon source such as uranium enriched minerals in fractures or in the wall rock, or from sorbed radium on, for example, fracture coatings. Because it is a gas, it readily moves into solution and, therefore, often far exceeds the concentration of its parent (^{226}Ra).

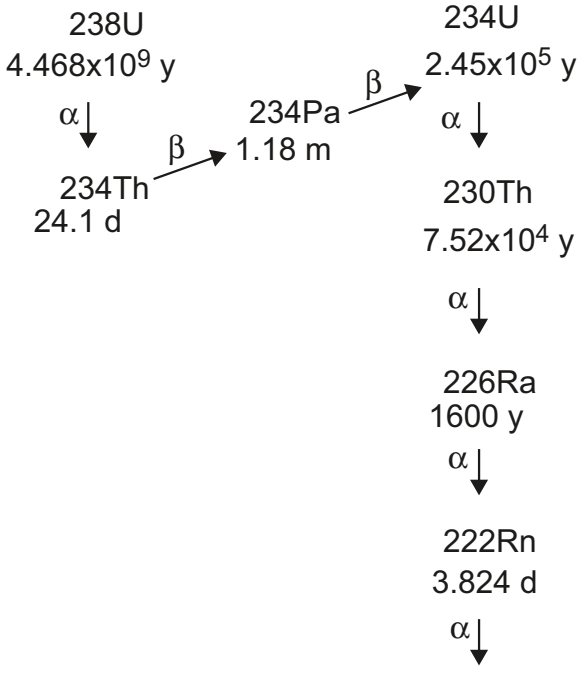

Figure 4-41. *The ^{238}U decay series.*

4.7.2 Uranium

Uranium contents have been measured in near surface and bedrock groundwaters and show an expected decrease with depth, partly coeval with decreasing bicarbonate values (Figure 4-42a and b). The near surface groundwaters show the largest range and also the highest values (up to 5 µg/L) which is attributed to the oxidising to mildly reducing conditions and the availability of bicarbonate for complexation; both near surface waters and groundwaters with bicarbonate contents lower than 25 mg/L bicarbonate show uranium contents lower than 1 µg/L. Shallow groundwaters of fresh and mixed brackish type show uranium contents below 4 µg/L, whereas the brackish and saline groundwaters at depths greater than about 300 m all show uranium contents below 1 µg/L which is in accordance with the low Eh measured at these depths (< –240 mV).

Analyses of uranium contents and uranium-series isotopes in the fracture coatings show recent redistribution of uranium within the last 300,000 y in the upper 100 m of bedrock /Drake et al. 2008/. Mobilisation in the upper 15 to 20 m is followed by an interval with variable redox conditions until mostly deposition prevails at depths greater than 60 m. Maximum uranium contents in the fracture coatings /Drake et al. submitted/ amount to approximately 50 ppm and the highest contents (around between 25 to 50 ppm U) are found at depths between 20 and 80 metres. At depths greater than 350 m the uranium contents in the fracture coatings decrease and are below 15 ppm.

Uranium isotope (^{238}U and ^{234}U) data show $^{234}U/^{238}U$ activity ratios (ARs) between 1 and 1.5 for the Laxemar near surface waters, whereas the groundwaters show ARs in the range 2 to 6 (Figures 4-43 and 4-44). There are a few exceptions of samples taken during the hydraulic testing programme where disturbances may have caused changes in redox conditions resulting in lower ARs. In common with the other trace element analyses, uranium and its daughters are very sensitive to perturbation and sampling procedures which may explain this behaviour. However, despite the scatter, the uranium contents in the Laxemar samples show expected trends, i.e. highest contents and lowest $^{234}U/^{238}U$ activity ratios indicative of oxidising conditions close to the surface, followed by lower contents and higher $^{234}U/^{238}U$ ratios at greater depths, typical for both reducing conditions and low bicarbonate content (cf e.g. /Gascoyne 2004/).

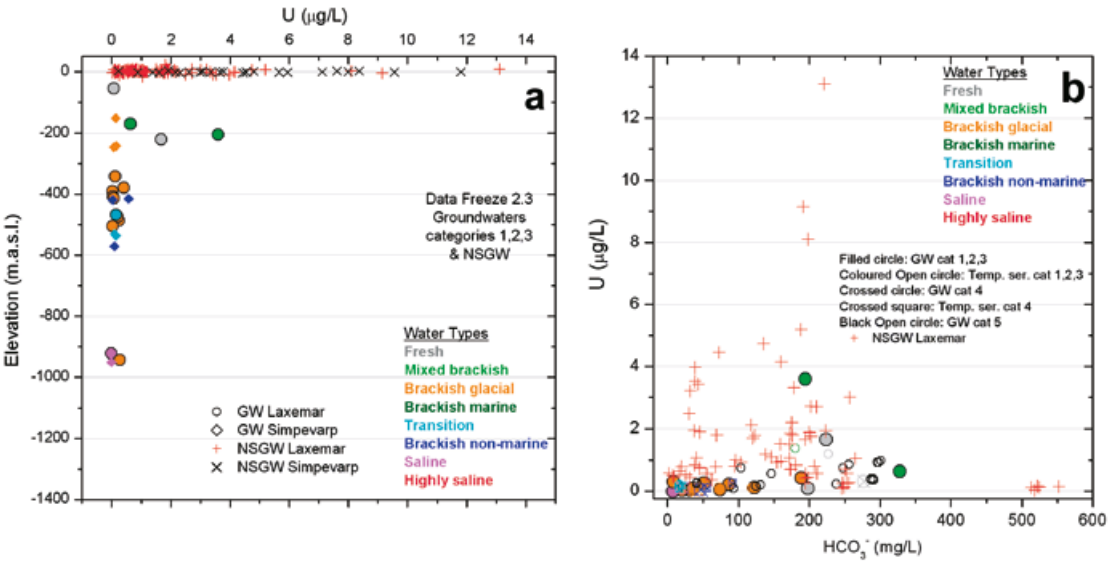

Figure 4-42. *Uranium content versus elevation (a) and bicarbonate (b) for near surface waters and groundwaters from the Laxemar subarea. All available data including categories 1 to 5 and time-series variations are presented in the plots.*

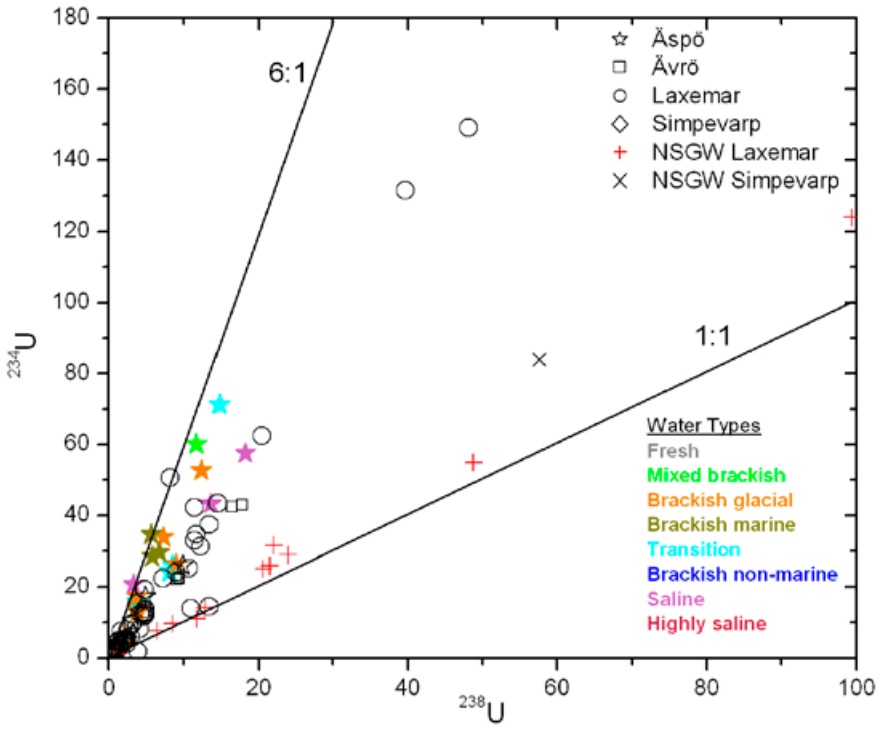

Figure 4-43. *^{234}U activity versus ^{238}U activity (mBq/L) for near surface waters and deeper groundwaters from the Laxemar-Simpevarp area.*

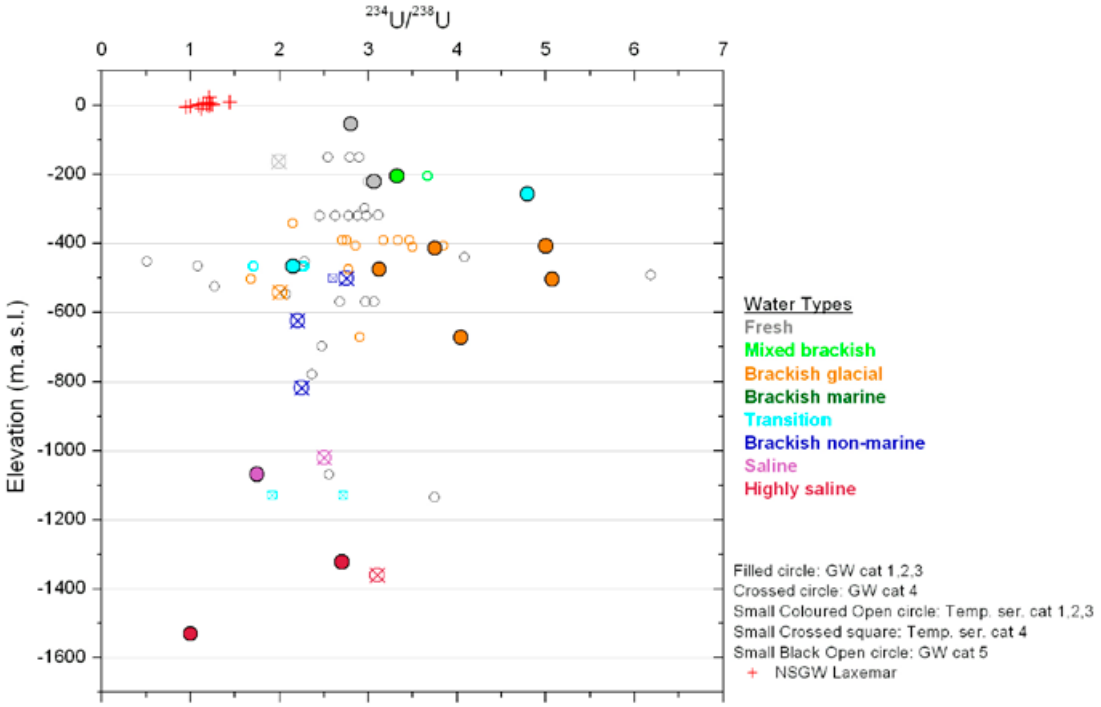

Figure 4-44. *$^{234}U/^{238}U$ activity ratio versus elevation for near surface waters and deeper groundwaters from the Laxemar subarea.*

4.7.3 Radium

Radium concentrations are generally low in the shallow, fresh (i.e. soil tube and percussion boreholes) groundwaters (Figure 4-45). Activities are below 0.5 Bq/L down to about 500 m where slightly higher values begin to appear, and still higher values are found in the deeper, more saline groundwaters, recording maximum values of 6.5 Bq/L at about 1,300 m depth. An inverse correlation between uranium and radium is expected because uranium concentrations normally decrease (due to lower redox potential and lack of HCO_3) as salinity increases, whereas radium is not directly affected by redox conditions and therefore tends to form soluble complexes as salinity increases. This is weakly indicated from Figure 4-48c but the scatter is large and the number of high category samples low.

4.7.4 Radon

Radon activity in the Laxemar subarea groundwaters ranges between almost 0 and 530 Bq/L. The variation with elevation and salinity (as Cl) and ^{226}Ra are shown in Figure 4-46a, b and c, respectively. Near surface groundwaters are low in radon, whereas the 1–3 category groundwater samples from cored boreholes and at depths exceeding 50 m usually show activities higher than 50 Bq/L. There is, however, a large variation in activity in the measured samples with category 4 to 5 samples (i.e. the less representative samples), tending to show low activities, suggesting sampling

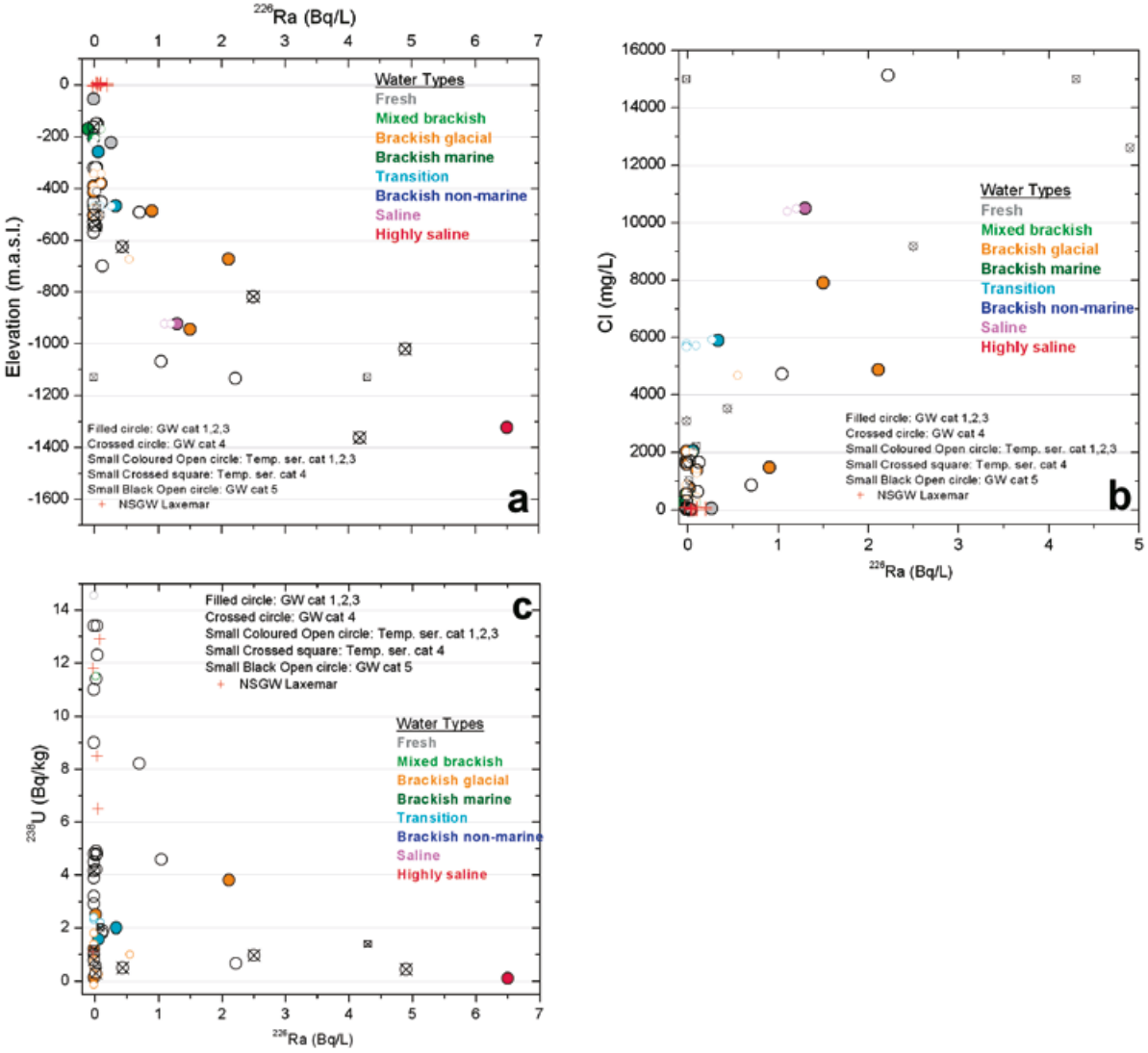

Figure 4-45. *Variation of radium concentration with elevation (a) with salinity given as Cl (b) and variation of ^{226}Ra with ^{238}U activity (c) in the Laxemar subarea groundwaters.*

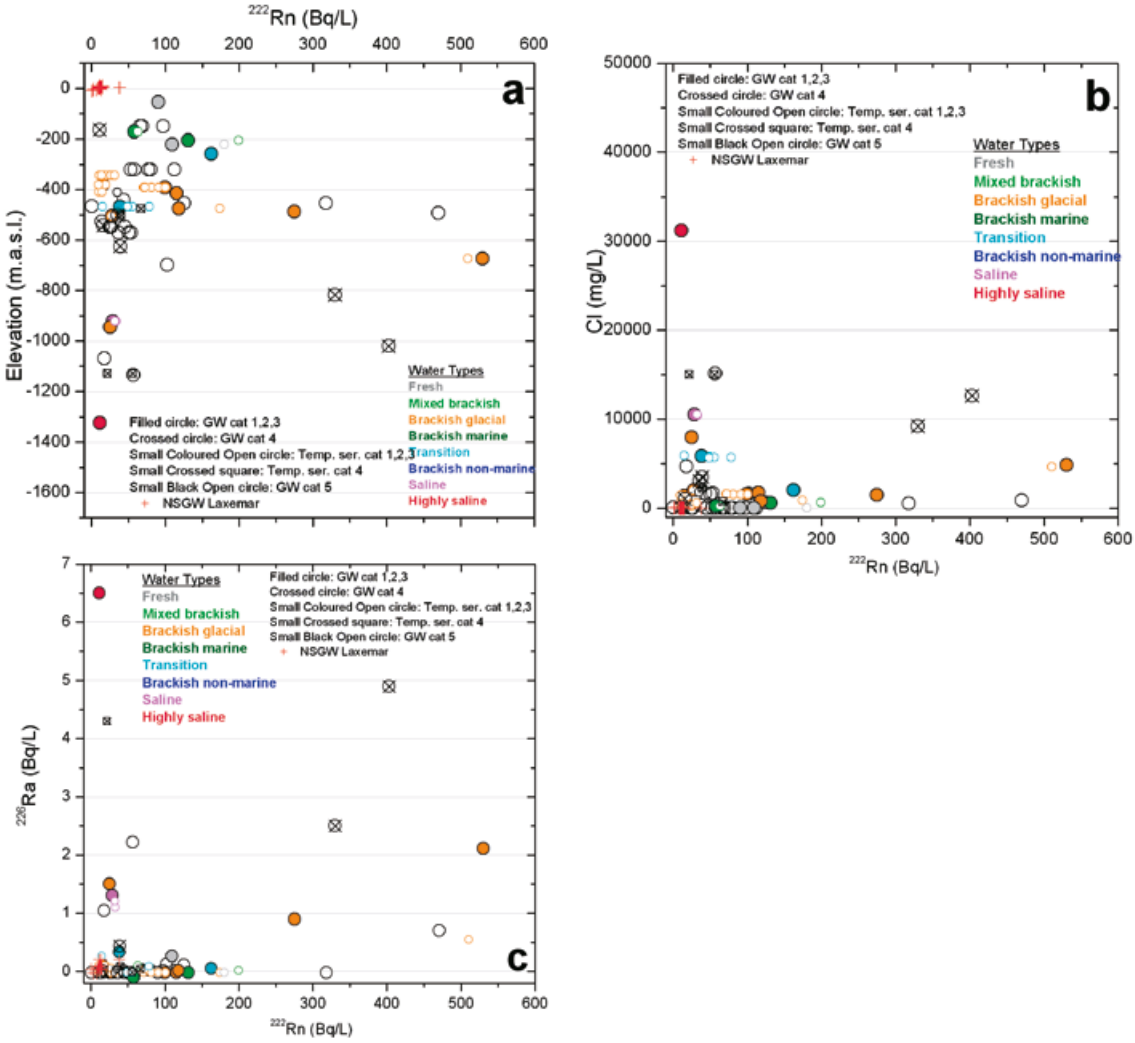

Figure 4-46. *Variation of radon with elevation (a) with salinity given as Cl (b) and with radon (c) in the Laxemar subarea groundwaters.*

problems. Most of the groundwaters show values below 200 Bq/L but somewhat higher activities (up to 530 Bq/L) are recorded in a few samples from about 450–1,000 m depth.

Generally, the radon activities are all well in excess (as high as three orders of magnitude) of the level for secular radioactive equilibrium with radium. This is in accordance with the fact that the radon in the groundwaters originates not only from radium in the groundwater, but also from radium present in the fracture coatings, or in the adjacent wall rock. Because ^{222}Rn has a relatively short (half life of 3.82 days), and assuming typical bedrock diffusivities, only the radon produced in the rock at millimetre to centimetre distances from the fracture can therefore reach the water-conducting fractures. Radon measurements from different fractures at about 450 m depth in the Äspö tunnel (i.e. the TRUE-1 site) show values between 350–650 Bg/L /Byegård et al. 2002/. Neither the host rock chemistry nor the fracture coating assemblages at Äspö deviate significantly from those in the Laxemar subarea, and therefore the low values measured in the Laxemar groundwaters, especially at great depth, are suspect and the interpretation uncertain.

4.7.5 Summary and conclusions

- The highest uranium values (up to 13 µg/L) are found in the near surface and shallow groundwaters representing relatively short residence times (possibly in the order of a few tens to thousands of years) and dynamic conditions with varying redox environments.

- At greater depths (< 250 m) groundwaters with longer residence times (some thousands years or older), lower bicarbonate contents and low Eh (< –240 mV) show uranium contents below 1 µg/L with most below 0.5 µg/L.
- There is good agreement with the uranium-series measurements on the fracture coatings which indicate a redistribution of uranium in the upper 100 m, with leaching in the uppermost 20 m and thereafter mainly deposition.
- This is also supported by the amounts of uranium in the fracture coatings where the highest values are found at depths between 20 to 80 m. However, both uranium contents in the groundwaters and the fracture coatings are relatively low.
- Radium in the Laxemar groundwaters shows increasing activities with increasing salinity (and thereby increasing depth), which is not unexpected.
- Although the radon measurements generally show a large scatter, a weak increase with depth is indicated for the category 1 to 3 samples except for groundwaters from greater than about 900 m depth.
- The radon activity exceeds the radium activity in all samples but there is no obvious correlation between the two. Furthermore, below about 900 m radon is very low which probably relates to sampling problems.

4.8 Groundwater mineral interaction

4.8.1 Background

Water/mineral reactions (that may or may not involve biogenic activity) are important for the hydrogechemical understanding and detailed description of the groundwater environment for two main reasons: a) recent water/mineral interaction with the groundwaters influences the present groundwater chemistry (e.g. dissolution/precipitation of calcite; oxidation/production of pyrite, ion exchange etc.; cf discussions in Sections 4.1 and 4.3), and b) the distribution and chemical/isotopic composition of certain minerals (e.g. calcite, pyrite and Fe-oxyhydroxide) provide information on former physico-chemical conditions which are important for the description of the long term stability of the site /Smellie et al. 2008/. Fracture minerals, and to some extent the adjacent bedrock, participate most actively in water/mineral interaction. Furthermore, fracture minerals may also serve as a redox and pH buffer in the case of recharging oxidising groundwaters (e.g. during glaciations and deglaciations). The most common fracture minerals in the crystalline rocks at Laxemar are chlorite, calcite, epidote, quartz, clay minerals, pyrite and hematite.

This section focuses on the possibility of using fracture minerals to derive palaeohydrogeological information and to indicate the available pH and redox buffer conditions provided by the minerals along the fracture system. The equilibria processes influencing the present groundwater chemistry are discussed in Sections 4.1 and 4.3 and concerns interaction between the groundwater and calcite, gypsum, fluorite, barite, quartz, goethite and iron sulphides, all of which have been identified in the fractures at Laxemar.

Calcite and to lesser extent sulphide and sulphate minerals are the phases that have been analysed for stable isotope composition ($\delta^{18}O$, $\delta^{13}C$, $\delta^{34}S$ and $^{87}Sr/^{86}Sr$) in order to provide information on their origin. Furthermore, calcite has been analysed for trace element composition and in a few samples also for fluid inclusions. The full results of the fracture mineral investigations from the Laxemar-Simpevarp area, including the palaeohydrogeological studies, are reported in /Drake and Tullborg 2009a/ and summarised below.

Calcites and sulphur minerals

The application of isotope systematics and detailed microscopy on the Laxemar-Simpevarp calcites /Drake and Tullborg 2009b/ has resulted in the identification of three general types of calcites based on stable isotope composition: a) hydrothermal calcite (Generation 3 and 4), b) warm brine type calcite originating from a fluid influenced by organic material (Generation 5a), and c) low temperature calcite precipitated from different groundwaters at low temperatures (probably less than 50 ºC) including temperatures close to present groundwater temperatures (Generation 5b). Fracture mineral assemblages of Generation 1 and 2 generally do not contain calcite (cf Section 2.2.5). Pyrite has been identified in

the same generations described for calcite, whereas sulphates, gypsum and barite are of Generation 5a, or slightly younger.

Hydrothermal calcite and pyrite

Calcite and pyrite belonging to the fracture minerals of Precambrian Generations 3 and 4 (cf Section 2.2.5) show typical hydrothermal signatures. The calcite shows a wide range in $\delta^{18}O$ values (–23.5 to –16‰ PDB), whilst the range for $\delta^{13}C$ (–6.5 to –2.1‰ PDB) is quite narrow and in agreement with inorganic carbon cycling (Figures 4-47 to 4-49). The hydrothermal origin is further evidenced by the homogenisation temperatures of the fluid inclusions (195–370°C). Furthermore, pyrite of Generation 3 shows typical hydrothermal/magmatic $\delta^{34}S$ values (–3 to +3‰ CDT; Figure 4-50).

The large range in $\delta^{18}O$ is probably due to varying degrees of water-rock interaction and successively decreasing temperatures, and the low amount of hydrothermal calcite in the upper 50 m of bedrock is most likely due to later dissolution and recrystallisation. The hydrothermal event responsible for the Generation 3 mineralisation is thought to be related to the Götemar and Uthammar granite intrusions ca 1,450 Ma ago (cf Section 2.2.5).

The $^{87}Sr/^{86}Sr$ ratios in the hydrothermal calcites are lower than those in the present groundwater, in the wall rock or in younger calcite (Figure 4-51) which indicate formation early in the history of the rock when the $^{87}Sr/^{86}Sr$ ratios were closer to the initial rock ratios. The high concentration of strontium in Generation 3 calcite is interpreted to be associated with extensive hydrothermal alteration of the wall rock adjacent to Generation 3 fractures.

Generation 4 minerals seem to be much less common; however, the few samples analysed generally show somewhat higher $\delta^{18}O$ than Generation 3 but similar $\delta^{13}C$ (Figure 4-47). This indicates a hydrothermal origin for Generation 4 in common with Generation 3 but with slightly lower formation temperatures, which is also supported by fluid inclusion results. The two salinity populations of fluid inclusions in calcite of Generation 4 with similar homogenisation temperatures (T_h) suggest mixing of two different fluids, such as brine and a more dilute fluid. Generation 4 is suggested to be Sveoconorwegian in age in common with the N-S trending dolerite dykes identified in in the westernmost parts of the Laxemar subarea (cf Section 2.2.3 and references therein).

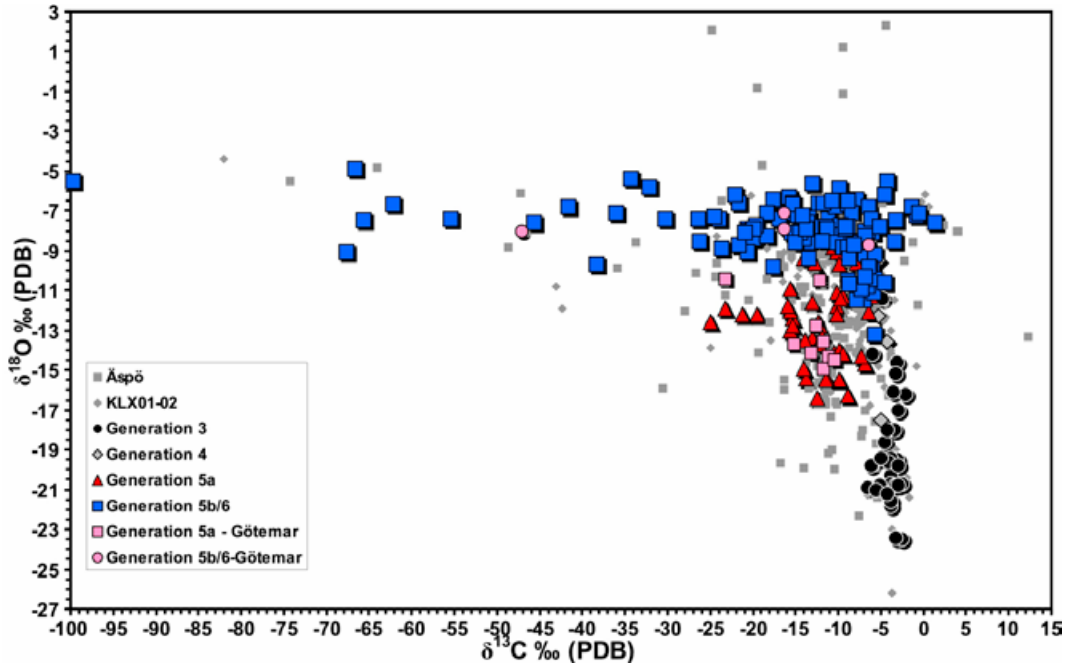

Figure 4-47. *$\delta^{18}O$ versus $\delta^{13}C$ in fracture filling calcites of different generations from the Laxemar and Simpevarp subareas and from the Götemar granite. Calcite samples from Äspö and KLX01-02 /Tullborg et al. 1999, Wallin and Peterman 1999, Bath et al. 2000, Milodowski et al. 2005/ are also shown but are not separated into different generations. Analytical errors are within the size of the symbols.*

Palaeozoic calcite, pyrite, gypsum and barite

The oldest Palaeozoic precipitates (Generation 5a) have $\delta^{18}O$ values ranging from –16.5 to –11‰ PDB and for the majority of samples $\delta^{13}C$ values between –16 to –9‰ PDB (Figures 4-47 to 4-49). Fluid inclusions in these calcites show salinities of 17–24 wt.% eq. $CaCl_2$ and T_h of 80–145°C. This corresponds to precipitation from 'warm brine' fluids, which has also been determined from earlier studies of fracture calcite at Äspö and Laxemar /Tullborg et al. 1999, Tullborg 2003, Milodowski et al. 2005/ as well as at Olkiluoto, Finland /Blyth et al. 2000/ and of fracture fluorite from the Götemar granite /Alm and Sundblad 2002/. Generation 5a is interpreted to have formed during the period of highest temperatures during the Palaeozoic. It is suggested that during this period, a several kilometre thick pile of marine and terrestrial sediments covered the Laxemar-Simpevarp area /Larson et al. 1999/.

The relatively low $\delta^{13}C$ compared with hydrothermal calcites is indicative of contribution of biogenic carbon and is probably the result of descending groundwaters containing organic input originating from the overlying, organic-rich sediments. One possible source may be alum shale, similarly proposed for asphaltite formation in Palaeozoic fractures in crystalline rock at Forsmark /Sandström et al. 2006/.

Fluid inclusion salinities of Generation 5a calcite are much higher than the salinity of the present groundwater at the site which at most is 8 wt.% total dissolved $CaCl_2$-dominated salts at about 1,500 m depth in KLX02. The wide range in $^{87}Sr/^{86}Sr$ and $\delta^{18}O$ may be due to: 1) the variable degree of water-rock interaction, and/or 2) mixing of groundwaters with very different origin and thereby of $\delta^{18}O$ (e.g. meteoric, marine and brine waters). The $^{87}Sr/^{86}Sr$ ratios of the Generation 5a minerals are considerably higher than for Phanaerozoic sea water ($^{87}Sr/^{86}Sr$: 0.707–0.7095 /Veizer et al. 1999/) and the strontium isotope ratios are probably reflecting water-rock interaction and possibly also a

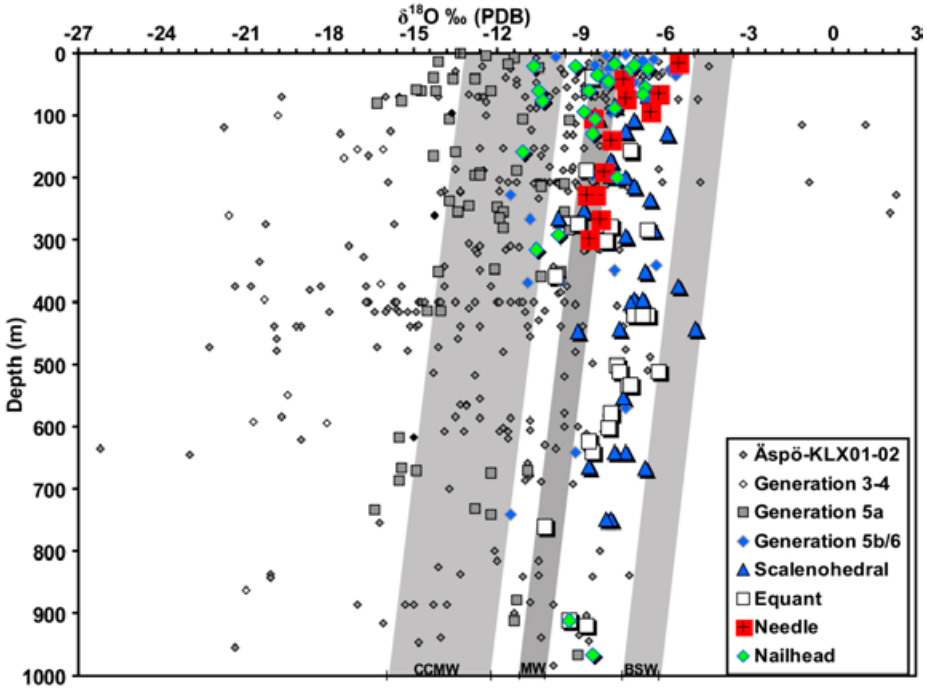

Figure 4-48. *$\delta^{18}O$ versus depth in fracture filling calcite of Generations 3–4, 5a and 5b/6 from the Laxemar subarea, the Simpevarp subarea and from the Götemar granite. Morphologies of calcite of Generation 5b/6 are indicated where observed. Calcite samples from Äspö and Laxemar (KLX01-02) /Tullborg et al. 1999, Wallin and Peterman 1999, Bath et al. 2000, Milodowski et al. 2005/ are also shown but are not separated into different generations. Shaded areas represent calcite precipitated in equilibrium with present day Baltic Sea water (BSW) and meteoric water (MW) as well as cold climate meteoric water (CMW) at temperatures increasing linearly from 7±2°C near the ground surface to 18±2°C at 1,000 m depth, and using fractionation factors by /O'Neil et al. 1969/ and the 'Extended data freeze Laxemar 2.3' groundwater data set. Analytical errors are within the size of the symbols.*

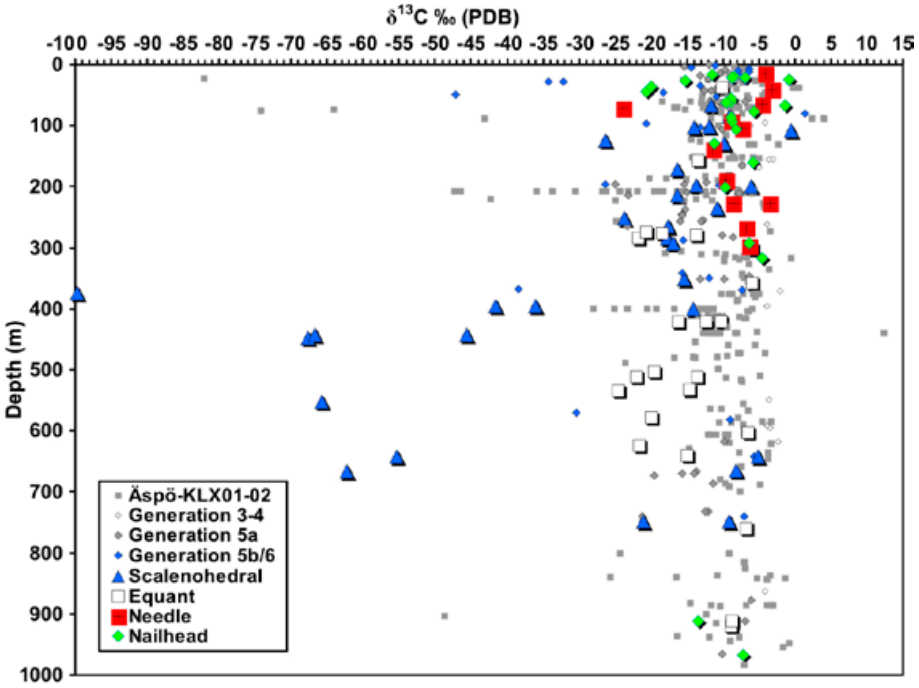

Figure 4-49. *$\delta^{13}C$ versus vertical depth in fracture filling calcite of Generations 3 to 4, 5 and 5b/6 from the Laxemar subarea, the Simpevarp subarea and from the Götemar granite. Morphologies of calcite of Generation 5b/6 are indicated where observed. Calcite samples from Äspö and Laxemar (KLX01-02) /Tullborg et al. 1999, Wallin and Peterman 1999, Bath et al. 2000 Milodowski et al. 2005/ are also shown but are not separated into different generations. Analytical errors are within the size of the symbols.*

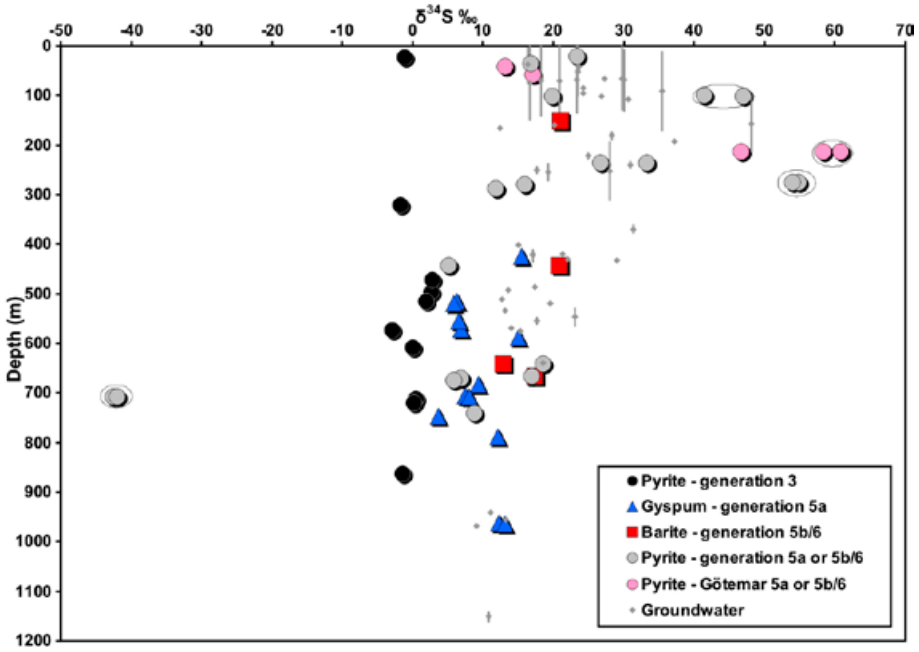

Figure 4-50. *$\delta^{34}S$ in fracture filling pyrite, gypsum and barite versus vertical depth. Samples are from the Laxemar and Simpevarp subareas and from the Götemar granite (plotted separately). Encircled values are two analyses of material from the same fracture surface. $\delta^{34}S$ in groundwater samples are also shown and y-axis bars define the borehole length of each section sampled (data are from the 'Extended data freeze Laxemar 2.3' groundwater data set). Analytical errors are within the size of the symbols.*

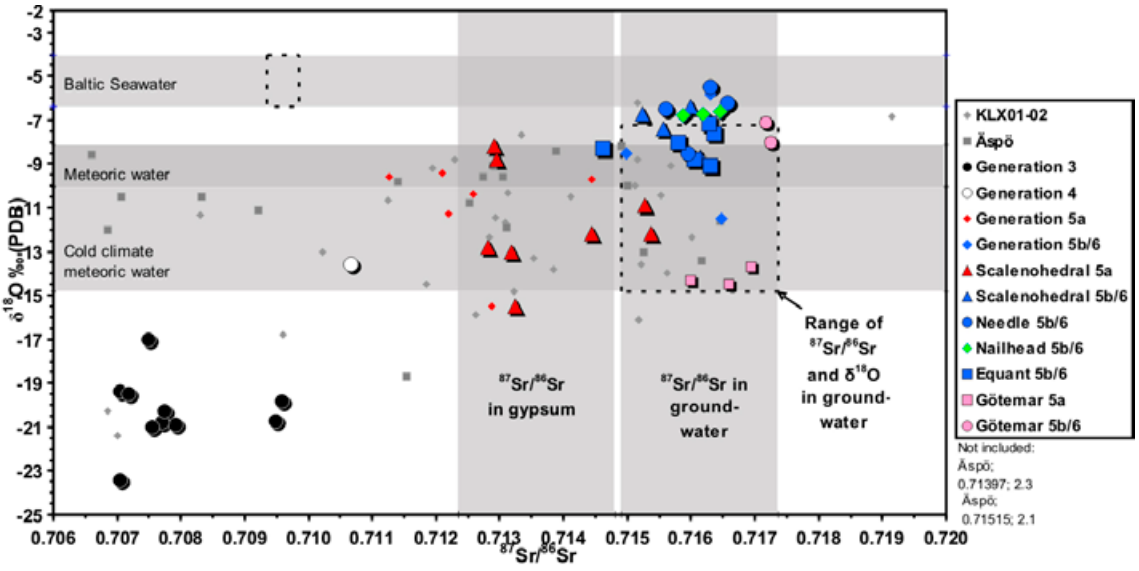

Figure 4-51. *$^{87}Sr/^{86}Sr$ ratio versus $\delta^{18}O$ in fracture filling calcites in the Götemar granite from the Laxemar subarea and the Simpevarp subarea. Crustal morphologies are indicated where observed. Calcite samples from Äspö and Laxemar (KLX01-02) /Tullborg et al. 1999, Wallin and Peterman 1999, Bath et al. 2000, Milodowski et al. 2005/ are also shown but are not separated into different generations. Shaded areas (y-axis) represent calcite precipitated in equilibrium with present day Baltic Sea water and meteoric water as well as cold climate meteoric water at 7–15°C using fractionation factors by /O'Neil et al. 1969/, data from the 'Extended data freeze Laxemar 2.3' groundwater data set. Shaded areas (x-axis) represent the range in $^{87}Sr/^{86}Sr$ in gypsum of Generation 5a as well as of the present groundwater in the Laxemar and Simpevarp subareas. Stippled areas represent the isotopic composition of the Baltic Sea water as well as of the present groundwater in the Laxemar and Simpevarp subareas. Analytical errors are within the symbol size.*

relatively long time span of precipitation. The positive correlation of $^{87}Sr/^{86}Sr$ with $\delta^{18}O$ in calcite indicates gradually lower formation temperatures of the different generations, in agreement with /Tullborg et al. 1999, Wallin and Peterman 1999, Bath et al. 2000, Tullborg 2003, Milodowski et al. 2005/.

Gypsum and probably some of the barite is Palaeozoic and their $\delta^{34}S$ compositions overlap with $\delta^{34}S$ of Palaeozoic sea water sulphate /Strauss 1997/ which suggests precipitation from descending sea water or fluids from presently eroded Palaeozoic sediments. The $\delta^{34}S$ values of the sulphates decrease with depth and below about 500 m (Figure 4-50) they are generally lower than for Palaeozoic sea water. Possible explanations include formation from a mixture of marine waters and non-marine waters with long residence times in the bedrock.

Late Palaeozoic-present low temperature precipitates

The low temperature minerals correspond to the Generation 5b/6 fracture minerals (cf Section 2.2.5). Absolute dating has not been possible and therefore these precipitates are referred to as 'Late Palaeozoic to recent' and represent different low temperature precipitates that may span periods of several hundreds of millions of years. These minerals are the most interesting from a palaeohydrogeological perspective since they may, at least partly, represent precipitates from groundwaters similar to the present. However, because the low temperature history of the area is very long it represents quite different hydrogeochemical environments. The precipitates analysed are calcites, pyrites and barite but for the latter two it has not been possible to distinguish which precipitates belong to Generation 5a and 5b respectively. Furthermore, minute grains of pyrite are common in fractures with late (Generation 6) calcites but this has not been possible to sample. The generally low formation temperatures are consistent with the absence of fluid inclusions in these calcites and therefore no independent information on formation temperatures exist.

The low temperature calcite has $\delta^{13}C$ in the range of –30 to –5‰ PDB (Figure 4-47 and 4-49), typical for descending biogenic CO_2, produced by breakdown of organic material. The very low $\delta^{13}C$ values (< –30‰ PDB) in some calcites suggest microbial breakdown of organic matter *in situ*, which produces bicarbonate with non-equilibrium low $\delta^{13}C$ values /cf Tullborg et al. 1999/. These calcites are found both in the upper part of the bedrock aquifer (~ 27–200 m) in accordance with similar findings at Äspö /Tullborg 2003/, and also down to about 670 m in the Laxemar subarea. The reason for low $\delta^{13}C$ calcite at greater depths in the Laxemar subarea include possible input of organic rich water to greater depths due to more extensive recharge compared with the Simpevarp subarea and Äspö. The low $\delta^{13}C$ calcites are of scalenohedral morphology which, according to /Milodowski et al. 2002, 2005/, is indicative of formation from saline groundwater. High $\delta^{13}C$ values (> –3‰ PDB) compatible with a marine origin, are only found in the upper –107 m elevation of the bedrock. The absence of low $\delta^{13}C$ values (< –13.5‰ PDB) and high $\delta^{18}O$ (> –8‰ PDB) below about 800 m in Generation 5b/6 (and 5a) calcites indicates a decrease in organic material supply, a change to a less hydraulically dynamic system, and a depth limit of major brackish marine input. Calcite with very low $\delta^{13}C$ is absent in the upper –27 m elevation probably due to open system conditions, which prevents extreme values to develop and may also be influenced by high $\delta^{13}C$ values from dissolved older calcite. Unlike older calcite, many of the Generation 5b/6 calcites have $\delta^{18}O$ values that indicate possible equilibrium with present meteoric water (–10 to –8‰ VSMOW) or brackish Baltic Sea water (–6.5 to –4‰ VSMOW) at ambient temperatures of 7 to 15°C (Figure 4-48). Large changes have occurred in both salinity and $\delta^{18}O$ in groundwater during the Quaternary, and the recorded distribution of groundwaters with different chemistry and origins at the site has most probably occurred at several earlier periods during this era.

The correlation between $\delta^{18}O$ and crystal morphology suggests that this is related to the salinity of the fluid from which the calcite precipitated (cf /Folk 1974, Milodowski et al. 1998ab, 2005/) which is also indicated by the highly saline fluid inclusions in scalenohedral calcites of Generation 5a origin. The variation in $\delta^{18}O$ values in calcite of all morphological types as well as the fact that all morphologies (except needle) are found at both the near surface and at great depths (Figure 4-48 and Figure 4-49), might be a result of the typically large changes in salinity and $\delta^{18}O$ related to the cycle of glaciations-deglaciations during the Quaternary. Many of the Generation 5b/6 calcites with $\delta^{18}O$ values in the range of calcite precipitated in equilibrium with meteoric water at ambient temperatures (Figure 4-51 and Figure 4-48) also show dominantly nailhead shapes, in agreement with a fresh water of temperate climate origin. Calcite that trends towards precipitation in equilibrium with Baltic Sea water at ambient temperatures is mostly present in the upper 100 m but also at greater depths (down to ~500 m) in deformation zones (Figure 4-51 and Figure 4-48). Note that the span for the temperatures in Figure 4-48 is quite narrow and is based on present temperatures in the boreholes. If the span of –6.5 to –4‰ $\delta^{18}O$ PDB and the temperature interval 7–15°C is used for all depths, this field includes mainly samples from the upper approximately 100 m. This calcite is dominantly scalenohedral and occasionally equant or needle shaped (near surface), indicating precipitation from saline or brackish groundwaters. However, below about 500 m, the dominance of scalenohedral and equant crystals with $\delta^{18}O$ values lower than typical Baltic Sea water signatures indicate precipitation from groundwaters of older deep saline origin. No low temperature marine precipitates (oceanic $\delta^{18}O$ is –3 to +3‰ VSMOW) similar to those observed at nearby Äspö (Figure 4-47), or potential precipitates from pronounced glacial meltwaters, have been identified. However, potential precipitates from meteoric water during a slightly colder climate than the present have been identified and are dominantly of fresh water, nailhead shaped type (Figure 4-48 and Figure 4-49).

$^{87}Sr/^{86}Sr$ ratios in calcites of Generation 5b/6 vary with the wall rock compositions. The Generation 5b/6 calcites might have precipitated in equilibrium with the present day groundwater because of the similar range in $^{87}Sr/^{86}Sr$-ratios, in contrast to most of the older calcites and all older gypsum. The $^{87}Sr/^{86}Sr$ ratios of calcite of Generation 5b/6 are considerably higher than those of the present Baltic Sea water (Figure 4-51), which is in agreement with a rapid change of the $^{87}Sr/^{86}Sr$ ratio in descending marine waters caused by water-rock interaction and especially ion exchange along the flow paths (cf Section 4.1). The large variation in $^{87}Sr/^{86}Sr$ ratios is probably also an effect of prolonged precipitation for this generation. Because the range in $^{87}Sr/^{86}Sr$ ratios for calcite of different morphologies overlaps, no relative chronological distinction of these different types can be identified. However, scalenohedral crystals generally have slightly lower $^{87}Sr/^{86}Sr$ ratios than the other types and might therefore be slightly older. The large variation in manganese content in calcite of Generation 5b/6, and also in Generation 5a, and the decrease in manganese contents with depth is in agreement with

earlier studies at Äspö and Laxemar /Tullborg 2003/. This variation in manganese content is at least partly due to varying redox conditions, as Mn^{2+} can be incorporated in calcite under reducing conditions. Possible explanations for the high manganese content at shallow to intermediate depth include sub-surface microbial manganese reduction of organic material, by which Mn^{2+} remains in solution and can be incorporated in calcite.

The $\delta^{34}S$ values in the sulphates decrease with depth (Figure 4-50). The few analysed barite samples of Generation 5b/6 have $\delta^{34}S$ values which overlap with those of the present groundwater /SKB 2006b/. The two barite samples from the uppermost 500 m show marine $\delta^{34}S$ signatures, whereas the $\delta^{34}S$ values of the two barite samples from depths greater than 500 m, show lower $\delta^{34}S$ values which indicates input of other sulphide sources, e.g. from dissolved Paleozoic gypsum. Pyrite of Generation 5b/6 has $\delta^{34}S$ values generally within the range of gypsum and barite, except at –100 m to –275 m and –707 m elevation. These very high $\delta^{34}S$ values in pyrite are probably due to closed system bacterial sulphate reduction (Rayleigh distillation) causing disequilibrium (e.g. /Ohmoto and Goldhaber 1997/), in accordance with observations from Äspö /Wallin 1992, Pedersen et al. 1997/ and also indicated by the large variation in $\delta^{34}S$ values between different samples and the quite large spread within single samples (cf /McKibben and Eldridge 1994, Ohmoto and Goldhaber 1997/). These depths correspond to were anaerobic sulphate reduction is the dominant current microbial process and where the highest $\delta^{34}S$ values occur (up to +48‰). Figure 4-50, indicates a closed system with microbial sulphate reduction, and therefore these pyrites may have formed during conditions similar to the present /McKibben and Eldridge 1994, Ohmoto and Goldhaber 1997/. However, heavy $\delta^{34}S$ values in barite related to the heavy $\delta^{34}S$ values in pyrite are not observed, indicating that these minerals are not co-genetic.

Palaeohydrogeological conclusions

At least two different events of hydrothermal fluid circulation during the Precambrian (in addition to post-magmatic mineralisations) have been possible to distinguish: a) Extensive fluid circulation resulting in precipitation of calcite, pyrite, and Ca-Al silicates (epidote, prehnite and laumontite) together with extensive wall rock alteration which occurred during a prolonged event related to the emplacement of the Uthammar and Götemar granites (dated to 1,450 Ma). Fluid inclusion homogenisation temperatures in the range of 195 to 370°C are in agreement with the mineral paragenesis found. b) A less defined and less extensive period of hydrothermal circulation took place during the late Sveconorweigian. This event is probably related to the intrusions of the N-S dolerite dykes (900 Ma) found in the westernmost part of the Laxemar subarea.

During the Palaeozoic when the area was covered by sediments, brine fluids formed and saturated the fracture system of the underlying crystalline bedrock. Temperatures in the range 80–145°C prevailed, probably as a result of the thick sedimentary pile. Organic-rich, reducing and highly saline fluids precipitated calcite, pyrite and gypsum.

During the Late Palaeozoic to recent period, calcite and pyrite showing organic and microbial influences precipitated at temperatures < 110°C, occasionally with closed system $\delta^{13}C$ or $\delta^{34}S$ signatures. The $\delta^{18}O$ values and $^{87}Sr/^{86}Sr$-ratios indicate that some of these calcites may have formed from fluids in equilibrium with water similar to present groundwaters at ambient temperatures. The calcites analysed represent precipitates from very different groundwaters (in terms of $\delta^{18}O$ and salinity) and calcites precipitated from different fluids in terms of microbial activity and salinity are often present in the same fractures or fracture system indicating that these fractures have been intermittently water conducting during a very long period of time. The frequency of both low $\delta^{13}C$ and microbially modified $\delta^{34}S$ values decreases with depth. Fresh water carbonates as well as the low $\delta^{13}C$ signatures are found at greater depths in the recharge areas (Laxemar) compared with discharge areas (Simpevarp). Intrestingly, low temperature oceanic or pure glacial precipitates have not been identified.

4.8.2 Changes in redox conditions and available redox buffer capacity

Different mineralogical and geochemical indicators, such as the distribution of Fe(II)/Fe(III) minerals and behaviour of redox sensitive elements like cerium and uranium, can be studied in order to reveal possible redox front development, for example, in the near surface bedrock environment. In addition,

although calcite is not redox sensitive *sensu stricto*, there is a secondary relationship due to interactions between the biosphere and the bicarbonate. Two different studies have been carried out at Laxemar, one focused on the Precambrian and one on recent redox features identified in the fractures and in the wall rock; the results are summarised in /Drake and Tullborg 2009a/:

1. Hydrothermally altered, red-stained (supposedly oxidised) wall rock samples have been compared to fresh wall rock nearby, and the differences in mineralogy and mineral and whole rock chemistry (especially the reducing capacity) have been determined /Drake et al. 2008/.
2. The position of a recent near surface redox front has been investigated based on mineralogical, geochemical and U-series disequilibrium analyses of mineral coatings along open fractures /Drake et al. 2009/.

The results from the hydrothermally altered and potentially oxidised wall rock, which is mainly related to the Generation 3 fracture minerals, show that the red-stained rock adjacent to the fractures displays major changes in mineralogy as summarised in Figure 4-52. Biotite, plagioclase and magnetite have been altered and chlorite, K-feldspar, albite, sericite, prehnite, epidote and hematite have been formed. However, the changes in chemistry are moderate with K-enrichment, Ca-depletion and constant Fe_{tot} documented.

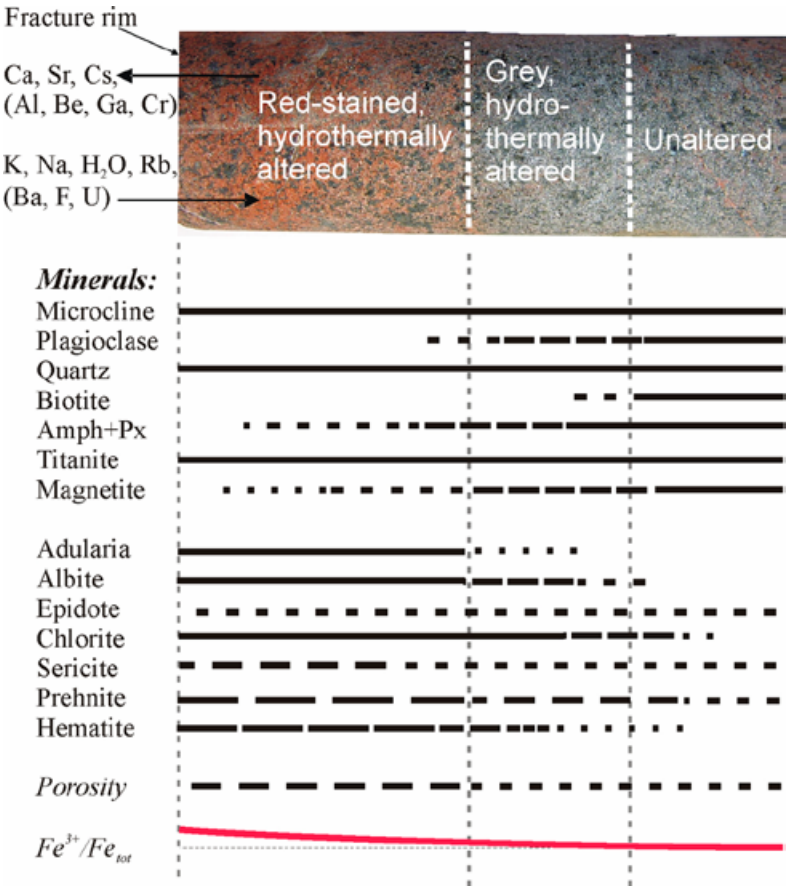

Figure 4-52. *Tentative sketch of the major features of the red-stained wall rock compared to the reference wallrock nearby, which consists of either partly hydrothermally altered (but not red stained) or unaltered rock, indicated by the stippled lines on the drill core photograph. The fracture rim is at the left side of the sketch characterised by fracture minerals such as prehnite, chlorite, epidote, calcite, quartz and fluorite. Arrows indicate which element is enriched or depleted in the red-stained rock compared to the reference rock. The horizontal lines (partly stippled) show were the major minerals occur adjacent to the fracture, as well as the difference in porosity (including microfractures). The lowermost line illustrates the change in Fe^{3+}/Fe_{tot} relative to a reference line. Figure adapted from /Drake et al. 2008/.*

The difference in Fe^{3+}/Fe_{tot}-ratio of the red-stained rock compared to the reference rock is considerably smaller than macroscopic observations suggest, and the average Fe^{3+}/Fe_{tot}-ratio is only 0.023 higher in the red-stained samples than in the reference samples when comparing each sample pair. This enrichment is mainly related to the replacement of magnetite by hematite and the generally slightly higher epidote content in the red-stained rock. The replacement of magnetite by hematite is also shown by the lower susceptibility of the red-stained rock compared to the unaltered rock /Mattsson et al. 2004/. However, because most of the Fe in the rock is contained in the silicate phases which show fairly constant Fe^{3+}/Fe_{tot} contents, the total change in Fe^{3+}/Fe_{tot} between the red-stained rock and the unaltered rock is not as high as susceptibility measurements suggest.

The mineralogical changes in combination with the modest oxidation and formation of minute hematite grains in porous secondary minerals in pseudomorphs after plagioclase have produced the red staining. Increased porosity is also characteristic for the red-stained rock. Moderate alteration in the macroscopically fresh reference rock shows that the hydrothermal alteration penetrates further from the fracture than the red staining. The increase in porosity in the red-stained rock may result in enhanced retention of radionuclides due to an increased sorptivity and diffusion close to the fracture.

Studies of the position of the near surface redox front in the boreholes show at what depths oxidising groundwaters within the last 1 Ma generally have been reduced by, for example, fracture minerals ± organic redox buffer. These investigations show that the redox front in the Laxemar area is generally positioned at about 15–20 m depth, depending locally on the bedrock hydraulic properties. The main features of the redox front are generally observed in the fracture mineralogy and geochemistry (Figure 4-53), and as a shift with increasing depth from: a) mainly goethite to mainly pyrite, b) positive cerium anomalies to slightly negative or insignificant cerium anomalies, and c) mobilisation and removal of uranium to mainly deposition.

Leaching of calcite in open fractures in the upper approximately 20–30 m further supports infiltration of very dilute recharge waters which probably have relatively low pH and may at least partly be charged with oxygen. Scattered goethite occurrences down to about 80 m and occasional signs of uranium removal at about 35–55 m depth, generally correlate with borehole sections of high conductivity (and/or high fracture frequencies) facilitating local downward percolation of oxidising groundwaters to greater depth. Removal of uranium during oxidising conditions within the last 300 ka, a period including both glaciations and interstadials, is not indicated in the analysed samples

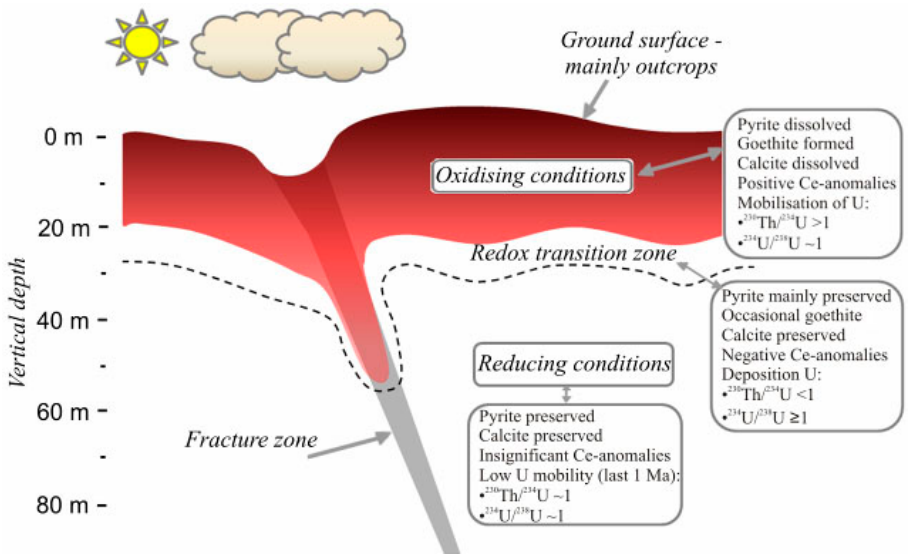

Figure 4-53. *Tentative sketch of the near surface redox front in the Laxemar subarea. The different fields represent the depth intervals were mineralogical, chemical and USD analyses of fracture coatings indicate recent oxidising conditions, reducing conditions or a transition zone between these. The study is based on a limited number of samples and deeper penetration of oxidising groundwaters along specific channels in highly transmissive fracture zones may occasionally have lasted for short periods of time, figure adopted from /Drake et al. 2009/.*

below about 55 m depth. Although penetration of glacial waters to much greater depths has been confirmed in the Laxemar-Simpevarp area /SKB 2006b/ this study conforms to the modelling carried out by /Guimerà et al. 1999/ and conclusions drawn by /Gascoyne 1999/ in that these glacial waters were not oxidising at repository depths. This is supported by present day observations whereupon oxygen in recharge waters is generally consumed within the upper approximately 20 m (± 5 m) and to slightly greater depths in bedrock volumes with increased hydraulic conductivity ($\geq 1\times10^{-7}$ m^2/s).

Concerning the available redox and pH buffer provided by the fracture minerals present along the groundwater pathways (cf Figure 4-54) it can be concluded that:

- The most efficient pH buffer is calcite which is present in most of the fractures and deformation zones although in lower amounts in the upper approximately 10–20 m of bedrock.
- The main inorganic redox buffer is Fe(II), which is present in chlorite, biotite and clay minerals and pyrite grains. The redox buffer has only been significantly decreased in the very near surface fractures (upper 20 metres) but may be partly lowered also in the upper approximately 50 m of bedrock.
- Despite earlier oxidising hydrothermal events and potential increased introduction of oxidising glacial meltwater during the Quaternary glaciations, there is still a large redox buffer capacity present in the fracture and wall rock minerals. Any potential build up of reducing capacity in the fracture minerals during recent periods of reducing groundwater conditions is difficult to estimate. Processes that could contribute to an increase in redox capacity include the production of Fe^{2+} and Mn^{2+} that may either precipitate (e.g. co-precipitation with calcite) or be sorbed on mineral surfaces due to ion exchange. In addition, iron sulphides may be formed due to bacterial activity of sulphate reducers. However, it can be concluded that the amounts of recent (Quaternary) minerals formed is probably small.

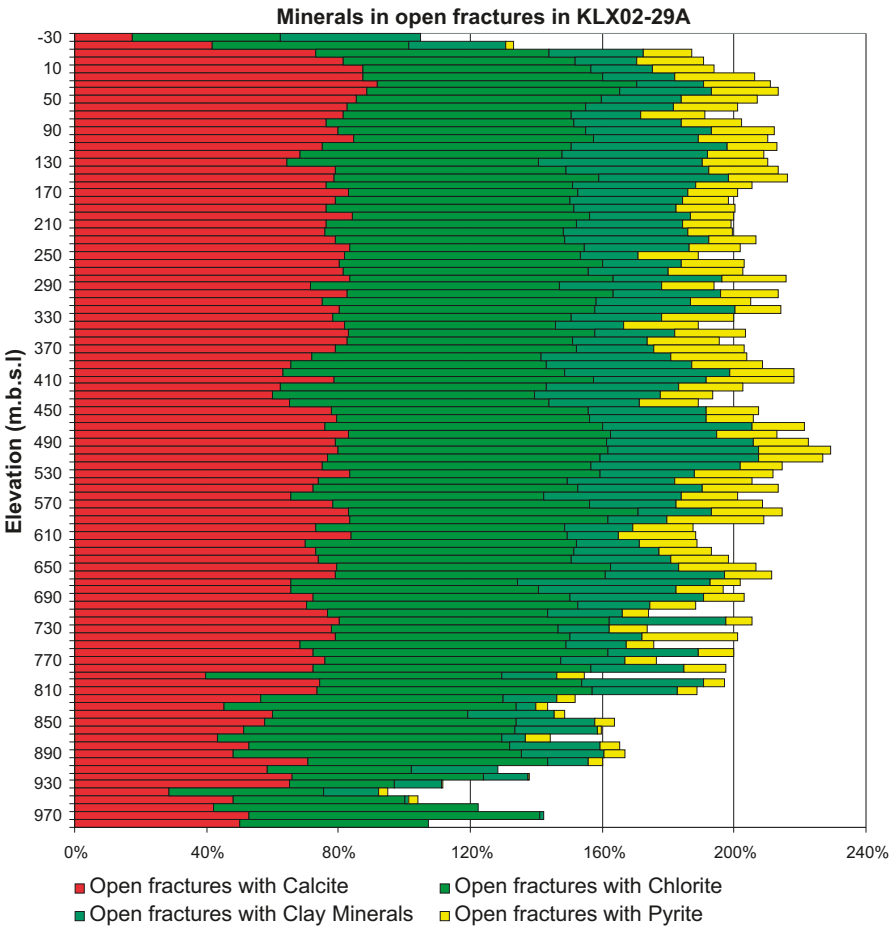

Figure 4-54. *Frequency of calcite, chlorite, clay minerals and pyrite in open fractures from the Laxemar subarea (borehole KLX02) shown as stacked % values. Please note that multiple minerals occur in the same fracture, hence the stacked % sum usually exceeds 100%.*

4.9 Porewater in the rock matrix

4.9.1 Background

The term 'porewater' as used here refers to the water in the connected pore space of the rock matrix that is accessible for diffusion-dominated interaction with groundwater circulating in nearby (micro-) fractures /Waber and Smellie 2008a/.

The mass of porewater contained in the low-permeability matrix of the crystalline rock at Laxemar is significant compared to the mass of groundwater circulating in the fractures. The interaction between porewater in the low permeable bedrock and groundwater in transmissive fractures depends on the degree of connectivity of the pore system, where solute transport can take place in the porewater, and on the differences in the chemical composition between the two systems. Porewater and fracture groundwater always tend to reach chemical and isotopic equilibrium given a long enough period of stable conditions. Thus, the porewater acts either as a sink or a source for solutes depending on the concentration gradient established between porewater and fracture groundwater and becomes therefore an archive of past fracture groundwater compositions and the palaeohydrogelogical history of a site. Elucidating this evolution is one of the major aims of the porewater investigations.

An established chemical and isotopic signature might be preserved in the porewater over long geologic time periods. The degree of preservation of such signatures depends on: a) the distance of the porewater sample to the nearest conducting fracture in three dimensions (i.e. the fracture network), b) the solute transport properties of the rock (i.e. diffusion coefficient, porosity), and c) the period of constant boundary conditions (i.e. constant fracture-groundwater composition). Constant boundary conditions over the time period considered greatly facilitate the interpretation of an observed porewater signature. In reality, however, overlap or superimposition of changes induced by variable boundary conditions seem more common, certainly in the first few metres of the rock matrix from the nearest water-conducting fracture, and over the Holocene and Pleistocene time period during which frequent climatic and hydrogeologic changes occurred (cf Section 2.5). In addition, the significance of the signature (taking account of the measurement error) depends on the chemical gradient between porewater and fracture groundwater /Waber and Smellie 2008a, Waber et al. 2009/. To conclude, no simple correlation between two independent variables (e.g. Cl^- and $\delta^{18}O$) can be expected and the porewater data have to be interpreted by taking all these influencing factors into account.

Porewater investigations at the Laxemar model site aimed at elaborating the hydrogeochemical evolution of the site based on the potential of porewater acting as an archive of what has happened over recent geological time (i.e. several hundreds to a few millions of years), and to define the potential of matrix diffusion to contribute to solute transport in the geosphere.

Porewater residing in the rock matrix cannot be sampled by conventional groundwater sampling techniques and therefore needs to be characterised by indirect methods based on drillcore material. Together with the above mentioned dependencies, it becomes obvious that porewater data obtained for a single sample from a borehole can only be interpreted to a limited degree. More information can be extracted if profiles are sampled along a borehole, and/or small scale profiles sampled from a water-conducting fracture into the host rock, and by comparing such data to present day fracture groundwater compositions in the closest water-conducting fracture(s). Within the SKB site investigation programmes at Oskarshamn and Forsmark, porewater investigations have been developed and tested for the first time in crystalline rocks /Waber and Smellie 2004, 2006abc, 2008b, and summaries in Waber and Smellie 2008a, Waber et al. 2008, 2009/.

4.9.2 Sampling strategy, methods and data uncertainty

The success of porewater investigations relies on obtaining the original freshly drilled saturated rock core material from boreholes and immediate on-site conditioning of such material within minutes after drillcore recovery (cf /Waber et al. 2009/ for details). In addition, rather large sized core samples are required due to the low porewater content and to minimise possible artefacts induced from the time of drilling to the time of analysis. Finally, there is also the great difficulty attached to predicting the location and orientation of a water-conducting fracture in a future borehole. Therefore, the porewater investigations initially aimed to characterise the composition of porewater that resides in as large as possible non-fractured and homogeneous rock portions. In these cases, core samples have been

collected at regular intervals along complete core lengths at least 5 metres from the nearest open fracture visible in the drillcore. Only at a later stage in the programme has sampling also focused on a fracture profile where samples were collected continuously along a profile extending (preferably perpendicular) to a water-conducting zone into the undisturbed host rock matrix.

Because of the inclinations of the dominating fracture zones in the Laxemar subarea (cf Section 2.2.2), in most cases intercepted by angled boreholes, the vertical distance between a porewater sample and an open (and possibly water-conducting) fracture might be less than the distance measured along borehole. In addition, a borehole provides only a one-dimensional section of a rock volume, such that in the other dimensions a water-conducting fracture might indeed occur closer to a selected porewater sample than observed form the core material alone. The existence of such a hidden fracture(s) can be assessed to some degree by quantitative modelling provided that high quality fracture groundwater data are available.

The chemical and isotopic compositions of the porewaters were derived using indirect methods such as out-diffusion and diffusive-exchange techniques, respectively, on originally saturated and intact drillcore material. All applied techniques have been continuously improved upon during the site investigation programme to minimise induced artefacts and the experimental and analytical errors /Waber and Smellie 2004, 2006abc, 2008a, Waber et al. 2008, 2009/.

Out-diffusion experiments were conducted on large-sized drillcore samples. The large size of approximately 200×50 mm (~ 1 kg) for the drillcore samples was chosen to minimise artefacts induced by the drilling process, by stress release, and by possible de-saturation during sample handling and transport. The effects of the drilling process and stress release were investigated by performing complementary experiments on cores from Äspö HRL (level 450 m) drilled using spiked drilling fluid and from 559–573 m borehole length in borehole KFM02B drilled at the Forsmark site. The rock sampled at the Äspö HRL is known to have undergone stress release prior to the drilling experiment due to the tunnel construction. In contrast, for borehole KFM02B, it was expected that the rock would be affected by both the drilling process and active stress release during drilling. The behaviour of the tracer concentrations in the core rim and core centre in both cases was compared and this revealed only minor contamination, i.e. the tracer penetration during drilling was limited to the millimetre range and appears mainly to depend on the average grain size of the rock samples /Waber et al. 2009/. For the Äspö HRL core material which was just affected by the drilling process, only about 0.7% of the total pore volume was mixed with drilling fluid. For the Forsmark KFM02B core, affected by both drilling and stress release, about 2.4% of the total pore volume was modified which converts to a maximum contamination of about 8% of the chloride concentration derived from the out-diffusion experiment. Such a small contamination lies within the experimental and analytical uncertainty of the experiment. The uncertainty attached to the derived porewater chloride concentration thus mainly depends on: a) the accuracy of the water-loss measurements which depends on the quality of core preservation and rapidity of measurement, and b) the heterogeneity of the rock sample. The uncertainty range of the obtained chloride concentrations in the porewater was thus estimated from the standard deviation of multiple water-loss measurements.

For chemically conservative components, the concentrations obtained in the experimental solutions of the out-diffusion experiments are thus converted to porewater concentrations using the geochemical porosity of an element. For the crystalline rocks of the Laxemar subarea the geochemical porosity of Cl^- is essentially equal to the water-loss (or connected) porosity. Porewater concentrations of chemical components are given in units of mg/kg_{H2O} rather than mg/L because of the mass-based basis of their derivation by indirect methods.

Concentrations for reactive components need to be corrected for water-rock interaction during the out-diffusion extraction experiment by applying geochemical modelling. For Laxemar, such corrections are of special interest for Mg^{2+} because of its potential as an indicator for a marine influence (e.g. Littorina and/or Baltic Sea water), and for SO_4^{2-} and Sr^{2+} because of their potential as indicators for SO_4^{2-}-rich porewater types (see below). Geochemical model calculations using mineral dissolution kinetics and mass balance considerations show that the contribution from mineral dissolution during the experiment is limited and for most elements, including Sr^{2+}, within a 10 percent maximum of the measured concentration in the experiment solutions /Waber et al. 2009/. However, the occurrence of Mg-bearing amphibole and pyroxene, in addition to biotite in the quartz monzodiorite, diorite and gabbro (e.g. /Waber and Smellie 2006b/), results in an increased contribution of Mg^{2+} to the

experiment solution of around 30% of the measured concentrations. This contrasts to the behaviour of the granitic rocks at Forsmark with minor biotite as the only Mg-bearing phase, and where this contribution was at a maximum of 10%. As a consequence, Mg^{2+} can only be used to some degree in experiment solutions from the Ävrö granite as a potential indicator of marine input to the rock matrix, but not for experiment solutions from quartz monzodiorite, diorite and gabbro. In the non-fractured rock matrix all rock sulphur occurs in sulphide minerals (mainly pyrite). The test water used in the out-diffusion experiments was in equilibrium with the atmosphere. Thus, pyrite oxidation induced by this initially present oxygen will result in a contribution of SO_4^{2-} to that originally present in the porewater. Model calculations show that for the SO_4^{2-}-rich chemical porewater type, this contribution (~ 10 mg/L) is less than about 3% of the SO_4^{2-} concentration measured in the experiment solution, and most of the SO_4^{2-} indeed seems to stem from the porewater /Waber et al. 2008/. This allows, as a first assumption, the recalculation of the SO_4^{2-} concentration in the porewater in a similar way to that for the conservative Cl^-. Whereas the uncertainty attached to such calculation might be somewhat larger compared to that of the porewater Cl^- concentration, it clearly allows the distinction between porewater with high SO_4^{2-} concentrations (i.e. > 10,000 mg/kg_{H2O}) and those with low or moderate SO_4^{2-} concentrations (i.e. < 1,500 mg/kg_{H2O}).

The water isotope composition, $\delta^{18}O$ and δ^2H, of porewater was derived using the isotope diffusive-exchange techniques on originally saturated and intact drillcore material /Waber and Smellie 2008a, Waber et al. 2009/. Continuous improvement of this technique allowed a reduction in the cumulated error as calculated by Gauss' law of error propagation for the first investigated borehole (KLX03) to the last (KLX17A), from about ± 2.2‰ VSMOW and ± 22‰ VSMOW to about ± 0.8‰ VSMOW and ± 7‰ VSMOW for $\delta^{18}O$ and δ^2H, respectively. In spite of the still substantial experimental error (especially on the hydrogen isotope composition), the obtained results allow certain statements about possible origins of the porewater when combined with other parameters.

Where available, the chemical and isotope composition of the porewater is compared to that of fracture groundwater sampled from nearby water-conducting fractures. Preferably such groundwater is sampled from fractures isolated by inflatable packers in the same borehole, or in neighbouring boreholes at similar depth. During the porewater/fracture groundwater interaction, the porewater composition is subjected to modification by the diffusive exchange (transient vs. steady state, species-specific diffusion coefficients) and water-rock interactions (larger reactive mineral surface area, longer residence time) in addition to the evolutionary processes identified for the fracture groundwaters. Furthermore, several of the fracture groundwater end members have similar water isotopic, but different chloride compositions and *vice-versa*. Therefore it is not surprising that a different relationship between these natural tracers is established in the porewaters compared to the fracture groundwaters where these components have been used in this report to trace the input of post glacial meltwater, Littorina/Baltic Sea and recent meteoric end member types into the bedrock groundwater system. The different distances of porewater samples to the nearest water-conducting fracture and the species-specific diffusion coefficients means that the superposition of two sequential events will result in different signatures. The behaviour of porewater signatures therefore differs from that of two mixing components mainly because it depends on the time of interaction with a specific fracture groundwater composition. In turn, the porewater might still have retained signatures of fracture groundwaters (e.g. glacial, warmer climate) that have been long since flushed from the fracture system by more recent fracture groundwaters.

4.9.3 Hydrogeological setting of porewater samples

Rock matrix porewater has been analysed from three boreholes (KLX03, KLX08 and KLX17A) in the Laxemar subarea drilled at different locations at an elevation above sea level of 15.8 m, 24.3 m and 27.6 m, respectively (Figure 3-1 and Figure 4-55). The boreholes were drilled at different inclinations up to 1,000 m borehole length into different rock types and different hydraulic and structural domains. The major rock types encountered by the boreholes are Ävrö granite and quartz monzodiorite with some minor intercalations of more mafic, dioritic rock types. Hydraulic logging has been performed on all three boreholes but unfortunately only a few reliable CCC (Complete Chemical Characterisation) groundwater analyses exist from water-conducting fracture zones. No drillcore samples exist from any of the upper 100 m percussion drilled part of the boreholes.

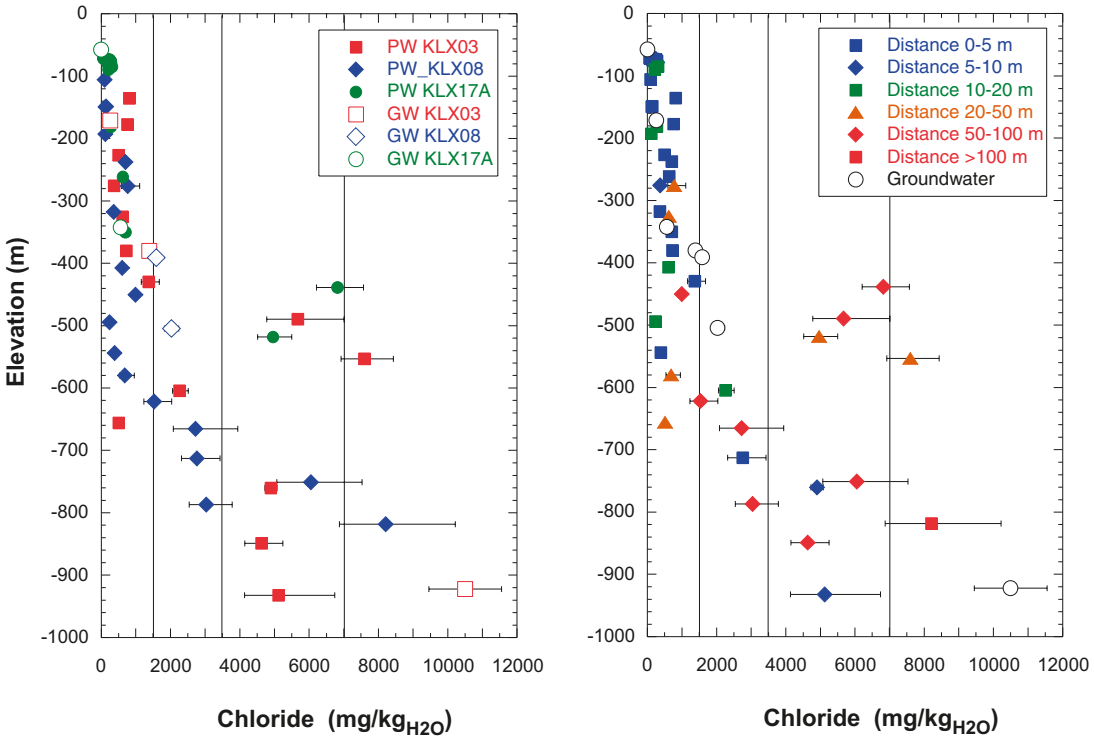

Figure 4-55. *Chloride concentration in porewater (PW, closed symbols) and related Category 1–3 groundwaters of boreholes KLX03, KLX08 and KLX17A of the Laxemar subarea on the left, compared with the distance of the porewater samples at one dimension from the nearest water-conducting fracture on the right.*

Borehole KLX03 was drilled at an inclination of 75° in hydraulic domain HRD-C which is comprised mostly of Ävrö granite (to about 620 m borehole length) and thereon of quartz monzodiorite. The major deformation zone ZSMEW946A was intersected between about 722–842 m borehole length. Borehole KLX08, situated north-east of KLX03 and comprising predominantly of Ävrö granite (until a transition to quartz monzodiorite at about 930 m borehole length), was drilled at an inclination of 60° initially in hydraulic domain HRD-N down to about 221 m depth, then through hydraulic domain HRD-EW007 from 211 to 702 m borehole length (with significant horizons of diorite/gabbro, up to 30 m in thickness, occurring in the Ävrö granite from below about 600 m), and finally hydraulic domain HRD-C to the end of the borehole at 991m borehole length, similar to KLX03. The westernmost borehole KLX17A was drilled at an inclination of about 61° down to 701 m borehole length through mainly Ävrö granite which continues to the bottom of the hole. It represents hydraulic domain HRD-W and intersects two major deformation zones at shallow levels, ZSMEW900A (100–130 m borehole length) and ZSMEW900B (220–250 m borehole length). A continuous profile of porewater samples was collected for some 20 m from a water-conducting fracture in the ZSMEW900A deformation zone down into the adjacent rock matrix, to investigate the most recent (i.e. Holocene to Pleistocene) interaction between porewater and fracture groundwater.

4.9.4 Porewater composition

In the Laxemar subarea, the chemical and isotopic composition of porewater extracted from drillcore material depends on the location of the three boreholes and the porewater samples with respect to the hydraulic domains and the occurrence of deformations zones. Nevertheless, there are some striking similarities between the chloride concentration, general chemical type and isotope composition of the porewater in samples from the three boreholes. The porewater data show a distinction between bedrock characterised by high transmissivity and a high frequency of water-conducting fractures at shallow to intermediate depths, and bedrock characterised by low transmissivity and a low frequency of water-conducting fractures at greater depths.

Chloride concentrations in matrix porewater cover a large range of less than 100 mg/kg_{H2O} to more than 8,000 mg/kg_{H2O} (Figure 4-55), which correspond largely to the span in salinity measured in the fracture groundwaters at depths from about 100–930 m (50–10,000 mg/L Cl. Low concentrations of less than 1,500 mg/kg_{H2O} occur at shallow levels down to about 430 m depth in borehole KLX03 and KLX17A and reach even to intermediate levels in borehole KLX08 (down to 620 m). These depth intervals are characterised with a high frequency of highly transmissive fractures. Most of the porewater at these levels is of a dilute Na-HCO_3 general type as deduced from out-diffusion experiment solutions corrected for mineral dissolution during the experiment.

A change in the porewater type to a general Na-Ca-SO_4 chemical type and associated with strongly elevated Cl^- concentrations occurs over a short interval of about 120 m in the Ävro granite starting below the dilute Na-HCO_3 type porewater. In all three boreholes this interval is characterised by a low frequency of transmissive fractures and in boreholes KLX03 and KLX08 it is located just above the transition from Ävro granite to quartz monzodiorite /Waber et al. 2009/. In boreholes KLX03 and KLX17A this type of porewater occurs between about 430–550 m depth and Cl^- contents range between about 5,000–7,600 mg/kg H_2O (Figure 4-54). In borehole KLX08 it occurs between about 620–750 m depth and Cl^- contents range between about 2,500–6,000 mg/kg H_2O. The Na-Ca-SO_4 type porewater differs from the other porewater types in the Ävro granite in having higher Ca^{2+}, Na^+, SO_4^{2-} and also Mg^{2+} and K^+ concentrations. Furthermore, differences are also observed in their Cl and Sr isotope compositions /Waber et al. 2009/ whereas $\delta^{18}O$ shows a significant variation at these locations. The Na-Ca-SO_4 type porewaters appear to have a common geochemical evolution that differs from that of the porewater above and below. Furthermore, they appear to have a restricted vertical distribution and so far have been only observed in the bedrock of the Laxemar subarea.

More dilute porewater, probably of Na-HCO_3 type (borehole KLX03) and Na-Ca-Cl-(HCO_3) type (borehole KLX08) occur again below the depth interval with Na-Ca-SO_4 type porewater (Figure 4-55). Here, Cl^- contents vary between about 500–3,000 mg/kgH_2O. In borehole KLX03 this change is associated with the occurrence of highly transmissive fractures, while such features seem absent in borehole KLX08 at similar depths.

Towards the bottom of boreholes KLX03 and KLX08 in the quartz monzodiorite at depths of 930 m and 820 m, respectively, Cl^- contents increase again to more than 5,000 mg/kgH_2O in KLX03 and more than 8,000 mg/kgH_2O in KLX08. In both boreholes, the high Cl concentrations at these depths are associated with porewater of the Na-Ca-Cl-(HCO_3) and Na-Ca-Cl chemical types, and coincide with a decrease in the frequency of water-conducting fractures. For borehole KLX17A no data are available from these depths.

4.9.5 Isotope composition of porewater

The ratio of the stable isotopes of waters infiltrating into the underground is, among others, dependent on the temperature during infiltration and the moisture source. This makes the stable isotopes valuable indicators of possible different origins of waters with similar Cl^- concentrations, such as, for example, glacial meltwater and present day infiltration. As for Cl^-, the isotope signature of fracture water will be transmitted to the porewater. It has to be kept in mind, however, that changes in the fracture water composition might strongly affect the water isotope composition, but not the chloride in the porewater (e.g. glacial versus meteoric) and *vice-versa* (e.g. Littorina Sea versus Baltic Sea water, brine versus warm climate meteoric).

Furthermore, repeating climatic cycles with similar or identical isotope composition in the fracture water will also leave their traces in the porewater and superimpose upon each other. Porewater isotope signatures obtained from individual samples collected in intervals as large as the 50 metres interval in the boreholes therefore might not be so indicative for a single event during the palaeohydrogeologcal evolution of the system, although this will depend on the distance to the nearest water-conducting fracture. The most obvious examples are locations where extreme signatures, such as glacial meltwater or warmer climate signatures, are preserved under certain circumstances. In contrast, a higher resolution and more information can be gained from porewater samples collected along a continuous profile (cf Section 4.9.8). In any case, the porewater isotope composition should not be interpreted without the chemical composition of the porewater.

The stable isotope composition of matrix porewater in the rocks at the Laxemar subarea covers a large range of $\delta^{18}O$ values between –14.3‰ and –1.8‰ VSMOW and $\delta^{2}H$ values between about –120‰ and –22‰ VSMOW. For comparison, the fracture groundwaters show $\delta^{18}O$ values in the range of –16 to –9‰ VSMOW and generally plot on or close to the Global Meteoric Water Line (GMWL) apart from the most saline types (cf Figure 4-56). The isotope compositions of most of the porewaters also plot parallel to the GMWL, suggesting that the majority of them are essentially meteoric in origin. However, several deviations from the GMWL are indicated suggesting porewaters with a different climatic origin. Moreover, the highest saline porewaters with the most enriched $\delta^{18}O$ values probably have been influenced by water-rock interaction.

In common with the Cl^- concentrations, the spatial distribution of $\delta^{18}O$ and $\delta^{2}H$ values of the porewater of borehole KLX03 resembles more that in borehole KLX17A compared to that in KLX08. Unlike the Cl^- concentrations in the porewater, however, the isotope concentration profile in borehole KLX08 is not simply shifted to greater depth, but is more complex in general. In the $\delta^{18}O$–$\delta^{2}H$ diagram, many of the porewater isotope compositions from borehole KLX08 plot further to the right of the GMWL compared to those of boreholes KLX03 and KLX17A, which may suggest one or more periods of warmer climate conditions (Figure 4-56).

In the more transmissive shallow to intermediate depths, the dilute Na-HCO_3 type porewater has an oxygen isotope composition ranging from $\delta^{18}O$ of around –8‰ VSMOW to cold climate signatures of around –14‰ VSMOW. Boreholes KLX03 and KLX17A show a maximum $\delta^{18}O$ depletion at depths between 250 and 500 m (Figure 4-57). In borehole KLX08 dilute Na-HCO_3 type porewater has a more enriched isotope signature down to a depth of about 300 m which could be interpreted as of a warm climate origin; this is followed by cold temperature signatures down to 500 m and again warm climate signatures from 550–600 m depth (cf /Waber et al. 2009/ for discussion).

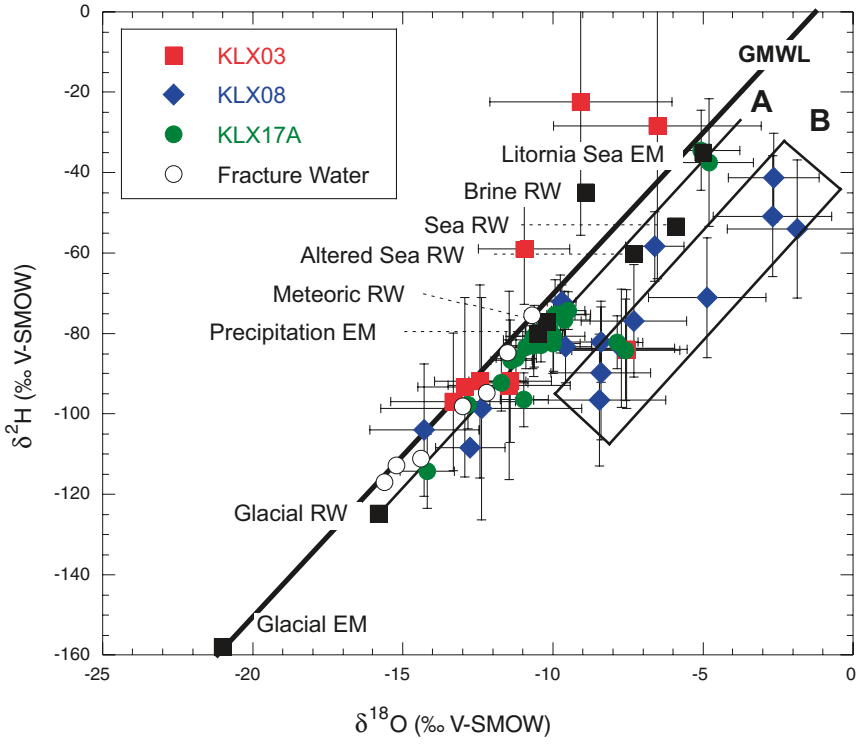

Figure 4-56. *$\delta^{18}O$ vs $\delta^{2}H$ diagram of porewater from the different boreholes in the Laxemar subarea. Note trend 'A' which covers most samples of porewater in KLX03 and KLX17A defined by the 'Littorina Sea water' to 'Glacial Reference Water' end-member compositions as used in the fracture groundwater modelling. Rectangle 'B' generally indicates the greater scatter/deviation of the KLX08 porewaters from the GMWL, possibly representing different climatic conditions compared to KLX03 and KLX17A. The isotope compositions of end member (EM) and reference fracture (RW) groundwaters are given for comparison. (GMWL = Global Meteoric Water Line).*

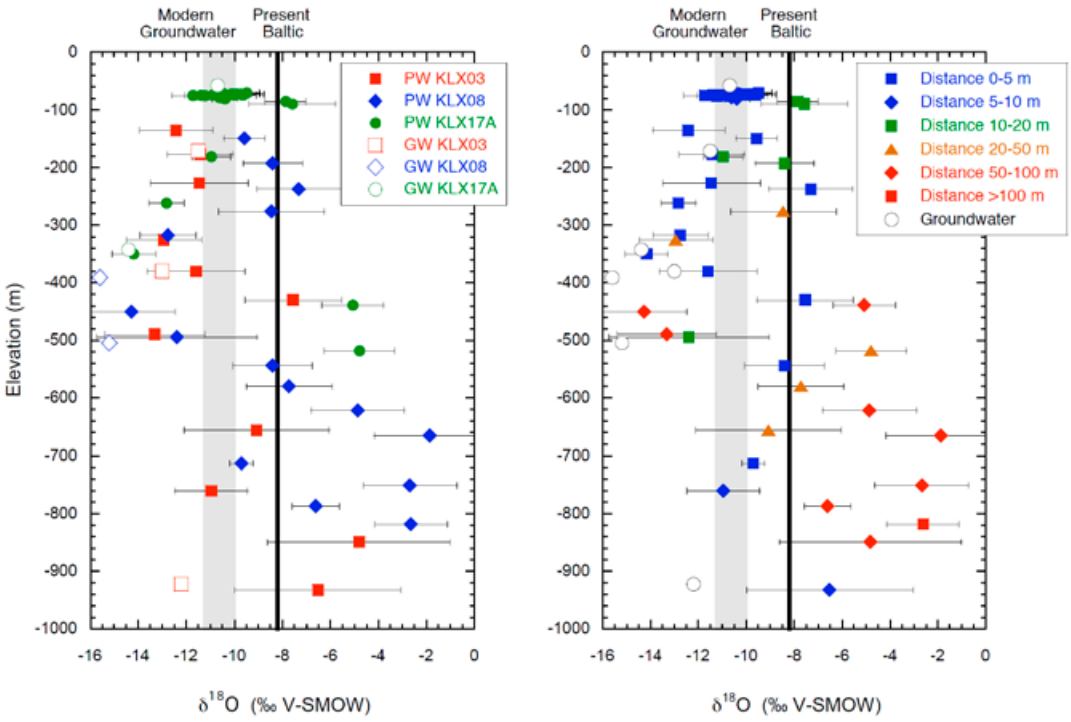

Figure 4-57. *Oxygen isotope composition, $\delta^{18}O$, of porewater (PW, closed symbols) and related groundwater (GW, open symbols, category 1–3 data) from boreholes KLX03, KLX08 and KLX17A of the Laxemar subarea on the left, compared with the distance of the porewater samples from the nearest water-conducting fracture on the right.*

The isotope compositions of the Na-Ca-SO_4 type porewaters restricted to intermediate depths cover a large range in common with the Cl^- concentrations. In boreholes KLX03 and KLX17A the $\delta^{18}O$ values vary between about –4‰ to –13‰ VSMOW, whereas more enriched values –2‰ to –10‰ VSMOW are observed for borehole KLX08 (Figure 4-57).

The Na-HCO_3 and Na-Ca-Cl-(HCO_3) type porewaters in the transition zone from Ävrö granite to quartz monzodiorite in boreholes KLX03 and KLX08, respectively, have $\delta^{18}O$ values between about –8‰ to –11‰ VSMOW (Figure 4-57). Further down these boreholes at depths of about 930 m and 820 m, respectively, the oxygen isotope composition becomes more enriched with $\delta^{18}O$ values between about –2‰ to –7‰ VSMOW.

4.9.6 Relationship between porewater and fracture groundwater

In boreholes KLX03 and KLX17A, generally equal chloride contents and oxygen isotope compositions are observed for porewater and fracture groundwater in the transmissive shallow to intermediate depths, down to at least (depending on location) about 380 m for porewater samples located within less than 5 metres from the nearest water-conducting fracture in the borehole. For such samples, a close to steady state situation is established for those components between the porewater and fracture groundwater of present day origin and, at intermediate depths, cold climate infiltration. No fracture groundwater data exist at this 0–360 m depth interval in borehole KLX08 to compare with the porewater data. This is unfortunate because many of the dilute Na-HCO_3 type porewater samples from this depth interval which are enriched in ^{18}O compared to the present meteoric recharge, are also distant to the nearest water-conducting fracture, and therefore may represent an older warm climate water. As discussed in /Waber et al. 2009/, even in the upper part of the bedrock, which is characterised by an interconnected fracture network of water-conducting fractures, large enough rock volumes may exist where very old porewater signatures can, at least in pockets or lenses, survive for a long period of time. However, why such signatures are not present in KLX03 and KLX17 is not known, unless the bedrock at these localities has different hydraulic properties.

Between about 380–430 m depth in boreholes KLX03 and KLX17A, where the most ^{18}O-depleted oxygen isotope compositions occur, a different resolution is highlighted for the two natural tracers with respect to their ability to identify compositional changes in the initial conditions (i.e. the matrix porewater) and boundary conditions (i.e. the fracture groundwater composition) as a function of time. Porewaters and fracture groundwaters have almost equally negative $\delta^{18}O$ values suggesting close to steady state conditions, whereas the chloride content of the porewater is only half that of the fracture groundwater indicating a transient state (Figure 4-55 and Figure 4-57). In borehole KLX08, a similar situation is established down to at least 500 m depth. Here, the difference in chloride content between dilute porewater and moderately mineralised fracture groundwater is even more pronounced, whereas the isotope signature is still similar within the uncertainty band. This can be explained by the porewater retaining a more pure cold temperature (or glacial) signature (but without having ever reached the pure end-member composition) compared to the fracture groundwater, which underwent more recent additional mixing with a more saline component.

Towards greater depths, fracture groundwater data are limited to one single analysis in borehole KLX03 at about 920 m depth. Porewater at this depth has a lower chloride content and is enriched in ^{18}O compared to the fracture groundwater (Figure 4-55 and Figure 4-57) and a transient state is established. Similar observations would also be expected for the 500–900 m depth interval, which includes the zone with Na-Ca-SO_4 type porewaters and from where fracture groundwater data are missing.

4.9.7 Solute transport in the rock matrix

The interpretation of porewater data in a broader hydrogelogical context requires knowledge of the solute transport properties of the various rock types. For the porewater samples such information was derived from measurements and modelling of the chloride concentration time series obtained from the out-diffusion experiments using large-sized (about 1 kg) originally saturated samples (/Waber et al. 2009/, cf Section 4.9.2).

For the rocks encountered in the Laxemar subarea, the water-loss porosity, i.e. the connected porosity were solute transport can occur in the rock matrix, depends on the rock type (Figure 4-58). The water-loss porosity is greatest in the Ävrö granite (0.69 ± 0.21 Vol%, n = 28), followed by the diorite (0.42 ± 0.16 wt%, n = 4) and the quartz monzodiorite (0.38 ± 0.20 Vol%, n = 9). In contrast to the water-loss porosity, the obtained pore diffusion coefficients for Cl^- are less dependent on the rock type although small differences related to the degree of foliation occur. The average pore diffusion coefficient for Cl^- is 5.8×10^{-11} $m^2/s \pm 2.7\times10^{-11}$ m^2/s for the Ävrö granite, 8.4×10^{-11} $m^2/s \pm 5.5\times10^{-12}$ m^2/s for the quartz monzodiorite, and 3.8×10^{-11} $m^2/s \pm 4.1\times10^{-11}$ m^2/s for the diorite /Waber et al. 2009/. Neither the water-loss porosity nor the Cl pore diffusion coefficient show a clear correlation with sample depth and only a slight tendency towards decreasing values with increasing depth is observed. This is also observed for the effective diffusion coefficient of Cl^- that is calculated from these data, which varies between 1.2×10^{-12} and 1.2×10^{-13} m^2/s at 25°C (cf Figure 4-58).

For the samples analysed for porewaters in the Laxemar subarea, differences in concentration between porewater samples and fracture groundwaters are especially observed if the distance to the nearest water-conducting fracture can be assumed to exceed 5–10 m. Keeping in mind the limitations of borehole investigations to roughly one dimension, and the relatively high fracture frequency at shallow depths, such a situation may have been established at shallow depths in borehole KLX08 and for two samples in borehole KLX17A, but more probably so below about 500 m depth in all three boreholes. The chemical and isotopic signatures preserved in such samples have been established a long time ago by palaeowaters which differ in composition from the fracture groundwaters sampled today, and are characterised by having very long residence times in the bedrock of several tens to hundreds of thousands of years (cf Section 4.10). Combined with diffusion being identified as the dominant transport process, it can be concluded that given enough time (e.g. compare the time dependence of diffusive exchange shown in Figure 6-42), matrix diffusion of solutes is efficient over at least decametres in the intact rock matrix /Waber et al. 2009/. The implications of these data for radionuclide retardation in the repository host rock should be examined in any future site-specific safety assessment.

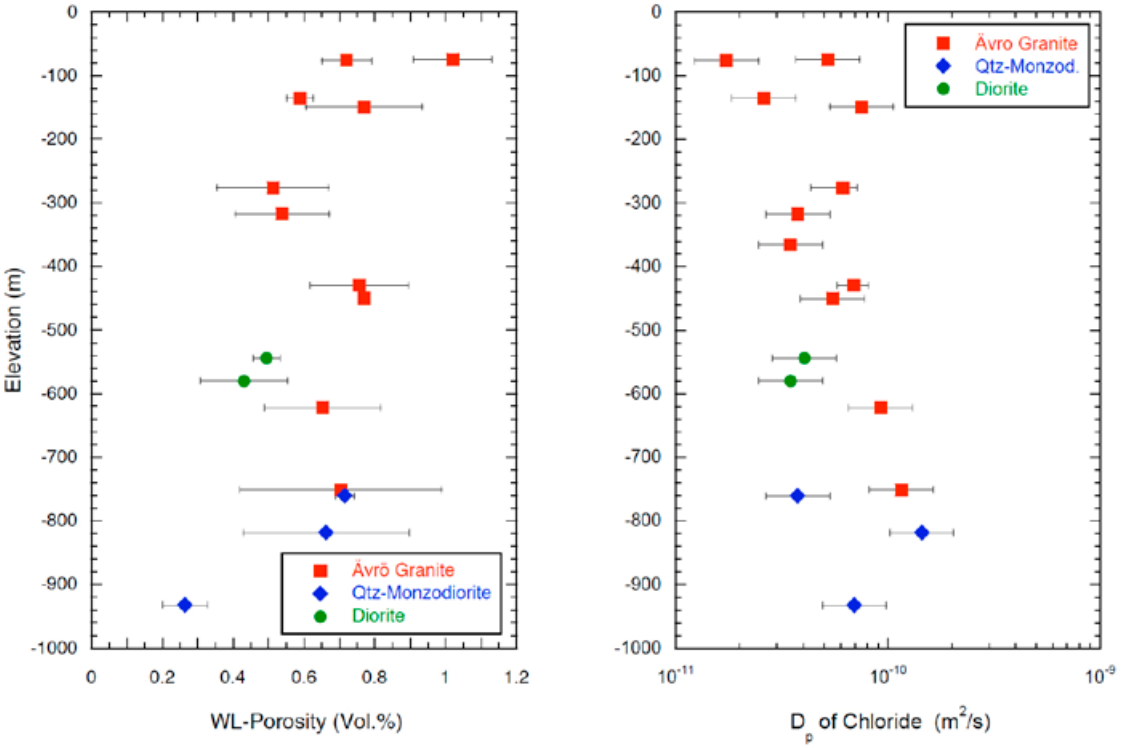

Figure 4-58. *Pore diffusion coefficients of chloride (right) and water-loss porosity of corresponding samples (left) as a function of rock type and elevation of porewater samples. The values were determined by out-diffusion of Cl^- from large-sized (approximately 1 kg), originally saturated samples and by subsequent water loss measurements on these samples /Waber et al. 2009/.*

With diffusion being identified as the dominant solute transport process in the rock matrix, the chemical and isotopic concentration of the porewater sample can be brought into an evolutionary context as a function of time (or space) using the fracture groundwaters to establish boundary conditions for the diffusion domain. Figure 4-59 illustrates schematically the concentration change induced in a porewater sample as a function of distance to the nearest water-conducting fracture and for time periods of 6,000 years and 12,000 years. In such a hypothetical system this could, for example, approximately correspond to the time of ingress of Littorina Sea water and the last deglaciation meltwater, respectively. A pore diffusion coefficient for chloride, Dp_{Cl}, at 25°C of 5.8×10^{-11} m^2/s corresponding to the average of the measured values for the Ävrö granite was used for the calculations. Note that at *in situ* temperatures of 10°C the Dp_{Cl} would be reduced by about a factor of 1.5 and the distances shown in Figure 4-59 and given below would be reduced by about a factor of 1.2 ($\sqrt{1.5}$). From Figure 4-59 it can be seen, for example, that a signature of a once established chloride content of Littorina Sea water (e.g. 6,500 mg/L) would be completely diluted in a porewater sample located 3.5 metres or less from a fracture above and below (i.e. distance between fractures = 7 m or less) or reduced by about 60% (i.e. to 3,900 mg/L) in a porewater sample located 5 metres from a fracture above and below, if fresh water would have circulated in both these fractures over the last 6,000 years (Figure 4-59, left). Similarly, a once established glacial isotope signature in a porewater sample (e.g. modern glacial with a $\delta^{18}O$ of –17‰ VSMOW) would be completely erased over a distance of 5 metres or less, changed to about 25% of the fracture water value (e.g. to about –15.5‰ VSMOW with a fracture water of –11‰ VSMOW) over a distance of 10 metres, or still be preserved at a distance of more than about 15 metres between the two fractures, assuming constant fracture water isotope composition over 12,000 years of interaction.

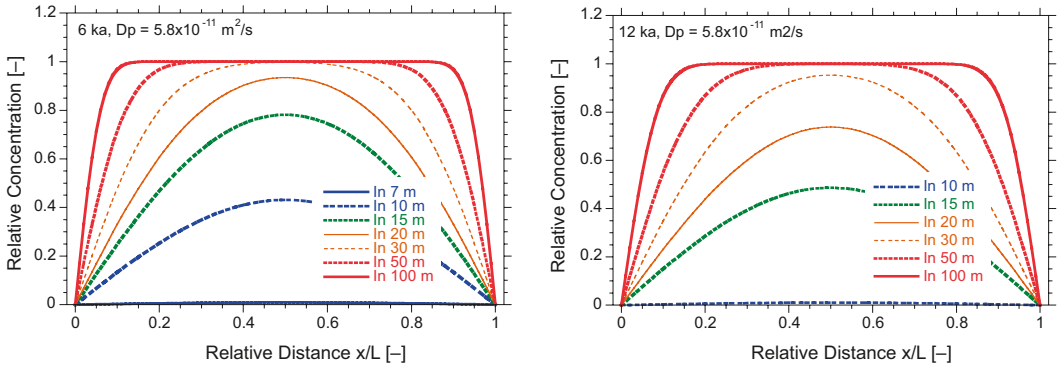

Figure 4-59. *Relative concentration changes induced on the porewater composition of a sample located at different relative distances between two water-conducting fractures for a time period of 6,000 years (left) and 12,000 years (right). The average pore diffusion coefficient for chloride, Dp_{Cl}, of 5.8×10^{-11} m^2/s measured for the Ävrö granite, was used in the calculations.*

4.9.8 Palaeohydrogeological evolution

The porewater of most of the samples is of meteoric origin as indicated by their oxygen and hydrogen isotope compositions that plot to the right of the Global Meteoric Water Line, GMWL (Figure 4-56). The majority of porewater samples from boreholes KLX03 and KLX17A, and a few samples from borehole KLX08 that in one dimension are far from the nearest water-conducting fracture in this borehole, plot along a line defined by the fracture groundwater 'Littorina Sea water' to 'Glacial Reference Water' end-member compositions as used in the fracture groundwater modelling (cf Section 4.2). A somewhat smaller range is covered by most of the porewater samples from borehole KLX08, and three samples located far from the nearest water-conducting fracture in KLX17A (2 samples) and KLX03 (1 sample), which all plot further to the right of the GMWL. Even allowing for the analytical uncertainties, and possible superimposition of different events during diffusion in the rock matrix, the variable isotope compositions preserved in the porewaters may represent: a) different periods of warm and cold (palaeo-) climatic signatures, or b) different diffusion pathways (i.e. different distances to the nearest water-conducting fracture) that may have influenced the isotopic signatures.

Modelling of this shallow bedrock system has been carried out on the fracture profile from borehole KLX17A /Waber et al. 2009/. The results have been interpreted as showing that the isotope signature enriched in ^{18}O and ^{2}H (together with the low chloride) and preserved in the samples most distant (> 15 m) from the water-conducting zone, have been established before the Weicheselian glaciation and should, therefore, represent a warm climate origin (Eemian Interglacial or older). This is in accordance with the fracture groundwater scenario outlined in Section 2.5.3. With respect to the other enriched samples which plot to the right of the GMWL (Figure 4-56) and include porewaters sampled closer to the water conducting fracture, it may be argued that these represent warm climate signatures introduced more recently in the Holocene, during post glacial time. This possibility is still under discussion.

The close to steady state situation established in boreholes KLX03 and KLX17A down to about 380 m depth between porewaters sampled close to a water-conducting fracture and the fracture groundwaters indicates that over short distances the exchange between porewater and fracture groundwater occurred relatively rapidly. The recorded low Cl^- concentrations, combined with isotope signatures similar to those of modern shallow groundwater and, with increasing depth, of a cold climate to glacial component, indicates that these porewaters have preserved signatures of the most recent climatic changes (i.e. Holocene). A similar explanation appears to account for the samples from borehole KLX08 at this depth interval. Signatures in the circulating fracture groundwaters of the most recent cold climate or glacial origin are preserved in the porewaters below these depths, down to about 350 m in KLX17A, 135 m in KLX03 and down to at least 500 m in KLX08 /Waber et al. 2009/.

Most prominent is the change in chemical and isotopic composition of the porewater in the Ävrö granite over a depth interval of about 120 m, starting at about 430 m in boreholes KLX03 and KLX17A and about 620 m depth in borehole KLX08. Geochemical model calculations show that mineralisation and isotopic composition of this Na-Ca-SO_4 porewater type cannot be explained by interaction with a known type of fracture groundwater and more advanced interaction with the Ävrö granite, but must originate from different processes. There are two possible sources to the measured Ca-Na-SO_4 waters at Laxemar discussed in Section 4.11 and /Waber et al 2009/: a) freeze-out mirabilite formation at shallow depths during permafrost (with subsequent breakdown and migration of Na-SO_4 waters to greater depths), and b) dissolution of old fracture gypsum (and migration of Ca-SO_4) during the last deglaciation whereupon glacial rebound may have reactivated sealed fracture systems of Palaeozoic age. This issue is still unresolved because of inadequate data.

4.9.9 Summary

- Porewater acts as a potential archive of the past hydrogeological history at the Laxemar subarea and its composition puts constraints on the interpretation of the palaeohydrogeological evolution of the site.
- Solute transport in the intact rock matrix appears to be dominated by diffusion, and matrix diffusion was identified to occur at least over several decametres into the rock matrix.
- Porewaters are generally of a dilute Na-HCO_3 type with Cl concentrations below 1,500 mg/kg_{H2O} down to about 420 m depth in KLX03 and KLX17A and down to about 620 m depth in KLX08. The associated isotope signatures suggest a meteoric influence from climatic conditions similar to those prevailing today in all boreholes and also from the Holocene temperature maximum in borehole KLX08.
- Cold climate influence from the last glaciation occurs in some porewater samples collected close to fractures between about 135–350 m depth in boreholes KLX03 and KLX17A, and down to about 500 m depth in borehole KLX08.
- A steady-state situation between pore water and fracture groundwater for both Cl concentration and isotope signatures is only established in some locations at shallow levels (to about 350 m depth) whereas transient states prevail for at least one of the natural tracers at intermediate levels.
- A distinct change in chemical and isotopic composition of the porewater to a highly mineralised Na-Ca-SO_4 type is observed between about 430–550 m in boreholes KLX03 and KLX17A and between about 620–750 m in borehole KLX08. Compatible fracture groundwater compositions have not been observed and the porewater signatures appear to have evolved a long time ago (before the Last Glacial Maximum) from fracture groundwater possibly influenced by freeze-out processes.
- In general terms, the porewater data indicate a change with increasing depth from waters of temperate meteoric origin, to glacial waters and finally to saline waters (i.e. a progressive change from dilute Na-HCO_3 to a saline Na-Ca-Cl type porewater) with a highly mineralised Na-Ca-SO_4 type porewater observed within a narrow depth interval at intermediate depths.
- Preliminary modelling of a porewater profile extending from a conducting fracture into the intact rock matrix indicate that changes in fracture groundwater composition during Holocene time left their (superimposed) signatures a few metres into the rock matrix. Further into the rock matrix, older (i.e. prior to the last glaciation), warm climate signatures are still preserved, lending additional support to the hydrogeochemical conceptual model.

(Note: The data presented and discussed in this section are based on primary borehole length measurements taken in the field and the elevation data calculated in Sicada. Adjusted elevation data based on single-hole interpretation measurements would only minimally modify the results, and therefore in this context are regarded to be unimportant for plotting purposes).

4.10 Groundwater residence time

4.10.1 Background

A key factor in understanding past and present groundwater evolution in the Laxemar-Simpevarp area is to constrain the average residence time for each of the major groundwater types. This can be approached qualitatively in terms of the major and trace element compositions of the groundwaters, i.e. in a broad sense based on aspects of water-rock reaction kinetics. Considering different groundwaters that have evolved in a similar geological environment such as the crystalline rocks in Laxemar, a greater groundwater mineralisation can be indicative of a greater residence time (i.e. higher contents of dissolved species as a result of water-rock interaction). Stable isotopes, such as δ^2H, $\delta^{18}O$, $^{11}B/^{10}B$, ^{37}Cl, $\delta^{13}C$, $\delta^{34}S$ and $^{86}Sr/^{87}Sr$, may give more detailed qualitative information on residence times, such as indications of climate change during recharge, increased water-rock interaction, etc. On a more quantitative level, because of their known half-life decay character, the radioactive isotopes of ^3H ($t½ = 12.343$ y), ^{14}C ($t½ = 5{,}730 \pm 40$ y), ^{36}Cl ($t½ = 301{,}000$ y) and non-radioactive ^4He have been used in the hydrochemical evaluation.

4.10.2 Qualitative information on residence time

The major rock-forming minerals in the Laxemar-Simpevarp area that are susceptible to groundwater reaction and alteration are K-feldspar, plagioclase, amphibole, quartz and micas (biotite/muscovite). These minerals give rise respectively to the redistribution and potential concentration in the rock matrix porewaters and fracture groundwaters of, for example, commonly Na, K, Ca, Rb, Ba and Sr. With slower flow to stagnant groundwater conditions with depth, accompanied by greater water-rock interaction, these constituents should also increase in concentration accordingly (except for the redox sensitive Fe which is, for example, dependent on microbial activity). There are clear indications from chloride, calcium and sodium of an increase in mineralisation with depth supporting the concept that very old groundwaters are present at the maximum depths sampled /Gimeno et al. 2009; cf Sections 4.1, 4.2 and 4.13/. The amounts of trace elements such as Sr, Rb, Cs and Li in groundwaters are rock dependent but they all show a tendency to increase in concentration with depth when away from the influence of the brackish marine Littorina type groundwaters. Since the influence of Littorina type groundwater is of minor importance in the Laxemar subarea compared to Forsmark, these trace element depth trends should be more indicative of water-rock interaction.

Additional qualitative indications of increased water-rock interaction with depth are provided by the behaviour of the stable isotopes $\delta^{18}O$ and δ^2H. The deep highly saline waters from Laxemar also show a significant deviation from the GMWL coeval with increased salinity and enrichment in deuterium (^2H) /Gimeno et al. 2009; cf Section 4.1/. Deep basement groundwaters in Canada (in particular) and Fennoscandia (to a much weaker extent) show a similar isotopic deviation. Based on such observations, rock matrix porewaters would be expected also to have similar δ^2H enrichments, which is the case for some of the porewater samples from KLX03 /Waber et al. 2009; cf Section 4.9/.

4.10.3 Quantitative information on residence time

Quantitative information on groundwater residence time can be derived from short lived and long lived radioisotopes. Within the Laxemar-Simpevarp hydrochemical programme the radioisotopes ^3H and ^{14}C are analysed routinely. In addition, ^{36}Cl analysis has been carried out on strategically-related groundwaters at a late stage in the programme. Helium (^4He) gas samples are routinely analysed at selected locations, and this input has been used as support, when possible, to the other dating methods, in particular the ^{36}Cl method cf /Smellie et al. 2008/.

Short residence times

Understanding present day flow conditions is crucial in determining, for example, the recharge input chemistry to the bedrock, the starting point for much of the bedrock hydrochemical modelling. Meteoric recharge waters of a young age (i.e. less than 55 years), are traced by their contents of atmospheric thermonuclear tritium from the 1950's still present in the recharge precipitation and shallow groundwaters. Figure 4-60 shows tritium versus elevation and includes category 1 to 5 data from percussion and cored boreholes from the Laxemar-Simpevarp area. The category 5 samples (Figure 4-60) show a wide scatter of tritium (^3H) activity contents with no obvious depth trend which

is attributed mainly to a large percentage of drilling fluid and the influence of open hole conditions prior to, and during tube sampling. The category 1 to 4 groundwater samples, in contrast, show a characteristic decrease in tritium to a depth of about 100 to 150 m, which represents the penetration limit of modern fresh meteoric groundwater. The persistent tritium contents (1–4 TU) with increasing depth are due to various sources of contamination, which are mentioned in Section 3.3.5 and also in /Smellie and Tullborg 2009/. Despite the problems with contamination from short circuiting and sampling activities, and the possible introduction of tritium from contaminated drilling fluid, it is notable that there exist a large number of groundwater samples at all depths with little or no tritium (< 0.8 TU; Figure 4-60). This underlines the heterogeneity of the flow system present in the Laxemar subarea.

Radiocarbon (^{14}C), with a half-life of 5,730 $\pm$ 40 years, extends the range of detection up to 35,000 years for groundwater residence time. Theoretically, this range should cover comfortably the period since the last deglaciation, in particular confirmation of the Littorina Sea transgression. However, radiocarbon dating is complex and a major problem has been to constrain the ^{14}C input signature to the bedrock.

Figure 4-61a and c shows $^{14}C_{(TIC)}$ versus elevation and $\delta^{13}C$, and Figure 4-61b and d, shows bicarbonate versus elevation and $^{14}C_{(TIC)}$ for the Laxemar-Simpevarp near surface water and groundwater samples. The groundwaters show $^{14}C_{(TIC)}$ values in the range of 19–80 pmC, HCO_3^- at 20 to 320 mg/L and $\delta^{13}C$ at –13 to –27‰ PDB (with the majority of samples in the range –15 to –20‰ PDB). The near surface waters in contrast show generally higher $^{14}C_{(TIC)}$ (45 up to 105 pmC) and larger span in HCO_3^- (from 40 to 550 mg/L) and $\delta^{13}C$ (–6 to –22‰ PDB). The general evolution of the $^{14}C_{(TIC)}$ can be described accordingly: The near surface recharge waters with high ^{14}C (around 100 pmC), low HCO_3^- (< 60 mg/L) and atmospheric $\delta^{13}C$ (> –8‰ PDB), will increase their HCO_3^- due to microbial degradation of organic material of variable age which, in turn, leads to dissolution of calcite with low or no ^{14}C.

This sequence of reactions is described in detail by /Gimeno et al. 2009/ and supported by geochemical modelling. The reactions indicate that shallow groundwaters with short residence times (modern tritium contents) show high HCO_3^- contents (200 to 350 mg/L), organically influenced $\delta^{13}C$ values (< –10‰ PDB) and, most importantly, a diluted ^{14}C signal (50 to 80 pmC, cf Figure 4-61e).

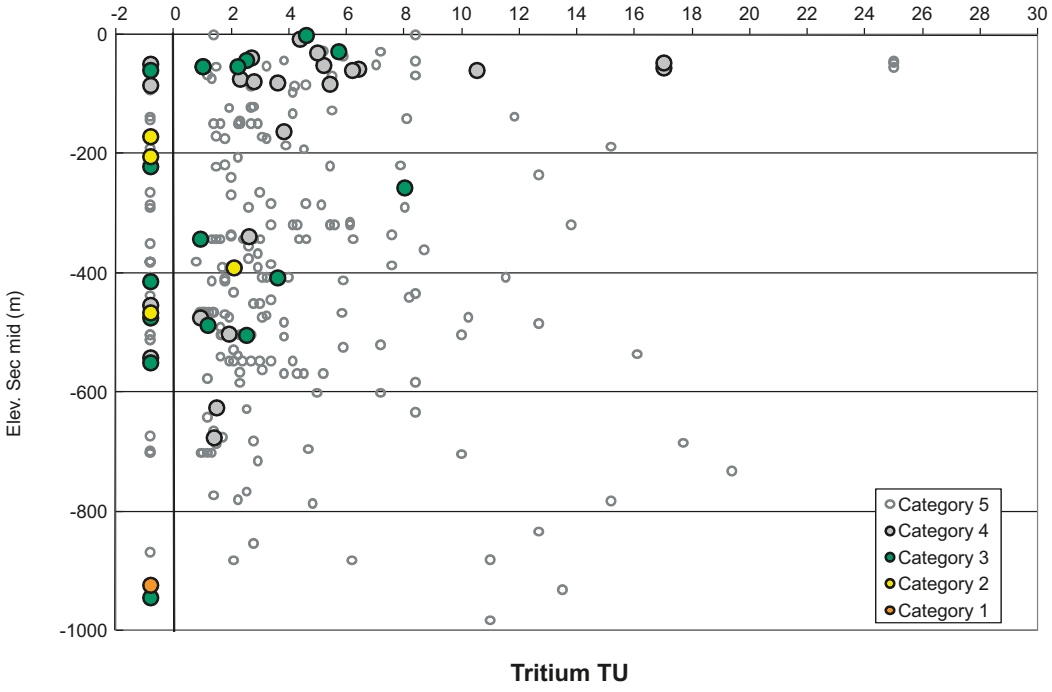

Figure 4-60. *Tritium versus elevation based on category 1 to 5 data from percussion and cored boreholes from the Laxemar-Simpevarp area. Data below zero reflect values under detection limit (0.8 TU).*

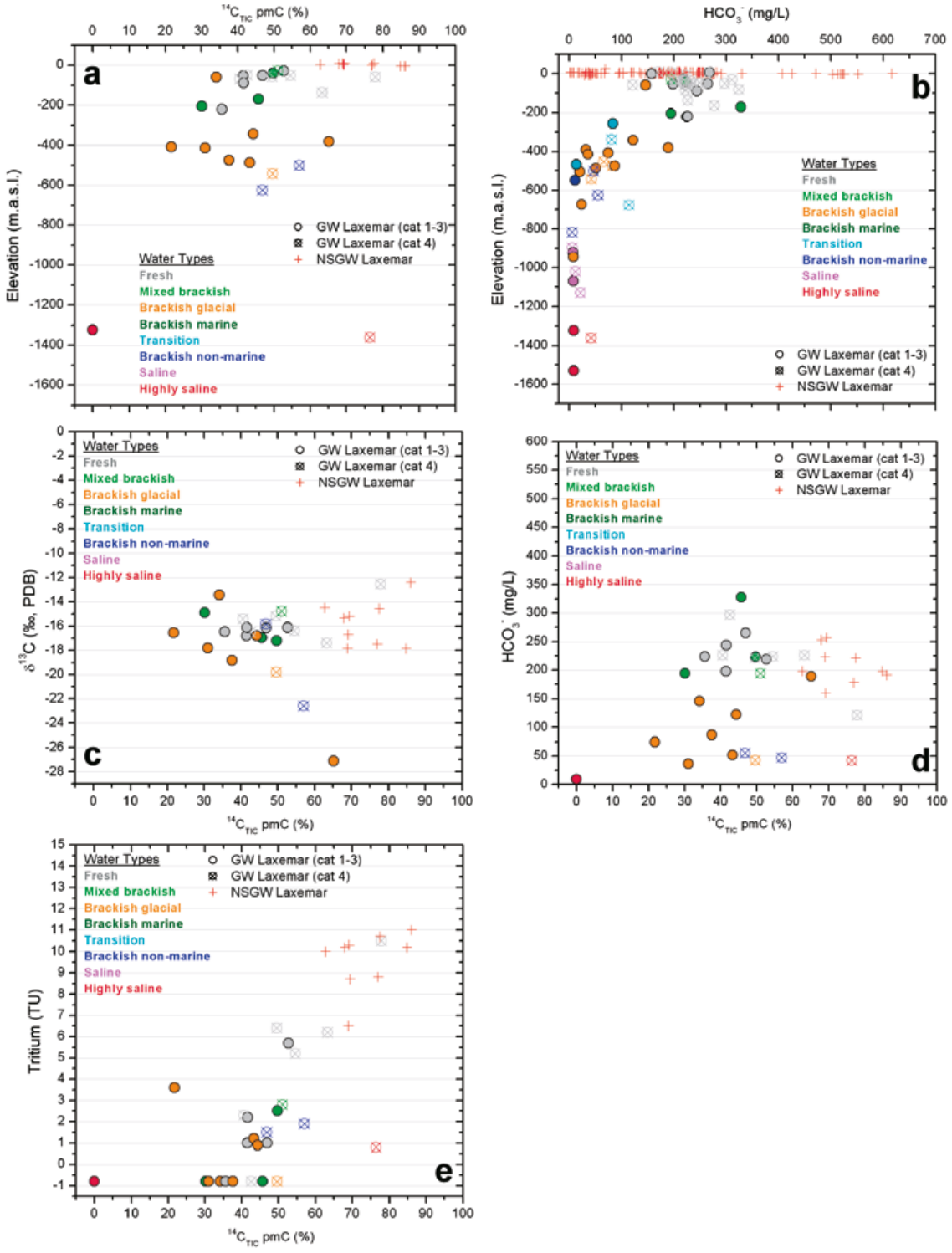

Figure 4-61. *Groundwater samples from the Laxemar subarea showing the distribution of $^{14}C_{(TIC)}$ pmC and bicarbonate versus depth (a and b), and $^{14}C_{(TIC)}$ versus $\delta^{13}C$ (c), bicarbonate (d) and tritium (e).*

Normally, groundwaters with HCO_3^- contents below 10 to 20 mg/L can not be successfully analysed for ^{14}C due to contamination with atmospheric carbon dioxide and/or drilling fluid. Because bicarbonate decreases with depth (cf Figure 4-61b), ^{14}C analyses from depths greater than 600 m are rare and those present are of dubious quality (i.e. not category 1–3 samples). This means that no ^{14}C analyses are available from the saline or highly saline groundwaters and only a few from groundwaters of brackish non-marine origin. The analysed groundwaters when plotted show mostly a large scatter (e.g. in bicarbonate versus $^{14}C_{(TIC)}$) but still there is an indication of decreasing bicarbonate with decreasing ^{14}C.

Mixing, and also the relatively high bicarbonate content in the drilling fluids, together with the many water samples with drilling fluid contents in the range 5 to 10%, complicate interpretating the original $^{14}C_{(TIC)}$ in undisturbed groundwaters (cf Figure 4-62 a and b). Nevertheless, the analyses of the brackish glacial waters indicate that the glacial component is very low in bicarbonate and $^{14}C_{(TIC)}$, implying that the carbon inventory is largely post glacial in age. However, there are reasons to believe that the depleted $\delta^{18}O$ in the groundwaters in the upper 600 m are mainly from the last deglaciation. Very low or non-detectable $^{14}C_{(TIC)}$ is fully compatible with this conclusion assuming that glacial water may have had a long residence time in the ice before entering the bedrock or, alternatively, is extremely low in bicarbonate content.

During an earlier model version attempts were made to correct the ^{14}C contents for reactions (calcite dissolution and organic breakdown), mainly based on $\delta^{13}C$. This was unsuccessful mainly due to the range of $\delta^{13}C$ values of the carbonates and the organic material. Therefore, straight forward calculation from a source term and processes identified failed to determine the ^{14}C age; the uncertainty is simply too large (G. Buckau, per. comm. 2007).

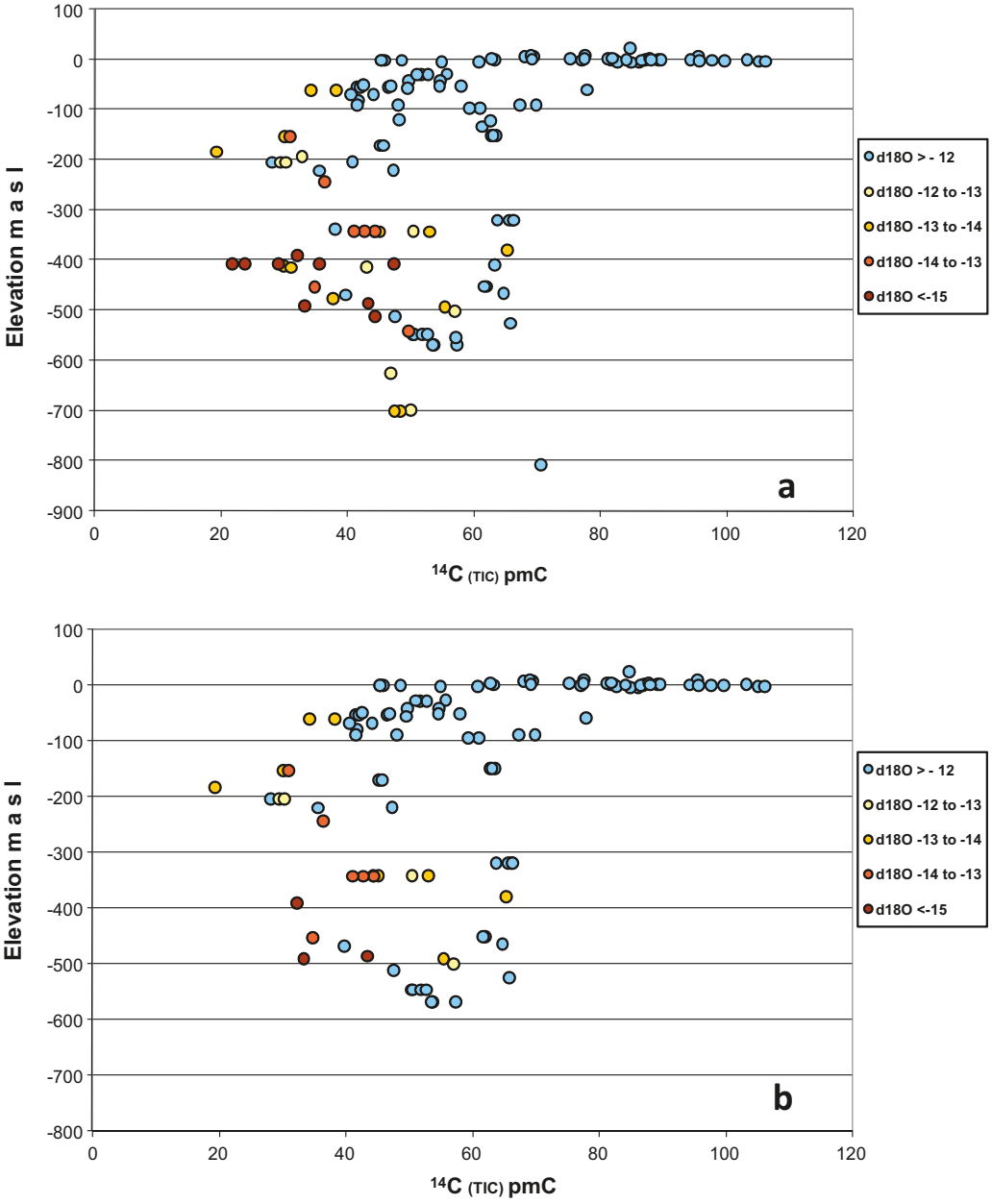

Figure 4-62. *$^{14}C_{(TIC)}$ versus elevation for all samples from the Laxemar- Simpevarp area except tube samples (a), and for all samples analysed with drilling water less than 5% (b).*

A small number of carbon-14 analyses of organic material from the groundwater have been carried out. The $^{14}C_{(org)}$ is generally greater (up to double) than the corresponding $^{14}C_{(TIC)}$, which is exemplified in KLX03:–170 m, KLX08:–390 m and KLX17:–342 m elevation. In these samples the $\delta^{13}C_{(TIC)}$ is also much higher than the $\delta^{13}C_{(org)}$, i.e. –17.8 to –15.7‰ PDB compared with –27.8 to –26.3‰ PDB, supporting the above theory that dissolution of ^{14}C-free carbonates has occurred. The $^{14}C_{(org)}$ in these samples varies between 64.6 to 71.0 pmC indicating that residence times of the organic material are in the order of 3,000 to 4,000 y. Apart for these three analyses, further interpretation was not possible because of suspected contamination, for example, very high $^{14}C_{(org)}$ in very old saline waters, and a single very low $^{14}C_{(org)}$ content in a groundwater sample with a marine (Littorina) component.

Long residence times

Helium-4 is continuously produced in rocks as alpha particles emitted in the decay of the naturally occurring radioactive elements, uranium and thorium, and their radioactive daughters. Helium-4 is the most abundant of the He isotopes ($^3He/^4He = 1.38\times10^{-6}$, /Andrews et al. 1989/). Because ^3He is rapidly diluted by ^4He produced in the geosphere and therefore has no characteristic value in the upper crust, ^4He is usually abbreviated to helium. For example, measurements at Äspö by /Mahara et al. 2008/ yielded $^3He/^4He$ ratios in the order of $1.4–4.3\times10^{-8}$. By comparing the measured ^4He concentrations in groundwater with the calculated *in situ* ^4He production rate (based on uranium and thorium concentrations in the host rock), information about groundwater residence time under closed system conditions, and/or indications of possible external input of helium into the system, can theoretically be obtained.

Gas analyses from the Laxemar-Simpevarp samples (cf Section 4.6) show generally decreasing carbon dioxide and increasing helium with depth indicating longer residence times with increasing depth. However, calculations of groundwater residence time based on helium production have yielded unrealistically old ages (hundreds of thousands to several millions of years), even for groundwaters with significant Littorina components and post glacial/glacial inputs /Gascoyne and Gurban 2009, Molinero et al. 2009/ Uncertainties in these calculations include:

- Possible helium transport from below (e.g. mantle origin). Lack of ^3He determinations (only total helium measured and assumed to correspond to ^4He).
- Possible contributions at all depths from uranium and thorium precipitated on fracture coatings and the altered host wall rock.
- Variation in porosity and diffusivity properties, for example, due to alteration of the fracture wall rock which may facilitate gas circulation.

The same uncertainties were recognised for Forsmark /Gimeno et al. 2009/ and considered common in fractured rock systems /Gascoyne and Gurban 2009/.

Chlorine-36 (with a half-life of 301,000 years) in groundwaters has three sources: a) cosmic radiation in the upper atmosphere and rain-out, b) spallation of Cl, K, Ca, and Ar in soil moisture and minerals, and c) subsurface production by neutron capture by ^{35}Cl (which makes up about 75% of total Cl). The thermal neutrons for this reaction are produced during spontaneous fission of ^{238}U and by interactions between α particles (from decay of U and Th) and light elements such as Al, Na, O, Mg and Si in the surrounding rocks /Florkowski et al. 1988/.

With time the ^{36}Cl will accumulate and decay until the rate of production equals the rate of decay (i.e. secular equilibrium) after a period of 1.5 million years. Groundwaters with ^{36}Cl values at secular equilibrium with *in situ* ^{36}Cl will therefore have been shielded from the atmosphere and resided in this rock for at least 1.5 million years.

Chlorine-36 has been measured in selected groundwaters from the Laxemar-Simpevarp area, ranging from the present Baltic Sea to near surface recharge waters, to deeper brackish marine (Littorina) and brackish non-marine groundwaters, and finally to saline groundwaters sampled from maximum depths /Gascoyne and Gurban 2009/. The variations of $^{36}Cl/Cl$ with Cl for the Laxemar-Simpevarp samples are shown in Figure 4-63, together with data from Forsmark /Gimeno et al. 2009/, older data from Äspö and Laxemar /Louvat et al. 1999/ and data from Olkiluoto /Pitkänen et al. 1996/. The brackish non-marine and deep saline samples have intermediate ratio values that are slightly higher

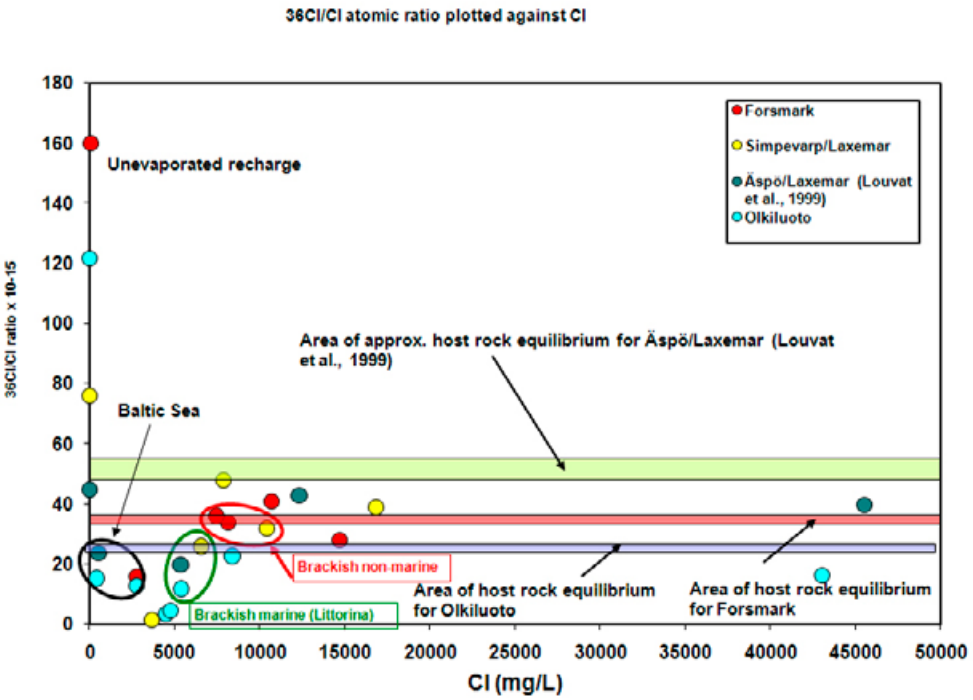

Figure 4-63. *^{36}Cl/Cl ratio versus Cl (from /Smellie et al. 2008/). In red are the Forsmark samples, in yellow are the Laxemar-Simpevarp data, in green the Äspö-Laxemar data from /Louvat et al. 1999/ and in light torquise the Olkiluoto data from /Gascoyne 2001/ .*

than other sites. Despite the relatively few analyses from each site a common pattern is indicated: a) high but variable values in the recharge waters with low chloride contents, b) Baltic Sea samples with relatively low ^{36}Cl/Cl ratios, c) Littorina influenced samples showing the lowest ^{36}Cl/Cl ratios, and d) highest values at greater depth in the brackish non-marine and saline groundwaters. In these last-mentioned groundwaters the ^{36}Cl/Cl starts to approach equilibrium with the bedrock. Similar results were also obtained in a study carried out by /Mahara et al. 2008/ on samples from the Äspö tunnel where groundwaters with Cl contents > 10,000 mg/L showed ^{36}Cl/Cl ratios close to equilibria with the bedrock.

As described above, the subsurface production is dependent on the contents of uranium and thorium and the equilibrium values are therefore different (indicated in the plot). Nevertheless, there is no doubt that the intermediate brackish non-marine and deeper saline groundwaters indicate long residence times which reflect early Quaternary times, and even pre-date the Quaternary period. That the brackish marine (Littorina) groundwater has a lower ratio than the Baltic Sea water indicates that its dissolved chloride has undergone additional shielding from atmospheric input, and/or undergone mixing with low ^{36}Cl groundwater from the bedrock. This is consistent with an overall older 'age' of this water type, but not old enough to receive a significant quantity of subsurface produced ^{36}Cl. In agreement with /Gascoyne 2001/ 'this provides strong support for the argument that these (brackish marine) waters are derived from the Littorina Sea'.

4.10.4 Conclusions

In summary, there is a range of qualitative (trace and major ion and stable isotope) and quantitative (isotopic) evidence based on depth relationships, that are generally supported by hydrogeological observations. This evidence shows:

- Recent to young fresh groundwaters, some showing signs of mixing, characterise the upper approximately 100 to 150 m of the bedrock. At these depths, because the hydraulic system is more dynamic, climatic changes have resulted in the cyclic introduction and flushing out of different groundwater types in post glacial time, such that residence times for individual groundwa-

ter types seem relatively short but very variable, i.e. possibly some decades up to a few thousand years depending on location. The heterogeneity of the system is demonstrated by the scattered occurrence of tritium free waters sampled in the upper 100 m and also measurements of cold climate signatures retained in a few sampling points.

- Groundwaters referred to as brackish glacial in type are generally mixtures of glacial waters and temperate climate meteoric water of post glacial origin based on their $^{14}C_{(TIC)}$ content. The saline component in these waters may be due to Littorina waters or older saline waters depending on location. The glacial component, assumed to be related to the phase of ice sheet coverage during the last glaciation, is generally low in bicarbonate and very low in $^{14}C_{(TIC)}$.
- The $^{14}C_{(TIC)}$ analyses support that the groundwater carbon inventory is mainly post glacial. Input of organic and inorganic carbon compounds of post glacial origin is detectable to a depth of approximately 500 m. Down to this depth there is a corresponding decrease in bicarbonate which becomes even less at still greater depths.
- Significantly older groundwaters, found at depths greater than around 600 to 1,000 m, are characterised initially by brackish non-marine groundwaters which become successively more mineralised with increasing depth (to saline in type) by water-rock interaction, mixing with (unknown) deep saline water, and diffusive exchange with the rock matrix porewater. Hydraulic conditions at these depths and preliminary ^{36}Cl data indicate very low groundwater flow or near stagnant conditions and suggest residence times that appear to be at least several hundreds of thousands of years.
- The presence of even more highly saline groundwaters (> 20,000 mg/L Cl) in the Laxemar subarea from depths greater than 1,400 m suggest still older groundwaters residing under effectively stagnant groundwater conditions.

4.11 Permafrost and freeze-out processes

4.11.1 Background

Under cold desert conditions permafrost formation is expected to precede the build-up and movement of a continental ice mass during the nearest glacial period in Fennoscandia /SKB 2006c/. This will cause the bedrock groundwaters to be frozen gradually, probably accompanied by a layer of concentrated salinity ahead of the advancing freezing front. Possible permafrost depths may vary significantly depending on a number of local conditions such as the climate at ground surface, geothermal heat flow, thermal properties of bedrock, chemical properties of groundwater, groundwater flow, vegetation, soil type and thickness and other surface conditions, for example, the presence of sea/lakes etc. When conditions for permafrost growth are favourable, and such conditions prevail for a long time, permafrost may accumulate to many hundreds of metres thick. Present day observations in northern Canada and elsewhere /Gascoyne 2000, Ahonen 2001, Ruskeeniemi et al. 2004/ indicate depths of about –400 to –500 m elevation. Given environmental conditions very favourable for permafrost growth, modelling of permafrost for Laxemar suggests a maximum permafrost depth of 270 m in a glacial cycle time perspective /SKB 2006d/. A recent climate modelling study has showed that the climate at Laxemar during Weichselian periods of ice free conditions may well support permafrost growth /Kjellström et al. 2009/.

When the permafrost is over-ridden by an ice sheet, it will subsequently decay and eventually disappear /SKB 2006d/, and some degree of water circulation in the upper parts of the bedrock will once again become established. During this phase the chemical and isotopic evidence of permafrost effects may be either altered by mixing processes or simply removed. Subsequently, following the maximum glacial extent, a deglaciation occurs with retreat of the ice sheet accompanied by the release of large volumes of meltwater into the bedrock (cf Section 4.11). This will make identification of any remaining hydrochemical evidence of permafrost even more uncertain. Both permafrost and deglaciation may influence, therefore, the hydrochemical character of the bedrock groundwaters to varying depths and degrees.

4.11.2 Freeze-out processes

The incremental freezing of surface water and particularly brackish bedrock groundwater ahead of the advancing continental ice sheet is believed to give rise to 'freeze-out' fluids of high salinity, possibly propagating down to several hundred metres. This is based on the fact that when water freezes slowly, most of the solutes present in the water will not be incorporated in the crystal lattice of the ice and will tend to accumulate at the propagating freeze-out front. This front, however, is not necessarily sharp, because freezing probably will take place over a range of temperatures, depending on the salinity and on the ratio between 'free' and tightly adsorbed water molecules.

The freeze-out hypothesis is largely based on laboratory experiments related to sea water freezing, where, for example, /Nelson and Thompson 1954/ were able to distinguish between the products of evaporation and freezing. The solid products from evaporation consisted of halite with subsidiary gypsum, and from freezing, hydrahalite and mirabilite. The most important difference during freezing is the removal of the SO_4^{2-} ion in mirabilite ($Na_2SO_4 \cdot 10H_2O$). However /Marion et al. 1999/, based on theoretical model and experimental evidence, demonstrated that gypsum also can precipitate spontaneously after mirabilite and at lower temperatures during sea water freezing, arguing that its inclusion is the most thermodynamically favoured pathway and close to that earlier proposed by /Gitterman 1937/. Moreover, from a theoretical point of view, depending on the Na/Ca ratio of the groundwater type present prior to permafrost activity, gypsum may be the first precipitated phase during freezing instead of mirabilite.

The 'freeze-out' concept, as described and discussed by /Bein and Arad 1992/, assumes that the formation of permafrost in a brackish lake or a restricted coastal sea environment (e.g. similar to that of the Baltic Sea or Hudson Bay in Canada) produced a layer of highly concentrated salinity ahead of the advancing freezing front. Since this saline water would be of high density, it subsequently would sink to lower depths (i.e. density driven intrusion), would avoid dilution by oceanic water, and potentially penetrate into the bedrock were it would eventually mix with formational groundwaters until groundwaters of similar density would be encountered.

Where the bedrock is not covered by brackish lake or restricted sea water, similar freeze-out processes may occur in the bedrock on a much smaller scale within the hydraulically active fractures and fracture zones, again resulting in formation of a higher density saline component in the residual fluids. The incremental downward propagation of the freeze-out front will eventually cease due to increased salinity, increased temperature, and a decrease in transmissivity which will hinder potential pathways for the residual fluids.

Freezing can also result in isotopic fractionation resulting in enrichment in the ice phase and such evidence includes ^{18}O and ^{2}H (and possibly ^{37}Cl), based on laboratory studies (e.g. /Zhang and Frape 2003, Ruskeeniemi et al. 2004/), and ^{10}B enrichment in the ice phase (i.e. ^{11}B enrichment in the residual fluids) advocated by /Casanova et al. 2005/ in studies of Fennoscandian groundwaters.

4.11.3 Evidence of permafrost processes at Laxemar

As pointed out above in Section 4.11.1, searching for evidence of permafrost processes is not expected to be an easy task because of subsequent flushing and dilution effects following permafrost decay. However, the residual saline fluids resulting from freeze-out may escape these effects because of entrapment in low transmissive parts of the bedrock, for example, in dead-end pathways, microfractures, lenses or pockets, or in the rock matrix itself as distinctive porewater compositions. With respect to the former, fortuitous drilling may intersect such reservoirs that could reveal hydrochemical and/or isotopic evidence of a permafrost freeze-out origin to the released groundwaters. Porewater studies perhaps would provide the best opportunity, but only if permafrost conditions have prevailed long enough for diffusion gradients to become established between water-conducting fractures containing the residual saline fluids and the rock matrix. From another angle, some of the dilute waters resulting from permafrost decay may have been involved in the subglacial formation of identifiable mineral phases (e.g. calcite) along fracture surfaces. Below are described and discussed the different possible permafrost indicators based on the groundwater data set of Laxemar-Simpevarp area.

Enrichment/Depletion of ^{18}O

Present day depleted $\delta^{18}O$ values (< –13.0‰ VSMOW) from the Laxemar-Simpevarp area characterise the brackish glacial and some of the brackish to saline non-marine groundwaters. There are two possible sources to these signatures: a) initially from freeze-out residual fluids during the establishment of permafrost conditions prior to the last phase of the ice sheet cover, and b) derived from glacial meltwaters during deglaciation. There may be some additional influence from past glacial cycles, particularly preserved at greater depths associated with the brackish to saline non-marine groundwaters, but it is impossible to descriminate between different timescales using ^{18}O. The depleted signatures in the upper approximately 600 m are believed to be dominantly from the last glaciation. At greater depths, both processes, i.e. density intrusion of ^{18}O during freeze-out and injection under high confining hydraulic pressures, may have been active.

Enrichment of ^{18}O resulting from permafrost would be expected to characterise the upper bedrock horizons, but the likelihood of such signatures surviving permafrost melting in the water-conducting fracture systems would be minimal. First, because of the dilute nature of the meltwaters (i.e. limited density intrusion), and then the mixing effects in the upper bedrock where some groundwater circulation associated with a warm based continental ice sheet would be active. Furthermore, with subsequent retreat and degradation of the ice sheet the glacial meltwaters under high confined hydraulic pressure would mix and flush out much of the remaining evidence of enriched ^{18}O waters. However, as mentioned above, there is the possibility that between the stages of permafrost decay and deglaciation ^{18}O-enriched water was resident in fracture systems for periods of sufficient duration to establish diffusion gradients with the rock matrix. Depending on the porewater composition prior to the last glaciation, present day matrix porewaters in the upper 400 to 500 m of bedrock may have retained a weak brackish water with an enriched ^{18}O signature, significantly more enriched than modern meteoric water. Unfortunately, such enriched signatures are not readily obvious from the porewater data (cf Section 4.9), although this is perhaps not surprising as both later glacial meltwater with depleted signatures and the range of meteoric recharge water signatures may have been superimposed on the matrix porewater system.

Boron isotope systematics

With respect to freezing processes, /Casanova et al. 2005/ suggest that permafrost would be accompanied by the preferential fractionation of ^{10}B into the ice component and ^{11}B into the residual fluid phase. Although subsequent glacial meltwaters would mix with the residual fluid, and additional mixing with different post glacial water incursions would also eventually occur with time, these modifications may be restricted to the more highly transmissive parts of the bedrock, whilst low transmissive parts may have preserved signatures of freeze-out fluids enriched in ^{11}B which could progressively return to the main fracture network and mix with the existing and more recent groundwaters /Casanova et al. 2005, Smellie et al. 2008/.

As summarised in /Smellie et al. 2008/, by analysing the boron isotopic data presently available for the Fennoscandian Shield it can be seen that groundwaters mainly from Äspö, but also from Palmottu, Olkiluoto and Hästholmen in Finland reported by /Casanova et al. 2005/, show a tendency for ^{11}B enrichment with depth, reaching maximae of 50 to 55‰ at about 90 and 500 m depth respectively. Below this level, ^{11}B decreases to the equivalent of marine values (around 40‰) at about 1,150 m depth (Figure 4-64; left-hand plot). These increases were suggested by /Casanova et al. 2005/ as indicating the selective uptake of $\delta^{10}B$ into ice related to freezing processes, and leaving residual fluids rich in $\delta^{11}B$.

The boron isotopic data for the Laxemar area (Figure 4-64; right-hand plot) show a slightly greater enrichment to a maximum of about 60 to 65‰ at depths from about 350 to 500 m. However, in the same figure the Simpevarp subarea $\delta^{11}B$ data are significantly higher, ranging to a maximum of 109‰ in borehole KSH01A. Furthermore, this highest value corresponds to several of the shallow soil pipe groundwaters in Laxemar. The reason for this is not readily obvious; possibilities include groundwater discharge localities, carbonate sources (overburden?), and perhaps wind blown salts of marine origin, or anthropogenic contamination from sewage or agricultural fertilizers. Interestingly, five of the seven shallow groundwater sampling points were identified as ‘outlet’ or ‘discharge’ points /SKB 2006a/ and the remaining two samples were collected more recently in 2007 and are not categorised. Of the five ‘discharge’ samples, four are from the Laxemar subarea and one from the Simpevarp subarea (Ävrö) at the coast close to borehole KAV01. However, with one exception (brackish at around 650 mg/L Cl) all are fresh meteoric in type (< 200 mg/L Cl) and show no clear discharge indications. The source of the high $\delta^{11}B$ values in these near surface soil pipe localities remains unresolved.

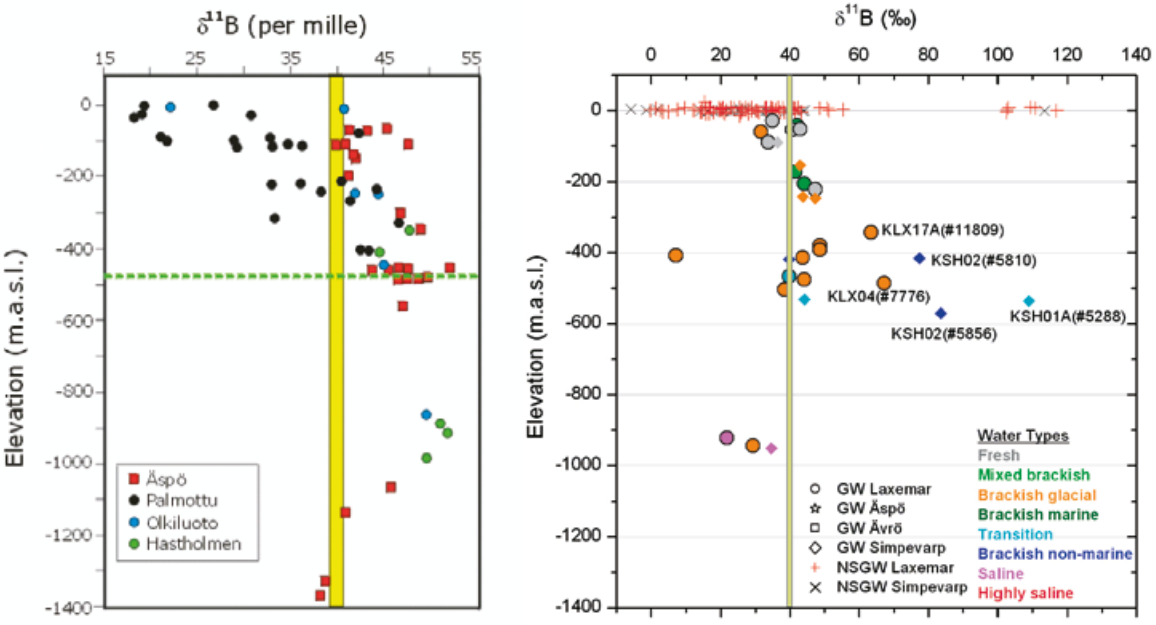

Figure 4-64. *$\delta^{11}B$ values as function of depth showing different Swedish and Finnish sites (left-hand plot) /Casanova et al. 2005/, and showing the Laxemar subarea (right-hand plot). In the former, the range of Baltic Sea water from /Casanova et al. 2005/ is represented by the vertical yellow infilled column (also right-hand plot), and the dashed horizontal line in the left-hand plot corresponds to the maximum permafrost depth calculated by /Boulton et al. 2001/ for southern Sweden.*

Taking the Laxemar-Simpevarp area (Figure 4-64; right-hand plot), the enrichment in ^{11}B is more pronounced, especially within the 300 to 550 m interval associated with some boreholes (KSH01A: –531.51 m, KSH02: –418.66 m and KSH02:– 570.90 m elevation) which are mainly brackish non-marine in type with chlorine contents ranging from 7,910 to 8,560 mg/L and also higher than normal amounts of sodium and sulphate when compared with other brackish non-marine groundwater types. It is interesting to note that /Gimeno et al. 2009/ report that these groundwater compositions can not be modelled using the present mixing assumptions. Furthermore, Na-Ca-SO_4 type compositions associated with chloride contents ranging from 2,500 to 7,600 mg/L, have been reported for porewaters at similar depth intervals (cf Section 4.9.4). These occurrences, together with the anomalously high $\delta^{11}B$ values in the groundwaters, may indicate possible influences of freezing that have accumulated at these depths prior to the last deglaciation.

In general, most of the analysed $\delta^{11}B$ values are between 20 and 60‰, in agreement with the published values by /Casanova et al. 2005/, who also noted that the Fennoscandian Shield groundwaters record the highest $\delta^{11}B$ values, even higher than the Canadian Shield groundwaters which are commonly enriched by water-interaction processes. Two of the shallow soil pipes also record very high ^{11}B values and the reason for this is presently not known.

The relationship between $\delta^{11}B$ and $\delta^{18}O$ in the Laxemar subarea is shown in Figure 4-65 which shows a wide range, although the most enriched ^{11}B values are associated with some of the most depleted ^{18}O signatures in the groundwaters, except for the near surface waters. This combination could reflect permafrost processes (cf Section 4.11.2). However, depleted ^{18}O can be equally well explained by the injection and mixing with later glacial meltwaters, although this possibility does not preclude the fact that depleted groundwaters may have existed prior to the last deglaciation.

Chlorine-37 data

As mentioned in Section 4.11.2, preferential fractionation of ^{37}Cl leading to its enrichment in the ice phase also may be a possible indicator of permafrost freeze-out processes. However, its fate may be similar to that described for ^{18}O in that near surface flushing during permafrost decay and subsequent deglaciation activity has most likely removed or destroyed any evidence, apart from potential preservation in low transmissive bedrock etc.

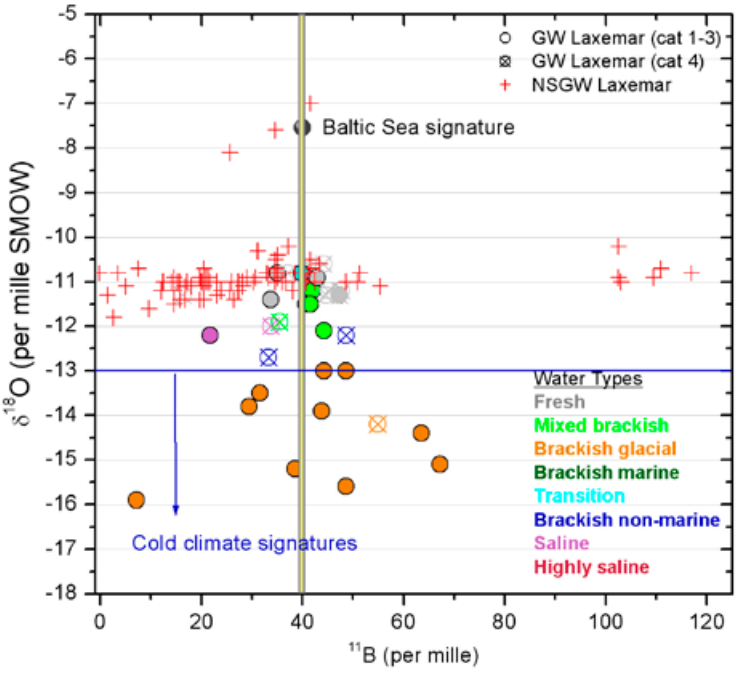

Figure 4-65. *$\delta^{11}B$ versus $\delta^{18}O$ for groundwaters from the Laxemar subarea (vertical line represents the Baltic Sea signature). The horizontal blue line indicates the cut-off for cold climate signatures ($\delta^{18}O < -13$‰ VSMOW).*

Figure 4-66a shows a general shift to more positive $\delta^{37}Cl$ values (i.e. indicative of non-marine derived groundwaters) at about 400 m, and there is a small increase with continuing depth suggested by the saline and highly saline groundwaters. The brackish glacial groundwaters mostly plot close to the marine 0‰ SMOC line and within the range of analytical error, with two exceptions located just outside the limit to the positive side of the plot.

Figure 4-66b shows the relationship between ^{37}Cl and ^{11}B where most data plot between 20 to 50‰ $\delta^{11}B$ and towards the positive, non-marine groundwater $\delta^{37}Cl$ values. Three brackish glacial groundwaters are anomalous, with two showing enriched and one showing depleted $\delta^{11}B$ values, and all three plot in the negative field suggesting marine-type groundwaters. If any general trend is present, it indicates a weak correlation between increasing enrichment of ^{37}Cl and a depletion of $\delta^{11}B$. This mostly reflects increasing depth and salinity (i.e. the transition from brackish glacial groundwaters to brackish non-marine to saline/high saline groundwaters), decreasing transmissivity and increasing water-rock interaction.

Figure 4-66c showing $\delta^{18}O$ versus $\delta^{37}Cl$ reflects in this case an increased enrichment in ^{18}O and ^{37}Cl which correlates with increasing depth and salinity. In the brackish glacial groundwaters this trend is interesting as enrichment in both ^{18}O and ^{37}Cl would be expected in the ice phase during permafrost formation. However, an alternative explanation is the mixing of glacial waters at different depths with deeper groundwaters of varying salinity and more enriched ^{18}O.

Porewaters

As pointed out above, porewater studies (cf Section 4.9) have recognised a brackish Na-Ca-SO_4 water type in the three boreholes investigated. This porewater occurs at depth intervals of about 430–550 m in boreholes KLX03 and KLX17A and at about 620–750 m in borehole KLX08 and appears to roughly correspond to the present deepest penetration of the brackish glacial groundwaters in the water-conducting fracture system. Interestingly, at or close to these levels in the bedrock fracture gypsum has been observed. As mentioned in Section 4.11.2, freeze-out processes can lead to either removal of Ca^{2+} and SO_4^{2-} by precipitation of gypsum or removal of the Na^+ and SO_4^{2-} ions in mirabilite ($Na_2SO_4 \cdot 10H_2O$). Thus, due to the highly metastable nature of mirabilite to temperature increase, present day evidence of freeze-out processes may therefore include the preservation of lens

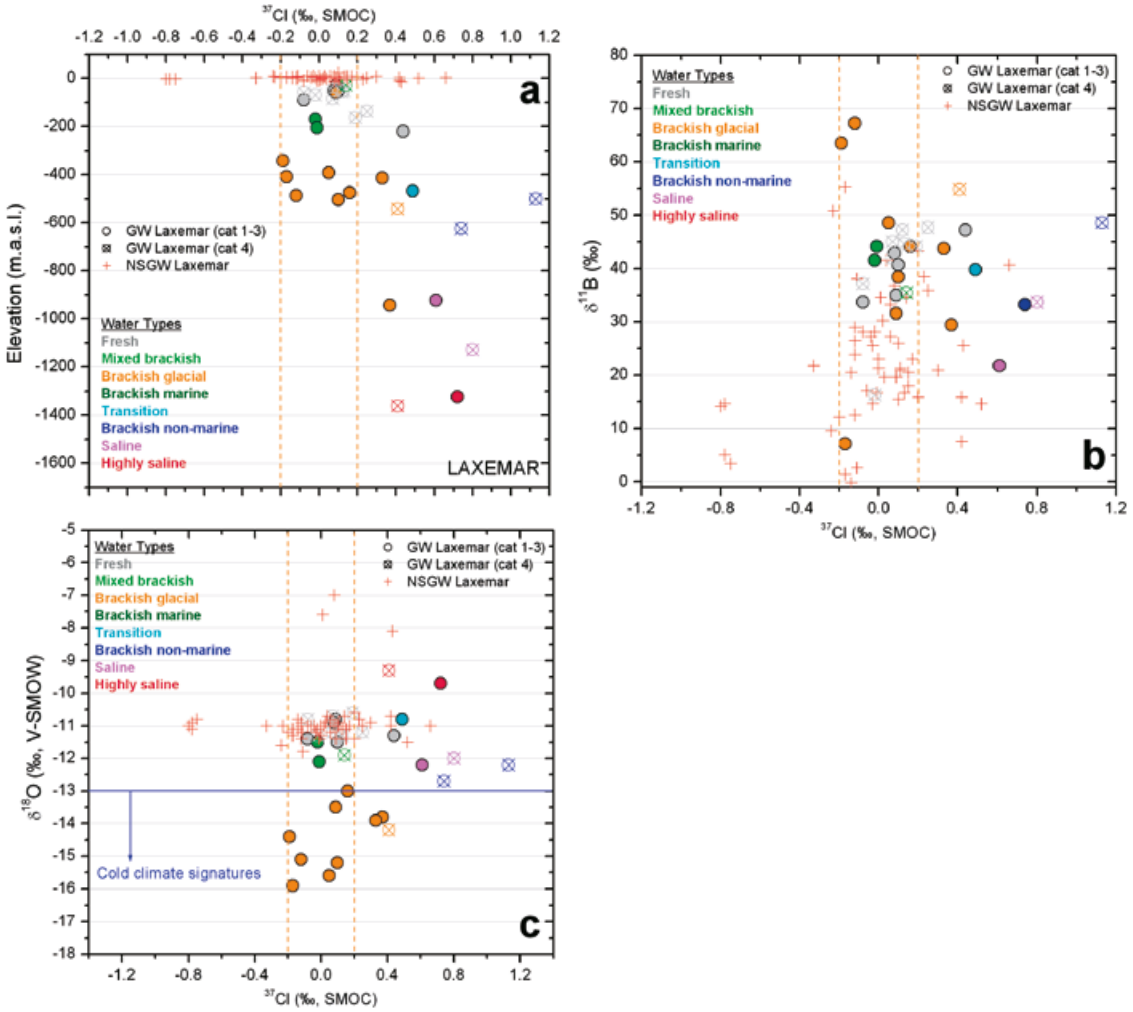

Figure 4-66. *$\delta^{37}Cl$ versus elevation (a) $\delta^{11}B$ (b) and $\delta^{18}O$ (c) for the Laxemar subarea groundwaters. Vertical lines represent the analytical error for $\delta^{37}Cl$ (± 0.2‰ SMOC) and the horizontal blue line in figure (c) indicates the cut-off for cold climate signatures ($\delta^{18}O$ < –13‰ VSMOW).*

or pockets of groundwater characterised by Na-Ca-SO_4 compositions. Dissolution of sulphate minerals appears to be the situation observed at Laxemar, both in some of the groundwaters and also the porewaters, as discussed above. However, the fracture gypsum recorded is old, probably Palaeozoic in age (cf Section 2.2.5), which precludes a last glaciation age of its formation. Therefore, there are two possible sources to the measured Ca-Na-SO_4 waters at Laxemar: a) freeze-out mirabilite (Na^+ and SO_4^{2-}), and b) dissolution of old fracture gypsum (Ca^{2+} and SO_4^{2-}) during the last deglaciation whereupon changes in rock stress may have reactiviated sealed fracture systems of Palaeozoic age. However, irrespective of the scenario, in both cases these components have accumulated at depths greater than the vertical extent of the modelled permafrost layer.

Modification of Br/Cl and Na/Cl by freezing processes

The possibility of producing deep brines from sea water freezing along the margins of continental ice masses has been proposed by /Starinsky and Katz 2003/. Based on laboratory freezing studies (e.g. /Herut et al. 1990/) they used sodium, chloride and bromide to differentiate between the formation of brines from evaporation and freezing processes. For example, 'during freezing sodium is first removed from the brine as mirabilite ($Na_2SO_4 \cdot 10H_2O$) at about –8°C reflecting a concentration factor of about ×4, followed by hydrohalite ($NaCl \cdot 2H_2O$) at a concentration factor around ×10. During evaporation, though, sodium is removed only as halite, as of and above a 10-fold concentration'. By plotting (Na/Cl) eq against (Br/Cl)eq ×100 should differentiate, therefore, between a cryogenic and evaporative origin to the Ca-chloride brines of the Canadian and Fennoscandian Shield environments.

The Laxemar groundwaters are presented in Figure 4-67 which shows some of the brackish glacial groundwaters, together with transition and brackish non-marine types, plotting close to the evaporation line. Considering the large glacial meltwater components comprising these brackish glacial groundwaters, this may not be so surprising. More difficult to explain is the brackish non-marine groundwater and transition types, although the latter does have a weak Littorina component. Two brackish glacial groundwaters mixed with deeper groundwater types plot on the freezing curve, as does one of the transition groundwaters. The highly saline groundwaters plot separately, which is not unusual as they represent a closed system characterised by stagnant groundwater conditions, and therefore not considered to be relevant to this particular discussion. In general, there is no convincing evidence from the available data that supports sea water freezing as a source of the saline to highly saline groundwaters in the Laxemar subarea.

Generally there are inconsistencies to this theory of sea water freezing. For example, /Pitkänen et al. 2003/ point out that the high salinities associated with many of the Finnish brine-type groundwaters are sensitive to lithological variations, indicating that water-rock interaction over very long time periods (hundreds of thousands of years; Section 4.10.3) is a significant process. It is therefore doubtful that sea water freezing initiated during the Quaternary as indicated by /Starinski and Katz 2003/ can be the sole explanation of deep brine chemistry.

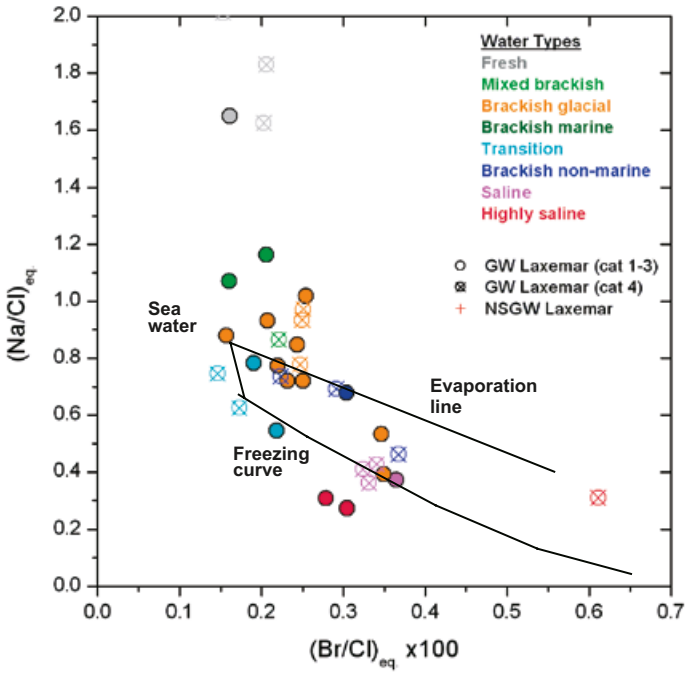

Figure 4-67. *Na/Cl versus Br/Cl for the Laxemar groundwaters. The freezing curve and evaporation line are based on /Herut et al. 1990 after Starinski and Katz 2003/.*

4.11.4 Conclusions

The main conclusions regarding potential permafrost activity are:

- Modelling of palaeoclimate and permafrost supports that permafrost conditions have prevailed for long periods of time at the Laxemar-Simpevarp area during the last glacial cycle, where the maximum depth of permafrost is in the order of 300 metres.
- Freeze-out processes have been demonstrated in the laboratory to give rise to the formation of mirabilite ($Na_2SO_4 \cdot 10H_2O$) and/or gypsum ($CaSO_4$). Following permafrost decay, a sulphate-rich water will result from the breakdown of mirabilite and/or dissolution of the gypsum.
- Enrichment of Ca-Na-SO_4 in porewaters and groundwaters is observed at Laxemar at depths close to the maximum penetration of the fracture brackish glacial groundwaters.
- The isotopes of oxygen, boron and chlorine can be sensitive to freeze-out conditions, either becoming enriched in the ice phase (^{18}O and ^{37}Cl) or in the residual fluid phase (^{11}B). These isotopes have been applied to the Laxemar groundwaters, in particular the brackish glacial type which mostly occurs at intermediate depths (about 300–600 m) and appears to have been reasonably well preserved in bedrock which shows a decrease in hydraulic conductivity with increasing depth.
- In common with earlier observations of $\delta^{11}B$ variations versus depth, the Laxemar-Simpevarp data show enrichment in ^{11}B compared with sea water which have accumulated in most of the groundwaters sampled at 200–600 m depth. This may be a result of freeze-out processes. In addition, the distribution of $\delta^{37}Cl$ shows a weak correlation between increasing enrichment of ^{37}Cl corresponding to a depletion of $\delta^{11}B$ in the brackish glacial groundwaters, supporting also a possible freezing effect.
- Although it is difficult to find clear evidence of permafrost influence on the groundwater composition, two samples (KLX13A:–408 m and KLX17A:–342 m elevation) show enriched ^{11}B together with depleted ^{18}O and possibly depleted ^{37}Cl, which may suggest a modification of the isotope systems related to freeze out processes.
- In the bedrock above the brackish glacial groundwaters, the isotopic indicators generally reflect a more dynamic and younger groundwater flow system, whilst below the groundwater system is characterised more by low flow to stagnant conditions, and the isotopes mainly reflect water-rock interaction processes.
- A number of porewater samples from depth intervals of about 430–550 m in boreholes KLX03 and KLX17A and 620–750 m in KLX08 show accumulated Na-Ca-SO_4 compositions. The origin of this sulphate is not clear but possible sources are dissolution of gypsum and/or modifications induced by freezing processes.

4.12 Cold climate recharge waters

Cold climate (or glacial melt) recharge waters largely derive from the degradation and retreat of continental ice sheets. Immense volumes of water are involved and penetration into the bedrock can be in excess of 1,000 m as evidenced in the Fennoscandian Shield. Their preservation today after a period dating back to at least the last deglaciation 14,000 years ago is therefore testament to the importance of high hydraulic gradients and rock permeability as major controls on groundwater flow and transport in fractured crystalline rocks. The nature of this glacial meltwater and its implications are detailed in /SKB 2006c/.

As described and discussed in Sections 4.1.2 and 4.1.3 evidence of cold climate recharge waters (typified by the brackish glacial types) is particularly widespread in the northwestern, western and central parts of the Laxemar subarea and more sporadically eastwards within the Simpevarp area. Today, they are present mainly within the 350 to 600 m depth interval, but may also be found at both shallower (5 to 250 m) and deeper (e.g. KLX04 at –945 m elevation) levels. The persistence of cold climate signatures (i.e. $\delta^{18}O < -13$‰ VSMOW) can be attributed mainly to variations in rock permeability were low hydraulically conductive parts of the bedrock have helped retain the brackish glacial groundwaters. The result is a laterally extensive distribution of brackish glacial groundwaters with a wide range of salinities (i.e. 500–6,500 mg/L Cl) irrespective of depth. Some exist mostly as horizons with some trapped as ‘pockets’ or ‘lenses’ at different depths. Some of the compositional heterogeneity largely reflects the location, the hydraulic properties, and the depth of sampling of the large-scale deformation zones which are the main sources of the sampled groundwaters.

The higher saline varieties of the brackish glacial groundwaters are considered to comprise a mixture of last deglaciation meltwaters with Old Meteoric ± Old Glacial + Saline waters, i.e. groundwaters thought to be present prior to the last deglaciation (cf Section 2.5.3). The less saline varieties have a greater meteoric water component which may range in age from soon after deglaciation to quite recent. In addition, especially in the southeastern part of the Laxemar subarea, a weak to intermediate component of marine (Littorina Sea) water introduced after the last deglaciation is also observed.

The $\delta^{18}O$ signatures of the deeper brackish to saline non-marine groundwaters, some of which are also significant (range –13.1 to –11.7‰ VSMOW), are impossible to evaluate in terms of timescale. They could represent the last deglaciation or, equally well, the product of earlier glaciation events.

4.12.1 Hydrochemistry of the glacial meltwater end member

The isotopic composition of the glacial end member involved in mixing at Laxemar (and Forsmark) has been assigned a $\delta^{18}O$ value of –21‰ VSMOW based on measured values of $\delta^{18}O$ in surface calcite deposits /Tullborg and Larson 1984/. In the Canadian Shield environment /Clark et al. 2000/ have assigned a value of –28‰ VSMOW, also partly based on subglacial bedrock carbonate concretions. The degree of $\delta^{18}O$ depletion will depend on local conditions during the freezing event. A slow and systematic freezing event under closed conditions will result in a progressive depletion in $\delta^{18}O$ in the residual water due to the preferential incorporation of the heavier isotopes in the ice.

The major dissolved ion concentrations in glacial meltwaters vary considerably, ranging from very dilute glacial waters from a Norwegian glacier used in these present studies, to a whole range of major dissolved ions from other glacier localities in northern and central Europe, Antartica and Alaska /Brown 2002/. The composition of the infiltrating glacial meltwater is important when later interpreting issues such as radiocarbon dating are considered. For example, bicarbonate contents (i.e. potential atmospheric CO_2 source of ^{14}C), may or may not date back to the last deglaciation event. Unfortunately, there is no way of being sure of the original composition of the glacial meltwater which may change depending on location and bedrock hydraulics along the margins of the retreating ice mass. Even dilute meltwaters introduced directly into the bedrock within a closed subglacial environment and under high confining pressure, may quickly mix both vertically and laterally (because of the high confining pressures) with other meltwaters containing major dissolved ion concentrations recharged from more open systems. This would be facilitated by an increase in interconnected hydraulic pathways in the upper bedrock opened by reactivation pressure-release mechanisms due to the melting ice mass. /Björnsson 1998/ records that summer melting adjacent to the steep front of an ice sheet (elevation several hundred metres) feeds an extensive network of intra- and sub-glacial meltwater channels, where freshly eroded bedrock material probably would be available. This may give rise to inorganic reactions thus changing the meltwater chemistry.

4.12.2 Other subglacial processes

Based on the review by /Brown 2000/ it was pointed out that basal ice and subglacial meltwaters from localities in Switzerland have yielded active bacterial populations comparable to those in the active layer of permafrost. This may influence the upper bedrock hydrochemistry in that:

- Oxidation of sulphide minerals and microbially-mediated oxidation of organic carbon at glacier beds could potentially provide acidity to the subglacial environment. The presence of liquid water at warm-based glaciers could sustain bacterial populations by supplying nutrients such as NO_3^- and NH_4^+ (from the surface) and Fe and SiO_2 (from subglacial sediments).
- Organic carbon derived from bedrock, soils and vegetation over-ridden during glacial advance may contribute to microbial mediation of redox reactions where the meltwaters are isolated from an atmospheric source of CO_2.

4.13 Origin and evolution of the deep saline groundwaters

4.13.1 Background

The origin and evolution of deep saline groundwaters in general, and partly in the Laxemar-Simpevarp area, are dealt with in some detail in /Smellie et al. 2008/. Groundwaters of high salinity are ubiquitous at depth in the Fennoscandian Shield and, as such, their origin and evolution form an integral part of the

hydrogeochemical site characterisation investigations. At the Swedish and Finnish sites characterised within the respective radwaste programmes, true brines (> 100 g/L TDS) are almost certainly present but have not been sampled due to limitations of the drilling programmes. Their influence as a brine component in presently sampled groundwaters at depths shielded from the effects of post glacial events is due mainly to mixing processes by upward molecular diffusion. To characterise these saline end members it is therefore important to understand fully the past and present (and potentially predict the future) hydrochemical evolution of the candidate site in question, and to use such information to help assess potential repercussions on long term repository safety and performance. Although being part of the hydrogeochemical programme, available evidence to the origin of the brine component in the sampled and characterised groundwaters is not immediately obvious and a more sophisticated and well planned approach would be required, for example, an extended programme of drilling to much greater depths.

The variability of the transition depth to a marked increase in salinity in the Fennoscandian Shield is illustrated in Figure 4-68. Comparison shows that the transition point to a more highly saline environment (10,000 to 15,000 mg/L Cl) is site dependent, with the Laxemar-Simpevarp area indicating a minimum depth at approximately 800 m to 900 m. In contrast, Olkiluoto and Oskarshamn (borehole KOV01 from the harbour at Oskarshamn) show this transition at shallower depths (~ 500–600 m).

A further 500 to 1,000 m drilling at the various sites may well have intercepted brine-type waters. The characterised deep groundwaters to around 1,000 m from the various sites are therefore mixtures of younger waters of different origin with variable amounts of deep, ancient brine waters. The antiquity of the brine component (at least hundreds of thousands of years) is suggested from ^{36}Cl dating of brackish-saline non-marine to highly saline groundwaters collected at different depths from the Äspö site /Louvat et al. 1999/, from the Forsmark site /Smellie et al. 2008/, and from the Laxemar-Simpevarp area (cf Section 4.10.3). Of the studied sites under discussion, perhaps those most likely to contain a deep brine component are: a) those subject to the deepest drillings (i.e. Laxemar), b) areas of potential 'regional' discharge (e.g. Simpevarp), and c) areas to some extent shielded from recharging waters (e.g. Forsmark).

Unravelling the contrasting palaeo-origins of the salinity may still be possible by careful interpretation of chemical and isotopic indicators not only in the groundwaters, but also associated with fracture filling materials from ancient, and continuously reactivated water-conducting fracture systems.

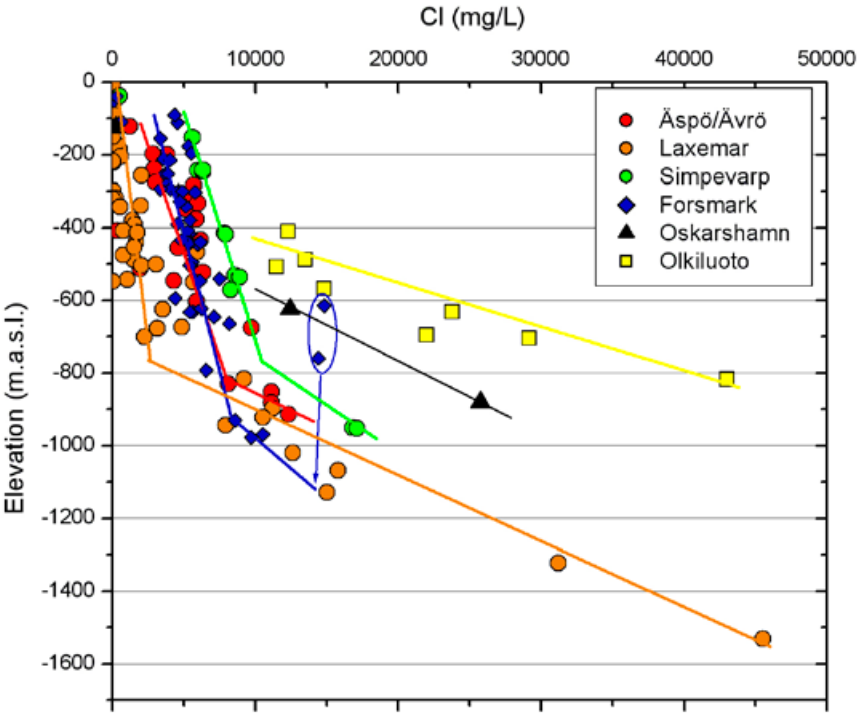

Figure 4-68. *Chloride versus elevation (categories 1–4) at selected Fennoscandian sites. (Note the most saline Forsmark samples (ringed in blue) may either be representative for the sampled depth or be the result of upconing (cf Smellie et al. 2008, Waber et al. 2008, Gimeno et al. 2009/ for discussion).*

4.13.2 Chemical and isotopic indicators

Indicators of a non-marine origin to brine-type compositions include high ratios of Ca/Na, Br/Cl, Li/Br and $^{37}Cl/^{35}Cl$ and long residence times influencing water-rock interactions are indicated by high $^{87}Sr/^{86}Sr$ ratios and enriched $\delta^{18}O$ and $\delta^{2}H$. Large volumes of deep-seated gases (e.g. ^{3}He) and the presence of enriched $\delta^{13}C$ are other indicators. In addition, the use of ^{36}Cl dating techniques can theoretically set a minimum age of 1.5 Ma to these brine-type groundwaters.

Indicators already addressed

High Ca/Na ratios at the Laxemar subarea have already been presented and discussed in Section 4.1.3 where a clear shift is observed from Na-Ca-Cl to Ca-Na-Cl type groundwaters with increasing depth and salinity (at about 600 m). Figure 4-69 shows that this transition is a general characteristic also in other groundwaters waters from the Fennoscandian Shield. At greater depths of about 800 to 1,000 m at the Laxemar subarea, where low flow conditions begin to prevail, these Ca-Na-Cl groundwaters indicate ages in the order of hundreds of thousands of years based on ^{36}Cl systematics (cf Section 4.10.3).

Br/Cl ratios are described in Section 4.1.4 and show in the Laxemar subarea a steady increase with depth to around 1,200 m which can be an indication of increasing water-rock interaction. Interestingly, this ratio decreases at highest salinities (~ 1,500 m depth), perhaps emphasising a separate, much older closed stagnant system, of slightly different origin. Additional salinity and modification of the Br/Cl ratio may have been influenced by freeze out processes during permafrost, but presently there is inadequate evidence to support this (cf Section 4.11).

Additional evidence of water-rock interaction is suggested from Figure 4-10 in Section 4.1.3 which plots the stable isotopes of $\delta^{18}O$ and $\delta^{2}H$. This shows a deviation above the GMWL coeval with increased salinity and enrichment in ^{2}H. This observation, although weak when compared to the deep brines in the Canadian Shield, does follow the general trend which is usually interpreted as indicating intensive water-rock interactions /Frape and Fritz 1989/.

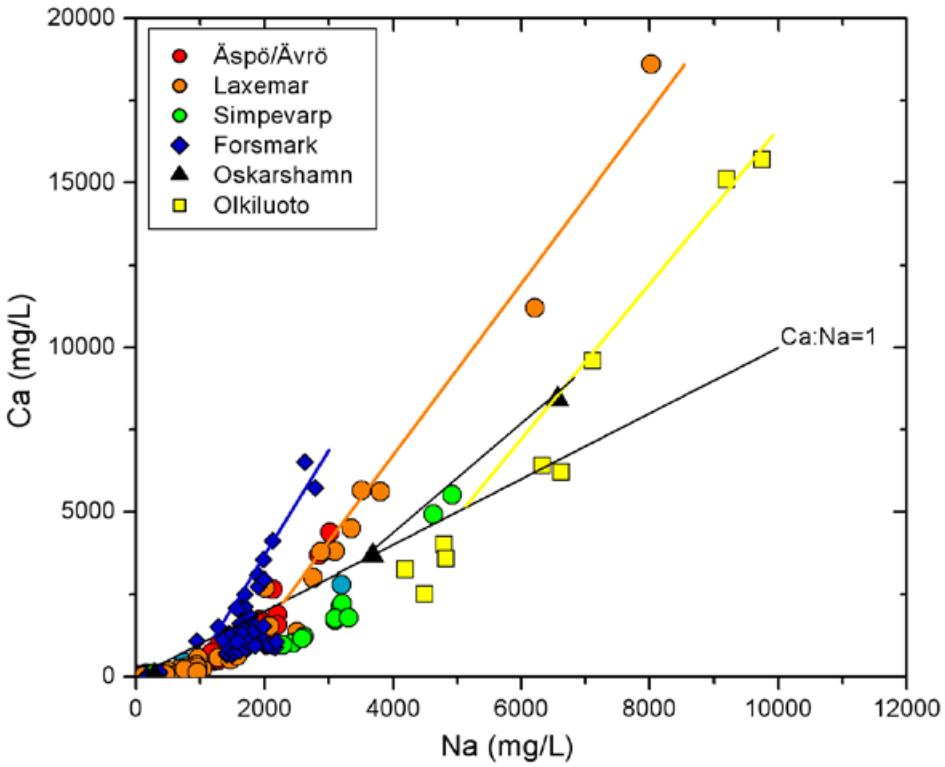

Figure 4-69. *Plot of calcium against sodium (categories 1 to 4) showing for all Fennoscandian groundwaters a shift from Na-Ca-Cl to Ca-Na-Cl type /Smellie et al. 2008/.*

Lithium

Because of a lack of category 1–3 samples for the Laxemar subarea at deep locations, Figure 4-70 presents a plot of all lithium data versus elevation. These data, even allowing for the many samples not considered representative (i.e. categories 4-5), show a clear increase in lithium from about 800 to 900 m to the maximum depths sampled.

Lithium versus chloride (Figure 4-71) shows enrichment of lithium compared with the sea water ratio for most of the saline waters except those from Olkiluoto and Forsmark. When the Laxemar subarea is compared to the other Fennoscandian sites (Figure 4-71), the following observations can be made: a) only the Forsmark brackish marine groundwaters plot along the sea water dilution line (up to 6,000 mg/L Cl) even though similar types of groundwaters exist at Simpevarp and to a lesser extent at Äspö/Ävrö (similar groundwaters from Olkiluoto may also fall into this category but there is a lack of available data), b) the Forsmark and Olkiluoto groundwaters show a depletion of lithium relative to the sea water Li/Cl ratio, and c) the Laxemar-Simpevarp area groundwaters all show an enrichment of lithium relative to chloride.

The large variability in lithium observed for saline waters from different areas also suggests the possibility of some lithological control, rather than a simple indication of increased water-rock interaction with depth. Unfortunately, systematic rock lithium data have not been included in the geochemical analytical protocol for the Forsmark and Laxemar-Simpevarp areas. Nevertheless, some analyses are available as part of the fracture mineralogy studies carried out in the Laxemar-Simpevarp area and surroundings. This covers lithium data from the Ävrö granite (7.63 mg/kg), quartz monzodiorite (< 2 mg/kg) and greisen (319 to 839 mg/kg) from the Laxemar subarea, and samples also from the Götemar granite (14 to 86.8 mg/kg) located north-east of Laxemar. What is perhaps most significant is that the groundwaters showing the greatest increase in lithium with depth come from borehole KLX02 where a single rock type dominates, i.e. the Ävrö granite. This suggests that water-rock interaction processes begin to be significant at Laxemar at depths greater than 800 m where low flow conditions begin to prevail.

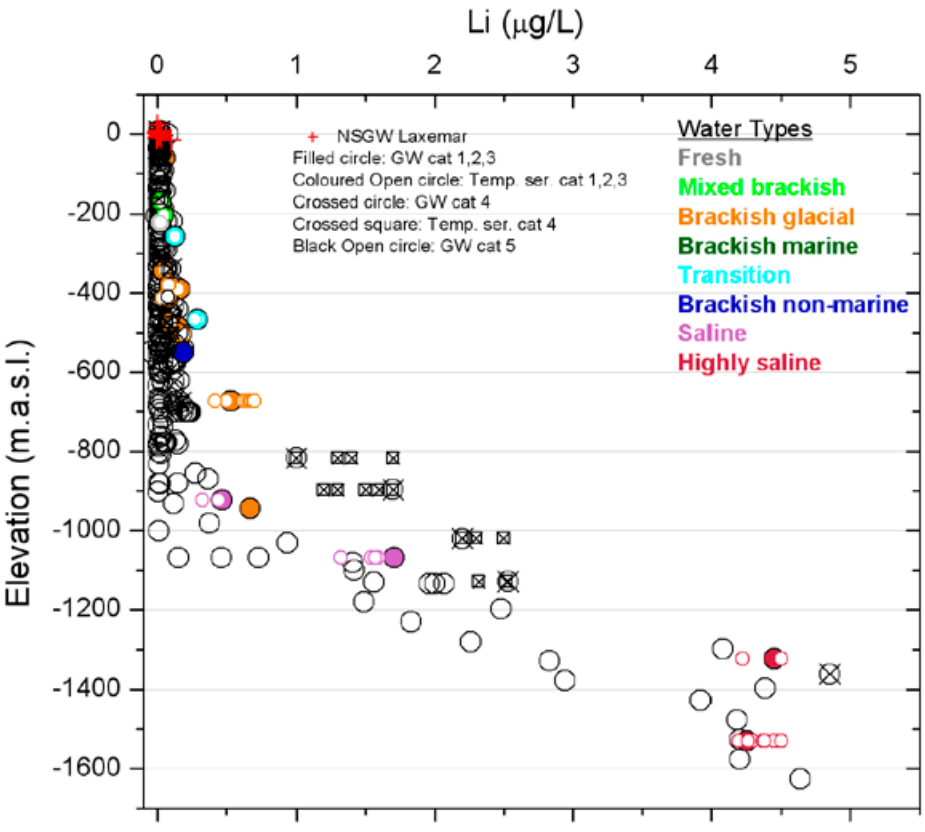

Figure 4-70. *Plot of lithium against elevation in groundwaters from the Laxemar subarea. Because of a lack of category 1 to 3 data at depth, all category 1 to 5 values have been plotted.*

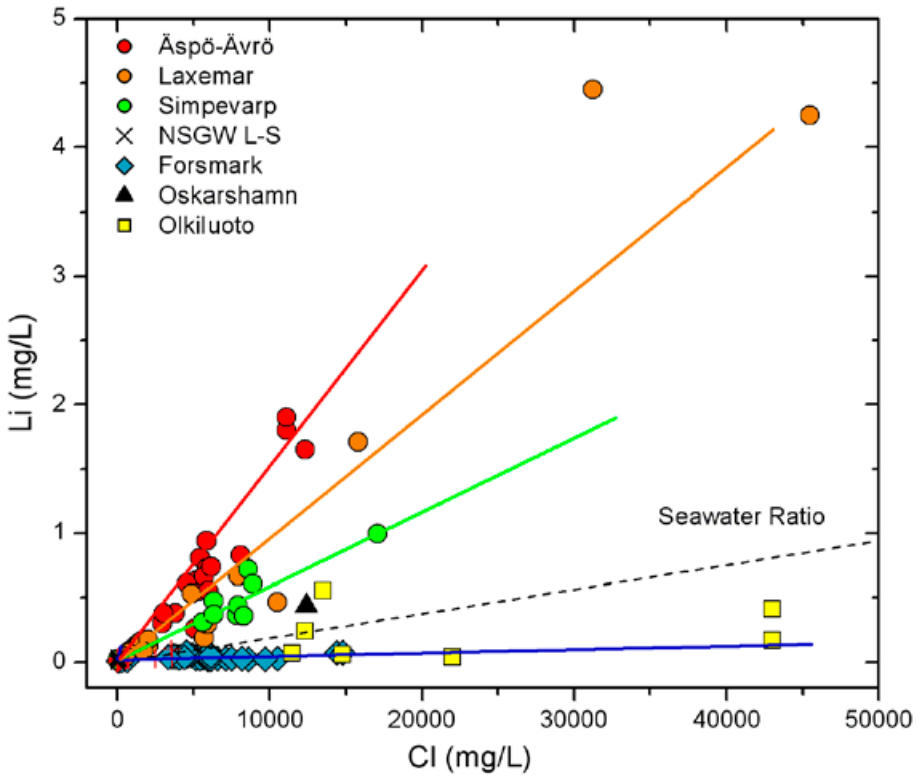

Figure 4-71. *Plot of lithium versus chlorite (categories 1 to 4) in groundwaters from different Fennoscandian sites related to the sea water dilution line /Smellie et al. 2008/.*

Caesium

Figure 4-72 shows the distribution of caesium in groundwaters from the Laxemar subarea. There is a clear increase in concentration related to depth commencing at around 800 m and becoming more accentuated with increasing depth. The highest value represents closed stagnant conditions, a trend that is typical also for some of the other trace elements such as yttrium, cerium and lanthanum.

Chlorine-37

Variations in the $^{37}Cl/^{35}Cl$ ratio expressed as $\delta^{37}Cl$ (SMOC), may reveal chloride sources of different origin (e.g. /Frape et al. 1996, Clark and Fritz 1997, Eastoe et al. 2007/). Generally, positive ^{37}Cl signatures in groundwaters are indicative of water-rock interaction chloride sources accumulated over long periods of geological time (e.g. evaporates, hydrothermal chloride), whilst negative signatures indicate chloride sources related to meteoric conditions and chloride isotope fractionation by diffusion processes. Oceanic marine water has a $\delta^{37}Cl$ of about 0‰ SMOC, while the much less saline modern Baltic Sea and palaeo-Baltic Seas have a signature of around –0.21‰ SMOC.

Figure 4-66a shows the plotted data with an analytical uncertainty of 0.2‰. There is a general shift to more positive $\delta^{37}Cl$ values (i.e. indicative of non-marine derived groundwaters) at about 400 m depth, and there is a small increase with continuing depth suggested by the saline and highly saline groundwaters. The brackish glacial groundwaters show values ranging from –0.2 to + 0.4‰ SMOC with only two samples plotting clearly outside the area of marine influence when including the range of analytical error.

Strontium isotope ratios

The distribution of strontium with increasing depth is similar to that of calcium, which is not unexpected considering their similar chemical behaviour and sources. Additional information on rock/water interaction may be derived from the isotope ratio of strontium, $^{87}Sr/^{86}Sr$, which continuously changes due to the production of radiogenic ^{87}Sr by the decay of ^{87}Rb (half-life 5×10^{10}a). In general,

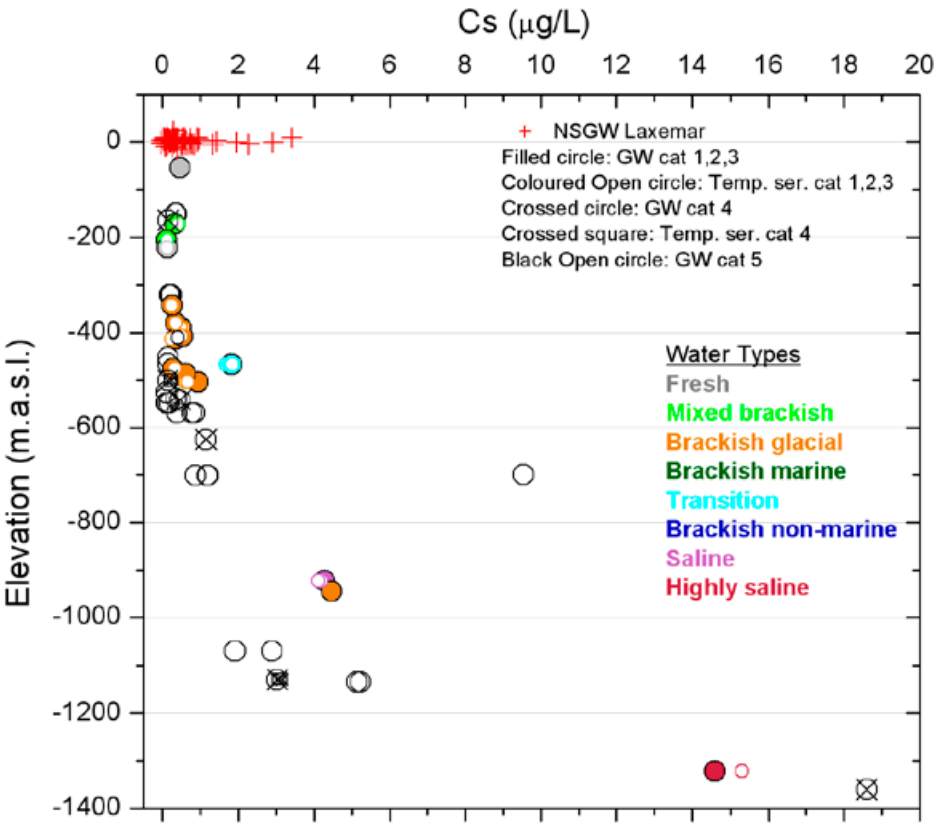

Figure 4-72. *Plot of caesium versus elevation (categories 1–4) in groundwaters from the Laxemar subarea.*

average ocean water shows a distinct strontium isotope signature (0.70906; /Faure 1982/) which is close to the measured values in the Baltic Sea waters (0.7092), whereas all other waters show higher strontium isotope ratios indicating contributions of radiogenic strontium. This is normally explained by water-rock interaction processes involving rubidium containing minerals such as K-feldspar and biotite. As shown in Section 4.1.7, the $^{87}Sr/^{86}Sr$ ratios show little variation in the groundwater at Laxemar and no correlation with Sr content, salinity or depth is indicated.

In conclusion, the strontium isotopes do not differentiate any increasing trend of water-rock interaction with depth, but rather reflect interaction at all levels within the bedrock. The same was concluded also for the Forsmark groundwaters /Smellie et al. 2008/.

Ca/Mg versus Br/Cl

Plotting Ca/Mg against Br/Cl is useful to illustrate the main groundwater evolutionary trends and has been presented and described already in Figure 4-12 (cf Section 4.1.4). A modified version is reproduced here (Figure 4-73) to achieve some perspective of the Fennoscandian deep groundwaters in relation to three well characterised Canadian brine occurrences located at Sudbury, Yellowknife and Thompson /Frape et al. 1984/. The main Laxemar (+ Olkiluoto, Simpevarp and maybe Oskarshamn) evolution pathway coincides clearly with the Sudbury site; this is true also for Forsmark although there may be a small deviation towards the Yellowknife site. In addition, the Ca/Na ratios for the Laxemar and Forsmark groundwaters coincide more closely with the Sudbury site. However, care should be taken not to overinterpret these observations; the main point is that these selected deep Fennoscandian groundwaters show an increasing brine component with depth which corresponds to some Canadian brine localities, and that the Forsmark groundwaters suggest a different evolution pathway from that indicated by the Laxemar-Simpevarp area groundwaters. Also indicated in this plot is the marked separation of the deepest and most saline groundwaters at Laxemar representing closed stagnant conditions.

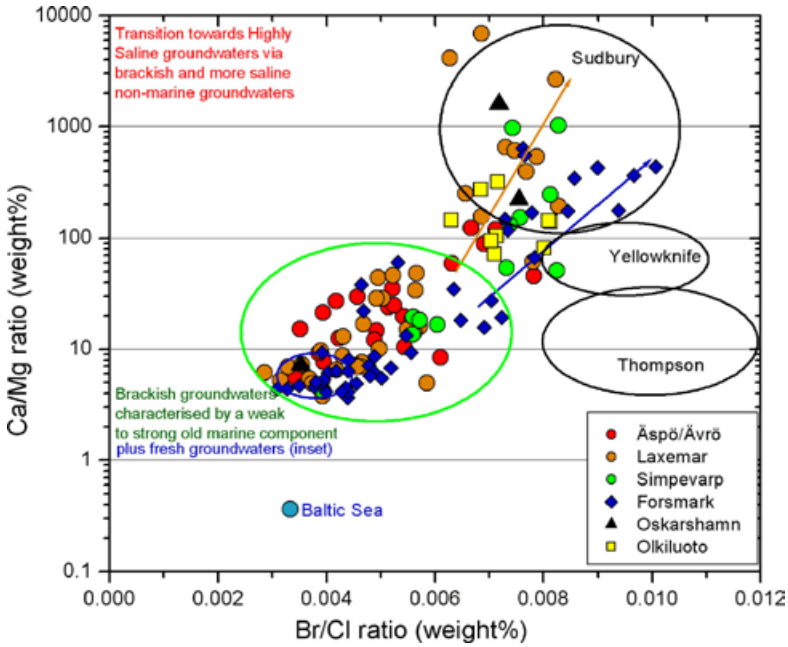

Figure 4-73. *Plot of Br/Cl versus Ca/Mg (weight %) (categories 1 to 4) showing potential major evolution trends with increasing depth for selected Fennoscandian sites. The brown arrow indicates the groundwater evolution trend for the Laxemar-Simpevarp area which shows an increasingly deep highly saline component in the groundwaters, and a similarity with Sudbury, one of the three Canadian localities characterised by deep brines (from /Smellie et al. 2008/ after /Frape et al. 1984/). Note the different trend shown by Forsmark indicated by the blue arrow. Fresh groundwaters are ringed in blue and the brackish groundwaters with a weak to strong Littorina component in green.*

4.13.3 Summary and conclusions

Despite the overall lack of data at depths greater than 1,000 m from Fennoscandian sites in general, there are indications that:

- Ca(Na)-Cl groundwaters of deep origin are common throughout the investigated sites and particularly well described at Laxemar.
- True brines (> 100 g/L TDS) have not yet been accessed despite drilling to about 1,700 m depth at Laxemar. In this deep borehole mixing is most prevalent to around 1,000 m depth, clearly indicated from hydrochemical and isotopic considerations. Diffusion processes probably dominate at depths greater than 1,200 m where closed stagnant conditions prevail.
- The deep saline groundwaters of the Laxemar-Simpevarp area show significant water-rock interaction enrichment with increasing depth which suggests an affinity to a non-marine origin, although a non-marine/old marine mixing origin cannot be excluded.
- Certain element ratios (e.g. Ca/Na, Ca/Mg and Br/Cl ratios) reveal similarities between the Laxemar site and other studied deep groundwaters in shield areas.
- Laboratory studies show that surface to near surface freezing of groundwater can produce a residual fluid of high salinity which, due to its high density, may migrate along hydraulically active fractures and settle at greater depth in the bedrock. Although permafrost conditions almost certainly occurred at Laxemar down to a depth of about 300 m, there is no hydrogeochemical evidence to indicate that such residual fluids have influenced the composition of the deep groundwaters at the site.
- The long term hydrochemical stability of the high saline groundwater environments and the near stagnant conditions is supported by ^{36}Cl age dating which indicates ages of at least hundreds of thousands of years. Low transmissive (low flow to stagnant) conditions coincide with greatest salinity at depths which are site specific. For example, at greatest depths in recharge areas (e.g. Laxemar subarea) and shallower depths in discharge areas (e.g. Simpevarp subarea).

4.14 Evaluation of uncertainties

4.14.1 Measured and modelled uncertainties in field data and interpretation methods

Before constructing the site descriptive hydrochemistry model various uncertainties have to be taken into account. These uncertainties are quantified and discussed below.

Major sources of uncertaintes

During every phase of the hydrogeochemical investigation programme, i.e. drilling, sampling, analysis, evaluation and modelling etc., uncertainties are introduced which have to be accounted for, addressed fully and clearly documented to provide confidence in the final result, whether it will be the site descriptive model or the repository safety analysis and design /Smellie et al. 2002/. Handling the uncertainties involved in constructing a site descriptive model has been documented in detail by /Andersson 2003/. The uncertainties can be conceptual uncertainties, data uncertainties, spatial variability of data, chosen scale, degree of confidence in the selected model, and error, precision, accuracy and bias in the predictions. Many of the uncertainties are difficult to assess and judge since they are the results of expert judgement and not mathematical modelling. There is no undisturbed groundwater sampled prior to drilling and therefore much of the uncertainty associated with sampling is based on indirect (e.g. short circuiting) or direct indications (e.g. drilling water content).

The sampling, analytical and modelling uncertainties are addressed and quantified in /Smellie et al. 2002, Nilsson 2009, Laaksoharju et al. 2008a, Bergelin et al. 2009, Gimeno et al. 2009, Gurban 2009/. Some of the identified uncertainties recognised during the modelling exercise are discussed below.

The following data uncertainties have been estimated, calculated or modelled for the Laxemar data:

- Disturbances from drilling activities, namely drilling water contamination, may be in the order of 10 to 70%. For modelling purposes the samples chosen (i.e. high quality samples used for the site descriptive model) generally have ≤10% drilling water content thus reducing the uncertainties.
- The effect on groundwater redox conditions from the presence of drilling water is unclear and therefore only waters with low drilling contents have been used in the redox modelling. In any case, however, the large buffer capacity of the rock and the microbial activity seem to stabilise the groundwater redox system.
- Influence of long transport times on the sampled groundwaters associated with pumping (e.g. in-/de-gassing of water through the tubing) may alter some of the water constituents in the order of ± 10%.
- Sample handling and preparation may alter some water constituents in the order of ± 5%.
- Individual analytical uncertainty for each chemical and isotopic constituent and their concentration values are reported by the different analytical laboratories. Furthermore, these uncertainty values are difficult to handle due to the large volumes of analytical data involved. General uncertainties as reported for the different methods and components are presented in /Nilsson 2009/. Analytical errors associated with laboratory measurements are generally ± 5% for major ions (Figure 4-74) but, for example, are less than ±2% for $\delta^{18}O$. However, for some elements the uncertainties can be larger as shown for bromide in Figure 4-75 (cf /Bergelin et al. 2009/). These effects on interpretation and modelling have been tested and reported in /SKB 2005, Gurban 2008/.
- The variability of the mean value of, for example, the measured chloride in groundwater during sampling (time series first/last sample) can be up to 25%, but the difference is generally much less /Gascoyne and Gurban 2008/.
- M3 model uncertainty is ±0.1 units within the 90% confidence interval; the effects on the modelling were tested in /SKB 2005/. Furthermore, the model uncertainties have been assessed in /Gimeno et al. 2009, Gurban 2009/ and the M3 model tested in detail in /Gomez et al. 2008/.

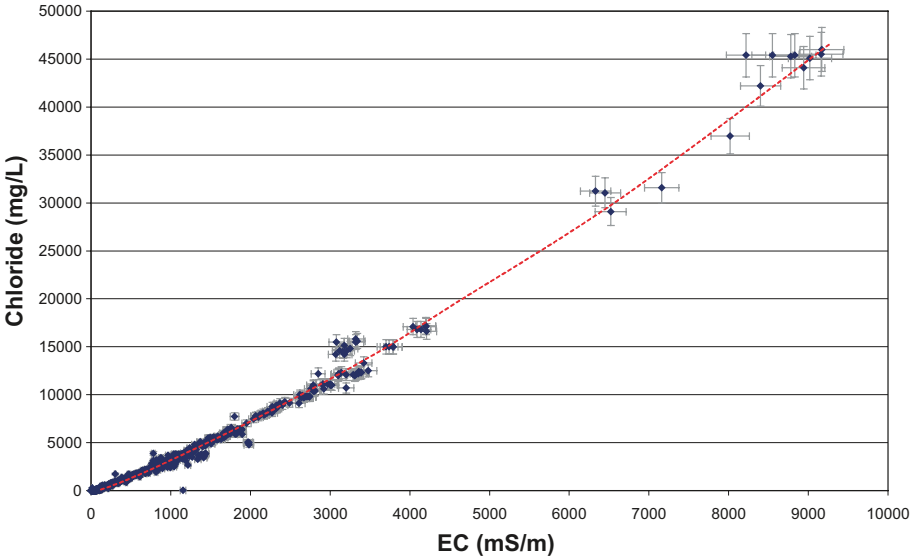

Figure 4-74. *Electrical conductivity versus chloride with a typical analytical error of ±5%.*

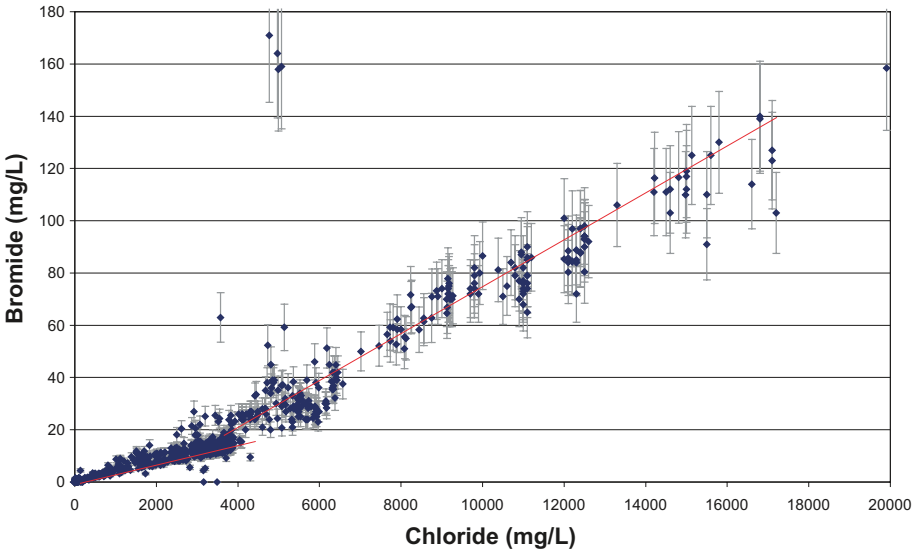

Figure 4-75. *Bromide values ('Extended data freeze Laxemar 2.3' dataset) plotted versus chloride concentrations. The short red line indicates a possible marine mixing line, the longer red line a possible non-marine mixing and/or evolution line, and the error bars correspond to ±15%. For discussion see /Nilsson 2009/.*

Conceptual models

In the construction of conceptual models, for example, the palaeohydrogeological conceptual model, errors can occur when evaluating the influence of old water end members in the bedrock where they can only be indicated by using certain element or isotopic signatures. The degree of uncertainty therefore increases generally with the age of the end member. Furthermore, the effect of porewater chemistry potentially altering the groundwater is not taken into account (cf Section 4.9.8).

The relevance of an end member participating in groundwater formation can be tested by introducing alternative end-member compositions or by using hydrodynamic modelling to test if old water types can reside in the bedrock during prevailing hydrogeological conditions. For this modelling stage a measure of verification is obtained by using statistical methods /Gimeno et al. 2009, Molinero et al. 2009/ to test the feasibility of the selected end member together with comparison with results of hydrogeological simulations.

Geochemical models

Uncertainties associated with using the PHREEQC code depend on the type of calculation performed. Analytical uncertainties and uncertainties concerning the thermodynamic data bases are of importance in speciation-solubility calculations.

Uncertainties in the conceptual model, in the selected end members and, again, in the thermodynamic data base, are of importance in mixing and reaction simulations. The associated errors can be addressed by reviewing the main source of uncertainties and performing sensitivity analyses. In this manner: a) uncertainties associated with the composition of selected end members have been evaluated /Gimeno et al. 2009, Appendix F/, b) solubility values for some critical mineral phases have been reviewed, corrected and verified in the WATEQ4F thermodynamic database /Gimeno et al. 2009; Appendix C/, c) sensistivity analyses concerning density data and activity coefficient calculations in waters with high ionic strength have been performed /Gimeno et al. 2009; Appendix B/, d) sensitivity analyses concerning the uncertainties due to pH on the calcite saturation states (Gimeno et al. 2009; Section 3.3.4.), and e) conceptual and redox modelling uncertainties have been evaluated /Gimeno et al. 2009; Appendix G/.

2D and 3D visualisation

The uncertainty resulting from 3D interpolation and 2D/3D visualisation depends on various aspects, i.e. data quality and distribution, and model uncertainties including the assumptions and limitations introduced. The uncertainties are therefore often site specific and the effect of 2D/3D interpolations can be tested by using quantified uncertainties, alternative models and comparison with independent models, such as hydrogeological simulations.

Modelling discrepancies

The discrepancies between different modelling approaches can be due to differences in the boundary conditions used in the models or in the assumptions made. During the whole site investigation phase discrepancies between models have been used as an important opportunity to guide further modelling, including validation and confidence building. The Cl and $\delta^{18}O$ values provided an important tool to compare the hydrogeological modelling with the hydrogeochemical site understanding and modelling. For example, descrepancies in the models has led to an important re-assessment of the hydrogeological modelling for the Laxemar subarea. For example, the use of different hydrogeochemical modelling approaches ranging from traditional geochemical approaches to advanced coupled modelling can be seen as a combined tool for confidence building. Agreement of process descriptions, independent of the modelling tool or approach, increases confidence in the modelling.

Of great importance to the modelling programme, in particular reducing the uncertainties in the site description model, has been the use of a common quality assured groundwater dataset restricting the modellers to use the best quality Category 1 to 3 samples for detailed modelling.

End-member tests

Thorough testing of the end members used in the M3 mixing modelling is presented in /Gimeno et al. 2008, 2009, Gurban 2008, 2009, Molinero et al. 2009/. These tests are an important tool for supporting the hydrogeochemical conceptual model and for integration between hydrochemistry and hydrogeology.

A Monte Carlo method has been developed /Gimeno et al. 2009/ to obtain an independent assessment of the feasibility of the chemical composition of the end members.

Effects of borehole perturbations

It is well known that site characterisation activities (mainly drilling activities) introduce perturbations in the system that can impact on the hydrochemistry of the groundwater samples collected at the site. It is of interest, therefore, to perform scoping calculations in order to evaluate how much disturbance can be allowed for a given groundwater sample at repository depth, and still meet, for example, the SKB suitability criteria /Molinero et al. 2008/.

It was concluded that suitability criteria related to TDS and pH would be fulfilled always for the Forsmark groundwaters, even for complete disturbance of the sample. The Ca+Mg criteria could be surpassed in the case of dilutions higher than 90 percent of the native groundwater sample. Furthermore, cation exchange processes have an effect by lowering the Ca+Mg concentrations in the groundwater, compared with a pure conservative mixing. Similar results can be assumed for Laxemar although the groundwaters are more dilute when compared to Forsmark.

The oxygen consumption capacity of the granite bedrock has also been evaluated by using reactive transport modelling. The modelling was made for the Forsmark site /Molinero et al. 2008/ but the results are not site specific and can therefore be applied to conditions at Laxemar. It was shown that a hypothetical contamination event by atmospheric oxygen at repository depth would be consumed in a relatively short period of time (about 1 year) if the maximum amounts of reported pyrite are included in the model. However, the model results have proved to be sensitive to uncertain parameters such as the exact mineralogical composition and the specific reactive surface area of such minerals. An interesting conclusion is that, in the base case considered in the model, the oxygen intrusion in a borehole would only affect a very short distance into the bedrock (of about 1 cm). The modelling documented in /Molinero et al. 2008/ supports these conclusions when the oxidising influence from drilling water on the groundwater composition was considered small, although the initially introduced drilling waters were not strongly oxidising as attempts to reduce oxidation (e.g. by flushing with nitrogen gas) formed part of the routine procedure during drilling. From another standpoint, the measured downhole redox potential measurements (Eh) values support further the reductive capacity of the groundwater system (Figure 4-76). For example, in one borehole after re-installation of the equipment (due to pump failure) the negative redox potenitial was re-established after 1–7 days indicating that possible oxygen contamination was consumed during this time period.

4.14.2 Temporal and spatial variability

Temporal and spatial variability is important in order to address how well the sampled groundwaters represent the described rock volume.

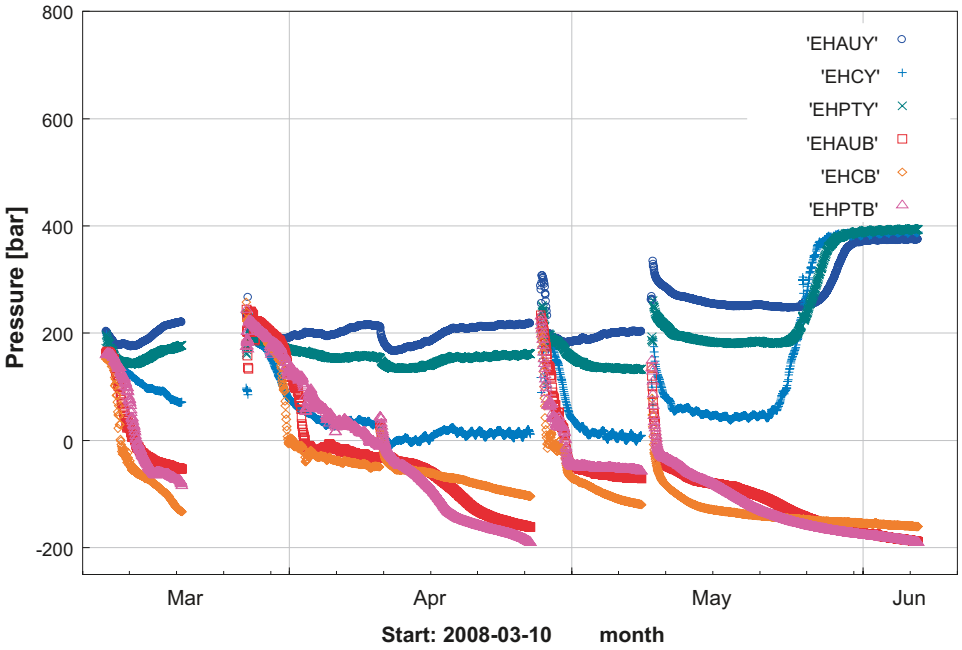

Figure 4-76. *Redox potential measurements (Eh, mV) in borehole KLX27A: 641.5–650.6 m borehole length using platinum, gold and glassy carbon electrodes in the borehole section (EHPTB, EHAUB and EHCB) and at the surface (EHPTY, EHAUY and EHCY) /Bergelin et al. 2009/. After re-installation of the equipment (due to pump failure) the negative redox potenitial was quickly re-established for the dowhole electrodes.*

Temporal variability of the groundwater character has been assessed by: a) comparing the electrical conductivity values measured shortly after drilling with the results obtained during hydraulic logging, b) evaluating open borehole values collected during hydrogeochemical logging (tube sampling), and c) by studying the time series data during hydrochemical sampling and during subsequent monitoring (cf /Gimeno et al. 2009, Gurban 2009/). Figure 4-77 illustrates a case in which sections sampled for complete chemical characterisation (CCC) in borehole KLX03 are compared with results from the resistivity logging and tube sampling.

The measurements were conducted during a time period of more than two years (June 2004–November 2006). Most of the samples obtained without pumping plot closer to the electrical conductivity values even though pumping during, for example, the CCC sampling, is at a low flow rate. Exceptions include samples from about 750 m borehole length (–701 m elevation) where some plot close to the electrical conductivity values obtained during pumping. This indicates sampling in, or close to, a transition zone between brackish and saline groundwaters (cf /Smellie et al. 2008, Gurban 2008/). In conclusion, the large amount of data from different measurements and time periods can be used to indicate the temporal variability of the groundwater in the bedrock.

To address the spatial variability 3D plots can be used to show how the measured samples vary in the 3D bedrock volume. To address the possible groundwater variability between the boreholes, coupled 3D modelling has to be used /Auqué et al. 2006/. The methodology used combines results from the hydrogeological modelling with a mixing and reaction-path simulation using PHREEQC. This coupling provides the theoretical but detailed compositional character of the groundwaters in a rock volume (constituted by a grid with about one million points) that represents the whole regional area (cf /Gimeno et al. 2008/).

4.14.3 Laxemar local scale hydrogeochemical site visualisation

The hydrogeochemical site visualisation (Section 6.2) is based on a systematic, step-wise approach to determine depth trends and hydrochemical groupings of the groundwater and porewater types as detailed in Section 4.1 and Section 4.9. Understanding of the system therefore reflects the interpreta-

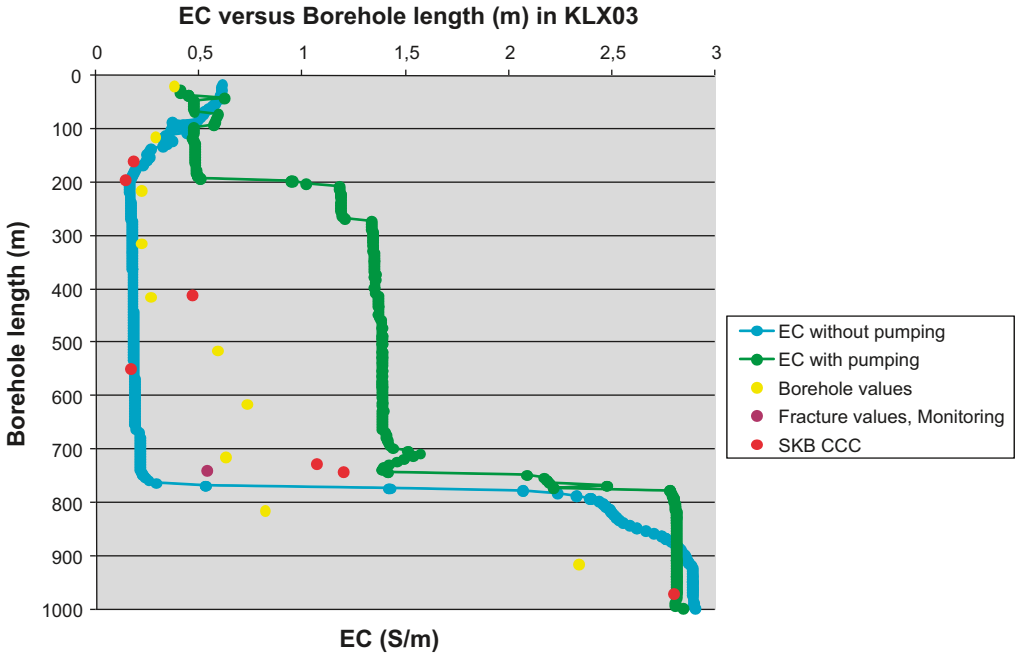

Figure 4-77. *Electrical conductivity measurements made during hydraulic logging of the freshly drilled borehole KLX03. The borehole values are compared with the conductivity of the samples taken after the hydraulic logging: 1) in the open borehole tube sampling (yellow dots), 2) with time series (red circles) taken during the complete chemical sampling (CCC) from fractures, and 3) the monitoring sections (brown) taken during the monitoring programme.*

tion of hydrochemical data which has undergone a rigorous quality check and categorisation; in other words a high degree of confidence. Coupled with the results of quality assured hydrogeological measurements and modelling, which in turn is based on geological models of high standard, the input ingredients to the hydrogeochemical visualisation should represent the best quality available at this moment of time. Uncertainties undoubtedly still remain, perhaps stemming from inadequacies in the geological model which may impact on the hydrogeological interpretation and possibly therefore on the integrity of the hydrogeochemical model and visualisation. However, the close agreement between all three disciplines indicates that the degree of uncertainty associated with the input data to the visualisation is low.

The upper 300–700 m of bedrock are fairly well characterised with corresponding low uncertainties. The main uncertainties are associated with the spatial lack of hydrochemical data, both laterally (particularly in the case of the porewater), and at depths greater than 700 m (particularly in the case of the fracture groundwater), such that a large degree of expert judgement has been used to extrapolate the hydrochemistry along the extent of the established cross-sections. There is, however, a greater geological and hydrogeological coverage documented to depth, in particular the latter, which has helped to extrapolate the hydrochemistry and porewater data, therefore reducing the uncertainties. Moreover, the uncertainties were further reduced with the realisation that at depths greater than 700 m, the fracture groundwater and porewater chemistries increase fairly uniformly in salinity and laterally appear to be quite homogeneous.

4.14.4 General confidence level

The following aspects of the hydrogeochemical model are associated with the highest confidence:

- The origin, major end members and major processes affecting the present water composition at the sampled locations.
- Current spatial distribution of groundwater types, even if the spatial resolution is relatively coarse.
- Existence of a redox transition zone detected in the fracture minerals.

The main reasons for this confidence are the many consistent time and spatial data to support the description concerning the origin, most of the major end members and major processes. Integration with hydrogeology supports the palaeohydrogeological description of the site. Various considerations such as reactive modelling, interpretation of different isotope ratios (Sr, S, C) buffer capacity measurements (Eh, pH) and microbial data support the process understanding.

The following aspects are associated with the lowest confidence:

- Understanding of measured levels of sulphide and ability to predict sulphide production.
- Undisturbed detailed groundwater composition at repository depth.
- Buffer capacity regarding Ca and Mg content under dynamic flow conditions.
- Detailed spatial variability and groundwater types associated with different rock domains. The results indicate poor correlation, possibly due to too few samples. The description is focussing on divisions into groundwater types.

The implications of these uncertainties need to be assessed in subsequent safety analysis within SR-Site.

5 Input from the hydrogeological modelling

5.1 Introduction

Close integration of hydrogeochemistry and hydrogeology is a necessary prerequisite to achieve site understanding. Hydrogeology requires hydrogeochemical information, for example, salinity distributions, groundwater end-member compositions, palaeohydrogeochemical input to help constrain model boundary conditions etc. Hydrogeology, on the other hand, can provide the groundwater flow parameters related to the geological framework so that the spatial distribution of hydrochemical signatures (laterally and vertically) can be interpreted and visualised. Within the SDM-Site Laxemar site descriptive modelling, the following steps have helped shape the interaction between hydrogechemistry and hydrogeology.

1) **Palaeo-conceptual model construction** for the site based on available Quaternary geological information. The model was used to set the boundary conditions for the hydrogeochemical and hydrogeological modelling.
2) **Parameter values and modelling results** such as major ions and isotopes and M3 mixing proportions were delivered to the hydrogeologists and used for flow model calibrations and comparisons.
3) **Collaboration** in the form of regular discussions focused on modelled output of boundary conditions and their relevance to the conceptual site modelling, and to the development of the palaeohydrogeological and palaeohydrogeochemical conceptual models.
4) **The Hydrogeochemical site descriptive model** is based on a common nomenclature of groundwater types and understanding of groundwater flow established through discussion and interaction.

5.2 Model interaction

Hydrodynamic assessment of the hydrochemical evolution is based on conservative hydrochemical constituents such as chloride and $\delta^{18}O$, and largely conservative constituents such as bromide. Chloride (and bromide) is used as an indicator of fresh versus saline water influences and $\delta^{18}O$, for example, is used to differentiate between glacial or marine waters. The predicted salinity distribution provides important feedback from hydrogeology and is used to understand the flow directions and salinity distribution in 3D and, consequently, provide support to the site descriptive hydrogeochemical models presented in Chapter 6. Outlined below are examples of hydrogeochemical input to the hydrogeological modelling.

Characteristic groundwater mixing features are illustrated in Figure 5-1 which plots $\delta^{18}O$ against elevation to show the distribution of cold climate input to the Laxemar bedrock. The glacial component, based on a cut-off of $^{18}O = < -13‰$ VSMOW, is characteristic and around 20–60% of glacial water seems to be present in many of the groundwater samples (cf Figure 4-22). This is also the case for many of the low category samples (Category 4 and 5) which have retained a glacial component despite dilution. The glacial component is detectable at the depth range 50–1,000 m but most prominent at the depth range of 300–600 m. It can also be added that the monitoring data from early 2008 and the new sampling of KLX27A confirms these observations.

The above observations at the Laxemar subarea indicate that the glacial water has not been affected by the Littorina Sea water influx to the same degree as was the case for Forsmark, or Äspö. The main hypothesis is that this was due to the fact that: a) the Laxemar subarea was not totally submerged by the Littorina Sea transgression, b) there was restricted access of the Littorina Sea to the Laxemar subarea along the bays and valley systems and this persisted for a relatively short time, and c) the Littorina Sea water in the valleys was diluted continuously by meteoric recharge run-off waters. This resulted in a diluted Littorina end-member water which was limited to the extent it could enter and move down through the bedrock by density intrusion, and become retained. Mixing with the brackish glacial groundwater was therefore either non-existent, i.e. at localities were the land had not been submerged, or at the most weak when emergence of the land occurred during uplift.

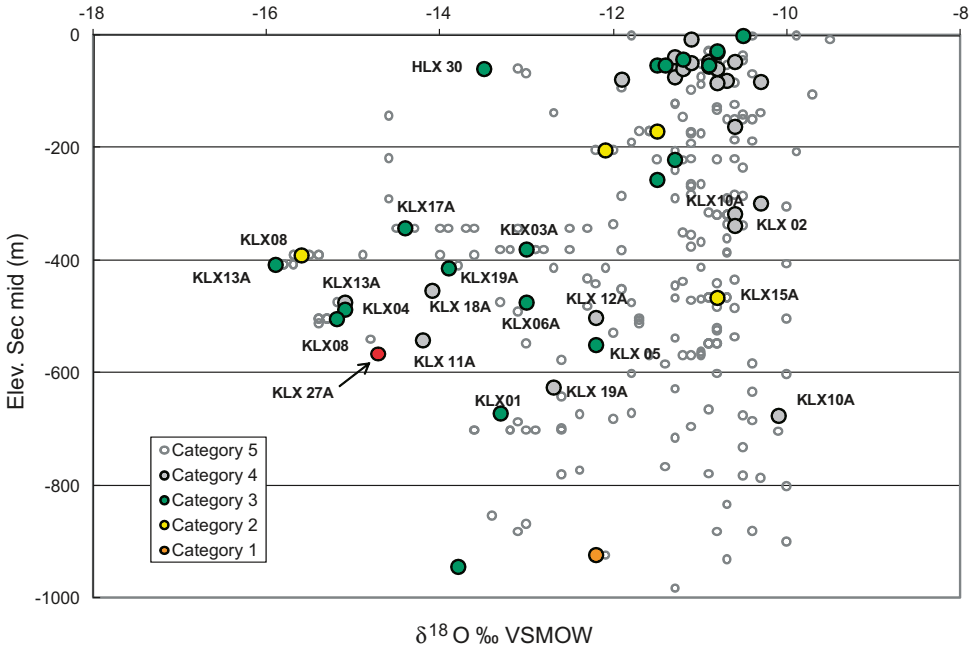

Figure 5-1. *$\delta^{18}O$ versus elevation based on Category 1-5 data from all percussion and cored boreholes. The results from the last borehole KLX27A also are included.*

Figure 5-2 a, b and c shows examples of hydrogeochemical and hydrogeological interaction, where modelled deep saline and mixing proportions of altered meteoric and glacial waters are the output from the hydrodynamic simulation model /Rhén et al. 2009/. The simulated proportions of these different input waters are displayed along a similar 2D cross-section to that used for the site descriptive model visualisation described in Chapter 6 (Figure 6-1). The realisations of deep saline groundwaters show similarities with the measured chloride and the mixing fractions of the Deep Saline end member (cf Figure 4-4 and Figure 4-21). The simulated distributions of the altered meteoric and glacial waters show similarities with the calculated mixing fractions of the same end members (cf Figure 4-22 and Figure 4-24). Overall, the description of the groundwater composition resulting from two independent modelling approaches is in general agreement, lending further confidence to the hydrogeochemical site description (cf /Rhén et al. 2009, Rhén and Hartley 2009/).

5.3 Reactive solute transport modelling

Coupled modelling of groundwater flow and reactive solute transport constitutes a powerful tool for quantitative integration of hydrogeological and hydrochemical understanding. For this reason, large scale and long term paleohydrogeochemical simulations have been performed by /Molinero et al. 2009/ based on key reactive transport processes that have influenced the Laxemar-Simpevarp area during the last 8,000 years. Two distinct flow regimes must be considered in order to simulate the hydrogeochemical evolution of the area since the last glaciation: a) Littorina Sea water intrusion (mainly density driven) into the bedrock containing previously infiltrated glacial meltwater, and b) meteoric flushing of the system (topographically driven) to present day conditions. The hydrogeochemical evolution of this long term, large scale and complex system has been numerically simulated by integration of the hydrogeological and hydrochemical models of the site. A comprehensive 3D hydrogeological model has been developed to simulate the groundwater flow evolution of the Laxemar area on a regional scale (hundreds of square kilometres) during the last 8,000 years /Hartley et al. 2007, Hunter et al. 2008/. This hydrogeological model corresponds to the regional model version 1.2. Note that the results have not been updated based on the current SDM-Site Laxemar flow modelling /Rhén et al. 2009/ and therefore are of more interest from a methodological rather than a quantitative point of view.

According to the current conceptual model for the site, it is thought that mineral dissolution/precipitation and cation exchange reactions are the main geochemical processes influencing the evolution of the major dissolved species and the pH of the system. The coupled modelling repro-

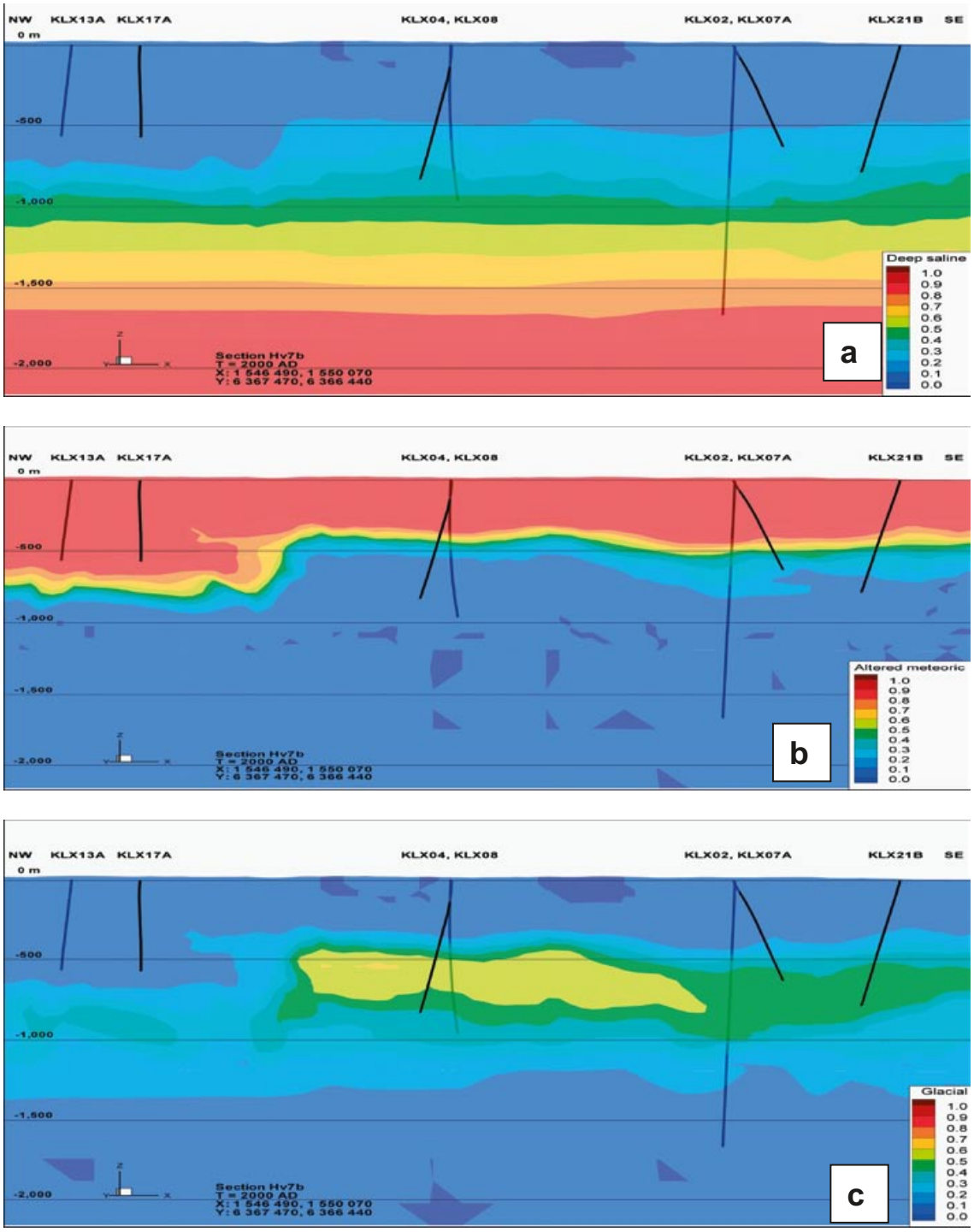

Figure 5-2. *Examples of information from the hydrogeological modelling studies used for calibrating the hydrogeochemical model: a) mixing proportions of deep saline, b) mixing proportions of altered meteoric water, and c) mixing proportions of glacial water /Rhén et al. 2009/.*

duces a granite weathering process typical of the shallow groundwater environment and shows the computed behaviour of some key minerals in the modelled domain. Carbonate evolution and silicate weathering processes are qualitatively well reproduced in this numerical transport model. Chlorite dissolution is computed simultaneously with quartz and clay minerals (illite) which are precipitating in the shallow part of the bedrock where the meteoric water undergoes water-rock interaction. These meteoric waters are close to equilibrium with respect to illite and quartz. However, the saturation state increases as a consequence of chlorite dissolution, and consequently there will be an increase of the silica and aluminium concentrations and pH values. The predictions during the time period 6000 to 2000 BC are presented in /Molinero et al. 2009/.

Figure 5-3 shows the comparison between: 1) computed results from conservative transport simulations, and 2) computed results of reactive transport simulations and measured values of pH and HCO_3^- concentrations; these two variables can be regarded as reactive indicators of the groundwater processes. Figure 5-3 is a qualitative illustration of the ability of coupled reactive transport numerical models to reproduce the hydrochemical behaviour of the groundwater system, and how these computed results can be improved upon, compared with the more static non-reactive solute transport models. The model takes into account matrix diffusion effects and the predictions of water conservative elements such as Cl and $\delta^{18}O$ are well predicted /Molinero et al. 2009/.

5.4 Concluding remarks

Interaction and integration between hydrogeochemistry and hydrogeology has been a common goal since the initiation of the site investigation programme in Laxemar. Important in the early stage was the use of a generalised palaeo-conceptual site model by the two diciplines which essentially was shared /Rhén et al. 2008, 2009/. As investigations progressed, hydrogeochemistry provided some insight into the present and past evolution of the different groundwater types within the approximate 0–1,000 m bedrock interval sampled in Laxemar. In turn, these observations provided an important platform for interaction for the hydrogeological modelling programme /Rhén et al. 2008, 2009/. From a hydrogeochemical perspective, the present hydrogeochemical site descriptive models discussed in Section 6 are the result of close hydrogeological interaction, where input concerning confirmation of flow directions, flow properties and possibilities to maintain different water types in the bedrock, have been of great importance in supporting the modelling results.

A more quantitative integration of hydrogeology and hydrochemistry has been done by means of combining hydrogeologic models with geochemical reactive transport processes. Computed model results have been checked by comparison with measured concentrations of major dissolved species. The results show that reactive transport simulations can reproduce most of the qualitative trends and characteristics observed in the hydrochemical data of the major components. It is worth noting that the reactive solute transport models have not been calibrated and/or adjusted to fit measured data. The current results can be seen as a first step towards a quantitative integration exercise of the hydrogeological and hydrochemical conceptual models of the site. Further applications of the model could be carried out by including, for example, the redox sensitive processes.

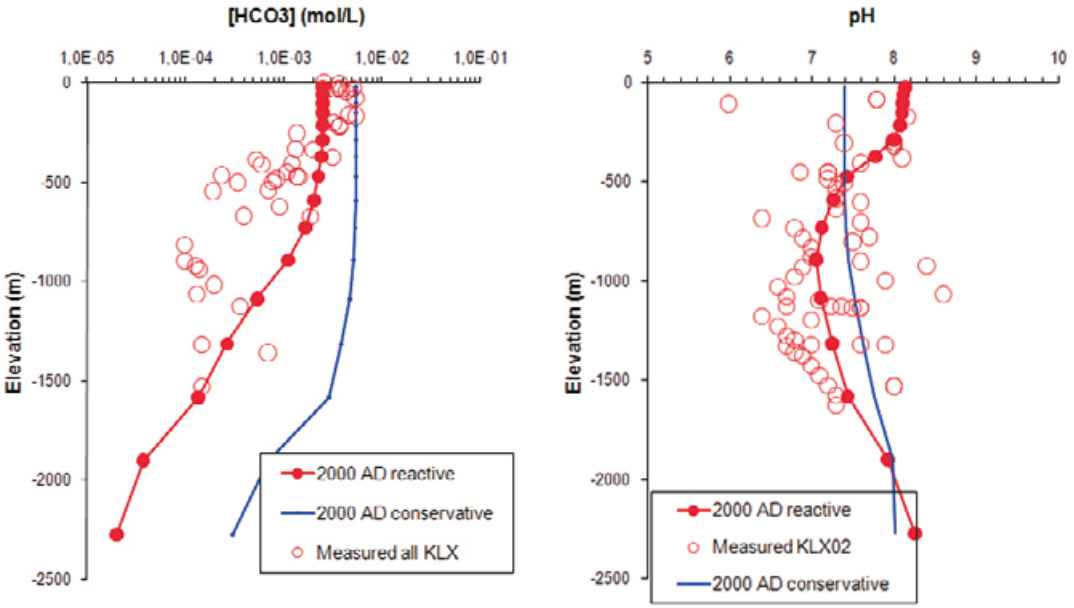

Figure 5-3. *Computed and measured concentrations of HCO_3^- (left) and pH (right) along a vertical profile located in the middle of the model domain. Computed results of a conservative transport run (blue) and a reactive transport run (red) are plotted to evaluate the influence of the geochemical processes on the dissolved concentrations.*

6 Hydrogeochemical site description

6.1 Introduction

The main aim of the hydrogeochemical site descriptive model is to present an understanding of the site based on measurements and model contributions described in the previous chapters. The site descriptive model is a combination of a quantitatively derived hydrogeochemical model (e.g. based on site measurements) and a qualitatively derived hydrogeochemical model (e.g. more descriptive, process-oriented conceptual model). The main objective is to describe the chemical composition and distribution of the groundwater and porewater in the bedrock and the groundwater close to the interface between bedrock and the overburden, and the hydrogeochemical processes involved in its origin and evolution. This description is based primarily on measurements of the groundwater composition, but also incorporates the use of available geological and hydrogeological site descriptive models. The description also serves as the basis for possible hydrogeochemical simulations of the palaeohydrogeochemical evolution of the site and also to predict future changes.

In this chapter, the Laxemar subarea hydrogeochemical site descriptive model, and its extension to the Simpevarp subarea, is presented together with a concluding summary of the main hydrogeochemical properties and characteristics of the Laxemar-Simpevarp area.

6.2 Hydrogeochemical visualisation

The Laxemar subarea 2D visualisation is based on the selection of five cross-sections that best represent the integration of geological and hydrogeological understanding, and the available hydrochemical data. Presented below are the three most illustrative examples which correspond to cross-sections #3, #2 and #5 presented in Figure 2-11 (cf Section 2.2.4), and these are illustrated in Figures 6-1, 6-2 and 6-3 respectively.

To provide a more realistic visualisation of groundwaters in a fractured crystalline rock environment (i.e. to avoid giving a porous medium impression to the bedrock), the groundwater types are shown confined to the major water-conducting fractures and deformation zones. The various groundwater types within these zones are colour coded and the transition from one groundwater type to another is indicated as being gradual and diffuse.

Cross-section #3 in Figure 6-1 has already featured in the Laxemar 1.2 and Laxemar 2.1 hydrogeochemistry model versions because of its orientation approximating to the west to east regional groundwater flow direction, and it also includes the Simpevarp subarea. This provides the opportunity to visualise changes in groundwater chemistry from recharge conditions to the west to discharge at the coastal margin to the east. Furthermore, this section is closely similar to the corresponding hydrogeological cross-section (denoted as # 7) used in the hydrogeological modelling, therefore allowing direct comparison between simulated (i.e. modelled) and measured values of, for example, Cl and $\delta\,^{18}O$.

6.2.1 Groundwaters

In the west and central part of the Laxemar subarea (Figure 6-1, NW-SE part of the cross-section), which exemplifies largely recharge conditions, the upper bedrock (down to about 100 to 250 m depth) is characterised by fresh, recharge waters. Some mixed type groundwaters are also present where the fresh waters have been influenced locally by brackish and glacial components and sometimes by a weak marine component derived from residual groundwaters in the overburden.

From about 250 m to 900 m depth brackish groundwaters (200 to 10,000 mg/L Cl) dominate, comprising mixtures of brackish non-marine groundwaters (present before the last deglaciation) with waters introduced during and after the last deglaciation. Of the latter types, brackish glacial groundwaters of variable distribution and salinity (and referred to as ‘a series of heterogeneous lenses’) are common in the Laxemar subarea, especially in the central, west and northwestern parts.

They occur mostly about the 300 to 600 m depth interval, but deeper occurrences are observed in borehole KLX04 down to about 900 m depth and also much shallower occurrences above 100 m. These shallow occurrences, together with other examples in the area at depths less than 250 m, may reflect preserved isolated pockets or lenses of glacial type water in rock volumes of lower hydraulic conductivity. In the southeastern part of the Laxemar subarea, of lower topography and closer to the coast, some of the groundwaters between about 250 to 600 m depth show weak Littorina signatures.

There are two main possibilities to explain the anomalously deep occurrence of brackish glacial groundwaters in borehole KLX04 that do not necessarily exclude each other: 1) borehole KLX04 may have been influenced during pump tests and sampling activities by short circuiting along sub-vertical fracture zones located close by, thus drawing down brackish glacial mixtures to greater depths, and 2) the same sub-vertical zones may have provided fast conduits to glacial meltwater movement at high confining pressures through the bedrock to greater than normal depths. However, it can not be excluded that if some of the other boreholes had been drilled to greater depths (> 1,000 m), they may have intercepted brackish glacial groundwaters similar to borehole KLX04. All three scenarios are possible, although present data suggest that deep penetration of glacial meltwaters greater than about 600 m is not common.

The majority of observations, both hydrochemical and hydrogeological, indicate that at about 600 m there is a change from intermediate to low flow conditions that persist to around 900 m depth. Within this approximate 600 to 900 m interval, which is dominated by brackish non-marine groundwaters, minor glacial components are observed but these may not necessarily represent the last deglaciation.

The transition from brackish non-marine to saline groundwaters occurs at about 900 m and continues to about 1,200 m. This saline type also appears to include minor glacial components even though chorine-36 dating supports a very old age for these groundwaters (hundreds of thousands of years, cf Section 4.10.4). Finally, at about 1,200 m, only observed in borehole KLX02, there is a transition to highly saline groundwaters at very low flow to effectively stagnant conditions where there is no evidence of glacial influence as indicated from the stable isotope data.

This described stratification of different groundwaters in the Laxemar subarea correlates generally with the hydrogeological depth zones employed in the hydrogeological DFN model (/Rhen et al. 2008/, and cf Section 2.3.3) i.e. at elevations 0 to –150 m, –150 to –400 m, –400 to –650 m, and > –650m.

In the Simpevarp subarea, (Figure 6-1, W-E part of the cross-section), the general groundwater compositional stages are also evident but appear to occur at shallower depths, i.e. brackish glacial groundwaters at about 100 to 300 m depth, the transition from brackish non-marine to saline groundwaters at around 500 m, and saline to highly saline groundwaters at 900 to 1,000 m depth. This probably reflects discharge conditions close to the Baltic Sea coastline as supported by the hydrogeological model /Rhén et al. 2009/. Another aspect that differentiates the Simpevarp and Laxemar subareas is the presence of a stronger Littorina Sea signature in Simpevarp, since this area is topographically low, was submerged for a much longer time period by the Littorina Sea, and subsequent flushing has been less efficient and is still on-going.

The visualisation shown in Figure 6-1 is based on a NW-SE cross-section (cf Section # 3; Figure 2-11) selected to approximately conform to the regional groundwater flow direction. Earlier versions of this section have been described in /SKB 2006ab/. This present version, based on more hydrochemical data and better hydogeological understanding, tries to capture the main groundwater components and their distribution within the Laxemar-Simpevarp area. In particular, the complex brackish groundwater interval from about 100 to 900 m (200 to 10,000 mg/L Cl) is subdivided into Brackish glacial (BG) and Brackish non-marine (BNM) groundwater types, with the presence of weak Littorina components in both groundwater types indicated by BG+L and BNM+L respectively (where the low order ‘L’ indicates a still weaker Littorina component). Where there is an absence of data, the possibility of brackish glacial is indicated by ‘BG?’ and of possible brackish non-marine by ‘BNM?’

At shallower depths (above 250 m) Fresh groundwater is denoted by ‘F’ and where there is a brackish glacial component by ‘F+G’. At the deepest levels, Saline and Highly Saline groundwaters are indicated by ‘S’ and ‘HS’ respectively, with probable locations indicated by ‘S?’ and ‘HS?’.

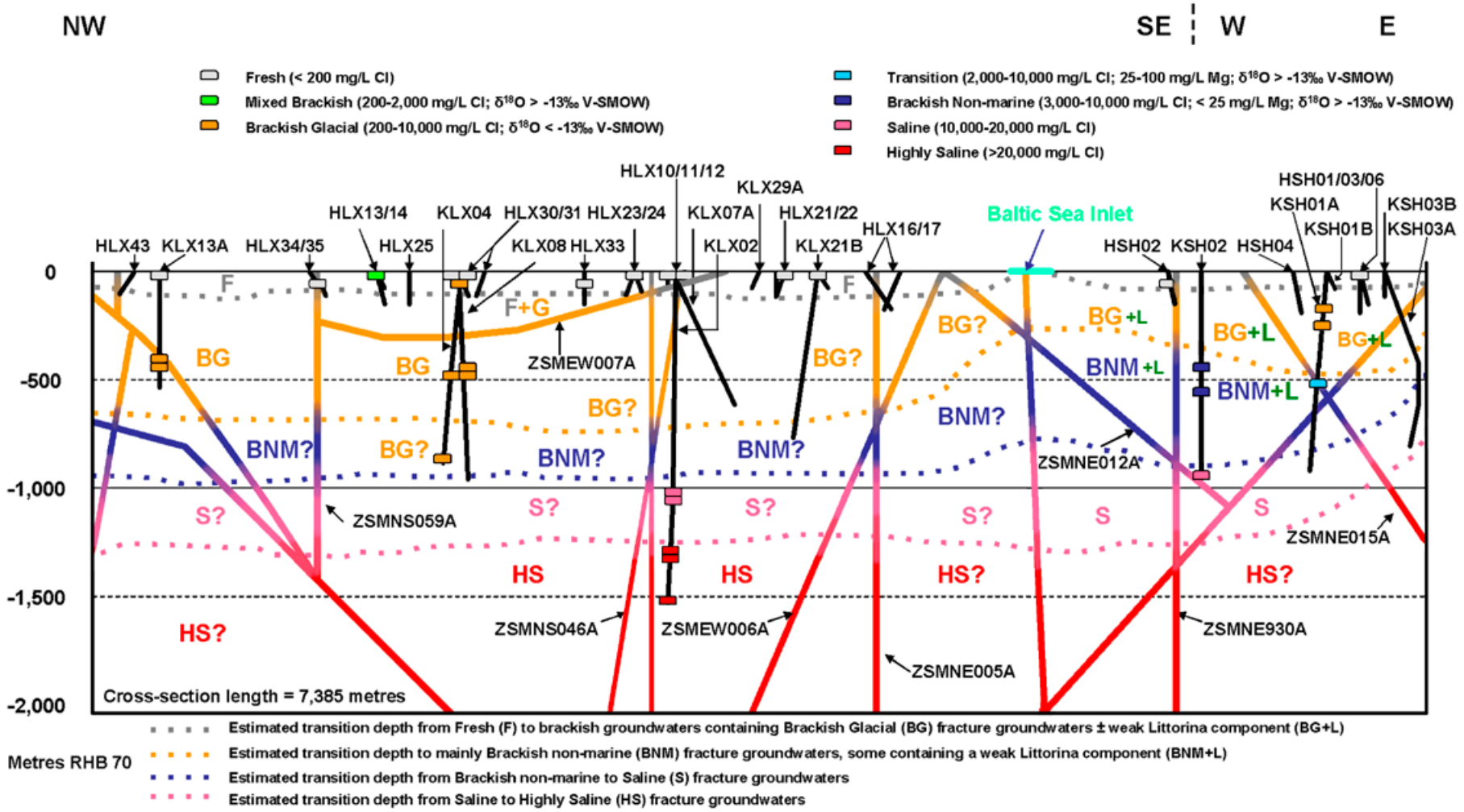

Figure 6-1. *Approximately NW-SE/W-E cross-section through the Laxemar-Simpevarp area (cf cross-section # 3 in Figure 2-11 for location). The visualisation is based on a 0 to –1,100 m RHB 70 vertical scale. Shown are: a) the location of the boreholes and the sections which have undergone hydrochemical sampling, b) the main fracture groundwater types (colour coded) which characterise the site, and c) the chloride distribution with depth along the major deformation zones. The dotted lines in different colours represent the approximate depths of penetration of the various fracture groundwater types along hydraulically active deformation zones. The main regional groundwater flow direction is from the west (recharge) to the east (discharge), approximately parallel to the section. (Cross-section length = 7,385 metres).*

These general observations are supported by the additional cross-sections (#2 and #5) shown in Figure 6-2 and Figure 6-3 below. The legend included in Figure 6-1 describing the different groundwater types applies also to the other two cross-sections.

The location of the brackish glacial groundwaters which characterise the central part of the Laxemar subarea visualised in Figure 6-1 is based on few measured data. The extent of the brackish glacial groundwaters is largely derived therefore from cross-section #2 visualised in Figure 6-2 which also traverses the central and western part of the Laxemar subarea, providing a much better spatial coverage of the groundwater chemistry. Noticeable is the dominance of the brackish glacial groundwaters and their distribution both laterally and vertically (with the exception of borehole KLX04). Also noticeable is the irregular distribution of the shallow fresh groundwaters and the presence of 'mixed types' close to the surface which may reflect localised and shallow recharge/discharge groundwater pathways which typify much of the Laxemar subarea. Only one data point exists for each of the brackish non-marine and saline groundwaters, and no data for the highly saline groundwaters. Once again, measured data from other sections (in this case Figure 6-2 and Figure 6-3) has helped to provide approximate transition depths between these groundwater types. Because of the low flow and stagnant groundwater conditions at depths of about 900 m downwards, extrapolation is much easier than in the shallow to intermediate depths which are more dynamic hydraulically.

Figure 6-3 (cross-section #5 in Figure 2-11) was chosen also to cover the western and southern parts of the Laxemar subarea (W-E part of the cross-section), in particular the southeastern part where a weak Littorina component resides in borehole KLX15A (associated with both brackish non-marine and brackish glacial groundwaters denoted by BNM+L/BNM$_{+L}$ and BG+L/BG$_{+L}$ respectively) and a very weak component in borehole KLX12A (associated with a brackish non-marine groundwater). The increased salinity trend to shallower depths to the east is similar to that shown in Figure 6-1 and represents a groundwater discharge feature towards the Baltic Sea coast in the Simpevarp subarea.

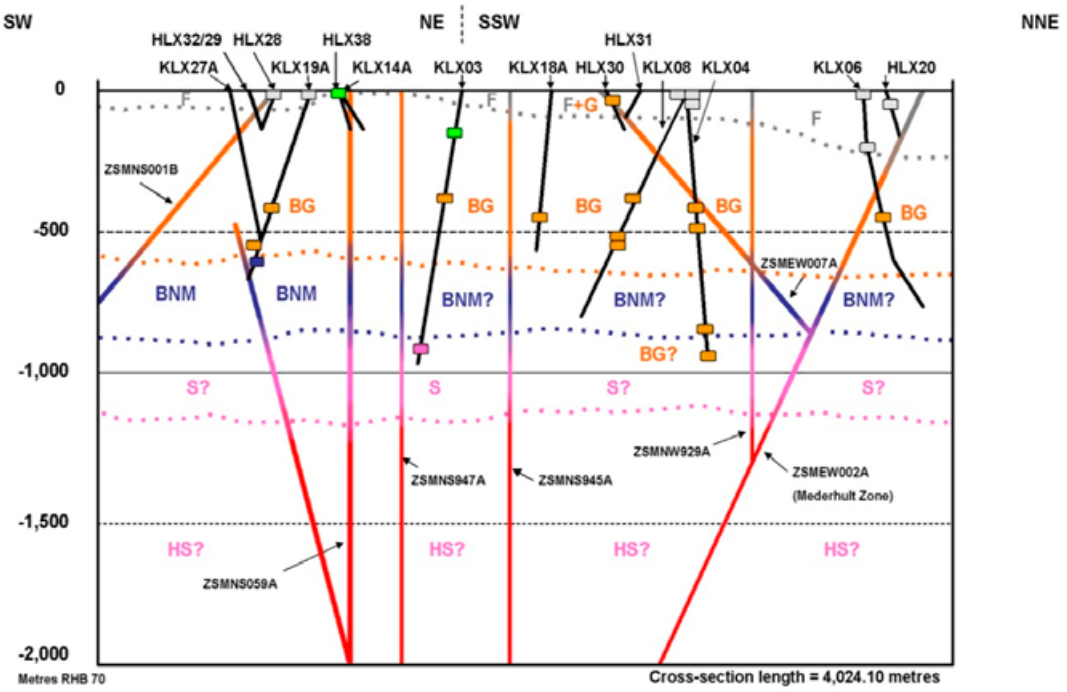

Figure 6-2. *Approximately NNE-SSW/NE-SW cross-section #2 through the north and west central part of theLaxemar subarea (cf Figure 2-11 for location). Shown are: a) the location of the boreholes and the borehole sections which have undergone hydrochemical sampling, b) the main fracture groundwater types (colour coded) which characterise the site, and c) the chloride distribution with depth along the major deformation zones. The dotted lines in different colours represent the approximate depths of penetration of the various fracture groundwater types along hydraulically active deformation zones. The main regional groundwater flow direction is into the plane of the cross-section from the west (recharge) to the east (discharge). (Cross-section length = 4,024 metres). Note: Data from borehole KLX27A have been used as support to delineate the extent of the brackish glacial groundwater.*

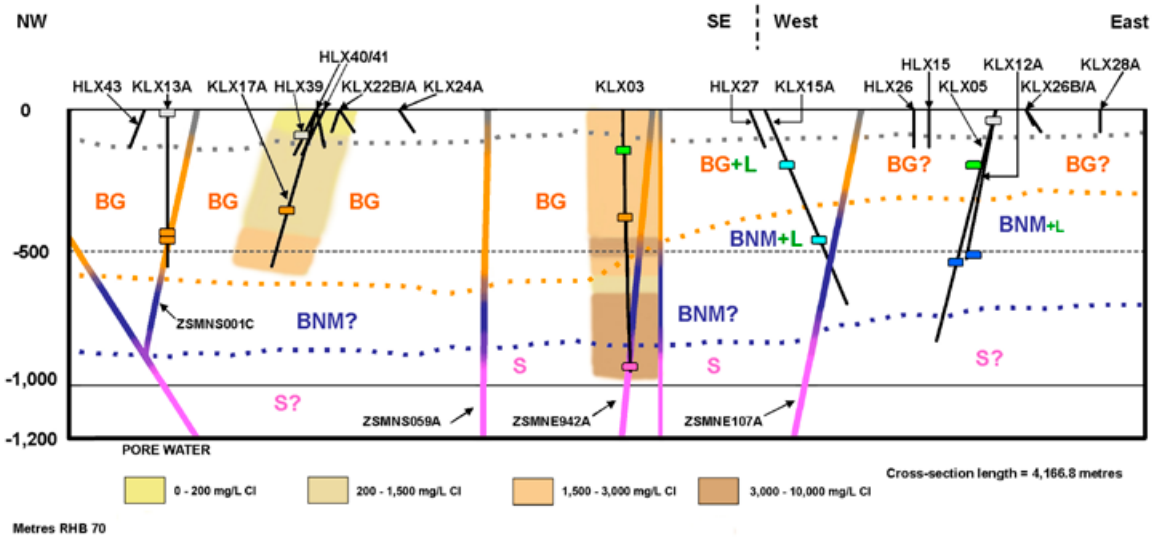

Figure 6-3. *Approximately NNW-SSE/W-E cross-section #5 through west central Laxemar to its eastern margin (cf Figure 2-11 for location). The visualisation is based on a 0 to –1,100 m RHB 70 vertical scale. Shown are: a) the location of the boreholes and the borehole sections which have undergone hydrochemical sampling, b) the main fracture groundwater types (colour coded) which characterise the site, c) the chloride distribution with depth along the major deformation zones, and d) the porewater chloride variation along boreholes KLX17A and KLX03. The dotted lines in different colours represent the approximate depths of penetration of the various fracture groundwater types along hydraulically active deformation zones. The main regional groundwater flow direction is from the west (recharge) to the east (discharge), approximately parallel to the section. (Cross-section length = 4,167 metres).*

6.2.2 Porewaters

Porewater data are available from three boreholes, KLX03, KLX08 and KLX17A, and are presented and described in Section 4.9. Because of limited data it is not possible to accurately establish the lateral spatial distribution of the porewater chloride compositions, and the vertical distribution is very much influenced by the nearest deformation zone. These porewater data are therefore visualised independently along the three investigated boreholes, two of which (boreholes KLX17A and KLX03) are shown in Figure 6-3. Of importance is that the changes in the chloride content with depth described for the different groundwater types in Section 6.2.1 are qualitatively supported by the porewater data, which in turn are influenced by the decrease in hydraulic conductivity (i.e. decrease in the frequency of open, water-conducting fractures) with depth.

6.3 Summary of site hydrogeochemical properties

In order to describe the groundwater system at Laxemar specific depth intervals are selected based on both hydrochemical and hydrogeological considerations. These intervals are: Near surface waters (0 to 20 m), shallow groundwaters (20 to 250 m), intermediate groundwaters (250 to 600 m), deep groundwaters (600 to 1,200 m) and very deep groundwaters below 1,200 m. The major hydrogeochemical characteristics are summarised in Table 6-1.

Near surface waters (0 to 20 m)

This depth interval is hydrogeologically active and dominated by recharge meteoric water or ***Fresh groundwater*** *(< 200 mg/L Cl) of Na-Ca-HCO_3 (SO_4) type showing large variations in pH and redox conditions. Available information is mainly from data collected in soil pipes which reflect effects from reactions and local mixing /Tröjbom et al. 2008, Gimeno et al. 2009/.*

The waters are usually high in tritium and some even show a slight annual variation in $\delta^{18}O$ values indicating that the average residence time for the near surface waters in the overburden is short, within a year to decades. In addition, some residual brackish near surface groundwaters

Table 6-1. The major hydrogeochemical characteristics.

Water types	Redox Reactions at present	Redox buffer	pH Reactions at present	pH buffer	Ion exchange	Ion exchange buffer	Precipitation/ dissolution reactions	SO_4^{2-}/S^{2-}
Surface and near surface waters 0–20 m Fresh waters of Na-HCO_3 type. Modern waters with high tritium	Fe(II) minerals →Fe^{3+} Organic degradation Aerobic/anaerobic microbial reactions Sulphate reducers (SRB)? Iron (III) reducers (IRB)?, Manganese (IV) reducers (MRB) Probably also methanogens	*Soil.* Organic matter Fe(II) min, Chlorite, Vermiculite, Biotite, Amphibole *Bedrock:* Biotite *Fracture minerals:* Fe(II)–min; Chlorite, Clays, (Pyrite)	Organic decay Calcite dissolution Aluminosilicate weathering Microbes	Organic decay Calcite dissolution Aluminosilicate weathering Microbes	Na/Ca Na to solution Ca to solid	*Soil:* Clay minerals, Vermuculite, Illite, Micas *Bedrock:* Biotite, Micas	Dissolution of calcite, silicates Fluorite	Sulphate: Pyrite dissolution, Sea Spray, Atmospheric deposition, leaching of marine sediments. Sulphide: Microbial S^{2-} production
Shallow groundwaters 20–250 m Fresh to mixed groundwater types. Partly modern waters with Tritium 0–12 TU. A few brackish glacial groundwaters and at Simpevarp also a weak brackish marine input.	Anaerobic system Decrease in oxidation of Fe(II) minerals Identified SRB, IRB, MRB Organic material and dissolved sulphate.	*Bedrock:* Micas *Fracture minerals:* pyrite,Fe(II) chlorite and clay minerals Dissolved; SO_4^{2-} Organic material	Calcite control Reactions with aluminosilicates Microbes	Calcite control Reactions with aluminosilicates Microbes	*Laxemar:* Na/Ca Na to solution Ca to solid *Simpevarp (Littorina mixing):* Na, Mg, K to solid Ca to solution	*Bedrock:* Micas *Fracture minerals*: Clay minerals Mixed layer clays (corrensite), illite	Equilibrium with fluorite, quartz, calcite	Sulphate: Leaching of marine sediments, Atmospheric deposition, Littorina influence. Sulphide: Microbial S^{2-} production
Intermediate groundwaters 250–600 m Mixed-brackish glacial, brackish non-marine in type. Low or absent tritium – detectable ^{14}C ages down to 500 m (last deglaciation and Holocene)	Organic material and dissolved sulphate Fe (III) minerals Microbial reactions SRB, IRB? Autotrophic Acetogens (AA) and Heterotrophic acetogens (HA), Methanogens (~ 400m depth) Equilibrium with FeS (am).	*Bedrock:* Micas *Fracture minerals:* pyrite, Fe(II) and Fe(II) chlorite and clay minerals etc. Dissolved: SO_4^{2-} Organic material Gases: CH_4, H_2	Calcite control Reactions with aluminosilicates Effect of microbes?	Calcite control Reactions with aluminosilicates Effect of microbes?	*Laxemar:* Na/Ca Na to solution Ca to solid *Simpevarp (Littorina mixing*): Na, Mg, K to solid Ca to solution	*Bedrock::* Micas *Fracture minerals*: Clay minerals Mixed layer clays (corrensite), illite	Equilibrium with fluorite, quartz, calcite Dissolution of gypsum	Sulphate: Dissolution of gypsum, Littorina influence in some waters Sulphide: Microbial S^{2-} production.
Deep groundwaters 600–1,200 m. Mainly brackish to saline non-marine waters. In addition some samples show a glacial input and a few indicate a weak marine input. Mainly older than 10,000 y.	Decreasing amount of organic material and dissolved sulphate. Microbial reactions Mainly SRB and AA and HA,	*Bedrock*: Micas *Fracture minerals:* Fe(II) minerals, pyrite Dissolved: SO_4^{2-} Gases: CH_4, H_2	Calcite control Reactions/equilibria with aluminosilicates Effect of microbes?	Calcite control Reactions/ equilibria with aluminosilicates Effect of microbes?	Small effect compared to mixing in the more saline groundwaters	*Bedrock*:: Micas *Fracture minerals*: Clay minerals Mixed layer clays (corrensite), illite	Equilibrium with fluorite, quartz, calcite Dissolution of gypsum	Sulphate: Dissolution of gypsum, Littorina influence in some waters. Sulphide: Microbial S^{2-} production Decreasing with depth.
Deep groundwaters > 1,200 m Highly saline, near stagnant to stagnant conditions. Older than 1.5 Ma based on ^{36}Cl.	Possible microbial reactions AA? AM? Gases:H_2 and CO_2	*Bedrock*: Micas *Fracture minerals:* Possibly less clay minerals, chlorite and pyrite Gases:CH_4, ,H_2	Calcite control Aluminosilicates equilibrium (albite, K-spar) Effect of microbes?	Calcite control Aluminosilicates equilibrium (albite, K-spar) Effect of microbes?	Small compared to mixing	Possibly less clay, chlorite and pyrite	Equilibrium with fluorite, quartz, calcite and gypsum	Relatively high sulphate in the deep waters due to gypsum equilibrium. Low sulphide

have been found in soil pipes located in till below lakes and sea sediments at Lake Frisksjön and Granholmsfjärden Bay. These waters are characterised by a strong marine influence (Baltic?) and/or by discharging deep groundwaters related to the main fracture zones in the area, which can indicate possibly longer residence times compared with other near surface groundwaters.

Based on groundwater observations and modelling, the hydrogeochemical evolution of the near surface groundwater is mainly determined by weathering reactions triggered by biogenic CO_2 input derived from organic matter decay (e.g. plant debris) and root respiration, clearly indicated by elevated bicarbonate. This input of CO_2 promotes a pH decrease and a CO_2 partial pressure increase in the waters, which may favour the dissolution of aluminosilicate mineral phases and carbonates (if present in the system) /Gimeno et al. 2009/. The result of these reactions is the release of cations (Na, Ca, Mg, K, etc), silica and increased alkalinity. Modelling indicates also that sodium, potassium and magnesium concentrations are mainly controlled by the incongruent dissolution of aluminosilicates and ion exchange processes. Dissolved calcium shows maximum concentrations of around 100 mg/L, although values recorded are usually below 80 mg/L. Calcite dissolution/precipitation, aluminosilicate weathering, fluorite equilibrium and cation exchange reactions control the calcium content in the near surface groundwaters. Bicarbonate reaches maximum concentrations of around 550 mg/L and calcite equilibrium is only achieved in groundwaters with the largest bicarbonate contents. Overall, calcite appears to contribute to the chemical and carbon isotopic character of these groundwaters more than what was expected as only small amounts of this mineral have been detected in the Laxemar-Simpevarp overburden (i.e. considerably smaller than in Forsmark).

Dissolved sulphate contents are always below 200 mg/L in these fresh groundwaters. The SO_4^{2-}/Cl ratio in most samples is greater than the sea water ratio and therefore a pure marine origin is not the sulphate source. The main processes controlling the sulphate concentrations seem to be pyrite oxidation, atmospheric deposition or direct influence from sea water deposition (sea spray), as well as the existence of microbial sulphate reducing activity.

Greater values and variability of silica and fluoride concentrations have been found in the near surface groundwaters of Laxemar-Simpevarp compared with other groundwater systems such as Forsmark. This would indicate a more important presence of easily alterable silica and fluoride-bearing minerals, and/or a more intense weathering in the Laxemar-Simpevarp overburden. Dissolved fluoride is mainly controlled by hornblende and mica dissolution but also fluorite participates as the solubility-limiting phase. Modelling indicates that dissolved silica concentrations are mainly controlled by the incongruent dissolution of aluminosilicates. Chalcedony and quartz are not the solubility-limiting phases for silica as they are oversaturated in most near surface groundwaters.

The variable and sometimes highly dissolved ferrous iron, sulphide and manganese concentrations indicate the presence of anoxic environments. This means that ongoing biogenically mediated reductive dissolution of Fe-silicates (e.g. Fe^{3+}-bearing clay minerals) or ferric and manganese oxyhydroxides (post-oxic environment), and bacterial S^{2-} production (sulphidic environment) take place already in the very shallow parts of the system. For example, complete redox sequences (from oxic to post-oxic, sulphidic and methanic environments) can be observed in soil profiles at scales of centimetres or metres. Different bacterial metabolic activities (IRB, MRB and SRB) may contribute to the dissolved ferrous iron, sulphide and manganese concentrations. However, inorganic processes are also involved in the control of these elements, such as reduction of ferric and manganese oxyhydroxides by dissolved sulphides as well as siderite and rhodochrosite equilibrium or iron monosulphide precipitation.

In the bedrock below outcrops devoid of overburden sediments, the reducing capacity is lower and oxygenated waters may reach greater depths. The occurrence of recent, low temperature Fe-oxyhydroxides (and other redox indicators, cf Section 4.8) indicates that the present redox front in the Laxemar subarea is located at about 20 m depth, followed by a zone reflecting seasonal and annual variations in recharging waters that usually extends to about 60 m depth. In any case, these oxidising pulses have not been intense enough to exhaust the reducing capacity of fracture filling minerals except for the shallowest parts of the rock.

No matrix porewater data are available from these very shallow levels.

Shallow groundwaters (20 to 250 m)

*This depth interval is dominated by **Fresh–Mixed brackish – (Brackish glacial)** groundwaters of Na-Ca-HCO_3 (SO_4) to Na-Ca-Cl-HCO_3 type, showing a transition to stable reducing conditions with increasing depth. The residence times of the groundwaters are in the order of decades to several thousands of years, and remnants of glacial water are a strong indication that occasionally groundwaters older than 14,000 years are still retained.*

These groundwaters are influenced by an active flow system where a large percentage of *Fresh groundwater* has persisted to varying depths depending on whether local recharge or discharge conditions prevail. These waters, compared with the near surface groundwaters, show almost the same chemical variability in the dissolved contents of major ions except for silica (lower) and fluoride (higher). This suggests a continuous weathering profile (i.e. water-rock dominated evolution) from the near surface recharge waters towards the deeper bedrock zones. The 20 to 250 m bedrock interval is also influenced by *Mixed brackish groundwaters* (260 to 840 mg/L Cl and 5 to 25 mg/L Mg) resulting from mixing with remnants of marine waters (e.g. the groundwater sampled in borehole HLX38). There are also sporadic occurrences of *Brackish glacial groundwaters* which are tritium free and depleted in $\delta^{18}O$ (–13.5‰ VSMOW). The ^{14}C contents below 40 pmC in these waters are indicative of longer residence times compared with other groundwater samples from similar depths (e.g. HLX30: –60.4 m elevation).

Incongruent dissolution of aluminosilicates and equilibrium with calcite, fluorite and quartz, are the main reactions controlling the major chemical contents. Ion exchange can also be important due to the input of dilute recharge waters at Laxemar and in association with Littorina Sea water influences at Simpevarp (cf Table 6-1).

The redox conditions in the upper 50 m or occasionally even down to 100 m depth probably vary, although accurate measurements do not exist and the depth resolution of the analysed samples does not allow more specific conclusions about conditions in the near surface part of the bedrock. However, such information can be obtained from the analysis of fracture minerals. For example, uranium-decay series analyses of fracture filling materials indicate a switch from mainly uranium removal (oxidising conditions) to mainly deposition (reducing conditions) occurring in the upper 100 metres of the bedrock.

The few data that exist for the redox characterisation of the groundwater are from depths greater than 150 m. At these depths potentiometrically measured Eh values are between –250 and –280 mV, indicating clearly reducing conditions in these dilute groundwaters. Contents of ferrous iron and sulphide in the groundwaters confirm the occurrence of post-oxic and sulphidic environments. Thus, all the data support the potential of microbial or water-rock interaction processes to create very reducing conditions already in the shallow parts of the system. The bedrock fractures at Laxemar contain the widespread presence of Fe(II) and Fe(III) minerals which play a fundamental role in the overall reducing capacity of the system. The reduction of iron and manganese are usually microbially mediated and iron- and manganese-reducing bacteria are commonly identified. Readily available Fe-oxyhydroxides are identified in the upper 100 m with potential single occurrences also at greater depths. The Mn-oxides in contrast appear to be less common and are only identitified in the upper 20 m of the fracture system. These phases are favourable for the activity of the iron- and manganese-reducing bacteria.

Porewater samples from the bedrock representing this depth interval are typically of dilute Na-HCO_3 chemical type with chloride contents of less than 1,000 mg/kg and isotope signatures ranging from present day infiltration to old meteoric water representing cool to temperate past climatic conditions. The porewaters are generally close to equilibrium with the surrounding fracture groundwaters.

Intermediate depth groundwaters (250 to 600 m)

*This depth interval is dominated by **Brackish glacial – Brackish non marine – Transition** groundwaters of Na-Ca-Cl-(HCO_3) type. Redox conditions are reducing and low Eh values (–245 to –303 mV) are typically controlled by the interplay between the iron and especially the sulphur systems. The significant portions of glacial waters at this depth interval, and the significant increase of non-marine groundwaters with depth, indicate that groundwaters older than 14,000 years are becoming increasingly important.*

The depth interval 250 to 600 m (of intermediate transmissivity) is characterised mainly by groundwaters with a glacial component recognised by their low $\delta^{18}O$ (< –13.0‰ VSMOW). This groundwater type is accordingly named *Brackish glacial* and is most common at around 300 to 600 m depth and shows a variable chemical composition resulting from different degrees of mixing with previously present *Brackish non-marine* groundwaters in the bedrock. In most cases the glacial waters are from the last deglaciation, but contributions from older glaciations cannot be excluded. Groundwaters labelled *Transition* groundwater types also characterise this depth interval. They have similar chloride contents (from 2,000 to 5,900 mg/L) as the brackish non-marine waters (mainly found at around 500 to 600 m depth), but are distinguished by their higher magnesium, potassium and $\delta^{18}O$ values, which suggest a weak brackish marine component, probably derived at localities affected by the Littorina Sea transgression.

Even though the overall compositional evolution of these intermediate groundwaters is mainly determined by mixing processes, different chemical and microbial reactions control the pH and redox conditions. Calcite equilibrium (the main pH control), fluorite and quartz equilibrium (controlling dissolved fluoride and silica) and gypsum dissolution are important chemical reactions. The bicarbonate contents of these groundwaters decrease in this depth interval and are generally low (below 50 mg/L) at depths greater than 500 m, indicating a transition to a less dynamic hydraulic regime deformation zones of lower hydraulic conductivity when approaching 500 to 600 m depth. High bicarbonate contents are mainly attributed to a temperate meteoric component and radiocarbon studies of the organic/inorganic carbon phases show that the carbon inventory present in the shallow to intermediate groundwaters is primarily post glacial. Additional sources and sinks for dissolved major components include the reaction with aluminosilicates, and cation exchange resulting from dilution with glacial meltwaters or increased concentration of Littorina waters.

All measured Eh values in these brackish groundwaters are clearly reducing (–245 to –303 mV), even in some very dilute short circuited groundwaters. The redox conditions seem to be mainly controlled by the interplay between the iron and sulphur systems that promote these reducing groundwater conditions at Laxemar (and Simpevarp). Measurable sulphide contents are present in most of the sections sampled but the representativity of the actual values are uncertain. Results from the monitoring programme indicate that the amounts of measured dissolved sulphide may be affected to an unknown extent by groundwater disturbances during sampling operations. However, despite this uncertainty, the presence of dissolved sulphide and sulphate-reducing bacteria (SRB), as well as the existence of equilibrium conditions with respect to amorphous ferrous iron monosulphides, indicate the presence of on-going sulphate reduction processes and the existence of clearly sulphidic environments. The key role played by SRB is also supported by the high $\delta^{34}S$ values and low SO_4 contents in many groundwater samples from about 100 to 450 m depth. Furthermore, isotope analyses of fracture pyrite indicate earlier biogenic precipitates, especially at depths from about 100 to 300 m supporting that sulphate reduction has been important over time. The long residence times of groundwaters under reducing conditions, and the actual data on the Fe(III)-oxyhydroxides in the fracture fillings, support the existence of crystalline phases, mainly hematite. The greater crystallinity and low surface areas of these ferric phases, together with the low Eh, is less favourable for iron-reducing bacteria at these depths. The reducing environment has preserved (and possibly increased) a large inorganic reducing capacity apparently provided by the presence of Fe(II)-bearing Al-silicates (chlorite and clay minerals, such as corrensite, smectite, mixed layer clays, illite/smectite) and sporadically distributed pyrite.

Dissolved manganese concentrations in groundwaters at these depths are variable but generally low and undersaturated with respect to rhodochrosite (except for some brackish glacial groundwaters) indicating that this mineral is not the manganese source. The common association of manganese with marine-type Littorina waters observed, for example, in the Simpevarp subarea and at Äspö, is also demonstrated in the Laxemar subarea where groundwaters with a weak marine component (transition type) show highest manganese. Generally, the significant manganese values associated with the Littorina waters may be due to processes in the sea bed sediments prior to the marine water intrusion. Manganese-reducing bacteria are identified in most groundwater samples analysed for microbes, but there is no correlation between the number of manganese-reducing bacteria and the observed Mn^{2+} concentrations in groundwaters and no suitable electon acceptors have been identified in the fracture fillings.

Similar porewaters of dilute Na-HCO_3 chemical type with chloride contents of less than 1,000 mg/kg described for depth interval 20 to 250 m, can extend down to about 430 m depth in boreholes KLX03 and KLX17A and in KLX08 down to about 620 m depth. At about 300 to 500 m depth the depleted O^{18} signature values in many porewater samples support the presence of a glacial component circulating for a considerable time period in the bedrock. Generally, at expected repository depths (–400 to –700 m elevation) the salinity increases to about 5,000 to 7,600 mg/L Cl and there is a change to a porewater of Na-Ca-SO_4 type, which may indicate the influence of permafrost conditions. In boreholes KLX03 and KLX17A this type of porewater occurs between about 430–550 m and in KLX08 between 620–750 m depth where it displays a larger variability in chloride contents from 2,700 to 6,000 mg/kg. Over the same interval close to steady state conditions are maintained between the porewaters and fracture groundwaters.

Deep groundwaters (600 to 1,200 m)

This depth interval is dominated by ***Brackish non-marine – Saline (±Brackish glacial and Transition)*** *groundwater of Na-Ca Cl-(SO_4) to Ca-Na Cl-(SO_4) type. This groundwater shows very low magnesium values and they are clearly reducing (–220 to –265 mV). Interpretation of chlorine-36 measurements on these groundwaters suggest long residence times of hundreds of thousands of years which is supported by low flow and stagnant hydraulic conditions.*

The dominating groundwater types in this interval are *Brackish non-marine groundwaters*, and the *Saline groundwaters,* which are residing in bedrock (including deformation zones) of low hydraulic conductivity. Traces of *Brackish glacial* and *Transition groundwaters* are also found. The existence of brackish glacial groundwaters at depths of about 650 and 950 m support a deeper input of glacial meltwater, probably from the last glaciation, but the possibility of them being older cannot be excluded. Furthermore, the possibility of anthropogenic effects during pumping and sampling has to be considered. Two interesting examples are KLX04:–944 m elevation and KLX01:–672 m elevation where brackish glacial waters are residing at greater depths. Earlier circulation of relatively fresh waters (> 1,000 mg/L Cl) over time at depth is also indicated by the precipitation of low temperature fresh water calcites at about 900 m depth in both these boreholes /Drake et al. 2009a, Milodowski et al. 2005/ possibly related to the large deformation zone ZSMEW007A and its surroundings.

In general, the depth interval from 600 to 1,200 m marks the transition from brackish non-marine to saline groundwater type, characterised by a steady increase in chloride to about 16,000 mg/L at about 1,000 to 1,200 m, low magnesium contents (< 10 mg/L) and enriched $\delta^{18}O$ values. These saline groundwaters also mark the transition from a Na-Ca Cl type groundwater to a deeper Ca-Na Cl type groundwater. Although there are inadequate data, this transition appears to occur at about 800 to 900 m depth.

The only mixing process in this part of the system corresponds to the superimposition of additional glacial groundwaters on the earlier relict groundwater system, although some of these may not be necessarily from the last deglaciation. Moreover, as the weathering profile characteristic of the Laxemar subarea does not penetrate so far, the evolution trends shown by the Laxemar and Simpevarp groundwaters are similar. Major and trace elements show a gradual and uniform increase (except magnesium) towards very high dissolved contents which eventually come close to that of the highly saline groundwaters (i.e. the Deep Saline end member) described below. The main chemical reactions within this depth interval are in equilibrium with calcite, quartz and fluorite and the dissolution of gypsum. Ionic exchange processes are only minor in effect.

There are no measured potentimetrical Eh values available from depths greater than 700 m at Laxemar. However, dissolved sulphide is detectable in the groundwaters and equilibrium conditions with respect to the amorphous monosulphides in groundwaters are widely established down to 900 m, indicating the importance of the sulphur system for controlling the redox.

In the depth interval 600 to 1,200 m the amount of fracture groundwater data related to porewater samples is limited to one single analysis in borehole KLX03 at about 920 m depth, where a transient state is established between porewater and fracture groundwater.

Very deep groundwaters (> 1,200 m)

*At great depths the groundwater becomes **Highly saline,** and Ca-Na-Cl-(SO_4) in type. Chloride reaches a maximum of 45,000 mg/L at –1,530 m elevation in KLX02. The bedrock at this depth is characterised by fractures and deformation zones with extremely low hydraulic conductivities and hence long residence times for the groundwater due to low flow and stagnant conditions. The redox information is limited, but very reducing conditions have been measured in borehole KLX02 recording –300 mV at –1,420 to –1,705 m elevation.*

These highly saline groundwaters are typically Ca-Na-Cl in type with low magnesium (< 5 mg/L) and $\delta^{18}O$ values enriched with respect to the previous saline groundwaters (–9‰ VSMOW). Furthermore, the $\delta^{18}O$/ $\delta^{2}H$ deviation above the Global Meteoric Water line is typical for deep saline groundwaters from shield areas (cf Section 4.13 and discussion in /Smellie et al. 2008/). The groundwater composition is determined by long term water-rock interaction processes including equilibrium with albite and K-feldspar, calcite, quartz, fluorite, gypsum and strontianite. There is no indication that any kind of advective flow occurs down to this level.

No porewater data are available from these depths but steady state conditions between porewater and groundwater are expected, reflecting the stagnant groundwater conditions that prevail.

7 Present status of hydrogeochemical understanding of the Laxemar site

7.1 Overall changes since previous model version

The previous hydrochemistry model version Laxemar 1.2 and model stage Laxemar 2.1 /SKB 2006bc/ concluded that the complex groundwater evolution and patterns at the Laxemar-Simpevarp area are a result of many factors such as: a) the present day topography and proximity to the Baltic Sea, b) past changes in hydrogeology related to glaciation/deglaciation, land uplift and repeated marine/lake water regressions/transgressions, and c) organic or inorganic alteration of the groundwater composition caused by microbial processes or water-rock interactions. The sampled groundwaters reflect to various degrees processes relating to modern or ancient water-rock interactions and mixing and these conditions are confirmed by the results of modelling within SDM-Site Laxemar.

The SDM-Site Laxemar hydrochemistry modelling has resulted in improved robustness of model versions Laxemar 1.2 and Laxemar 2.1 concerning site understanding. Additional hydrochemical data from strategically located boreholes, reflecting a greater temporal and spatial understanding of the groundwaters, support previous understanding of the site, for example, in relation to groundwater origin and evolution, the major hydrochemical processes that distinguish the site, the selected major end members for conceptualisation and modelling purposes and, importantly, the close agreement with hydrogeology on the palaeohydrogeological description of the site. Improved process understanding has been achieved through different isotopic approaches (e.g. Sr, S, C, O, H, B, Cl and the U-decay series), more reliable Eh and pH measurements, integration of microbial measurements from Laxemar with that from other Fennnoscandian sites, and various modelling applications (e.g. geochemical reactive modelling, modelling of groundwater mixing proportions, coupled transport modelling and modelling indicating groundwater residence times).

Matrix porewater studies are now established, giving support to the understanding of the palaeo system and to the hydrogeochemical and hydrogeological conceptual modelling of the site, in addition to providing evidence that matrix diffusion in crystalline rock is active over distances of metres to tens of metres.

7.2 Overall understanding of the site

Explorative analyses and modelling of groundwater chemistry data measured in samples from cored boreholes, percussion boreholes, porewater from bedrock and shallow soil boreholes have been used to evaluate the hydrogeochemical conditions at the site in terms of origin of the groundwater and the processes that control the groundwater composition. Although the data set is rather limited, the results provide an overall understanding of the site. The effects from changing climate (and shoreline movement), on the measured groundwater, matrix porewater and fracture minerals, have been determined with respect to origin, reactions and evolution.

7.2.1 Post glacial evolution

Several water types which are now present in the bedrock can be associated with past climatic events in the late Pleistocene, including interglacials, glaciations, deglaciations and associated changes in the shoreline in connection with marine/non-marine transgressions and regressions. Amongst these, the last deglaciation and post glacial period are the most important for groundwater development in the Fennoscandian Shield, especially in terms of land uplift and shore level displacement as well as the development of the Baltic Basin.

The post glacial development reveals that when the ice sheet melted and retreated from the Laxemar-Simpevarp area around 12,000 BC, glacial meltwater was hydraulically injected under considerable head pressure into the bedrock. The exact penetration depth is unknown, but, according to hydraulic simulations depths exceeding several hundred metres are possible. Although the last deglaciation

of the Laxemar-Simpevarp area coincided with the end of the Yoldia period, there are no signs of Yoldia Sea water in the bedrock. The Ancylus Lake (8800 to 7500 BC) was lacustrine and developed after the deglaciation. This period was followed by the brackish Littorina Sea (7500 BC to present). During the Littorina Sea stage, the salinity was considerably higher than at present, reaching a maximum of about 15‰ in the period 4500 to 3000 BC. Dense brackish sea water from the Littorina Sea initially penetrated most of the rock in the Simpevarp subarea, and probably a more diluted variety penetrated the eastern and southeastern parts of the bedrock at Laxemar (low topographic areas and along valleys). This resulted in a density-driven intrusion that affected the groundwater in the more conductive parts of the bedrock. In the areas not covered by the Littorina Sea water, meteoric water circulation became established around 12,000 BC forming a freshwater layer on top of the older saline water. Driven by the land uplift, this meteoric water started to gradually flush out the older groundwater types. However, this has been limited, and consequently post glacial water dominates at depths of about 20–300 m and remnants of glacial water still dominate within the approximate 300–600 m depth interval. An alternative or an additional process is that the Littorina signature was diluted in the bedrock as a result of meteoric water infiltration driven by land uplift.

The Holocene evolution therefore has had most influence on the groundwater chemistry in the Laxemar-Simpevarp area, but at greater depths (> 600 m) this is not restricted to post glacial time. At these depths the hydrochemistry of the Laxemar-Simpevarp area cannot be explained without recognising an older groundwater component. The present groundwaters therefore are a result of mixing and reactions over a long period of geological time. Furthermore, the interfaces between different groundwater types are not sharp and reflect the anisotropy in the bedrock hydrostructural properties.

7.2.2 General groundwater features

The general major groundwater features at the Laxemar subarea are summarised in Figure 7-1. The latest known salinity input to the Laxemar subarea is from the Littorina Sea stage, and is very limited. This also means that most of the brackish waters, and certainly groundwaters with a salinity content exceeding 6,000 mg/L Cl, are older than the Littorina period and most of the saline components are even older than the last glaciation. Cold climate signatures mainly associated with the last deglaciation are found mostly at 300–600 m depth. Magnesium, commonly used as an indicator of marine input and present in some groundwaters at depths of 200–600 m, is interpreted as a possible Littorina influence.

At shallower depths, the upper approximately 150 m are characterised by modern meteoric recharge water with measurable tritium (1–5 TU); groundwaters at greater depths are either tritium free or record 1–4 TU due to drilling or sampling contamination. Down to about 200 m high bicarbonate (> 150 mg/L HCO_3) characterises the groundwaters. This is partly due to calcite dissolution but even more importantly ongoing organic decomposition in combination with microbial reduction of iron, manganese or sulphate.

Consistent negative redox measurements below 100 m indicate reducing conditions in the bedrock of the Laxemar-Simpevarp area and pH ranges between 7.5 and 8.6 for all representative groundwaters measured.

7.2.3 Groundwater evolution and composition

The main processes determining the overall geochemical evolution of Laxemar-Simpevarp groundwater systems are mixing and reaction processes. Mixing has taken place between different types of waters (end members) over time, making discrimination of the main influences complex. In addition to mixing processes and their superimposition effects, different chemical reactions have taken place in the system due to the interaction between waters, minerals and/or microbial activity (e.g. aluminosilicate and carbonate dissolution/precipitation, cation exchange, gypsum dissolution, main redox reactions, etc.). Some elements (Cl or $\delta^{18}O$) behave conservatively in groundwater while others are affected by chemical reactions to differing degrees, especially the redox sensitive elements.

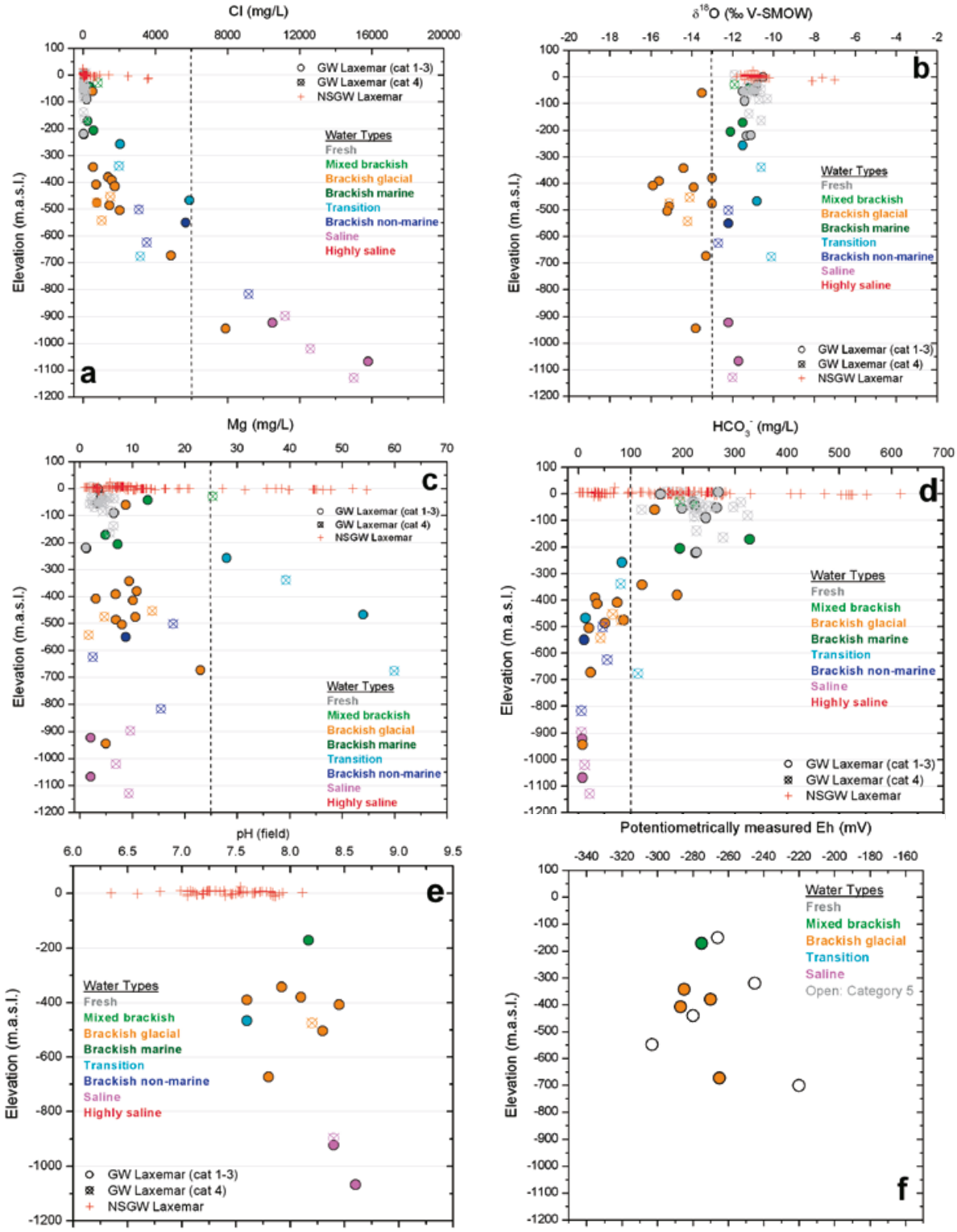

Figure 7-1. *Distributions of key parameters versus depth in groundwaters from Laxemar: chloride (a); vertical dashed line indicates maximum possible penetration depth for Littorina water (= 6,000 mg/L Cl), $\delta^{18}O$ (b); vertical dashed line at $\delta^{18}O$ = –13‰ VSMOW indicates the upper limit for the classification of water with a glacial component, magnesium (c); vertical dashed line at 25 mg/L indicates the lower limit for groundwater with a marine component, bicarbonate (d); vertical dashed line at 100 mg/L indicates upper limit for most of the waters at repository depth, pH (e), and redox potential (f).*

The overburden (near surface/shallow system down to 150 m depth) is dominated by water-rock interactions between the recharging meteoric water and the soil, till sediments and bedrock (Figure 7-2). Weathering and potential calcite dissolution under acidic conditions in the near surface bedrock environment is promoted and controlled by biogenic input of carbon dioxide. This gives rise to pH values usually above 7, calcium concentrations mostly between 50 and 200 mg/L, and bicarbonate concentrations up to 600 mg/L in the near surface waters (down to around 20 m depth). Concentrations then decrease to very low values at great depths. However, bicarbonate locally reaches values up to 100–200 mg/L in some of the brackish glacial groundwaters hosted in the upper approximate 500 m.

In the intermediate to deep bedrock system (150–1,000 m depth), groundwater mixing processes usually dominate and the effects of reactions between the groundwaters and the minerals in the fracture fillings will be superimposed on mixing signatures. The temporal sequence of the deep groundwater evolution and the composition is illustrated in Figure 7-3 assuming that there is a continuous recharging and downward advective flow of groundwater to maximum depths of around 1,000 m. Below this depth, low flow and stagnant conditions prevail and solute transport is increasingly diffusion controlled.

It is envisaged that prior to the last glaciation there existed a concentration profile extending from dilute meteoric waters in the near surface of the bedrock to highly saline, brine type compositions at around 1,000 m depth and deeper. These highly saline groundwaters, believed to be similar in composition to those sampled at maximum depths today (see red rectangle in the deepest part of the bedrock, Figure 7-3), indicated high contents of chloride, calcium, sodium, potasium and sulphate, low values of magnesium and bicarbonate, a more or less constant Ca/Sr ratio, and enriched oxygen-18 signatures. Then, with the onset of the last glaciation/deglaciation, the input of dilute waters (meteoric or glacial meltwaters) over time modified the pre-existing concentration profile from the surface to depth. The cold climate signature depleted the oxygen-18 signature and waters with low pCO_2 and high pH values entered the system. These different mixtures promoted calcite precipitation and cation exchange due to dilution, i.e. led to a decrease of calcium and increase of sodium in the groundwaters.

The nearest major event is the input of a marine component (Littorina Sea) into the bedrock following several diagenetic processes during its passage through marine sediments. This water is thought to have passed into the bedrock down to different depths depending on the coastal proximity

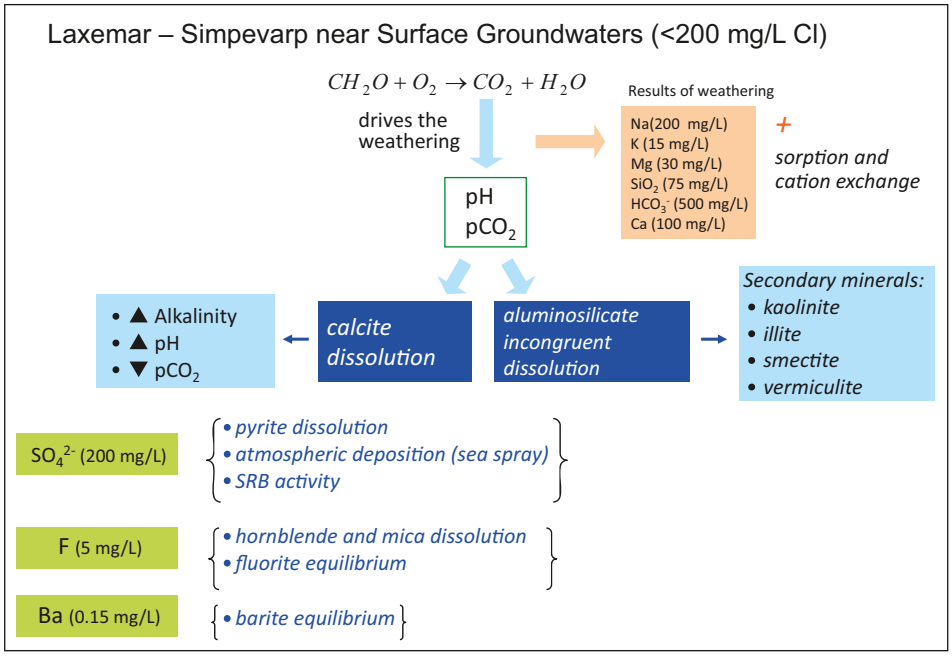

Figure 7-2. *The evolution of the near surface groundwater in the Laxemar-Simpevarp area where typical weathering reactions control the hydrochemistry; SRB = Sulphate-Reducing Bacteria.*

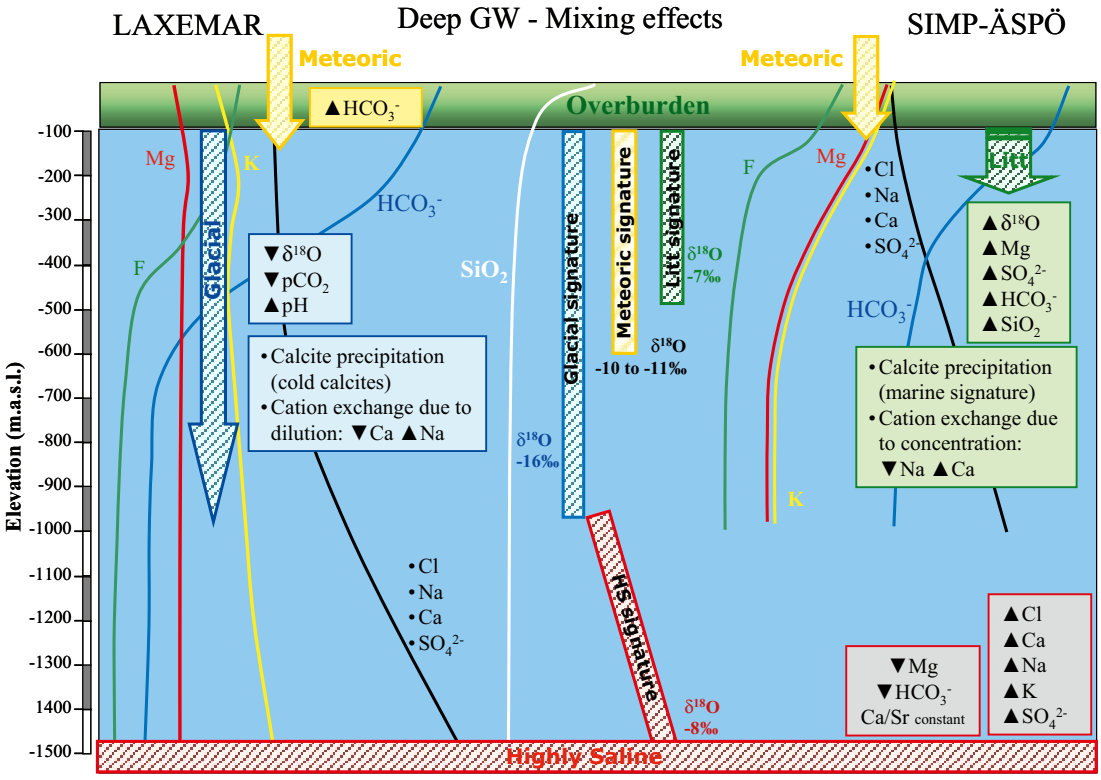

Figure 7-3. *The evolution of the groundwater in the Laxemar (left zone) and Simpevarp (right zone) subareas. Coloured trend lines indicate relative measured variations of different elements with depth. Also indicated are element or isotope increases/decreases associated with reactions and end-member influences. The end members are: Meteoric (yellow), Littorina (green), Glacial (blue) and Deep or Highly saline (red). The central part of the profile shows the common evolution of silica (in white) and the relative $\delta^{18}O$ variations with depth for both subareas.*

(more in Simpevarp and Äspö than Laxemar), on the rock hydraulic properties, and on the salinity of the pre-existing waters (i.e. glacial to brackish glacial waters with depleted oxygen-18 signatures). Eventually, the higher density of these Littorina waters displaced the previous dilute waters and resulted in the groundwaters becoming more enriched in oxygen-18, magnesium, sulphate, bicarbonate and silica. This was followed by calcite precipitation and cation exchange to produce a decrease of sodium and an increase in calcium in the waters. Finally, the continuous input of meteoric waters produced a superimposed dilution profile (more marked in the recharge areas such as at Laxemar).

Modelled groundwater mineral equilibrium features which are supported by mineralogical and microbial observations are shown in Figure 7-4. The pH buffering capacity in Laxemar at depths greater than 100 m appears to be controlled by the carbonate system, and modelling indicates that this water is in equilibrium with calcite.

According to data analyses and modelling of the redox system, reducing conditions currently prevail at depths greater than about 20 m. Most of the Eh values determined at the Laxemar subarea are in the brackish glacial groundwaters (at depths between 100 and 700 m). The iron and the sulphur systems are very important for the control of redox processes in the groundwaters at Laxemar-Simpevarp. Iron (II) and (III) minerals are widely distributed in the studied systems and the presence of IRB has been documented. However, the bioenergetic calculations and the redox modelling approach performed from a partial equilibrium assumption for iron reduction and sulphate reduction processes indicate that sulphate reduction is the thermodynamic favoured processes.

All the data indicate that the system has retained a significant reducing capacity to the present day. The key role played by SRB in the stabilisation of these reducing conditions is supported by several lines of evidence, including the microbially influenced $\delta^{34}S$ values found in pyrites from the Laxemar-Simpevarp area at shallow to intermediate depths, and the low $\delta^{13}C$ values found in calcites

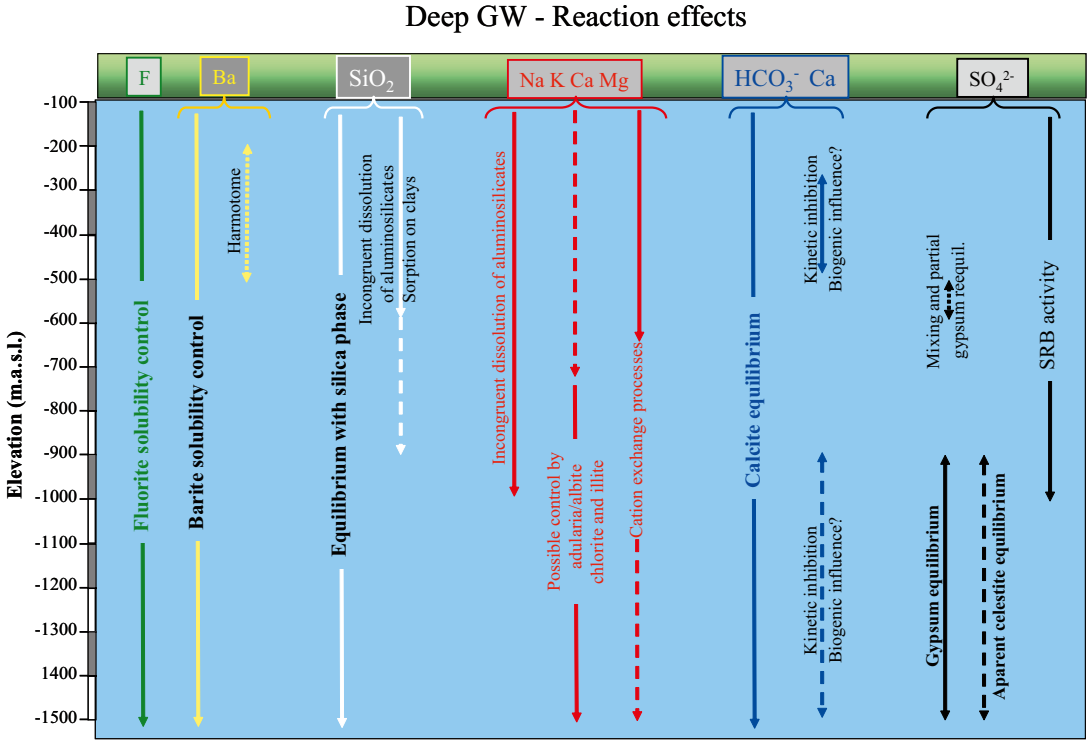

Figure 7-4. *Modelled groundwater equilibrium features which are supported by mineralogical and microbial observations.*

from fracture fillings from the same area. The importance of the SRB at great depths (> 700 m) at the Laxemar subarea remains unclear. They are not documented in the one existing sample from below 700 m depth (KLX03:–922 m elevation) and moreover no Eh measurements are available from these depths.

The major groundwater characteristics are (cf Table 6.1):

- The 0–20 m depth interval is hydrogeologically active (residence times in the order of years to decades) and dominated by modern recharge meteoric water or Fresh groundwater (< 200 mg/L Cl) of Na-Ca-HCO_3 (SO_4) type showing large variations in pH and redox conditions.
- The 20–250 m depth interval is dominated by Fresh–Mixed Brackish–Brackish Glacial groundwaters of Na-Ca-HCO_3 (SO_4) to Na-Ca-Cl-HCO_3 type, showing a transition to stable reducing conditions with increasing depth. The residence times of the groundwaters are in the order of decades to several thousands of years.
- The 250–600 m depth interval is dominated by Brackish Glacial–Brackish Non-marine–Transition groundwaters of Na-Ca-Cl-(HCO_3) type. Redox conditions are reducing and low Eh values (–245 to –303 mV) are typically controlled by the interplay between the iron and especially the sulphur systems. The significant portions of glacial waters in this depth interval, and the equally significant increase of non-marine groundwaters with depth, indicates that groundwaters older than the last deglaciation at around 14,000 years ago are becoming increasingly important.
- The 600–1,200 m depth interval is dominated by Brackish Non-marine–Saline (±Brackish Glacial and Transition) groundwater of Na-Ca Cl-(SO_4) to Ca-Na Cl-(SO_4) type. These groundwaters show very low magnesium values and are clearly reducing (–220 to –265 mV). Interpretation of chlorine-36 measurements suggests long residence times of hundreds of thousands of years; this is supported hydrogeologically by low flow to stagnant conditions.
- The pH values are between 7.2 and 8.6 in the groundwaters and do not show any clear variation trend with depth. pH is mainly controlled by calcite dissolution-precipitation reactions and, probably, by microbial activities. Of secondary importance is the influence of other common chemical processes, such as aluminosilicate dissolution-precipitation or cation exchange.

7.2.4 Rock matrix porewater

Porewaters have been analysed from boreholes KLX03, KLX08 and KLX17A representing sampled depths from about 600 to 1,000 m. Taken together, similarities in the preserved porewater compositions indicate a clear change from waters of temperate meteoric origin, to glacial waters and finally to much older saline waters with increasing depth. Generally, this is in agreement with the surrounding fracture groundwater compositions and the hydraulic properties of the bedrock. In the upper approximately 300 m of bedrock, the porewater is of a dilute Na-HCO_3 type and present day meteoric influence dominates in the porewaters in KLX03 and KLX17A. In contrast, warmer climate meteoric influences from temperature maximums prior to the last glaciation and during the Holocene may have influenced some samples distant to the nearest water-conducting fracture (most common in KLX08). Cold climate influence from the last glaciation occurs in the still dilute Na-HCO_3 type porewaters between about 300–360 m depth in boreholes KLX03 and KLX17A, and down to about 500 m in borehole KLX08.

A distinct change in chemical and isotopic composition to a highly mineralised Na-Ca-SO_4 type porewater is observed between about 430–550 m depth in boreholes KLX03 and KLX17A, and between about 620–750 m in borehole KLX08. Potentially, two different processes may have given rise to this unusual composition: a) interaction with a known fracture groundwater type and/or intensified rock-water interaction, and/or b) the result of permafrost related freeze-out processes. This issue is still unresolved because of a lack of data.

Preliminary modelling of a sampled porewater profile at shallow depth in borehole KLX17A, which extends from a conducting fracture (at about 105 m borehole length) into the intact rock matrix, indicates that the isotope signature enriched in ^{18}O and ^{2}H (together with the low chloride) is preserved in the porewater samples most distant (> 15 m) from the water-conducting zone. It is thought that these porewaters were established before the last glaciation and should, therefore, represent a warm climate origin. This is in accordance with the fracture groundwater scenario. With respect to the other enriched samples which include porewaters sampled closer to the water conducting fracture, it may be argued that these represent warm climate signatures introduced more recently in the Holocene, during post glacial time. These possibilities are still being discussed.

7.2.5 Dissolved gases and colloids

The main gas in samples from the Laxemar-Simpevarp area groundwaters is nitrogen followed by carbon dioxide in the more shallow groundwaters, and helium in the deeper parts of the system. Other gases present are helium, methane, argon and hydrogen. The available data indicate that the total gas content is less than would be expected in Fennoscandian Shield groundwaters. This indicates either an open system (high outflux) or low influx of gases from below. Although their concentrations generally increase with depth, the gases are not oversaturated at the depths at which they were sampled. There are few samples taken for gas analyses and the isotopic composition of important gases such as hydrogen and methane is missing. The description of the origin of gases should therefore be considered as preliminary.

The number of colloids found in Laxemar-Simpevarp groundwaters was approximately in the order of 10^6/mL. The measured colloid concentration is in agreement with measurements from other crystalline groundwater environments. Both inorganic and organic colloids exist at Laxemar and some colloids are probably microbes and potentially viruses (phages).

7.2.6 Confidence

There is generally a high confidence in the description and understanding of the current spatial distribution of groundwater composition, mainly due to the consistency between different analyses and modelling of the chemical data, but also due to the general agreement with the hydrogeological understanding of the area. In addition, the existence of a near surface redox reaction zone appears to be well established based on the shallow groundwater chemistry. Furthermore, indications from the Laxemar-Simpevarp area as a whole point to a bedrock that has a sufficiently large buffering capacity to maintain pH values in the range 7.5 to 8.5 and Eh values lower than –200 mV. One important remaining uncertainty concerns the increased sulphide concentrations measured in the on-going moni-

toring programme. Initial drilling and pumping may have disturbed the system or may have facilitated sulphate reduction, but this issue remains to be resolved. The monitoring programme should also support the overall understanding of the long term behaviour of other groundwater parameters such as iron, manganese, DOC and tritium.

7.3 Summary of important issues in site understanding

7.3.1 General

The site investigations in the Laxemar-Simpevarp area have produced a good hydrogeochemical understanding of the site, both of present and past conditions, and have emphasised the different groundwater behaviour. Looking at the conditions in the focused volume, these do not represent a site characterised by a continuous and systematic hydrogeochemical evolution from surface recharge to the maximum depths sampled. Instead, the large variation in hydrogeological properties and climate have resulted in a complicated addition (of e.g. brackish marine waters) and mixing of water types of different origin.

Major hydrogeochemical issues of importance to site understanding are addressed below which include: a) the redox buffering capacity of the bedrock system, b) changes in groundwater composition with depth based on palaeohydrogeochemical events, c) the presence of sulphide in groundwaters, and d) the presence of methanogenic bacteria and methane in groundwaters.

7.3.2 Bedrock redox buffer capacity

The mineralogical and geochemical studies performed on the fracture fillings from the Laxemar subarea indicate that the transition from oxidising to reducing conditions mainly takes place in the upper 20 m, as deduced from the occurrences of recent, low temperature Fe-oxyhydroxides and the results of the U-series analyses. Importantly, the presence of Fe^{2+}-bearing minerals (mainly chlorite and pyrite) in the fracture fillings at all depths indicates that past oxidising episodes have not exhausted the reducing capacity of the fracture minerals, even in the shallowest part of the system. In fact, both chlorite and unaltered pyrite have been identified in the fractures ín the Laxemar-Simpevarp area even in the uppermost 100 m of the bedrock. These findings, together with the significant Fe(II) content of the host rock (also in the red-stained altered wall rock), suggest that the buffering capacity against infiltrating dilute groundwater remains efficient.

7.3.3 Glacial meltwaters

Glacial signatures are most prominent at depths between 300–600 m. Assuming similar conditions for a future glaciation as experienced during the last glaciation, it is likely that large volumes of glacial meltwaters will penetrate to repository depth in the focused volume. Accepting this scenario, the probability of the glacial meltwaters retaining their oxidising character for a long period of time is unlikely considering the buffer capacity of the bedrock and the fracture system mentiond above in Section 7.3.2. This assumed outcome is supported by detailed mineralogical studies from the Laxemar-Simpevarp area and Äspö, all of which indicate that even though glacial meltwater signatures are found in the bedrock, there are no signs of this water having been oxidising at depths below 100 m.

7.3.4 Calcium variability in groundwater

A groundwater calcium content of more than 1 mM/L is the limit set for repository safety analysis used in SR-Can /SKB 2006b/. This is based on a preliminary assessment on the stability of bentonite colloids. Shallow groundwaters in Laxemar are characterised by relatively low calcium contents and a few groundwaters sampled from intermediate depth also show low calcium contents, although still exceeding 1 mM/L. Calcium content in groundwater is governed by mixing and reactions, in this latter case particularly ion exchange with sodium in the bedrock.

With regard to potential effects of dilute groundwater on the buffer material, there are two critical events that may entail potential lowering of the calcium content; the incursion of dilute glacial melt-waters (described above) and less probable is the subsequent meteoric recharge following land uplift.

7.3.5 The presence of sulphide

Sulphate and sulphide have been measured in the groundwaters at Laxemar and several sulphur sources for the dissolved sulphate in the groundwater have been identified. These include meteoric water (deposition of atmospheric sulphate, sea spray and weathering of sulphide mineral), relict marine water (smaller portions of Littorina water), leaching of marine clays, dissolution of gypsum in the fractures, and deep saline groundwater that may include leached evaporites.

The sulphur isotope ratios in the dissolved sulphate show large variations indicating that sulphide has been produced in the system and also that microbial sulphate reduction is ongoing. Furthermore, sulphate-reducing bacteria are present at all depths sampled, but show wide variations in population levels. Measurements of sulphide at different sampling occasions have yielded very ambiguous results and continued sampling in conjunction with the monitoring programme has been initiated to determine the reason for these observations. Hence, more information is needed prior to any future detailed interpretations. It is probable that the relatively high concentrations of reduced iron (Fe^{2+}) in the groundwater system, together with the S^{2-} values, will be controlled by Fe-monosulphide solubility during undisturbed conditions. In conclusion, the magnitude and variability of sulphide at repository depth remain an open question.

7.3.6 Microbes and methane

The contents of methane in the groundwaters in the Laxemar subarea are generally low (below 0.2 mL/L) except for two sections: KLX03: –171 m and KLX03: –380 m elevation. The KLX03: –380 m section is the only section at Laxemar showing significant numbers of anaerobic and heterotrophic methanogenic bacteria. All other sections show numbers of methanogens below the detection limit.

7.4 Implication for further modelling

The *in situ* concentration of sulphide needs further monitoring, sampling and modelling, as the potential implications of these uncertainties are important and need to be assessed in SR-Site study.

8 Acknowledgements

This study forms part of the SKB site investigation programme, managed and supported by the Swedish Nuclear Fuel and Waste Management Company (SKB), Stockholm. The ChemNet, SKB and Sierg reviewers are acknowledged for helping to improve this report. Carl-Henrik Walgren, Kent Werner and Ingvar Rhen are thanked for reviewing the geology, surface hydrology and hydrogeology sections respectively.

9 References

Andersson J, 2003. Site descriptive modelling – strategy for integrated evaluation. SKB R-03-05, Svensk Kärnbränslehantering AB.

Ahonen L, 2001. Permafrost occurrence and physiochemical processes. Posiva, Tech. Rep. (2001-05), Posiva, Helsinki, Finland.

Alexeev S V, Alexeeva L P, 2003. Hydrogeochemistry of the permafrost zone in the central part of the Yakutian diamond-bearing province, Russian Hydrogeological Journal, 11, 574–581.

Andrews J N, Davis S N, Fabryka-Martin J, Fontes J-CH, Lehmann B E, Loosli H H, Michelot J-L, Moser H, Smith B, Wolf M, 1989a. The in situ production of radioisotopes in rock matrices with particular reference to the Stripa granite, Geochimica et Cosmochimica Acta, 53, 1803–1815.

Appelo C A J, Postma D, 2005. Geochemistry, groundwater and pollution. Balkema, Rotterdam, The Netherlands. (2nd. edition).

Apps J A, van de Kamp P C, 1993. Energy gases of abiogenic origin in the Earth's crust. The future of energy gases. U.S. Geological Survey Professional Papers. United States Government Printing Office, Washington., pp. 81–132.

Auqué L F, Gimeno M J, Gómez J, Puigdoménech I, Smellie J, Tullborg E-L, 2006. Groundwater chemistry around a repository for spent nuclear fuel over a glacial cycle. Evaluation for SR-Can. SKB TR-06-31, Svensk Kärnbränslehantering AB.

Auqué L, Gimeno M J, Gómez J, Nilsson A-C, 2008. Potentiometrically measured Eh in groundwaters from the Scandinavian Shield. Applied Geochemistry, 23:1820–1833.

Ball J W, Nordstrom D K, 2001. User's manual for WATEQ4F, with revised thermodynamic data base and test cases for calculating speciation of major, trace, and redox elements in natural waters. U.S. Geological Survey, USA. Open File Report 91-183.

Banwart S A, 1999. Reduction of iron (III) minerals by natural organic matter in groundwater. Geochimica et Cosmochimica Acta, 63, 2919–2928.

Berg C, Bergelin A, Wacker P, Nilsson A-C, 2006. Forsmark site investigation. Hydrochemical characterisation in borehole KFM08A. Results from the investigated section at 683.5–690.6 (690.8) m. SKB P-06-63, Svensk Kärnbränslehantering AB.

Bergelin A, Nilsson K, Lindquist A and Wacker P, 2008. Oskarshamn site investigation. Complete chemical characterisation in borehole KLX27A. Results from borehole section 641.5 to 650.6 m. SKB P-08-77. Svensk Kärnbränslehantering AB.

Bein A, Arad A, 1992. Formation of saline groundwaters in the Baltic region through freezing of sea water during glacial periods. Journal of Hydrology, 140, Elsevier Science B.V., 75–87.

Björck S, 1995. A review of the history of the Baltic Sea 13-8 ka, Quaternary International, 27, 19–40.

Blomqvist R, Ruskeeniemi T, Kaija J, Ahonen L, Paananen M, Smellie J, Grundfelt G, Pedersen K, Bruno J, Pérez del Villar L, Cera E, Rasilainen K, 2000. The Palmottu Natural Analogue Project. Phase II: transport of radionuclides in a natural flow system. European Commission, Final Report, Phase II, EUR 19611 EN, 171 p.

Blyth A, Frape S, Blomqvist R, Nissinen P, 2000. Assessing the past thermal and chemical history of fluids in crystalline rock by combining fluid inclusion and isotopic investigations of fracture calcite. Applied Geochemistry 15, 1417–1437.

Boulton G, Gustafson M, Schelkes K, Casanova J, Moren L, 2001. Palaeohydrology and geoforcasting for performance assessment in geosphere repositories for radioactive waste disposal (PAGEPA). EUR 19784 EN, Luxembourg.

Brown G H, 2002. Glacier meltwater hydrochemistry. Applied Geochemistry, 17, 855–883.

Byegård J, Ramebäck H, Widestrand H, 2002. Use of radon concentrations for estimation of fracture apertures. SKB IPR-02-68, Svensk Kärnbränslehantering AB.

Byrne R H, Lee J H, Bingler L S, 1991. Rare earth element complexation by PO_4 ^3- ions in aqueous solution. Geochimica et Cosmochimica Acta, 55, 2729–2735.

Byrne R H, Liu X, Schijf J, 1996. The influence of phosphate coprecipitation on rare earth distribution in natural waters. Geochimica et Cosmochimica Acta, 60, 3341–3346.

Carlsten S, Mattson K-J, Stråhle A, Wahlgren C-H, 2008. Geological single-hole interpretation of KLX27A. SKB P-08-48, Svensk Kärnbränslehantering AB.

Casanova J, Négrel P, Blomqvist R, 2005. Boron isotope fractionation in groundwaters as an indicator of past permafrost conditions in the fractured crystalline bedrock of the Fennoscandian Shield. Water Research, 39, 362–370.

Cederbom C, Larson S Å, Tullborg E-L, Stiberg J P, 2000. Fission track thermochronology applied to Phanerozoic thermotectonic events in central and southern Sweden. Tectonophysics, 316, 1-2, 153–167.

Clark I, Fritz P, 1997. Environmental Isotopes in Hydrogeology. Lewis, 328 pp.

Clark I D, Douglas M, Raven, K, Bottomley D, 2000. Recharge and preservation of Laurentide glacial meltwater in the Canadian Shield. Ground Water, 38, 735–742.

Degueldre C, 1994. Colloid properties in groundwater from crystalline formations. PSI Bericht Nr 94-21 and NAGRA report NTB-92-05.

Dideriksen K, Christiansen B C , Baker J A, Frandsen C, Balic-Zunic T, Tullborg E-L, Mørup S, Stipp S L S, 2007. Fe-oxide fracture-fillings as a palæo-temperature and -redox indicator: Structure, crystal form, REE content and Fe isotope composition. Chemical Geology, 244, 330–343.

Drake H, Sandström B, Tullborg E-L, 2006. Mineralogy and geochemistry of rocks and fracture fillings from Forsmark and Oskarshamn: Compilation of data for SR-Can. SKB-R-06-109, Svensk Kärnbränslehantering AB.

Drake H, Page L, Tullborg E-L, 2007. Oskarshamn site investigation, 40Ar/39Ar dating of fracture minerals. SKB-P-07-27, Svensk Kärnbränslehantering AB.

Drake H, Tullborg E-L, 2008. Oskarshamn site investigation. Mineralogy in water conducting zones. Results from boreholes KLX03, KLX04, KLX06, KSH01A+B, KSH02 and KSH03A. SKB P-08-41, Svensk Kärnbränslehantering AB.

Drake H, Tullborg E-L, Annersten H, 2008. Red-staining of the wall rock and its influence on the reducing capacity around water conducting fractures. Applied Geochemistry, 23: 1898–1920.

Drake H, Tullborg E-L, 2009a. Fracture mineralogy Laxemar, Site-descriptive modelling, SDM-Site Laxemar. SKB R-08-99, Svensk Kärnbränslehantering AB.

Drake H, Tullborg E-L, 2009b. Paleohydrogeological events recorded by stable isotopes, fluid inclusions and trace elements in fracture minerals in crystalline rock, Simpevarp area, SE Sweden. Applied Geochemistry, 24. 715–732.

Drake H, Tullborg E-L, MacKenzie A B, 2009. Detecting the near surface redox front in crystalline bedrock using fracture mineral distribution, geochemistry and U-series disequilibrium. Applied Geochemistry, 24, 1023–1039.

Drever J I, 1997. The geochemistry of natural waters: surface and groundwater environments. Prentice Hall. Upper Saddle River, N.J. 436 pp.

Eastoe C J, Peryt T M, Petrychenko O Y, Geisler-Cussey D, 2007. Stable chlorine isotopes in Phanerozoic evaporites. Applied Geochemistry, 22, 575–588.

Eydal H S C, Pedersen K, 2007. Use of an ATP assay to determine viable microbial biomass in Fennoscandian Shield groundwater from depths of 3–1,000 m, Journal of Microbiology Methods, 70, 363–373.

Florkowski T, Morawska L, & Rozanski K, 1988. Natural production of radionuclides in geological formations. Nuclear Geophysics, 2, 1–14.

Folk R L, 1974. The natural history of crystalline calcium carbonate; effect of magnesium content and salinity. Journal of Sedimentary Petrology, 44, 40–53.

Follin S, Stephens M B, Laaksoharju M, Nilsson A-C, Smellie J A T, Tullborg E-L, 2008. Modelling the evolution of hydrochemical conditions in the Fennoscandian Shield during Holocene time using multidisciplinary information. Applied Geochemistry, 23, 2004–2020.

Frape S K, Fritz P, 1987. Geochemical trends from groundwaters from the Canadian Shield. In: (eds.) P. Fritz and S.K. Frape. Saline waters and gases in crystalline rocks. Geological Association in Canada Special Paper 33, 19–38.

Frape S K, Byrant G, Blomqvist R, Ruskeeniemi T, 1996. Evidence from stable chlorine isotopes for multiple sources of chloride in groundwaters from crystalline shield environments. In: Isotopes in water resources management 1996. IAEA-SM-336/24, Vol. 1, 19–30. et al. 1996 Fredén C, 2002. Berg och Jord, Sveriges Nationalatlas. 208 pp.

Garrels R M, Christ C J, 1965. Solutions, minerals and equilibria. New York, Harper & Row, 450 p.

Gascoyne M, 1999. Long-term maintenance of reducing conditions in a spent nuclear fuel repository. A re-examination of critical factors. SKB R-99-41, Svensk Kärnbränslehantering AB.

Gascoyne M, 2001. 36Cl in Olkiluoto groundwaters: Evidence for intrusion of Litorina Sea water. POSIVA OY Working Report 2001-20.

Gascoyne M, 2004. Hydrogeochemistry, groundwater ages and sources of salts in a granitic batholith on the Canadian Shield, southeastern Manitoba. Applied Geochemistry, 19, 519–560.

Gascoyne M, Laaksoharju M (ed), 2008. High-level radioactive waste disposal in Sweden: Hydrogeochemical characterisation and modelling of two potential sites. Applied Geochemistry, 23:7. Elsevier.

Gascoyne M, Gurban I, 2009. Determination of Residence Time: ^{4}He and ^{36}Cl in Laxemar Groundwaters. In: B. Kalinowski (ed) 2009. Background complementary hydrogeochemical studies Model, Site descriptive modelling, SDM-Site Laxemar. SKB R-08-111, Svensk Kärnbränslehantering AB.

Gimeno M, Auqué L F, Gómez J, 2007. Water-rock interaction modelling issues. In: SKB (2007), Hydrogeochemical evaluation of the Forsmark site, modelling stage 2.1-issue report. SKB R-06-69, Appendix 3, Svensk Kärnbränslehantering AB.

Gimeno M J, Auqué L F, Gómez J B, Acero P, 2008. Water-rock interaction modelling and uncertainties on mixing modelling. SDM-Site Forsmark. SKB R-08-86, Svensk Kärnbränslehantering AB.

Gimeno M J, Auqué L F, Gómez J, Acero P, 2009. /Water-rock interaction modelling and uncertainties of mixing modelling./ SDM-Site Laxemar. SKB R-08-110, Svensk Kärnbränslehantering AB.

Gitterman K E, 1937. Thermal analysis of sea water. CRREL TL287. USA Cold Regions Research and Engineering Laboratory,Hanover, NH.

Gómez J B, Laaksharju M, Skårman E, Gurban I, 2006. M3 version 3.0: Concepts, methods, and mathematical formulation. SKB TR-06-27, Svensk Kärnbränslehantering AB.

Gómez J, Laaksoharju M, Skårman E, Gurban I, 2009. M3 version 3.0: Verification and Validation. SKB report in preparation.

Grenthe I, Stumm W, Laaksoharju M, Nilsson A-C, Wikberg P, 1992. Redox potentials and redox reactions in deep groundwater systems. Chemical Geology, 98, 131–150.

Gurban I, 2009. M3 modelling of the hydrogeochemical parameters of Laxemar-Simpevarp gropundwaters. In: B. Kalinowski (ed), 2008, SKB R-08-111, Svensk Kärnbränslehantering AB.

Hallbeck L, Pedersen K, 2008a. Characterization of microbial processes in deep aquifers in the Fennoscandian Shield. Applied Geochemistry, 23, 1796–1819.

Hallbeck L, Pedersen K, 2008b. Explorative analyses of microbes, colloids and gases. SDM-Site Forsmark. SKB R-08-111, Svensk Kärnbränslehantering AB.

Hallbeck L, Pedersen K, 2009. Explorative analysis of microbes, colloids and gases, Site descriptive modelling, SDM-Site Laxemar. SKB R-08-109, Svensk Kärnbränslehantering AB.

Haveman Pedersen K, 2002. Distribution of culturable anaerobic microorganisms in Fennoscandian shield groundwater, FEMS Microbiol Ecology, 39, 129–137.

Heginbottom J A, Dubreuil M A, Harker P A, 1995. Canada – Permafrost, in: National Atlas of Canada, 5th Edition, National Atlas Information Service, Natural Resources Canada, MCR 4177.

Herut B, Starinsky A, Katz A, Bein A, 1990. The role of sea water freezing in the formation of subsurface brines. Geochimica et Cosmochimica Acta, 33, 1321–1349.

Kalinowski B (ed), 2009. Background complementary hydrogeochemical studies. SDM Site Laxemar. SKB R-08-111, Svensk Kärnbränslehantering AB.

Kjellström E, Brandefelt J, Näslund J O, Smith B, Strandberg G, Wohlfarth B, 2009. Climate conditions in Sweden in a 100,000 year time perspective. SKB TR-09-04, Svensk Kärnbränslehantering AB.

Klungness G D, Byrne R H, 2000. Comparative hydrolysis behavior of the rare earths and yttrium: the influence of temperature and ionic strength. Polyhedron 19. 99–107.

Kukkonen I T, Safanda J, 2001. Numerical modelling of permafrost in bedrock in northern Fennoscandia during the Holocene. Special Issue of Global and Planetary Change. Vol. 29, Issues 3-4, 259–273.

Kölling M, 2000. Comparison of different methods for redox potential determination in natural waters. In:L. Schüring, H.D. Schulz, W.R. Fischer, J. Böttcher and W.H.M. Duijnisveld (eds.), Redox. Fundamentals, processes and applications. Springer. Chapter 4, 42–54.

Laaksoharju M, Degueldre C, Skårman C, 1995. Studies of colloids and their importance for repository performance assessment. SKB TR 95-24, Svensk Kärnbränslehantering AB.

Laaksoharju M, Wallin B (eds), 1997. Evolution of the groundwater chemistry at the Äspö Hard Rock Laboratory. Proceedings of the second Äspö International Geochemistry Workshop, June 6–7, 1995. Äspö HRL, SKB ICR-97-04, Svensk Kärnbränslehantering AB.

Laaksoharju M, 1999. Groundwater Characterisation and Modelling: Problems, Facts and Possibilities. Dissertation TRITA-AMI-PHD 1031; ISSN 1400-1284; ISRN KTH/AMI/PHD 1031-SE; ISBN 91-7170-. Royal Institute of Technology, Stockholm, Sweden. SKB TR-99-42, Svensk Kärnbränslehantering AB.

Laaksoharju M, Tullborg E-L, Wikberg P, Wallin B, Smellie, J, 1999. Hydrogeochemical conditions and evolution at the Äspö HRL, Sweden. Applied Geochemistry, 14, 835–859.

Laaksoharju M (ed), 2004. Hydrogeochemical evaluation for Simpevarp model version 1.2. Preliminary site description of the Simpevarp area. SKB R-04-71, Svensk Kärnbränslehantering AB.

Laaksoharju M (ed), Smellie J, Gimeno M, Auqué L, Gomez , Tullborg E-L, Gurban I, 2004. Hydrochemical evaluation of the Simpevarp area, model version 1.1. SKB R 04-16, Svensk Kärnbränslehantering AB.

Laaksoharju M, Smellie J, Tullborg E-L, Gimeno M, Molinero J, Gurban I, Hallbeck L, 2008a. Hydrogeochemical evaluation and modelling performed within the site investigation programme. Applied Geochemistry, 1761–1795.

Laaksoharju M, Smellie J, Tullborg E-L, Gimeno M, Molinero J, Hallbeck L, Moliner J, Waber N, 2008b. Bedrock hydrogeoghemistry Forsmark. SKB R 08-47, Svensk Kärnbränslehantering AB.

Landström O, Tullborg E-L, 1995. Interactions of trace elements with fracture filling minerals from the Äspö Hard Rock laboratory. SKB TR 95-13, Svensk Kärnbränslehantering AB.

Langmuir D, Melchior D, 1985. The geochemistry of Ca, Sr, Ba and Ra sulfates in some deep brines from the Palo Duro Basin, Texas. Geochimica et Cosmochimica Acta, 49, 2423–2432.

Langmuir D, Riese A C, 1985. The thermodynamic properties of radium. Geochimica et Cosmochimica Acta, 49, 1593–1601.

Larsson-McCann S, Karlsson A, Nord M, Sjögren J, Johansson L, Ivarsson M, Kindell S, 2002. Meteorological, hydrological and oceanographical information and data for the site investigation program in the communities of Östhammar and Tierp in the northern part of Uppland. SKB T-02-02, Svensk Kärnbränslehantering AB.

Lindborg T, 2006. Description of surface systems. Preliminary site description Laxemar subarea – version 1.2 SKB R-06-11, Svensk Kärnbränslehantering AB.

Louvat D, Michelot J, Aranyossy J, 1999. Origin and residence time of salinity in the Äspö groundwater system. Applied Geochemistry 14, 917–925.

Luo Y R, Byrne R H, 2001. Yttrium and Rare Earth Element Complexation by Chloride Ions at 25°C. Journal of Solution Chemistry, Vol. 30, No. 9, 837–845.

Luo Y R, Byrne R H, 2004. Carbonate Complexation of Yttrium and the Rare Earth Elements in Natural Waters. Geochimica et Cosmochimica Acta, Vol. 68, No. 4, pp. 691–699.

Luo Y, Millero F J, 2004. Effects of temperature and ionic strength on the stabilities of the first and second fluoride complexes of yttrium and the rare earth elements. Geochimica et Cosmochimica Acta, Vol. 68, No. 21, pp. 4301–4308.

Mahara Y, Hasegwa T, Miyakawa K, Ohta T, 2008. Correlation between dissolved 4He concentration and 36Cl in groundwater at Äspö, Sweden. Applied Geochemistry 23, 3305–3320.

Mattsson H, Thunehed H, Triumf C-A, 2004. Oskarshamn site investigation. Compilation of petrophysical data from rock samples and in situ gamma-ray spectrometry measurements. Stage 2 – 2004 (including 2002). SKB-P-04-294, Svensk Kärnbränslehantering AB.

Marion G M, Farren R E, Komrowski A J, 1999. Alternative pathways for sea water freezing. Cold Regions Science and Technology, 29, 259–266.

McKibben M A, Eldridge C S, 1994. Micron-scale isotopic zoning in minerals; a record of large-scale geologic processes. Mineralogical Magazine, 58A, 587–588.

Millero F J, 1985. The physical chemistry of natural waters. Pure Applied Chemistry, 57, 1015–1024.

Milodowski A E, Gillespie M R, Pearce J M, Metcalfe R, 1998a. Collaboration with the SKB EQUIP programme; Petrographic characterisation of calcites from Äspö and Laxemar deep boreholes by scanning electron microscopy, electron microprobe and cathodoluminescence petrography, WG/98/45C. British Geological Survey, Keyworth, Nottingham.

Milodowski A E, Gillespie M R, Naden J, Fortey N J, Shepherd T J, Pearce J M, Metcalfe R, 1998b. The petrology and paragenesis of fracture mineralization in the Sellafield area, west Cumbria. Proceedings of the Yorkshire Geological Society, 52, 215–241.

Milodowski A E, Fortey N J, Gillespie M R, Pearce J M, Hyslop E K, 2002. Synthesis report on the mineralogical characteristics of fractures from the Nirex boreholes in the Sellafield area. British Geological Survey Technical Report WG/98/8.

Milodowski A E, Tullborg E-L, Buil B, Gomez P, Turrero M-J, Haszeldine S, England G, Gillespie M R, Torres T, Ortiz J E, Zacharias J, Silar J, Chvatal M, Strnad L, Sebek O, Bouch J E, Chenery S R, Chenery C, Shepherd T J, McKervey J A, 2005. Application of Mineralogical, Petrological and Geochemical tools for Evaluating the Palaeohydrogeological Evolution of the PADAMOT Study Sites. PADAMOT Project Technical Report WP2.

Molinero J, Salas J, Arcos D, Duro L, 2009. Integrated hydrogeological and geochemical modelling of the Laxemar-Simpevarp area during the recent Holocene (last 8000 years). In: Kalinowski, B. (ed.), /Background complementary hydrogeochemical studies/. SKB R-08-111, Svensk Kärnbränslehantering AB.

Nelson KH, Thompson TG, 1954. Deposition of salts from seawater by frigid concentration. J. Mar. Res. 13, 166–182.

Nilsson A-C, 2009. Quality of hydrochemical analyses in data freeze Laxemar 2.3. In: B. Kalinowski (ed) 2009. Background complementary hydrogeochemical studies Model , Site descriptive modelling, SDM-Site Laxemar. SKB R-08-111, Svensk Kärnbränslehantering AB.

Nordstrom D K, Puigdomènech I, 1986. Redox chemistry of deep ground-waters in Sweden. SKB TR 86-03, Svensk Kärnbränslehantering AB.

Nordstrom D K, Plummer L N, Langmuir D, Busenberg E, May H M, Jones B F, Parkhurst D, 1990. Revised chemical equilibrium data for major water-mineral reactions and their limitations. In: Melchior, D C, Basset R L (eds), Chemical Modelling of Aqueous Systems II. ACS Symposium Series 398–413.

Nyman H, Sohlenius G, Strömgren M, Brydsten L, 2008. Oskarshamn site investigation – Depth and stratigraphy of regolith. SKB R-08-06, Svensk Kärnbränslehantering AB.

Näslund J-O (ed) 1); Wohlfarth B (ed) 2);Alexanderson H, Helmens K, Hättestrand M, Jansson P, Kleman J, Lundqvist J, Brandefelt J, Houmark-Nielsen M, Kjellström E, Strandberg G, Luise Knudsen K, Krog Larsen N, Ukkonen P, Mangerud J, 2008. Fennoscandian paleo-environment and ice sheet dynamics during Marine Isotope Stage (MIS) 3. Report of workshop held September 20–21, 2007 in Stockholm, Sweden SKB R-08-79 Svensk Kärnbränslehantering AB.

Ohmoto H, Goldhaber M B, 1997. Sulfur and carbon isotopes, 3rd ed. In: H L Barnes (ed), Geochemistry of hydrothermal ore deposits. John Wiley & Sons, New York, NY, USA.

O'Neil J R, Clayton R N, Mayeda T K, 1969. Oxygen isotope fractionation in divalent metal carbonates. Journal of Chemical Physics, 51, 5547–5558.

Parkhurst D L, Appelo C A J, 1999. User's Guide to PHREEQC (Version 2), a computer program for speciation, batch-reaction, one-dimensional transport, and inverse geochemical calculations. Water Resources Research Investigations Report 99-4259, 312 p.

Pedersen K, 2001. Diversity and activity of microorganisms in deep igneous rock aquifers of the Fennoscandian Shield. In Subsurface microbiology and biogeochemistry. Fredrickson, J K, Fletcher M (eds), New York: Wiley-Liss Inc, 97–139.

Pedersen K, 2005. Äspö Hard Rock Laboratory. MICROBE. Analysis of microorganisms and gases in MICROBE groundwater over time during MINICAN drainage of the MICROBE water conducting zone. SKB IPR 05-29, Svensk Kärnbränslehantering AB.

Pedersen K, Ekendahl S, Tullborg E-L, Furnes H, Thorseth I, Tumyr O, 1997a. Evidence of ancient life at 207 m depth in a granitic aquifer. Geology, 25, 827–830.

Pedersen K, 2007. Microorganisms in groundwater from borehole KLX08 – numbers, viability, and metabolic diversity. Results from sections 197.0–206.7 m, 396.0–400.9 m and 476.0–485.6 m. Oskarshamn site investigation. SKB P-07-59, Svensk Kärnbränslehantering AB.

Pedersen K, Arlinger J, Eriksson S, Hallbeck A, Hallbeck L, Johansson J, 2008. Numbers, biomass and cultivable diversity of microbial populations relate to depth and borehole-specific conditions in groundwater from depths of 4–450 m in Olkiluoto, Finland. ISME-J doi:10.1038/ismej.2008.43.

Peterman Z, Wallin B, 1999. Synopsis of strontium isotope variations in groundwater at Äspö Hard Rock Laboratory, Southern Sweden. Applied Geochemistry, vol. 14:7, pp 953–962.

Pitkänen P, Snellman M, Vuorinen U, 1996. On the origin and chemical evolution of groundwater at the Olkiluoto site. Posiva Oy , Report POSIVA-96-04.

Pitkänen P, Luukkonen A, Ruotsalainen P, Leino-Forsman H, Vuorinen U, 1999. Geochemical modelling of groundwater evolution and residence time at the Olkiluoto site. Posiva Tech Rep. (98-10), Posiva, Helsinki, Finland.

Pitkänen P, Partamies S, Luukkonen A, 2004. Hydrogeochemical interpretation of baseline groundwater conditions at the Olkiluoto site. Posiva Tech. Rep. (2003-07), Posiva, Helsinki, Finland.

Puigdomenech I, Ambrosi J-P, Eisenlohr L, Lartigue J-E, Banwart S A, Bateman, K, Milodowski A, West, J M, Griffault L, Gustafsson E, Hama K,Yoshida H, Kotelnikova S, Pedersen K, Michaud V, Trotignon L, Rivas Perez J, Tullborg E-L, 2001. O2 depletion in granitic media. The REX project SKB TR-01-05.

Påsse T, 1997. A mathematical model of past, present and future shore level displacement in Fennoscandia. SKB TR 97-28, Svensk Kärnbränslehantering AB.

Rhén I, Forsmark T, Hartley L, Jackson C P, Roberts D, Swan D, Gylling B, 2008. Hydrogeological conceptualisation and parameterisation, Site descriptive modelling. SDM-Site Laxemar. SKB R-08-78, Svensk Kärnbränslehantering AB.

Rhén I, Forsmark T, Hartley L, Jackson C P, Joyce S, Roberts D, Swift B, Marsic N, Gylling B, 2009. Bedrock Hydrogeolology: model testing and synthesis, Site descriptive modelling. SDM-Site Laxemar. SKB R-08-91, Svensk Kärnbränslehantering AB.

Rhén I, Hartley L, 2009. Bedrock hydrogeology Laxemar, Site descriptive modelling SDM-Site Laxemar, SDM-Site Laxemar, SKB R-08-92, Svensk Kärnbränslehantering AB.

Ruskeeniemi T, Ahonen L, Paananen M, Frape S, Stotler R, Hobbs M, Kaija J, Degnan P, Blomqvist R, Jensen M, Lehto K, Moren L, Puigdomenech I, Snellman M, 2004. Permafrost at Lupin. Report of Phase II. Permafrost project GTK-SKB-POSIVA-NIREX-OPG. Report YST-119, Geol. Surv. Finland, Helsinki, Finland.

Samper J, Delgado J, Juncosa R, Montenegro L, 2000. CORE2D v 2.0: A Code for non-isothermal water flow and reactive solute transport. User's manual. ENRESA Technical report 06/2000.

Sandström B, Page L, Tullborg, E-L, 2006. Forsmark site investigation. 40Ar/39Ar (adualaria) and Rb-Sr (adularia, prehnite, calcite) ages of fracture minerals. SKB P-06-213, Svensk Kärnbränslehantering AB.

Sandström B, Tullborg E-L, Smellie J, MacKenzie A B, Suksi J, 2008. Fracture mineralogy of the Forsmark site. Final report. SKB P-08-102, Svensk Kärnbränslehantering AB.

Schijf J, Byrne R H, 2004. Determination of SO4[beta]1 for yttrium and the rare earth elements at I = 0.66 m and t = 25[deg]C-Implications for YREE solution speciation in sulfate-rich waters. Geochimica et Cosmochimica Acta 68(13), 2825–2837.

SKB, 2004a. Hydrogeochemical evaluation for Simpevarp model version 1.2. Preliminary site description of the Simpevarp area. SKB R-04-71, Svensk Kärnbränslehantering AB.

SKB, 2004b. Preliminary site description Forsmark area–version 1.1. SKB R-04-15, Svensk Kärnbränslehantering AB.

SKB, 2005. Hydrogeochemical evaluation. Preliminary site description Forsmark area – version 1.2. SKB R-05-17, Svensk Kärnbränslehantering AB.

SKB, 2006a. Hydrogeochemical evaluation. Preliminary site description Laxemar subarea – version 1.2. SKB R-06-12, Svensk Kärnbränslehantering AB.

SKB, 2006b. Hydrogeochemical evaluation. Preliminary site description Laxemar subarea – version 2.1. SKB R-06-70, Svensk Kärnbränslehantering AB.

SKB, 2006c. Site descriptive modelling. Forsmark stage 2.1. Feedback for completion of the site investigation including input from safety assessment and repository engineering. SKB R-06-38, Svensk Kärnbränslehantering AB.

SKB, 2006d. Climate and climate-related issues for the safety assessment SR-Can. SKB TR-06-23, Svensk Kärnbränslehantering AB.

Smellie J, Laaksoharju M, Tullborg E-L, 2002. Hydrogeochemical site descriptive model – a strategy for the model development during site investigations. SKB R-02-49, Svensk Kärnbränslehantering AB.

Smellie J, Tullborg E-L, Nilsson A-C, Gimeno M, Sandström B, Waber N, 2008. Hydrogeochemical evlauation. Forsmark area (version 2.2/2.3). SKB R-08-84, Svensk Kärnbränslehantering AB.

Smellie J, Tullborg, E-L, 2009. Documentation related to categorisation of the 'Extended data freeze Laxemar 2.3' groundwater samples In Kalinowski: SKB R-08-111, Svensk Kärnbränslehantering AB.

Sohlenius G, Hedenström A, 2008. Description of regolith at Laxemar-Simpevarp. Site descriptive modelling SDM-Site Laxemar. SKB R-08-05, Svensk Kärnbränslehantering AB.

Starinsky A, Katz A, 2003. The formation of natural cryogenic brines. Geochimica et Cosmochimica Acta, 67, 1475–1484.

Stumm W, Morgan J, 1996. Aquatic chemistry, 3rd ed. John Wiley, New York.

Svensson U, 1996. SKB Palaeohydrogeological programme. Regional groundwater flow due to advancing and retreating glacier-scoping calculations. In: SKB Project Report (U 96-35), Svensk Kärnbränslehantering AB.

Söderbäck B (ed), 2008. Geological evolution, palaeoclimate and historical development of the Forsmark and Laxemar-Simpevarp areas. Site descriptive modelling, SDM-Site. SKB R-08-19, Svensk Kärnbränslehantering AB.

Tröjbom M, Söderbäck B, Kalinowski B, 2008. Hydrochemistry of surface water and shallow groundwater. Site descriptive modelling SDM-Site Laxemar. SKB R-08-46, Svensk Kärnbränslehantering AB.

Tullborg E-L, Landström O, Wallin B, 1999. Low-temperature trace element mobility influenced by microbial activity; indications from fracture calcite and pyrite in crystalline basement. Chemical Geology, 157, 199–218.

Tullborg E-L, 2003. Palaeohydrogeological evidences from fracture filling minerals – Results from the Äspö/Laxemar area. Material Research Society Symposium, Vol 807, 873–878.

Tullborg E-L, Smellie J, Mackenzie A B, 2003. The use of natural uranium decay series studies in support of understanding redox conditions at potential radioactive waste disposal sites. Material Research Society Symposium, 807, Scientific basis for Nuclear Waste Management XXVII, 571–576.

Tullborg E-L, Drake H, Sandström B, 2008. Palaeohydrogeology: A methodology based on fracture mineral studies. Applied Geochemistry, 23, 1881–1897.

Veizer J, Ala D, Azmy K, Bruckschen P, Buhl D, Bruhn F, Carden G A F, Diener A, Ebneth S, Godderis Y, Jasper T, Korte C, Pawellek F, Podlaha O G, Strauss H, 1999. 87Sr/86Sr, δ13C and δ18O evolution of Phanerozoic sea water. Chemical Geology, 161, 59–88.

Vilks P, Miller H, Doern D, 1991. Natural colloids and suspended particles in the Whiteshell Research area, Manitoba, Canada, and their potential effect on radiocolloid formation. Applied Geochemistry 8, 565–574.

Waber H N, Smellie J A T, 2004. Oskarshamn site investigations Borehole KSH02: Characterisation of matrix porewater (Feasibility Study). SKB P-04-249, Svensk Kärnbränslehantering AB.

Waber H N, Smellie J A T, 2005. Forsmark site investigation. Borehole KFM06: Characterisation of porewater. Part I: Diffusion experiments. SKB P-05-196, Svensk Kärnbränslehantering AB.

Waber H N, Smellie J A T, 2006a. Oskarshamn site investigation. Borehole KLX03: Characterisation of porewater. Part 1: Methodology and analytical data. SKB P-06-12, Svensk Kärnbränslehantering AB.

Waber H N, Smellie J A T, 2006b. Oskarshamn site investigation. Borehole KLX03: Characterisation of porewater. Part 2: Rock properties and diffusion experiments SKB P-06-77, Svensk Kärnbränslehantering AB.

Waber H N, Smellie J A T, 2006c. Oskarshamn site investigation. Borehole KLX08: Characterisation of porewater. Part 1: Methodology and analytical data. SKB P-06-163, Svensk Kärnbränslehantering AB.

Waber H N, Smellie J A T, 2007. Forsmark site investigation. Borehole KFM01D, KFM08C, KFM09B: Characterisation of porewater. Part I: Diffusion experiments and porewater data. SKB P-07-119, Svensk Kärnbränslehantering AB.

Waber H N, Smellie J A T, 2008a. Oskarshamn site investigation. Borehole KLX17A: Characterisation of porewater. Part 1: Methodology and analytical data. SKB P-08-43, Svensk Kärnbränslehantering AB.

Waber H N, Smellie J A T, 2008a. Characterisation of porewater in crystalline rocks. Applied Geochemistry 23, 1834–1861.

Waber H N, Smellie J A T, 2008b. Oskarshamn site investigation. Borehole KLX17A: Characterisation of porewater. Part 1: Methodology and analytical data. SKB P-08-43, Svensk Kärnbränslehantering AB.

Waber H N, Gimmi T, Smellie J A T, 2008. Porewater in the rock matrix. Site descriptive modelling. SDM-Site Forsmark. SKB R-08-105, Svensk Kärnbränslehantering AB.

Waber H N, Gimmi T, Smellie J A T, deHaller A, 2009. Porewater in the rock matrix. Site descriptive modelling. SDM-Site Laxemar. SKB R-08-112, Svensk Kärnbränslehantering AB.

Wahlgren C-H, Curtis P, Hermanson J, Forssberg O, Öhman J, Fox A, La Pointe P, Drake H, Triumf C-A, Mattsson H, Thunehed H, Juhlin C, 2008. Geology Laxemar Site descriptive modelling SDM-Site Laxemar. SKB R-08-54, Svensk Kärnbränslehantering AB.

Wallin B, 1992. Sulfur and oxygen isotope evidence from dissolved sulphates in groundwater and sulphide sulphur in fissure fillings at Äspö, south-eastern Sweden. SKB PR 25-92-08, Svensk Kärnbränslehantering AB.

Wallin B, Peterman Z E, 1999. Calcite fracture fillings as indicators of paleohydrology at Laxemar at the Äspo Hard Rock Laboratory, southern Sweden. Applied Geochemistry, 14, 953–962.

Werner K, Bosson E, Berglund S, 2005. Description of climate, surface hydrology, and near surface hydrogeology. Simpevarp 1.2. SKB R-05-04, Svensk Kärnbränslehantering AB.

Werner K, 2008. Description of hydrology and near-surface hydrogeology at Laxemar-Simpevarp. Site descriptive modelling. SDM-Site Laxemar. SKB R-08-71, Svensk Kärnbränslehantering AB.

Werner K, Öhman J, Holgersson B, Rönnback K, Marelius F, 2008. Meteorological, hydrological and hydrogeological monitoring data and near surface hydrogeological properties data from Laxemar. Site descriptive modelling, SDM-Site Laxemar. SKB R-08-73, Svensk Kärnbränslehantering AB.

Westman P, Wastegård S, Schoning K, Gustafsson B, 1999. Salinity change in the Baltic Sea during the last 8,500 years: evidence causes and models. SKB TR-99-38, Svensk Kärnbränslehantering AB.

Wohlfarth B, 2009. Ice free conditions in Fennoscandia during Marine Isotope Stage 3. SKB TR-09-12, Svensk Kärnbränslehantering AB.

Wood S A, 1990a. The aqueous geochemistry of rare earth elements and Ytrium. 1. Review of available low-temperature data for inorganic complexes and the inorganic REE speciation of natural waters. Chemical Geology, 82, 159–186.

Wood S A, 1990b. The aqueous geochemistry of rare earth elements and Ytrium. 2. Theoretical predictions of speciation in hydrothermal solutions to 350 ºC at saturation water-vapor pressure. Chemical Geology, 88, 99–125.

Zhang M, Frape S K, 2003. Evolution of Shield brine water composition during freezing. Ontario Power generation, Report No: 06819-REP-01200-10089-R00.

Äspö Hard Rock Laboratory. Proceedings of the second Äspö International Geochemistry Workshop, June 6–7, 1995. Äspö HRL ICR-97-04, Svensk Kärnbränslehantering AB.